Ministério da Saúde

FIOCRUZ
Fundação Oswaldo Cruz

INSTITUTO OSWALDO CRUZ
Pós-Graduação em Biologia Celular e Molecular

Detalhamento morfológico e análise da expressão proteica do nematoide *Angiostrongylus costaricensis* em suas diferentes fases evolutivas

Karina Mastropasqua Rebello

Orientador(es): Dra. Ana Gisele da Costa Neves Ferreira
Dr. Henrique Leonel Lenzi (*in memoriam*)

RIO DE JANEIRO
ANO 2012

Ministério da Saúde

FIOCRUZ
Fundação Oswaldo Cruz

INSTITUTO OSWALDO CRUZ

Pós-Graduação em Biologia Celular e Molecular

Karina Mastropasqua Rebello

Detalhamento morfológico e análise da expressão proteica do nematoide *Angiostrongylus costaricensis* em suas diferentes fases evolutivas

Tese apresentada ao Instituto Oswaldo Cruz como parte dos requisitos para obtenção do título de Doutor em Biologia Celular e Molecular

Orientador(es): Dra. Ana Gisele da Costa Neves Ferreira
Dr. Henrique Leonel Lenzi (*in memoriam*)

RIO DE JANEIRO
ANO 2012

Rebello, Karina Mastropasqua

Detalhamento morfológico e análise da expressão proteica do nematoide *Angiostrongylus costaricensis* em suas diferentes fases evolutivas./Karina Mastropasqua Rebello.- Rio de Janeiro: 2012.

xviii, 131f.

Tese (Doutorado) – Instituto Oswaldo Cruz, Biologia Celular e Molecular, 2012.

1.Angiostrongylus costaricensis.2.Morfologia.3.Proteômica.4.Proteases. I.Título

Ministério da Saúde

FIOCRUZ
Fundação Oswaldo Cruz

INSTITUTO OSWALDO CRUZ

Pós-Graduação em Biologia Celular e Molecular

AUTOR: Karina Mastropasqua Rebello

TÍTULO DA TESE

Detalhamento morfológico e análise da expressão proteica do nematoide *Angiostrongylus costaricensis* em suas diferentes fases evolutivas

ORIENTADOR (ES): Dra. Ana Gisele da Costa Neves Ferreira
Dr. Henrique Leonel Lenzi (*in memoriam*)

Aprovada em: 31/07/2012

EXAMINADORES:

Dr. Delir Corrêa Gomes Maués da Serra Freire - Presidente

Dr. Carlos Graeff Teixeira

Dra. Leila Maria Lopez Bezerra

Dra Patrícia Cuervo Escobar - suplente

Dr. Marcelo Machado Pelajo - suplente

Rio de Janeiro, 31 de Julho de 2012

Dedico aos meus pais Adelino e
Sandra e aos meus irmãos
Rodrigo e Fernanda
e
Ao meu querido e eterno orientador
Dr. Henrique Lenzi (in memoriam)

Tantas vezes pensamos ter chegado, tantas vezes é preciso ir além.
Fernando Pessoa

Agradecimentos

Ao Mestre e querido orientador Dr. Henrique Lenzi (*in memoriam*), pela amizade, maravilhosa convivência, inúmeros ensinamentos, histórias regadas a chás e biscoitos... enfim, por tudo. Obrigada por ter tido o privilégio de ser sua aluna.

À minha orientadora Dra. Ana Gisele Costa Neves Ferreira, pela orientação, confiança, paciência, imenso auxílio principalmente no final da tese, estímulo e por todo o aprendizado durante esta caminhada científica.

Aos meus pais Adelino e Sandra, meus eternos incentivadores, pelo amor e apoio incondicionais e aos meus irmãos Rodrigo e Fernanda, que estão sempre vibrando com cada conquista minha.

Ao Dr. Richard Hemmi Valente, pelo incentivo à pesquisa, pelas incontáveis contribuições durante a realização desta tese e nos artigos dela resultantes.

Ao Dr. Jonas Perales, por todo apoio científico, amizade e incentivo durante a elaboração deste projeto.

À Dra. Ester Maria Mota, pelos ensinamentos e esclarecimentos sobre o *Angiostrongylus costaricensis* e por todo auxílio para a realização desta tese.

À Dra. Aleksandra Oliveira Menezes, pela amizade, colaboração científica e imensa ajuda com a análise dos resultados desta tese.

Ao Dr. James McKerrow, por me aceitar em seu laboratório na UCSF para realização do meu doutorado sanduíche em São Francisco, Califórnia.

À minha amiga Daniela Beghini, pelos inúmeros ensinamentos das técnicas proteômicas, pela amizade eterna, pela ótima convivência no laboratório e pela ajuda no desenvolvimento desta tese.

Aos Drs. Alex Donat Chapeaurouge (Henk) e André Texeira (Pink), pelo auxílio na utilização do espectrômetro de massas.

Às minhas ex-alunas de iniciação científica Caroline Siqueira e Erika Ribeiro que me auxiliaram na elaboração de alguns experimentos desta tese.

Aos amigos e ex-companheiros de laboratório André Gubler e Thayssa Gusmão, pela amizade, divertida convivência e inestimável ajuda nos *zip-tips* no início deste trabalho.

Às amigas e companheiras de laboratório Joelma Saldanha, Viviane Tostes e Monique Nunes, pelo apoio técnico para realização deste trabalho, amizade e convivência maravilhosa.

Ao amigo Rubem Mena Barreto, pela amizade, divertida convivência e colaboração científica.

À amiga Claudia d´Avila Levy, pela amizade, ensinamentos, colaboração científica e revisão da tese.

Ao Dr. Marcelo Pelajo, pela revisão da tese e pelo apoio para a realização do projeto.

Ao Dr Paulo Carvalho pelo imenso auxílio nas análises dos resultados de espectrometria de massas.

Aos colegas de laboratório Aline Garcia, Viviane Bastos, Giselle Brunoro, Surza Lucia, Monique Trugilho, Carolina Nicolau, Karen Trinta, Tamires Souza, Priscila Brandão e Matheus Tempone, pela convivência.

Às técnicas do Laboratório de Patologia do IOC responsáveis pela manutenção do ciclo do *A. costaricensis* e pela manutenção do biotério: Andréa da Silva, Iolanda Pedro, Juciara de Souza e Thatiane Cristina Barros.

Ao Laboratório de Biologia de Helmintos Otto Wucherer da UFRJ e seus integrantes, pela colaboração científica imprescindível na parte de microscopia.

À amiga Claudia Calvet, pela maravilhosa convivência durante o meu doutorado sanduíche na UCSF e por toda ajuda na ambientação ao laboratório.

Ao amigo Dan Sjoka, pela imensa ajuda durante a minha estada na UCSF com os experimentos e ambientação no laboratório.

Aos meus avós Othello e Francisca (*in memoriam*) que sempre rezaram por mim e sempre se orgulharam da neta cientista.

À Plataforma de Microscopia Eletrônica do Instituto Oswaldo Cruz (IOC-FIOCRUZ), pela aquisição das belíssimas imagens de microscopia eletrônica de varredura.

À Plataforma de Microscopia Confocal Eletrônica do Instituto Oswaldo Cruz (IOC-FIOCRUZ), pela aquisição das imagens de microscopia de luz e confocal. Em especial, agradeço ao Igor José da Silva, técnico responsável por operar o microscópio.

À Coordenação do Programa de Pós Graduação em Biologia Celular e Molecular do Instituto Oswaldo Cruz, pelo apoio e suporte financeiro em eventos científicos.

À agência de fomento CAPES, pela minha bolsa de estudos durante o doutorado dentro e fora do país (PDSE).

Lista de Figuras

Lista de Tabelas

Lista de Abreviações

2DE – Eletroforese bidimensional

A – Ânus

AA – Angiostrongilíase abdominal

AFA – Mistura de ácido acético, formaldeído e etanol

APMSF – Fluoreto de (4-aminofenil)-metanosulfonila

BAPNA – p-nitroanilida de benzoil-arginina

BDR – *Bursal dorsal rays* (raios bursais dorsais)

BLASTp – *Basic local aligment search tool- protein*

BVR – *Bursal ventral rays* (raios bursais ventrais)

$CaCl_2$ – Cloreto de cálcio

CHAPS- *3-[(3-Colamidopropil)-dimetilamonio]-1-propano sulfonato*

COI – Citocromo c subunidade I

CP – C*ephalic pappilae* (papilas cefálicas)

DNA – *Deoxyribonucleic acid (*ácido desoxirribonucleico)

DMSO – Dimetil sulfóxido

DTT– Ditiotreitol

E-64 – *Trans*-epoxysuccinyl-L-leucylamida (4-guanidina) butano

EDTA – Ácido etileno-diamino tetracético

EGTA – Ácido etilenoglicol-bis(2-amino-etil-éter)-N,N,N',N'- tetra-acético

ESI – *Electrospray ionization* (ionização por eletrospray)

EV – *Esophageal valve* (válvulas esofágicas)

GO – *Gene Ontology*

HCl – Ácido clorídrico

HE- Hematoxilina-eosina

HSPs – *Heat shock proteins* (proteínas de choque térmico)

IEF– *Isoelectric focusing* (focalização isoelétrica)

KCl – Cloreto de potássio

kDa – Quilodalton

L– Linear

LA – *Lateral alae* (ala lateral)

L1 – Larva de primeiro estágio

L3 – Larva de terceiro estágio

MALDI-TOF – *Matrix-assisted laser desorption ionization – time of flight* (ionização por dessorção a laser auxiliada por matrix – tempo de vôo)

MCVL – Microscopia confocal de varredura a laser

MEV – Microscopia eletrônica de varredura

mRNA – *Messenger ribonucleic acid* (ácido ribonucleico mensageiro)

MudPiT – *Multidimensional protein identification technology*

NaOH – Hidróxido de sódio

NL– Não linear

O – *Oral opening* (abertura oral)

PBS – Salina tamponada com fosfato

PCR – *Polymerase chain reaction* (reação em cadeia da polimerase)

PFF – *Peptide fragment fingerprint*

pI – Ponto isoelétrico

PMSF – Fluoreto de fenilmetilsulfonila

PSD – *Post source decay* (tipo de fragmentação utilizada em espectrometria de massas)

PTMs – Modificações pós-traducionais

PVDF – Polivinildifluoreto

RFLPs – *Restriction fragment length polymorphism* (polimorfismo no comprimento de fragmentos de restrição)

S – *Spicule* (espículo)

SCX – *Strong cation exchange* (cromatografia líquida de troca catiônica forte)

SDS – *Sodium dodecyl sulfate* (dodecil sulfato de sódio)

SDS-PAGE - *Sodium dodecyl sulfate polyacrylamide gel electrophoresis (*eletroforese em gel de poliacrilamida contendo dodecil sulfato de sódio)

SEM – *Scanning electron microscopy* (microscopia eletrônica de varredura)

SPITC – *4-sulfophenyl isothiocyanate*

T – *Tail* (cauda)

TE – *Tail end* (final da cauda)

V – Volts

v/v – relação volume por volume

Resumo

Angiostrongylus costaricensis é o nematoide causador da angiostrongilíase abdominal, uma parasitose de ampla distribuição na América Latina. Este trabalho teve como objetivos a caracterização da morfologia e a determinação dos padrões de expressão proteica dos diferentes estágios de desenvolvimento deste helminto. Para o estudo morfológico, utilizamos microscopia de luz, microscopia eletrônica de varredura e microscopia confocal a laser. Métodos bioquímicos clássicos e proteômicos foram utilizados nas análises de expressão proteica, incluindo a caracterização de proteases e proteínas imunorreativas. Larvas de primeiro estágio (L1) foram obtidas das fezes de roedores *Sigmodon hispidus* infectados e larvas de terceiro estágio (L3) foram coletadas de moluscos *Biomphalaria glabrata* previamente infectadas com L1. Vermes adultos foram recuperados das artérias mesentéricas de roedores. Os dados morfológicos se mostraram compatíveis com os descritos anteriormente para *A. costaricensis*. Entretanto, várias novas estruturas foram observadas, tais como detalhes das estriações cuticulares nos espículos de machos adultos, uma aba de cutícula protetora cobrindo a abertura vulvar, o gubernáculo e a válvula esofágica-intestinal. Algumas características taxonômicas foram redescritas e outras, como o número correto de papilas ao redor da boca e atrás da abertura cloacal, foram documentadas pela primeira vez. Os extratos celulares dos vermes adultos de ambos os sexos mostraram perfis similares por eletroforese bidimensional, com 60% de todos os *spots* proteicos focalizando entre pH 5-7 e com massas moleculares de 20,1 a 66 kDa. Dentre as proteínas mais abundantes, 53 foram identificadas e se mostraram associadas aos seguintes termos do *Gene Ontology – Biological Process*: “processo metabólico de macromoléculas”, “processo de desenvolvimento”, “resposta à estresse” e “regulação biológica”. Os *immunoblots* de fêmeas e machos adultos mostraram padrões similares de proteínas reativas, identificadas por MS/MS como proteínas de choque térmico, proteína putativa DAuer e galectinas, entre outras. Nos ensaios de zimografia, apenas os extratos dos estágios larvares mostraram atividade gelatinásica, caracterizada em L1 e L3 como serino- e metaloproteases, respectivamente. Vermes adultos e larvas hidrolisaram hemoglobina em solução, atividade enzimática atribuída à presença de aspártico-proteases. Nossos resultados contribuem para a melhor compreensão da biologia do *A. costaricensis* e representam um primeiro passo na busca por proteínas candidatas para o diagnóstico e o tratamento desta infecção parasitária.

Abstract

Angiostrongylus costaricensis is a nematode that causes abdominal angiostrongyliasis, a widespread human parasitism in Latin America. This study aimed to characterize the morphology and to determine the protein expression profiles of different developmental stages of this helminth. For the morphological analyses, we used optical microscopy, scanning electron microscopy and confocal laser scanning microscopy techniques. Classical biochemical and proteomic methods were employed for the analysis of protein expression, including the characterization of proteases and immunoreactive proteins. First-stage larvae (L1) were obtained from the feces of infected *Sigmodon hispidus* rodents and third-stage larvae (L3) were collected from mollusks *Biomphalaria glabrata* previously infected with L1. Adult worms were recovered from rodent mesenteric arteries. The morphological data were compatible with the previous descriptions of *A. costaricensis*. However, several novel anatomical structures were visualized, such as details of the cuticular striations of the spicules in male worms, a protective flap of cuticle covering the vulvar aperture, the gubernaculum and the esophageal-intestinal valve. Some taxonomic features were redescribed and others, such as the correct number of papillae distributed around the oral opening and the papillae behind the cloacal opening, were documented for the first time. Total cellular extracts from both sexes of adult worms showed similar bidimensional electrophoresis profiles, with 60% of all protein spots focusing between pH 5–7 and presenting molecular masses from 20.1 to 66 kDa. A total of 53 different dominant proteins were identified in our dataset and were mainly associated with the following over-represented Gene Ontology Biological Process terms: “macromolecule metabolic process”, “developmental process”, “response to stress”, and “biological regulation”. Female and male immunoblots showed similar patterns of reactive proteins, identified by MS/MS as heat shock proteins, a putative abnormal DAuer Formation family member and galectins, among others. Proteolysis of gelatin was observed by zymography only in the larval stages. The gelatinolytic activities of L1 and L3 extracts were ascribed to serino- and metallo-proteases, respectively. Adult worms and larvae extracts were able to hydrolyze hemoglobin in solution, an enzymatic activity completely inhibited by aspartic proteases inhibitors. Our results contribute to a better understanding of the biology of *A. costaricensis* and represent a first step in the search for candidate proteins for diagnostic assays and the treatment of this parasitic infection.

Índice

I. Introdução

1. Filo Nematoda: um dos mais numerosos e diversos do planeta

As infecções causadas por helmintos (palavra derivada do grego *helmins/helminthos*, que significa "verme") estão entre as doenças crônicas humanas de maior prevalência mundial (Brooker *et al.*, 2006). O grupo dos helmintos se divide em dois grandes filos de interesse na parasitologia humana: Platyhelminthes e Nematoda (Faust *et al.*, 1970). O filo dos platelmintos é composto de vermes acelomados achatados dorso-ventralmente, tais como o *Schistosoma mansoni*, a *Fasciola hepatica* e a *Taenia solium*; o filo Nematoda é o segundo maior do reino animal e engloba vermes pseudocelomados cilíndricos, com extremidades afiladas e simetria bilateral (Rey, 2008). Estima-se a existência de mais de um milhão de espécies de nematoides, das quais apenas 20.000 foram descritas. Ainda que a maioria dos nematoides seja de vida livre (*e.g*. *Caenorhabditis elegans*), existem muitos exemplos de espécies parasitas de seres humanos, animais e plantas causando doenças de importância sócio-econômica em todo o mundo (Blaxter, 1998; Lambshead *et al.*, 2003). Das 342 espécies de helmintos parasitas de humanos conhecidas, 138 pertencem ao filo Nematoda (Crompton, 1999). Estes dados revelam a importância dos nematoides como um dos principais responsáveis pelas helmintoses humanas (Brooker *et al.*, 2006).

Os nematoides apresentam sistema digestivo completo, com boca, esôfago, intestino e ânus (Murray *et al.*, 2006). Seu sistema nervoso é simples, composto basicamente por um anel nervoso circum-esofágico e cordões nervosos longitudinais. São considerados animais dioicos (sexo separado em indivíduos distintos) e com dimorfismo sexual, sendo as fêmeas maiores do que os machos. O aparelho reprodutor feminino consiste de um ou dois ovários alongados e tubulares conectados a um útero terminando na abertura vulvar. O aparelho reprodutor masculino é formado por um ou dois testículos tubulares e vasos deferentes que se unem posteriormente ao reto e terminam na cloaca, onde são encontradas estruturas acessórias, como os espículos (um ou dois) e o gubernáculo. Em algumas espécies de nematoides, como por exemplo, no *Angiostrongylus costaricensis*, existe ainda a presença da bolsa copuladora (Chitwood & Chitwood, 1974). A superfície dos nematoides é coberta por uma

cutícula secretada pela hipoderme. Além de recobrir o corpo do helminto, a cutícula também é encontrada nas porções iniciais da boca, faringe, vulva e ânus (Page & Winter, 2003). Entre a parede do corpo e os aparelhos reprodutor e digestivo encontra-se o pseudoceloma, cavidade preenchida por fluido. A movimentação dos vermes ocorre através da contração das fibras musculares longitudinais estriadas sobre o esqueleto hidrostático (Ruppert *et al.*, 1996).

2. Nematoides parasitas e saúde pública

As helmintoses são um grave problema de saúde pública em diversas regiões tropicais e subtropicais, incluindo a América Latina e a África. O filo Nematoda abrange os vermes filariais, causadores da filariose linfática e da oncocercose, e os vermes intestinais, também conhecidos como geo-helmintos (Hotez *et al.*, 2008).

Os principais vermes filariais que infectam o homem são *Wuchereria bancrofti, Brugia malayi, Brugia timori, Onchocerca volvulus, Loa loa, Mansonella streptocerca, Mansonella ozzardi, Mansonella pertans* e *Dracunculus medinensis* (Walther & Muller, 2003; Taylor *et al.*, 2010; CDC, 2011). A transmissão destes vermes ocorre através da picada de dípteros hematófagos infectados. Estima-se que cerca de 120 milhões de pessoas estão infectadas com *Wuchereria bancrofti*, *Brugia malayi* e/ou *Brugia timori*, vermes causadores da filariose linfática (Erickson *et al.*, 2009). A oncocercose, transmitida pelo *O. volvulus*, é uma das principais causas de cegueira e doença de pele na América Latina e na África (Hotez *et al.*, 2008). Em todo o mundo existem mais de 120 milhões de pessoas em risco de contrair a doença, com cerca de 18 milhões de pessoas infectadas (Gustavsen *et al.*, 2011). *Loa loa* é o verme causador da doença denominada loaíase, um tipo de filariose subcutânea que afeta milhões de indíviduos que vivem em florestas e savanas africanas. No entanto, é uma verminose menos difundida do que a filariose linfática e a oncocercose, sendo restrita à África Central (Boussinesq, 2006). Os vermes *M. streptocerca* e *D. medinensis* causam a filariose subcutânea (Fischer *et al.*, 1997; Iriemenam *et al.*, 2008), enquanto o *M. ozzardi e* o *M. pertans* são causadores da filariose da cavidade serosa, pois parasitam a cavidade do abdômen (Simonsen *et al.*, 2010; Medeiros *et al.*, 2011). Estes últimos estão presentes em partes da África, América Central, América do Sul e

algumas ilhas do Caribe (Fischer *et al.*, 1997; Iriemenam *et al.*, 2008; Simonsen *et al.*, 2010; Medeiros *et al.*, 2011).

Para infectar o homem, os geo-helmintos precisam passar por embrionamento no solo, sob condições adequadas de temperatura e umidade. Os principais geo-helmintos que infectam a espécie humana são os nematoides intestinais *Ascaris lumbricoides*, *Trichuris trichiura*, *Strongyloides stercoralis* e os ancilostomídeos *Ancylostoma duodenale* e *Necator americanus* (Hotez *et al.*, 2008). A infecção ocorre através da ingestão de ovos larvados e, no caso dos ancilostomídeos, também pode ocorrer através da penetração ativa da larva na pele intacta. Estima-se que aproximadamente 4,5 bilhões de pessoas estejam infectadas por *A. lumbricoides, T. trichiura, S. stercoralis, A. duodenale* e/ou *N. americanus* em todo o mundo (Horton, 2003; Utzinger & Keiser, 2004; Bethony *et al.*, 2006; Ziegelbauer *et al.*, 2012)

Os nematoides do gênero *Angiostrongylus* são parasitas de roedores e pequenos mamíferos carnívoros (Anderson, 2000). Eles habitam as artérias pulmonares de seus hospedeiros, com exceção do *Angiostrongylus costaricensis* (Morera & Céspedes, 1971) e do *Angiostrongylus siamensis* (Ohbayashi *et al.*, 1979), cujo *habitat* são as artérias mesentéricas. Neste gênero existem pelo menos 22 espécies (Morera & Cespedes, 2002; Maldonado Jr *et al.*, 2012) (Tabela 1), sendo que apenas duas foram relatadas infectando humanos e representam risco à saúde pública: *A. costaricensis* e *A. cantonensis* (Chen, 1935), agentes etiológicos da angiostrongilíase abdominal e da meningoencefalite eosinofílica, respectivamente (Eamsobhana *et al.*, 2010). O *A. costaricensis* é endêmico no continente americano, com casos relatados principalmente na Costa Rica (Morera, 2001) e na região sul do Brasil (Agostini *et al.*, 1983; Ayala, 1987). O *A. cantonensis,* por outro lado, possui uma distribuição mais ampla, sendo encontrado principalmente no continente asiático, nas ilhas do Pacífico. Entretanto, também existem casos da presença do nematoide descritos na Índia, Caribe, Austrália, América do Norte (Campbell & Little, 1988; Pien & Pien, 1999), Cuba (Aguiar *et al.*, 1981), Haiti (Raccurt *et al.*, 2003) e Jamaica (Lindo *et al.*, 2002). Em 2007, notificou-se o primeiro caso no Brasil, descrito como transmissão autóctone de meningoencefalite eosinofílica no estado do Espírito Santo (Caldeira *et al.*, 2007). Recentemente, foi descrito um caso inédito de angiostrongilíase abdominal causada por *A.*

cantonensis (Sawanyawisuth *et al.*, 2010). Alguns poucos trabalhos na literatura também descrevem a existência de *A. costaricensis* parasitando gambás e guaxinins (Sly *et al.*, 1982; Brack & Schropel, 1995; Miller *et al.*, 2006).

Tabela 1: Diferentes espécies de *Angiostrongylus* e sua distribuição geográfica (baseado em Morera & Cespedes, 2002; Maldonado Jr *et al.*, 2012).

Hospedeiro	Parasito	Distribuição geográfica	Descrito por
Carnívoros	*A. vasorum*	Europa, America do Sul, Australia, Brasil	Baillet, 1866
	A. raillieti	Brasil	Travassos, 1927
	A. gubernaculatus	Estados Unidos	Dougherty, 1946
	A. chabaudi	Itália	Biocca, 1957
Roedores	*A. costaricensis*	America Central e America do Sul	Morera & Céspedes, 1971
	A. tateronae	Oeste Africano	Baylis, 1928
	A. cantonensis	Ásia, Pacífico, Brasil	Chen, 1935
	A. sciuri	Turquia	Merdevenci, 1964
	A. sandarasae	Leste da Ásia	Alicata, 1968
	A. mackerrasae	Australia	Bhaibulaya, 1968
	A. dujardini	França	Drozdz & Doby, 1970
	A. schmidti	Estados Unidos	Kinsella, 1971
	A. malaysiensis	Sudeste da Ásia	Bhaibulay & Cross, 1971
	A. siamensis	Tailandia	Ohbayashi, Kamiya & Bhaibulaya, 1979
	A. lenzii	Brasil	Souza *et al*., 2009
	A. petrowi	Itália	Tarjymanova & Tschertkova, 1969
	A. ryjikovi	Estados Unidos	Jushkov, 1971
	A. morerai	Argentina	Robles, Navone & Kinsella, 2008
	A. michiganensis	Estados Unidos	Ash, 1967
	A. ondatrae	Russia	Schultz, Orlow & Kutass,1933
	A. blarini	Estados Unidos	Ogren, 1954
	A. soricis	Polônia	Soltys, 1954

3. *Angiostrongylus costaricensis* – o parasito

O *Angiostrongylus costaricensis* foi descrito pela primeira vez em 1971, por Morera e Cespedes, na Costa Rica, quando foram isoladas três fêmeas e um macho de um paciente infectado, durante uma cirurgia (Maldonado Jr *et al.*, 2012). A espécie recém-descrita foi originalmente agrupada em um novo gênero denominado *Morerastrongylus* (Chabaud, 1972), mas esta nomenclatura não foi aceita em uma revisão posterior sobre a classificação de nematoides (Anderson, 1978).

O *Angiostrongylus costaricensis* (Morera & Céspedes, 1971) é um helminto nematoide pertencente à família Metastrongylidae que habita os ramos íleo-cecais da artéria mesentérica superior de seus hospedeiros vertebrados. No homem, causa um processo inflamatório agudo intestinal denominado angiostrongilíase abdominal (Morera, 1973).

Durante o ciclo biológico do helminto, larvas de primeiro estágio (L1) atravessam as paredes da mucosa intestinal do hospedeiro vertebrado e caem na luz do intestino, sendo liberadas junto com as fezes. Moluscos terrestres, como lesmas e caramujos, podem ingerir as L1 ou estas podem penetrar ativamente por sua mucosa. No interior do molusco, as L1 sofrem duas mudas: de L1 para L2 e de L2 para L3, sendo esta última a forma infectante para o hospedeiro vertebrado. As larvas de terceiro estágio são liberadas junto ao muco secretado pelos moluscos. O mamífero se infecta ao ingerir alimentos contaminados com o muco contendo as larvas ou o próprio molusco infectado (Figura 1) (Morera & Cespedes, 1971).

No roedor, o hospedeiro definitivo, as L3 podem seguir duas vias migratórias: linfático/venosa-arterial e/ou venosa-portal hepática. Na primeira (preferencial), as L3 se transformam em vermes adultos juvenis no sistema linfático abdominal e atingem o sistema sanguíneo arterial através da circulação pulmonar. Seguem então para os ramos íleos-cecais da artéria mesentérica superior, seu *habitat* definitivo. Os parasitos que seguem a via venosa-portal hepática penetram nos vasos sanguíneos venosos das vilosidades intestinais e são levados pela corrente sanguínea até o fígado, onde se transformam em vermes adultos. Após o 30° dia de infecção, migram contra a corrente sanguínea para as veias mesentéricas intestinais, onde as

fêmeas eliminam os ovos que são embolizados no fígado e nos pulmões (Mota & Lenzi, 2005).

Os vermes adultos apresentam dimorfismo sexual, sendo o macho menor, com 20 mm de comprimento, e a fêmea maior, com 33 mm. Ao ingerir alimentos crus, água ou moluscos contaminados com L3, o homem se infecta e desenvolve a angiostrongilíase abdominal. Devido à intensa reação inflamatória que ocorre na parede intestinal, as L1 não são eliminadas junto às fezes humanas. Como as larvas ficam retidas na mucosa intestinal, o ciclo biológico não se completa e, portanto, o homem é considerado um hospedeiro incidental parasito (Graeff-Teixeira *et al.*, 1991b).

O nematoide *A. costaricensis* é um verme filiforme, apresentando a extremidade anterior arredondada, com uma abertura oral circular coberta por três pequenos lábios. Ao redor da boca estão dispostas, em dois círculos, seis papilas cefálicas sensoriais, sendo duas delas ofidiais. A cutícula é estriada transversalmente e as formas larvares apresentam uma ala bilateral que se estende ao longo do corpo, exceto nas extremidades anterior e posterior (Morera, 1973).

A fêmea adulta mede cerca de 33 mm de comprimento e 0,33 mm de largura (Maldonado Jr *et al.*, 2012). O esôfago é claviforme e tem comunicação direta com a abertura bucal; o intestino retilíneo abre-se próximo à extremidade posterior; o poro excretor é pequeno e localiza-se ventralmente próximo à junção esôfago-intestinal; seu aparelho reprodutor apresenta um aspecto helicoidal, com dois ovários espiralados ao redor do intestino terminando em uma vulva situada pouco depois do ânus, localizado ventralmente (Morera, 1973). Os machos medem em torno de 20 mm de comprimento e 0,30 mm de largura e apresentam o tubo digestivo igual ao das fêmeas (Maldonado Jr *et al.*, 2012). O aparelho reprodutor masculino é composto por um testículo localizados ao redor do intestino, cujo canal se abre em uma bolsa copuladora provida de dois espículos estriados e um gubernáculo (Morera, 1973; Thiengo *et al.*, 1997).

Ao longo do seu ciclo biológico, o *A. costaricensis* apresenta larvas de primeiro, segundo e terceiro estágios (Morera, 1973). L1 e L3 exibem o tubo digestivo igual ao descrito para os vermes adultos, assim como a presença do poro excretor na face ventral próximo à junção esôfago-intestino. As L1 têm em

torno de 0,26-0,29 mm de comprimento e 0,01-0,02 mm largura. As L3 são mais robustas do que as L1 e apresentam 0,46-0,48 mm de comprimento e 0,03 mm de largura (Morera, 1973; Thiengo *et al.*, 1997). As L2 apresentam 0,28-0,31mm de comprimento e 0,02 mm de largura (Morera, 1973; Thiengo *et al.*, 1997).

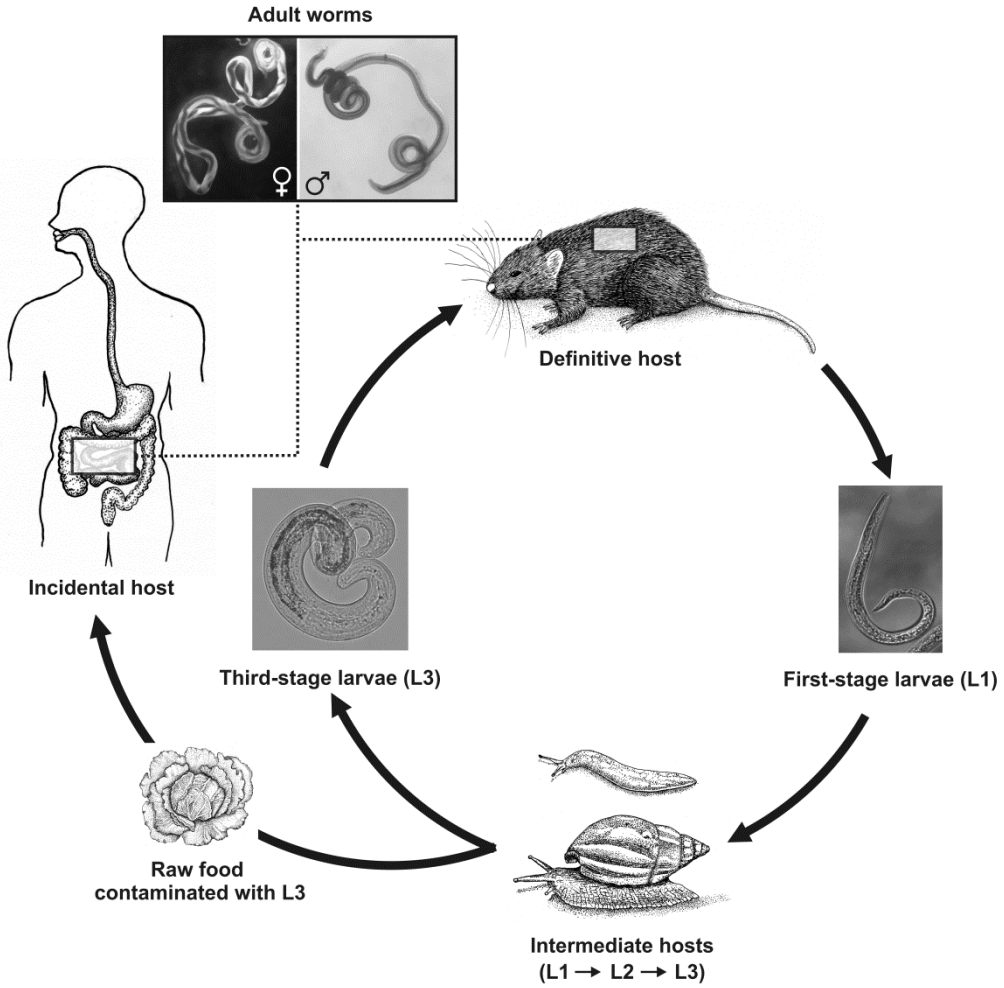

Figura 1: Ciclo biológico do *Angiostrongylus costaricensis* (Rebello *et al.*, 2011).

4. Angiostrongilíase abdominal – a doença

O primeiro relato de angiostrongilíase abdominal ocorreu em 1952, em crianças da Costa Rica (Céspedes, 1967). Quase 20 anos depois, neste mesmo país, foi observada a infecção natural de *Sigmodon hispidus* e *Rattus rattus* pelo parasito (Morera & Cespedes, 1971). A angiostrongilíase abdominal (AA) é um problema de saúde pública em diversos países da América Latina, especialmente na Costa Rica e na região sul do Brasil. Existem relatos da

doença e/ou da presença do parasito desde os Estados Unidos até o norte da Argentina (Ubelaker & Hall, 1979; Demo & Pessat, 1986; Morera, 1988; Duarte *et al.*, 1991; Hulbert *et al.*, 1992; Juminer *et al.*, 1992; Sanchez, 1992). Um caso suspeito de AA foi relatado na África (Baird *et al.*, 1987). No Brasil, já existem casos relatados nos estados de Minas Gerais (Rocha *et al.*, 1991), Espírito Santo (Pena *et al.*, 1995), Distrito Federal (Barbosa *et al.*, 1980; de Magalhaes *et al.*, 1982), São Paulo (Ziliotto *et al.*, 1975; Iabuki & Montenegro, 1979), Santa Catarina, Paraná e Rio Grande do Sul (Agostini *et al.*, 1984; Ayala, 1987), sendo a região sul o local com maior número de registros de casos da doença (Agostini *et al.*, 1983; Graeff-Teixeira *et al.*, 1991a). O primeiro surto da doença relatado ocorreu na Guatemala, onde a folha de hortelã crua (comida separadamente ou como ingrediente do ceviche) foi o provável veículo de infecção (Kramer *et al.*, 1998).

Até o momento, não existe um tratamento específico para a doença e os anti-helmínticos disponíveis comercialmente não são eficientes, podendo agravar o quadro clínico do paciente, pois podem induzir migração ectópica dos vermes e desencadear trombose arterial (Morera & Bontempo, 1985). A ausência das larvas nas fezes gera um resultado falso negativo no exame parasitológico convencional; o diagnóstico preliminar da doença é baseado na presença de eventos inespecíficos, tais como febre, dor abdominal, anorexia, vasculites, granulomas eosinofílicos e eosinofilia tecidual, que podem ser facilmente confundidos com outras etiologias (Graeff-Teixeira *et al.*, 1991b).

Ao exame clínico, a presença de uma massa dura à palpação na fossa ilíaca direito, acompanhada com leucocitose e eosinofilia sanguínea são sugestivos de AA. (Graeff-Teixeira *et al.*, 1991b). A massa endurecida pode ser confundida com enterite regional, tuberculose intestinal ou linfoma. Até o momento, a confirmação dos casos suspeitos de AA só é feita através de intervenções cirúrgicas, seguidas de exames histopatológicos de biopsia ou de peças cirúrgicas (Rey, 2001). Três achados são fundamentais: eosinofilia, vasculite eosinofílica e granuloma com eosinofilia Os casos de rápida evolução da doença são considerados graves e levados à cirurgia para ressecção das alças intestinais afetadas (Morera & Bontempo, 1985).

As lesões causadas por *A. costaricensis* ocorrem mais frequentemente na região íleo-cecal, apêndice e cólon ascendente (Kramer *et al.*, 1998;

Abrahams-Sandí, 2007). Estas lesões caracterizam-se por inflamação, hipertrofia e presença de zonas de necrose no intestino (Abrahams-Sandí, 2007). Em alguns casos, podem existir ulcerações que eventualmente evoluem para perfuração do órgão (Waisberg *et al.*, 1999). Microscopicamente, é possível observar granulomas com infiltrado eosinofílico na parede intestinal e vasculite eosinofílica (Graeff-Teixeira *et al.*, 1991a). Existem ainda relatos de lesões extra-intestinais encontradas no fígado (Quiros *et al.*, 2011) e artéria espermática (Ruiz & Morera, 1983). Estas últimas são raras e consideradas de localização ectópica (Abrahams-Sandí, 2007).

Estudos utilizando ferramentas não invasivas para diagnóstico da AA mostraram que os testes sorológicos disponíveis não são eficazes devido à reação cruzada com outros nematoides e à diversidade de resposta humoral dos pacientes (Graeff-Teixeira *et al.*, 1997; Geiger *et al.*, 2001). Mais recentemente, sugeriu-se a utilização da reação em cadeia da polimerase (PCR) como método alternativo eficaz para o diagnóstico da AA, mas os resultados ainda são preliminares (da Silva *et al.*, 2003).

Diante das dificuldades de diagnóstico e tratamento da angiostrongilíase abdominal, as medidas profiláticas tornam-se muito importantes na prevenção da doença: deve-se lavar bem as mãos após a manipulação de verduras e evitar a manipulação e o consumo de moluscos (Zanini & Graeff-Teixeira, 1995). A utilização de hiploclorito de sódio, vinagre e o cozimento em solução contendo sal se mostraram efetivos na inativação das larvas infectantes L3 de *A. costaricensis* (Zanini & Graeff-Teixeira, 2001), desde que usados de modo adequado.

5. Conhecendo melhor o *A. costaricensis:* abordagens metodológicas propostas no estudo do nematoide

Como descrito anteriormente, o conhecimento sobre a biologia do *Angiostrongylus costaricensis* ainda é bastante limitado. Sua morfologia foi pouco documentada na literatura e a maior parte dos dados baseia-se em descrições com câmara clara. A morfologia interna está pobremente descrita, limitando o conhecimento da anátomo-fisiologia desse helminto. De modo similar, não existem estudos sistemáticos sobre a bioquímica do *A. costaricensis*, incluindo informações sobre o perfil de expressão proteica em

suas diferentes fases de desenvolvimento. Neste trabalho, pretendemos avançar nestas duas vertentes: a) caracterização morfológica do helminto, utilizando microscopia de luz e modernas técnicas de microscopia eletrônica de varredura e confocal a laser; b) caracterização bioquímica, incluindo a descrição do perfil global de expressão proteica (proteômica) e a identificação de suas proteínas antigênicas e enzimas proteolíticas. As abordagens complementares da morfologia e da proteômica permitirão que, futuramente, proteínas de interesse selecionadas possam também ser estudadas *in situ*, através de imunomarcações sobre cortes do parasito e análise por microscopia. A seguir, descreveremos brevemente as principais abordagens metodológicas empregadas nesta tese.

5.1. Caracterização morfológica / microscopia

Para estudar a superfície das diferentes fases de desenvolvimento do *A. costaricensis,* utilizamos a microscopia eletrônica de varredura (MEV), metodologia amplamente empregada nos estudos de topografia de helmintos (Lanfredi *et al.*, 1998; Marques *et al.*, 2004). A MEV é uma técnica de alta resolução que permite grande profundidade de foco, dando à imagem uma aparência tridimensional. A imagem é formada pela incidência de elétrons na amostra desidratada ou seca, sob condições de vácuo. A incidência do feixe de elétrons na amostra promove a emissão de elétrons secundários. A imagem eletrônica de varredura representa, em tons de cinza, o mapeamento e a contagem de elétrons secundários e retroespalhados emitidos pelo material. Para a homogeneização da emissão de elétrons secundários, as amostras são previamente metalizadas. A etapa de metalização consiste na precipitação a vácuo de uma película de um metal condutor (comumente o ouro) sobre a superfície as amostra. Esta técnica permite o estudo detalhado da superfície de diferentes espécimes (Maliska, 2004).

Para analisar as estruturas internas do parasito, fizemos cortes histológicos para serem analisados por microscopia de luz. Nesta metodologia, a resolução e a precisão são limitadas pelo espalhamento de luz que decorre dos sistemas ópticos tradicionais (Halton, 2004). Assim, de modo complementar, utilizamos a microscopia confocal de varredura a laser (MCVL), que possibilita a aquisição de imagens das estruturas internas utilizando o

parasito inteiro. A microscopia confocal utiliza laser como fonte de luz para a aquisição das imagens. Nesta técnica, um feixe de iluminação extremamente fino se desloca sobre cada ponto da amostra gerando fótons que são selecionados, de acordo com a profundidade de foco, por um orifício denominado “pinhole”. A imagem produzida de cada plano focal é denominada corte óptico. A imagem da espécime analisada pode ser reconstruída eletronicamente através da sobreposição dos cortes ópticos, formando uma imagem 3D (Vermelho *et al.*, 2011). Assim, é possível gerar imagens de alta qualidade que permitem o estudo de detalhes da morfologia interna do material analisado como, por exemplo, a reconstrução tridimensional do sistema nervoso de platelmintos (Halton & Gustafsson, 1996).

A interface entre a microscopia e a bioquímica pode ser explorada de diversas maneiras nos estudos sobre helmintos. Como exemplos, podemos citar proteínas de interesse imunolocalizadas em cortes histológicos de *Schistosoma mansoni* e *Setaria digitata* (Havercroft *et al.*, 1991; Krushna *et al.*, 2009). Nas pesquisas por novas drogas para o controle dos parasitos, o monitoramento de suas mudanças morfológicas pode indicar o grau de eficácia / toxicidade dos compostos testados (Halton, 2004). O conhecimento dos detalhes anatômicos do parasito também é importante na seleção de subproteomas relevantes a serem explorados. Um trabalho recente sobre proteômica do tegumento do *S. mansoni* ilustra bem esta abordagem (van Balkom *et al.*, 2005). Neste trabalho foram identificadas 740 proteínas, das quais 43 foram reconhecidas como proteínas específicas de tegumento. Muitas não mostraram homologia com nenhuma proteína disponível no banco de dados de *S. mansoni*, demonstrando que a superfície de *S. mansoni* apresenta proteínas específicas e únicas, crucias para a sobrevivência do parasita (van Balkom *et al.*, 2005).

5.2. Caracterização bioquímica/proteômica

O termo proteoma foi cunhado originalmente para descrever o conjunto de proteínas expressas pelo genoma de um organismo, sob condições definidas (Wilkins *et al.*, 1996). Atualmente, a proteômica é definida como um conjunto de técnicas bioquímicas que permite a análise em grande escala de proteínas e peptídeos de uma célula, um tecido ou um organismo. Pode ser

encarada também como uma ferramenta fundamental para a compreensão da função dos genes (Mallick & Kuster, 2010). As proteínas definem o fenótipo de um organismo e representam os alvos principais da maioria dos agentes terapêuticos conhecidos. Informações sobre sequências de DNA, ainda que muito úteis, pouco nos dizem acerca dos mecanismos dinâmicos complexos que ocorrem no interior dos organismos. A análise da transcrição de mRNAs revela o padrão de expressão gênica diferencial nestas amostras, mas nem sempre apresenta correlação direta com os níveis de proteínas efetivamente expressas (Cox & Mann, 2011). Por sua vez, a proteômica permite não só a identificação e a quantificação das proteínas, mas também a determinação de suas modificações, interações, atividades e, eventualmente, funções biológicas (Fields, 2001; Zhu *et al.*, 2003).

O estudo em larga escala de proteínas foi dificultado durante um bom tempo em função de limitações técnicas. Infelizmente, não existe uma PCR para proteínas e o grau de complexidade destas moléculas é maior do que os polímeros de ácidos nucleicos estudados na genômica e na transcriptômica (Graves & Haystead, 2002; Patterson & Aebersold, 2003). Nos últimos anos, evoluções metodológicas, principalmente nas técnicas de eletroforese bidimensional, cromatografia líquida e espectrometria de massas, permitiram o desenvolvimento da proteômica de modo extraordinário, com perspectivas de aplicações em diversos campos da Biologia, incluindo a Parasitologia (Ashton *et al.*, 2001).

Estudos proteômicos sobre helmintos nematoides ainda são pouco numerosos. A maior parte das pesquisas foi realizada usando como modelo o *Caenorhabditis elegans*, primeiro organismo multicelular a ter seu genoma totalmente sequenciado (Consortium, 1998). Os dados proteômicos contribuíram significativamente para o melhor conhecimento da biologia deste nematoide, facilitando, por exemplo, a anotação de seu genoma (Merrihew *et al.*, 2008) e a identificação de suas principais vias de sinalização (ex.: TGF-ß e insulina) e de seus processos metabólicos (Shim & Paik, 2010). Exemplos mais recentes de estudos proteômicos em nematoides incluem trabalhos com *Haemonchus contortus* (Millares *et al.*, 2012), *Heterodera glycines* (Chen *et al.*, 2011), *Heligmosomoides polygyrus* (Hewitson *et al.*, 2011), *Brugia malayi* (Bennuru *et al.*, 2011; Wongkamchai *et al.*, 2011) e *Angiostrongylus*

cantonensis (Song *et al.*, 2012). Estes trabalhos analisaram os perfis de expressão proteica de extratos totais destes helmintos e/ou de seus produtos de excreção/secreção. Estas análises descritivas são importantes para se conhecer as proteínas que viabilizam a sobrevivência e a proliferação dos parasitos, contribuindo para o entendimento da fisiologia destes organismos e a detecção de suas proteínas imunogênicas (Yatsuda *et al.*, 2003; Bakker *et al.*, 2004 ; Craig *et al.*, 2006).

5.2.1. Eletroforese bidimensional e cromatografia líquida

Estudos proteômicos normalmente envolvem a análise de misturas complexas de proteínas. Para reduzir a complexidade, as amostras devem ser fracionadas, permitindo a identificação eficiente de seus constituintes. Durante muitos anos, a eletroforese bidimensional foi a técnica mais utilizada para fracionar misturas proteicas (Righetti, 2009). Como descrita originalmente (O'Farrell, 1975), consistia na separação de proteínas com base em duas propriedades físico-químicas independentes: ponto isoelétrico e volume/massa molecular. Inicialmente, o gradiente de pH era estabelecido por anfólitos carreadores de diferentes pKs misturados a géis de poliacrilamida cilíndricos. Esta técnica sofreu modificações e tornou-se mais reprodutiva com a introdução do gradiente imobilizado de pH (IPG) estabelecido por anfólitos copolimerizados no gel de poliacrilamida (*Immobilines*™) (Bjellqvist *et al.*, 1982).

Na primeira etapa da técnica, também denominada primeira dimensão, a amostra aplicada em uma fita de gel contendo o gradiente imobilizado de pH é submetida a um campo elétrico (Rabilloud *et al.*, 2010). As proteínas carregadas migram horizontalmente no gel até atingirem o pH em que sua carga líquida é zero (pI ou ponto isoelétrico). Esta técnica é conhecida como focalização isoelétrica (do inglês IEF - *Isoelectric Focusing*). Posteriormente, a fita da primeira dimensão é submetida à eletroforese tradicional em gel de poliacrilamida (segunda dimensão) na presença de SDS (SDS-PAGE), de forma a permitir uma segunda separação das proteínas de acordo com seus volumes moleculares. Após coloração apropriada (ex.: Coomassie blue, nitrato de prata), as cadeias polipeptídicas fracionadas no gel são visualizadas na

forma de manchas (*spots*). Elas podem ser excisadas do gel, tripsinizadas e submetidas à identificação por espectrometria de massas (Görg *et al.*, 2004).

A eletroforese bidimensional é um método de separação eficiente porque permite o fracionamento simultâneo de centenas de proteínas de uma amostra complexa, fornecendo informações úteis sobre ponto isoelétrico, massa molecular, abundância relativa e modificações pós-traducionais, verificadas pela alteração da mobilidade eletroforética. Possibilita também a comparação quantitativa dos mapas bidimensionais gerados, permitindo a identificação de proteínas diferencialmente expressas. Entretanto, como qualquer técnica analítica, apresenta limitações, dentre as quais destacamos: método trabalhoso, difícil de automatizar, com sensibilidade limitada e pouco eficiente para fracionar proteínas de baixa solubilidade ou com extremos de pH e massa molecular (Gorg *et al.*, 2009).

Nos últimos anos, a cromatografia líquida vem sendo cada vez mais utilizada como técnica de fracionamento em substituição à eletroforese bidimensional. Atualmente, é considerada o estado da arte em metodologias proteômicas (Fröhlich & Arnold, 2006; Zhang *et al.*, 2010). Nesta abordagem *gel free* (também conhecida como *shotgun proteomics*), as proteínas são inicialmente digeridas (geralmente com tripsina) e o fracionamento posterior é centrado na separação de peptídeos. No caso de amostras mais complexas (ex.: extratos celulares, plasma), são utilizadas pelo menos duas separações cromatográficas em sequência, normalmente uma coluna de troca iônica seguida de uma fase reversa hifenada diretamente com o espectrômetro de massas (Link *et al.*, 1999), técnica originalmente conhecida como MudPiT (*Multidimensional Protein Identification Technology*) (Washburn *et al.*, 2001).

Além de ser facilmente automatizada, a proteômica *gel free* permite a detecção de componentes menos abundantes e com propriedades físico-químicas extremas. Por outro lado, trabalhar com peptídeos ao invés de proteínas aumenta muito a complexidade da amostra. Muitas vezes, no caso da identificação apenas de peptídeos não-proteotípicos (característicos de várias proteínas), só é possível determinar a família a qual a proteína pertence, sem definir exatamente sua identidade individual. A estimativa do número de isoformas presentes também é mais difícil através da abordagem centrada em peptídeos, assim como a visualização de processamentos proteolíticos das

proteínas (Nesvizhskii & Aebersold, 2005). A lista final de proteínas na amostra pode ser inferida a partir do conjunto de peptídeos identificados (Nesvizhskii & Aebersold, 2005).

5.2.2. Espectrometria de massas

Para identificar os componentes proteicos fracionados como descrito acima, emprega-se a espectrometria de massas, uma ferramenta analítica capaz de determinar as massas moleculares de peptídeos e proteínas na forma ionizada (íons moleculares). Quando submetidos à ação de campos elétricos e/ou magnéticos, diferentes íons moleculares podem ser separados porque assumem comportamentos (ex.: trajetória espacial, velocidade e/ou direção) que dependem diretamente da razão entre sua massa e sua carga (*m/z)* (Canas *et al.*, 2006). Esta ferramenta permite a determinação da massa de peptídeos, assim como a identificação de sua estrutura primária, sua quantificação e a caracterização de modificações pós-traducionais. O espectrômetro de massas é um instrumento constituído dos seguintes componentes: fonte de ionização (onde o analito é ionizado e dessorvido/transferido para a fase gasosa), analisador de massas (onde ocorre a determinação da m/z do analito) e detector de íons (sistema que detecta a presença do analito) (Lane, 2005).

Dois tipos principais de fonte de ionização são utilizadas na análise de proteínas e peptídeos: ionização por eletrospray (*ESI - Electrospray Ionization*) e ionização por desorção a laser auxiliada por matriz (*MALDI - Matrix Assisted Laser Desorption Ionization).* Geralmente, estas fontes podem ser combinadas com um ou mais analisadores, permitindo a construção de equipamentos de alto desempenho. Os principais tipos de analisadores utilizados em proteômica são: quadrupolo (Q), armadilha de íons (*íon traps* tridimensionais ou lineares), tempo de vôo (TOF - *Time of Flight*), orbitrap e ressonância ciclotrônica de íons com transformada de Fourier (FT-ICR) (Yates, 2004).

Em equipamentos híbridos, como o MALDI-TOF/TOF e o ESI-LTQ-Orbitrap utilizados nesta tese, é possível determinar a massa (MS ou MS1) de vários peptídeos simultaneamente. Em seguida, pode-se selecionar um precursor de uma determinada m/z e induzir sua fragmentação (MS/MS ou MS2) (Steen & Mann, 2004). O método de fragmentação mais utilizado em

proteômica é a dissociação induzida por colisão (CID – *Collision-Induced Dissociation*) entre o peptídeo e moléculas de um gás inerte, geralmente hélio. A energia liberada nas colisões é convertida em energia interna, que promove migração intramolecular de prótons, desestabilizando diferentes ligações químicas. Como consequência, pode haver a formação de dois conjuntos de íons-fragmento: a) os que retêm a carga residual (próton) no lado N-terminal (fragmentos das séries a, b, c, dependendo da ligação que é fragmentada); e b) os que retêm a carga residual na região C-terminal (fragmentos das séries x, y, z, dependendo da ligação que é fragmentada) (Aebersold & Goodlett, 2001).

Ainda que possa ocorrer em vários locais, a fragmentação é preferencial nas ligações peptídicas (são as ligações de menor energia), gerando fundamentalmente íons das séries b e y. Picos adjacentes de cada uma destas séries diferem entre si pela massa de um resíduo de aminoácido, tornando teoricamente possível a determinação da sequência do peptídeo por *de novo sequencing*. Entretanto, na prática, este método de interpretação de espectros de fragmentação pode bastante trabalhoso e difícil. Desta forma, na maior parte das vezes, a identificação da proteína é feita baseando-se na comparação com bancos de dados (*Peptide Fragment Fingerprinting* ou *Database Search Method*) (Forner *et al.*, 2007). Para isto, utilizam-se algoritmos de busca (ex.: Mascot, Sequest) capazes de comparar os espectros MS/MS obtidos experimentalmente com espectros MS/MS teóricos. Estes últimos são gerados após a digestão *in silico* de sequências de proteína depositadas em bancos de dados (ex.: NCBI, UniProt) e a fragmentação teórica de seus peptídeos (Yates *et al.*, 2009).

II. Justificativa e Objetivos

Estudos sobre o *Angiostrongylus costaricensis* e a angiostrongilíase abdominal são escassos, restringindo-se, em sua maioria, a relatos epidemiológicos e de complicações da doença, descrição de métodos não-invasivos de diagnóstico humano, tratamento experimental da infecção murina e/ou caracterização de hospedeiros intermediários e definitivos. A dificuldade de diagnóstico e o desconhecimento sobre o parasito e a doença contribuem para sua ampla distribuição nas Américas.

Utilizando técnicas modernas de microscopia e bioquímica, este trabalho pretendeu contribuir para o avanço do conhecimento biológico sobre o *Angiostrongylus costaricensis*. Nosso objetivo geral foi detalhar a morfologia e o perfil de expressão proteica das diferentes fases evolutivas deste nematoide parasita do homem. Os dados obtidos estão apresentados na forma de três artigos científicos, além de duas seções de resultados complementares. Nossos objetivos específicos nestes trabalhos foram:

Artigo 1: Avaliar a morfologia do parasito em suas diferentes fases evolutivas (vermes adultos, L1 e L3) utilizando microscopia eletrônica de varredura (MEV) e microscopia de luz;

Resultados complementares 1: Analisar as estruturas internas do parasito em suas diferentes fases evolutivas (vermes adultos, L1 e L3) utilizando microscopia confocal de varredura a laser (MCVL) e microscopia de luz de cortes histológicos;

Artigo 2: a) Analisar os perfis de expressão proteica de vermes adultos (machos e fêmeas) utilizando eletroforese bidimensional e espectrometria de massas; b) através de *immunoblotting* com soros de camundongos infectados, identificar proteínas imunorreativas de vermes adultos que possam ser candidatas a biomarcadores;

Artigo 3: Caracterizar o conteúdo de proteases dos extratos das diferentes fases evolutivas (vermes adultos, L1 e L3) utilizando substratos proteicos;

Resultados complementares 2: a) Caracterizar o conteúdo de proteases dos extratos das diferentes fases evolutivas (vermes adultos, L1 e L3) utilizando substratos sintéticos fluorogênicos; b) Purificar a(s) serino-protease(s) presente(s) no extrato de L1 por cromatografia de afinidade em coluna de benzamidina.

III. Metodologia e Resultados

Artigo 1

Morphological aspects of Angiostrongylus costaricensis by light and scanning microscopy (a submeter à revista Acta Tropica)

Morphological aspects of *Angiostrongylus costaricensis* by light and scanning electron microscopy

Karina M Rebello[1,2], Rubem Menna-Barreto[3], Vanessa Moutinho[4], Ester Mota[2], Jonas Perales[1], Ana Gisele da Costa Neves-Ferreira[1], Aleksandra Menezes[5*],Henrique Lenzi[2†]

[1]Laboratório de Toxinologia, Instituto Oswaldo Cruz, Fiocruz, Av. Brasil 4365, Manguinhos, 21040-900 Rio de Janeiro, RJ, Brazil

[2]Laboratório de Patologia, Instituto Oswaldo Cruz, Fiocruz, Av. Brasil 4365, Manguinhos, 21040-900 Rio de Janeiro, RJ, Brazil

[3]Laboratório de Biologia Celular, Instituto Oswaldo Cruz, Fiocruz, Av. Brasil 4365, Manguinhos, 21040-900 Rio de Janeiro, RJ, Brazil

[4]Laboratório de Biologia de Helmintos Otto Wucherer, Instituto de Biofísica Carlos Chagas Filho, Universidade Federal do Rio de Janeiro, Av. Carlos Chagas Filho, s/n Bloco G, 40296-710, Rio de Janeiro, Brazil

[5]Grupo de Sistemática e Biologia Evolutiva (GSE), Pólo Barreto, Universidade Federal do Rio de Janeiro - Campus Macaé - Avenida São José do Barreto, 764 - São José do Barreto - Macaé - Rio de Janeiro CEP: 27910-970, Brazil

†*in memoriam*

[*] corresponding author (alek@macae.ufrj.br)

Abstract

Angiostrongylus costaricensis is a parasitic nematode that can cause severe gastrointestinal disease in humans, known as abdominal angiostrongiliasis. This paper presents a new description of first and third larvae and male and female adult worms of *Angiostrongylus costaricensis* by scanning electron and light microscopy. The morphological data were compatible with the previous descriptions of *A. costaricensis*. However, several novel anatomical structures were described by scanning electron microscopy, such as details of the cuticular striations of the spicules in male worms and a protective flap of cuticle covering the vulvar aperture. Other taxonomic features were also visualized by light microscopy, including the gubernaculum and the esophageal-intestinal valve. The use of two microscopy techniques allowed a detailed analysis of the morphology and ultrastructure of this nematode. Some taxonomic features were redescribed, and others, such as the correct number of papillae distributed around the oral opening and the papillae behind the cloacal opening, were documented for the first time by SEM, thus permitting clarification of the taxonomy of this nematode.

Keywords: *Angiostrongylus costaricensis*, morphology, SEM, light microscopy

1. Introduction

Angiostrongylus costaricensis is an intestinal parasitic nematode that causes abdominal angiostrongyliasis (AA), a widespread and poorly studied human disease of Latin America. This nematode has been reported in several Brazilian states including Minas Gerais (Rocha et al., 1991), Espírito Santo (Pena et al., 1995), Distrito Federal (Barbosa et al., 1980; de Magalhaes et al., 1982), São Paulo (Iabuki and Montenegro, 1979; Ziliotto et al., 1975), Santa Catarina, Paraná and Rio Grande do Sul (Agostini et al., 1984; Ayala, 1987). In Brazil, the highest number of recorded cases has been reported in the South region of the country, which is considered endemic for the disease (Agostini et al., 1983; Graeff-Teixeira et al., 1991).

The life cycle of *A. costaricensisis* is characterized as heteroxenic and requires two hosts: a vertebrate (the definitive hosts are rodents) and an invertebrate (the intermediate hosts are slugs and terrestrial mollusks). The first stage larvae (L1) are expelled in the feces. These larvae can penetrate mollusks through oral (Morera, 1973) or percutaneous infection (Mendonca et al., 1999), where they become infective after two moltings (L1 to L2 to L3). The third stage larvae (L3) are expelled along with the mucus secretion of the mollusks (Morera and Céspedes, 1971; Thiengo, 1996). When rodents ingest mollusks, food, or water contaminated with L3, the infective larvae penetrate the intestinal wall. Humans can acquire the infection by the ingestion of fruits, vegetables, raw food, or water contaminated with infective larvae. The larvae then migrate through the blood and the lymphatic vessels to the heart and enter the arterial circulation to reach the mesenteric arteries. There, the L3 grow to maturity and become adults. Eggs are deposited in the mesenteric arteries and are carried through the blood to the capillaries in the intestinal wall, where they develop into larvae (L1). Ultimately they reach the intestinal lumen and are expelled in feces.

The details of the morphology of *A. costaricensis* adult worms and the larval stages have previously been described (Morera, 1973). Redescription by light microscopy (Ishih et al., 1990; Thiengo et al., 1997) revealed details of the external surface architecture of the different *Angiostrongylus costaricensis* developmental stages. In the present work, we use light and scanning electron microscopy (SEM) to contribute to the descriptions of novel morphological features to the characterization of the parasite.

2. Material and Methods

2.1 Parasites

A. costaricensis at different developmental stages was maintained at the Pathology Laboratory of Instituto Oswaldo Cruz (FIOCRUZ) through successive passages in slugs (*Biomphalaria glabrata*) and rodents (*Sigmodon hispidus*). Adult worms were recovered by dissection of the mesenteric arteries of rats following 40 days of infection and were segregated by gender. First-stage larvae (L1) were obtained from the feces of infected rodents and were passed through a discontinuous Percoll gradient (Graeff-Teixeira et al., 1999) to separate fresh L1 from small debris and bacteria. Third-stage larvae (L3) were collected from mollusks previously infected with L1.

2.2 Ethics

All procedures with animals were approved by the Animal Ethics Committee at Fiocruz (CEUA license # P0246/05) and conducted in accordance with the International Guiding Principles for Biomedical Research Involving Animals, as issued by the Council for the International Organizations of Medical Sciences.

2.3 Preparation for scanning electron microscopy and light microscopy

For scanning electron microscopy, the parasites were fixed in hot AFA (2% glacial acetic acid, 3% formaldehyde, and 95% ethanol) or 2.5% glutaraldehyde in 0.1 M sodium cacodylate buffer (pH 7.2) at room temperature for 1 hour. Samples were post-fixed with 1% OsO_4, 0.8% potassium ferricyanide and 2.5 mM $CaCl_2$ added to the same buffer for 1 h at 25°C. The parasites were dehydrated in an ascending acetone series, dried by the critical point method with CO_2, mounted on aluminum stubs coated with a 20 nm thick gold layer, and examined with a Jeol JSM6390LV scanning electron microscope (Tokyo, Japan).

In addition, some adult worms were fixed in Milloning's solution and stained with Carmin chloride. Fresh specimens and fixed samples were also analyzed by light microscopy using a Zeiss Axio Observer Z1 (Oberkochen, Germany).

3. Results

3.1 Larval stages

First stage larvae have a cylindrical body form (Fig 1a) and are covered by a transversely striated cuticle (Fig 1d). At the anterior end, we observed a triangular oral opening surrounded by six cephalic papillae (Fig 1b). Broad and lateral double alae extended nearly the entire larval body length, from slightly posterior to the cephalic extremity, and terminated before the tail (Fig 1c, 1d). An excretory opening was located at the ventral side of the body (Fig 1c). The posterior end was ventrally curved and slender, and the tail ends were sharply pointed (Fig 1f). The anus was located at the ventral surface near the tip of tail (Fig 1e).

Third-stage larvae were slightly bigger in diameter than L1. The body shape was similar, but the tails were conical (Fig 2c, 2d), and the lateral alae were thicker and shorter (Fig 2c, 2e, 2f). The six L3 cephalic papillae were more widely separated than the cephalic papillae of L1 (Figs 2a, 2b). The excretory pore (not shown) and the anus were observed on the ventral surface, with the latter adjacent to the tip of tail (Fig 2e).

3.2 Adult worms

Males and females had distinct sexual dimorphisms, but both had elongated and slender bodies. The anterior end of both sexes was round with a circular oral opening and three lips around the mouth surrounded by six sensory papillae (Figs 3a, 3b, 4h). Two amphidial pores were also located on each side of the oral aperture (Figs 3b, 4h). The oral aperture was directly connected to the claviform-shaped esophagus (Fig 5a). At the esophageal-intestinal junction, we observed cylindrical valves (Fig 5b). Furthermore, an excretory pore was observed on the ventral surface near the anterior end (data not shown). The cuticle along the body was transversally striated, and longitudinal lateral alae were absent (Fig 3a).

The female reproductive system was tubular and consisted of two ovaries, each of which connected to an oviduct and a uterus (Fig 5h). The two uteri joined to form the vagina, which opened to the exterior by a cuticle-covered vulva (Figs 3c, 5e). The eggs were transparent, ovoid, thin-shelled, and had granular contents when fertilized (Fig 5c). The posterior end was ventrally bent, roughly conical, and had a terminal projection (Figs 3c, 3d, 3f).

The male reproductive system was a single tube differentiated into two testes (Fig 5i), which lied at the free end of a convoluted or recurved tube. This tube led into the seminal vesicle and vas deferens and terminated in the muscular ejaculatory duct that emptied into the cloaca (Fig 4a). Behind the cloacal opening, there were three papillae (Fig 4c, 4d). A pair of copulatory spicules protruded through the cloacal opening (Fig 4f). The two spicules were slender, striated, had sharply pointed distal ends, and were not projected (Fig 4g). The muscular movements and the body contractions exposed the spicules (Fig 4f). The sperm were small and round in shape (Fig 5d). The posterior end of the male *A. costaricensis* worms contained a copulatory bursa (Figs 4a, 4c, 4e-4g, 5f). The bursa was supported by finger-like structures, referred to as rays, associated with the muscle tissue. This nematode had two pairs of dorsal bursal rays and two pairs of ventral bursal rays (Fig 4b).

4. Discussion

The taxonomic position of the *Angiostrongylus* genus is predominantly based on morphological characteristics, such as rays of the copulatory bursa, host group specificity, and the sites where the adult worms reside within the host. Drozdz (1970) had separated the *Angiostrongylus* genus into two subgroups based on the morphological characteristics of the caudal bursa. It was further subdivided into two subgenera – *Angiostrongylus* and *Parastrongylus* – based on the morphology of the lateral rays of the caudal bursa. *Angiostrongylus* has a ventrolateral ray that arises independently from the mediolateral and posterolateral rays, which emerge as a single trunk.

Scanning electron microscopy of the different developmental stages of *A. costaricensis* revealed details of several structures of taxonomic importance. Ishih et al., (1990) described six cephalic papillae, each lying in two rows around the oral opening

of adult worms. As proposed by using light microscopy, in the present study it was shown that there were only six sensory papillae placed around the mouth and two amphidial pores (Thiengo et al., 1997). We observed that *A. costaricensis* has a mouth that opens into a buccal capsule, whereas food moves into the esophagus. The buccal capsule is cylindrical and lacks a bulb at its posterior end unlike most other nematodes. The esophagus is connected to the intestine via an esophageal-intestinal valve, a muscular structure usually referred to as the cardia. These structures can have varied functions, such as regulating the rate or direction of food intake to the intestine, providing secretory material for extra- or intra-corporeal digestion, or possibly for lubrication, as previously described in others nematodes, including *Ostertagia bison* (Hoberg et al., 2008; Lichtenfels and Pilitt, 1991) and *Pseudomarshallagia enlongata* (Hoberg et al., 2010).

Our SEM results revealed a flap structure that closes the vulvar aperture, a cuticular outgrowth that occurs at the female genital opening and is similar to the cementum found in other nematodes. The function of the flap is to ensure fertilization (Chitwood and Chitwood, 1974). Among plant or insect parasites, vulvar flaps have primarily been described in *Tylenchida* and *Aphelenchida* (Nickle, 1970), and among animal parasites they have been described in *Ostertagiinae* (Durette-Desset et al., 1999; Hoberg and Lichtenfels, 1994). To date, vulvar flaps had not previously been observed in *Angiostrongylus* species.

The position, number, and morphological characteristics of the rays of the copulatory bursa are important taxonomic parameters for identifying *Angiostrongylus* species. Our results by light microscopy are in agreement with previously published data (Morera and Cespedes, 1971). The copulatory bursa was slightly asymmetric and well developed. The dorsal ray was short and bifurcated into arms that terminated in

sharp tips. On the ventral side behind the bifurcation, there was a conspicuous papilla. The lateral rays emerged from a common trunk and were widely separated from the ventral rays. The mediolateral and posterolateral rays were fused at the proximal half. The anterolateral ray was thicker and separated from the common trunk immediately after its emergence from the trunk. The externodorsal ray arose adjacent to the lateral trunk and was well separated from the dorsal ray. Its distal end was knoblike. The ventral rays were fused except at the tips and the ventrolateral ray was slightly longer than the ventrolateral ray (Maldonado Jr et al., 2012).

Using light microscopy, previous reports described three papillae behind the cloacal opening (Morera and Céspedes, 1971; Thiengo et al., 1997). For the first time, we report these structures by scanning electron microscopy. The gubernaculum is a sclerotized accessory piece of the male reproductive system. Male specimens of *Angiostrongylus* spp. display two branches that come together just prior to termination in the cloaca, and their function is to guide spicules during the copula. The presence of the gubernaculum was previously observed in males of *A. costaricensis* (Morera and Cespedes, 1971; Thiengo et al., 1997), and we clearly confirm this by micrography.

In the present work, *A. costaricensis* spicules were shown to be slender and similar in size to what has been previously described (Morera and Cespedes, 1971; Thiengo et al., 1997), and we confirm by scanning electron microscopy the striated nature of the spicules. Additionally, we provide a novel hypothesis as to how the spicules are projected during copula. The spicules are associated with muscle, which is attached to the body wall of the worms. The contraction of these muscles should causes the spicules to extrude from the body, and when the muscles relax they pull the spicules within the body.

The use of both light microscopy and SEM allowed for a detailed analysis of the morphology and ultrastructure of this nematode. Some taxonomic features were redescribed, but the accurate number of papillae distributed around the oral opening and the papillae behind the cloacal opening were documented for the first time by SEM. The observation of esophageal valves by light microscopy provides a novel and important detail for morphological characterization of this species.

Acknowledgments

This research was supported by Brazilian financial support from the Conselho Nacional de Desenvolvimento Científico e Tecnológico (PAPES V), the Coordenação de Aperfeiçoamento de Pessoal de Nível Superior (CAPES), the Conselho Nacional de Desenvolvimento Científico e Tecnológico (CNPq), and the Fundação Carlos Chagas Filho de Amparo a Pesquisa do Estado do Rio de Janeiro (FAPERJ). We are very thankful to the Plataforma de Microscopia Eletrônica (IOC/FIOCRUZ), where all scanning electron microscopy micrographs were obtained. We are also grateful to Heloisa M. N. Diniz for processing the figures. Karina M Rebello received funding from CAPES for her PhD fellowship.

References

Agostini, A.A., Marcolan, A.M., Lisot, J.M., Lisot, J.U., 1984. Abdominal angiostrongyliasis. Anatomo-pathological study of 4 cases observed in Rio Grande do Sul, Brazil. Mem Inst Oswaldo Cruz 79, 443-445.

Agostini, A.A., Peixoto, A., Caleffi, A.L., Dexhaimer, A., Camargo, R.R., 1983. Angiostrongilíase abdominal: três casos observados no Rio Grande do Sul. Rev Assoc Med Rio Grande do Sul 27, 200-203.

Ayala, M.A., 1987. Abdominal angiostrongyloidiasis. 6 cases observed in Parana and in Santa Catarina, Brazil. Mem Inst Oswaldo Cruz 82, 29-36.

Barbosa, H., Raick, A.N., Magalhaes, A.V., Otero, P.M., 1980. [Abdominal angiostrongylosis]. AMB Rev Assoc Med Bras 26, 178-180.

Chitwood, B.G., Chitwood, M.B., 1974. Introduction to Nematology, Baltimore, Maryland.

de Magalhaes, A.V., de Andrade, G.E., Koh, I.H., Soares Mdo, C., Alves, E., Tubino, P., dos Santos Fde, A., Raick, A.N., 1982. [A new case of abdominal angiostrongyliasis]. Rev. Inst. Med. Trop. Sao Paulo 24, 252-256.

Drozdz, J., 1970. Revision of the classification of the genus Angiostrongylus Kamensky 1905 (Nematoda: Metastrongyloidea). Ann. Parasitol. Hum. Comp. 45, 597-603.

Durette-Desset, M.C., Hugot, J.P., Darlu, P., Chabaud, A.G., 1999. A cladistic analysis of the Trichostrongyloidea (Nematoda). Int. J. Parasitol. 29, 1065-1086.

Graeff-Teixeira, C., Camillo-Coura, L., Lenzi, H.L., 1991. Clinical and epidemiological aspects of abdominal angiostrongyliasis in southern Brazil. Rev Inst Med Trop São Paulo. 33, 373-378.

263 Graeff-Teixeira, C., Geiger, S., Walderich, B., Hoffmann, W., Abrahams, E., Schulz-
264 Key, H., 1999. Isolation of *Angiostrongylus costaricensis* first-stage larvae from rodent
265 feces on a Percoll gradient. J. Parasitol. 85, 1170-1171.
266 Hoberg, E.P., Abrams, A., Ezenwa, V.O., 2008. An exploration of diversity among the
267 Ostertagiinae (Nematoda: Trichostrongyloidea) in ungulates from Sub-Saharan Africa
268 with a proposal for a new genus. J. Parasitol. 94, 230-251.
269 Hoberg, E.P., Kumsa, B., Pilitt, P.A., Abrams, A., 2010. Synlophe structure in
270 *Pseudomarshallagia elongata* (Nematoda: Trichostrongyloidea), abomasal parasites
271 among Ethiopian ungulates, with consideration of other morphological attributes and
272 differentiation within the Ostertagiinae. J. Parasitol. 96, 401-411.
273 Hoberg, E.P., Lichtenfels, J.R., 1994. Phylogenetic systematic analysis of the
274 Trichostrongylidae (Nematoda), with an initial assessment of coevolution and
275 biogeography. J. Parasitol. 80, 976-996.
276 Iabuki, K., Montenegro, M.R., 1979. Appendicitis caused by Angiostrongylus
277 costaricensis. Presentation of a case. Rev. Inst. Med. Trop. Sao Paulo 21, 33-36.
278 Ishih, A., Rodriguez, B.O., Sano, M., 1990. Scanning electron microscopic observations
279 of first and third-stage larvae and adults of *Angiostrongylus costaricensis*. Southeast
280 Asian J. Trop. Med. Public Health 21, 568-573.
281 Lichtenfels, J.R., Pilitt, P.A., 1991. A redescription of *Ostertagia bisonis* (Nematoda:
282 Trichostrongyloidea) and a key to species of Ostertagiinae with a tapering lateral
283 synlophe from domestic ruminants in North America. J. Helminthol. Soc. W. 58, 231-
284 244.
285 Maldonado Jr, A., Simões, R., Thiengo, S., 2012. Angiostrongyliasis in the Americas,
286 Zoonosis, pp. 303-320.

Mendonca, C.L., Carvalho, O.S., Mota, E.M., Pelajo-Machado, M., Caputo, L.F., Lenzi, H.L., 1999. Penetration sites and migratory routes of *Angiostrongylus costaricensis* in the experimental intermediate host (*Sarasinula marginata*). Mem Inst Oswaldo Cruz 94, 549-556.

Morera, P., 1973. Life history and redescription of *Angiostrongylus costaricensis* Morera and Céspedes, 1971. Am J Trop Med Hyg. 22, 613-621.

Morera, P., Cespedes, R., 1971. Angiostrongilosis abdominal. Uma nueva parasitosis humana. Acta Med Costarric. 14, 173-189.

Morera, P., Céspedes, R., 1971. *Angiostrongylus costaricensis* n. sp. (Nematoda: Metastrongyloidea), a new lungworm occuring in man in Costa Rica. Rev Biol Trop. 18, 173-185.

Nickle, W.R., 1970. A taxonomic review of the genera of the aphelenchoidea (fuchs, 1937) thorne, 1949 (Nematoda: Tylenchida). J Nematol 2, 375-392.

Pena, G.P., Andrade Filho, J., de Assis, S.C., 1995. *Angiostrongylus costaricensis*: first record of its occurrence in the State of Espírito Santo, Brazil, and a review of its geographic distribution. Rev. Inst. Med. Trop. São Paulo 37, 369-374.

Rocha, A., Sobrinho, J.M., Salomao, E.C., 1991. [Abdominal angiostrongyliasis. The first indigenous case reported in Minas Gerais]. Rev Soc Bras Med Trop 24, 265-268.

Thiengo, S., 1996. Mode of infection of *Sarasinula marginata* (Mollusca) with larvae of *Angiostrongylus costaricensis* (Nematoda). Mem Inst Oswaldo Cruz 91, 277-278.

Thiengo, S.C., Vicente, J.J., Pinto, R.M., 1997. Redescription of *Angiostrongylus (Paranstrongylus) costaricensis* Morera & Céspedes (nematoda: metastrongyloidea) from brazilian strain. Rev Bras Zool 14, 839 - 844.

310 Ziliotto, A., Jr., Kunzle, J.E., Fernandes, L.A., Prates-Campos, J.C., Britto-Costa, R.,
311 1975. Angiostrongyliasis: report of a probable case. Rev. Inst. Med. Trop. Sao Paulo 17,
312 312-318.

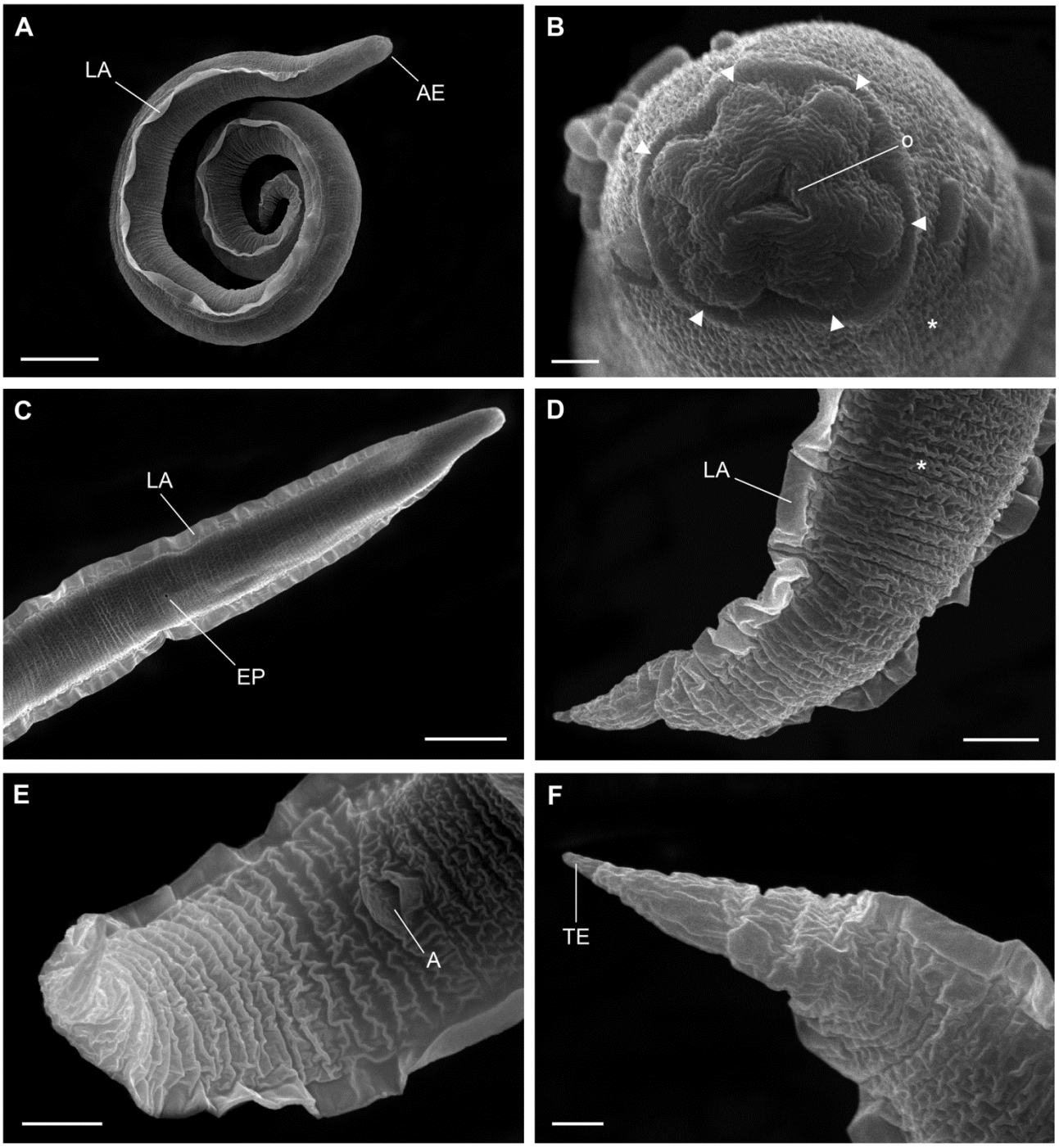

Fig. 1: Micrographs of the first-larval stage of *A. costaricensis*. **(A)** Whole body of L1, showing the anterior extremity (A) and the lateral alae (L). Scale bar = 10µm; **(B)** Details of anterior extremity showing the six cephalic papillae (arrowhead) around the oral opening (O). Scale bar = 1µm; **(C)** Ventral view of the larvae showing the excretory pore (E) and the lateral alae (L) on both sides. Scale bar = 10µm; **(D)** Details of the posterior end showing the transversal striations (*) and the notch (N) at the beginning of the tail (T). Scale bar = 2µm; **(E)** Ventral view of the posterior end showing the anus (A). Scale bar = 2µm (A); **(F)** Details of the extremity of the tail (T). Scale bar = 1µm.

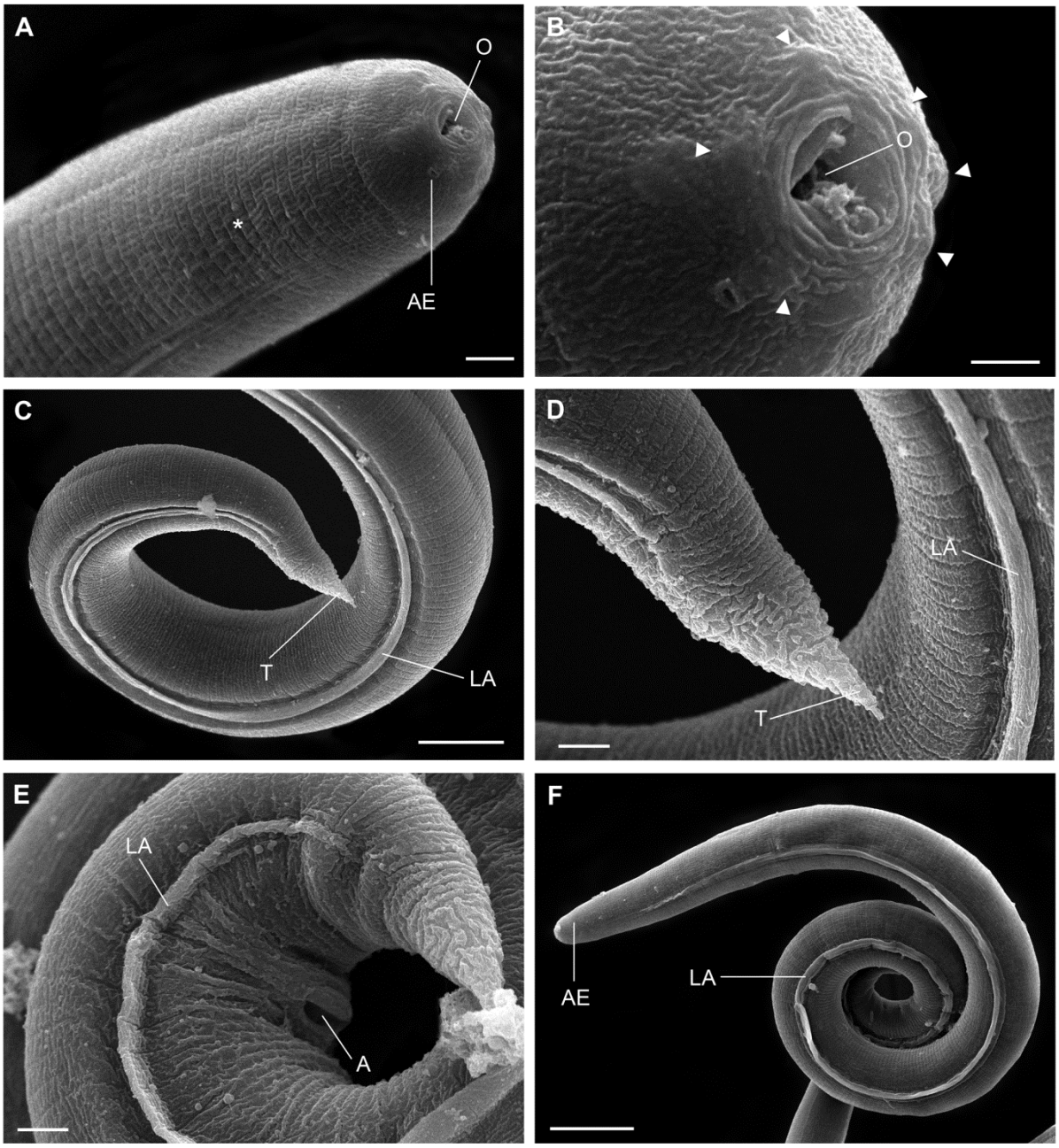

Fig. 2: Micrographs of the third-larval stage of *A. costaricensis.* **(A)** Lateral view of the anterior portion with transversal striations (*) and the anterior extremity (A) with the oral opening (O). Scale bar = 2µm; **(B)** Details of the anterior extremity showing six cephalic papillae surrounding the oral opening (arrowhead). Scale bar = 1µm; **(C)** Posterior portion showing the lateral alae (L) and the tail (T). Scale bar = 10µm; **(D)** Details of the posterior end, showing the tail end (T). Scale bar = 2µm; **(E)** Posterior end showing the anus (A) next to the tail. Scale bar = 2µm; **(F)** Whole body of L3, showing the anterior extremity (A) and the lateral alae (L). Scale bar = 20µm

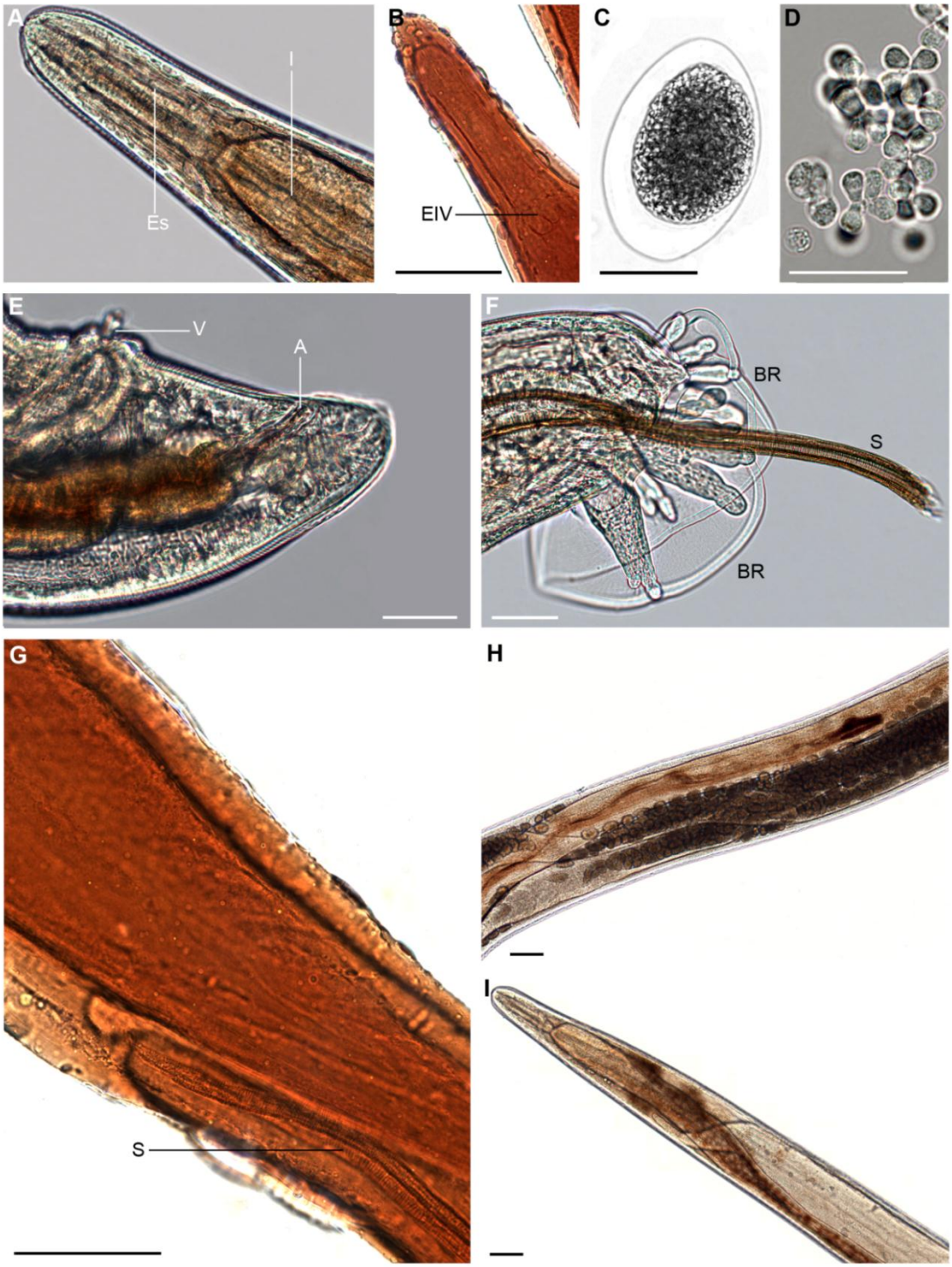

Fig. 3: Light microscopy of *Angiostrongylus costaricensis*. **(A)** Anterior portion showing the esophagus (Es) and intestine (I) of adult worms; **(B)** Anterior portion showing the esophageal-intestinal valves (EIV) between the esophagus and the intestine of the adult worms; **(C)** Fertilized egg with the shell; **(D)** Sperm; **(E)** Lateral view of the posterior portion of the female adult worm showing the vulva with the flap (V) and the anus (A); **(F)** Male posterior end with the copulatory bursa with the bursal rays (BR) and a visible spicule (S); **(G)** Male posterior portion showing the gubernaculum (arrowhead) and the beginning of the spicules (S); **(H)** Lateral view of the female showing the two tubular ovaries spiraling around the intestine; **(I)** Anterior portion of male adult worm showing the intestine and the beginning of the testicles (Scale bar 500 µm)

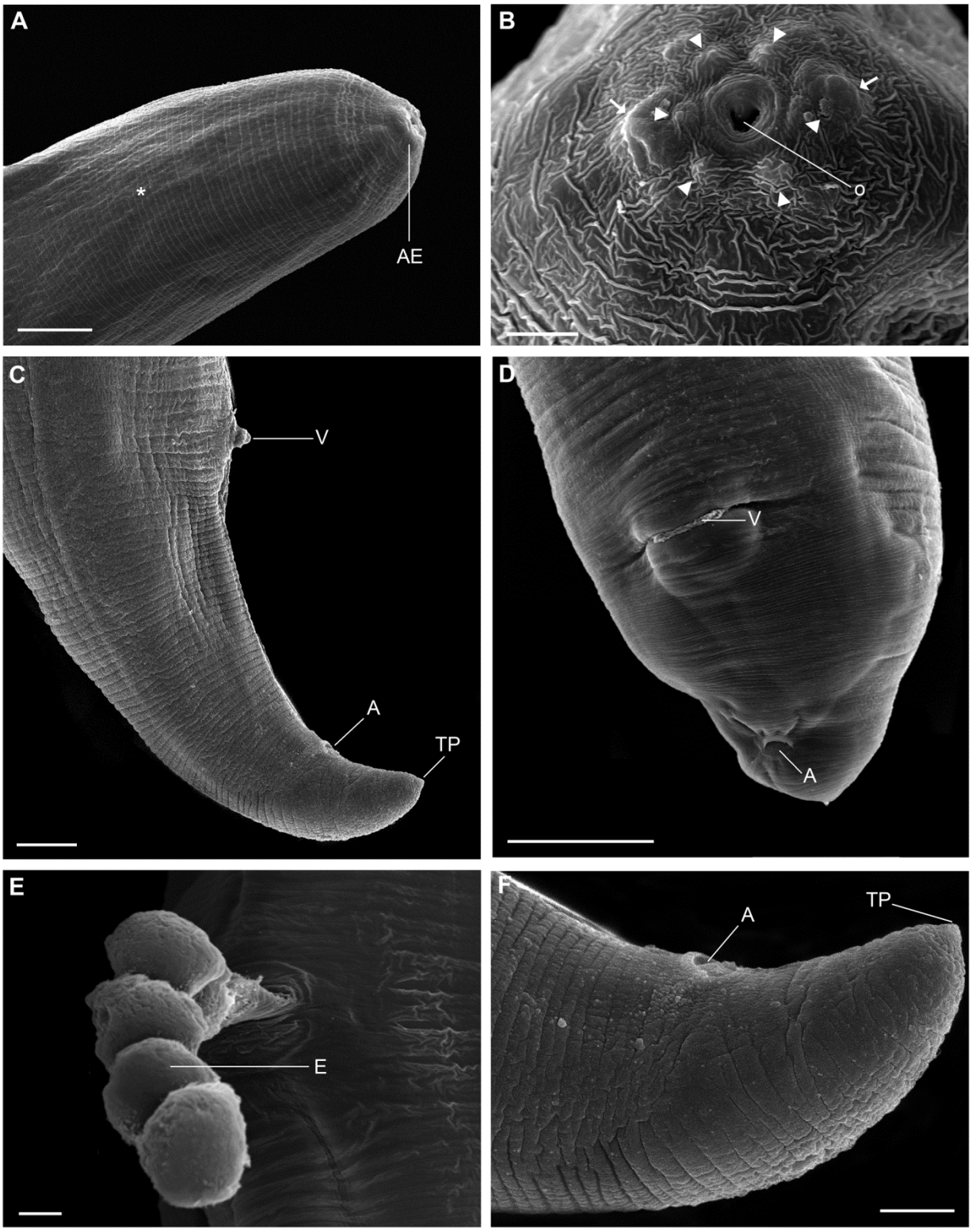

Fig. 4: Micrographs of the adult female *A. costaricensis*. **(A)** Anterior portion showing the anterior extremity (A) and the cuticle with transversal striations (*). Scale bar = 20µm; **(B)** Anterior extremity showing six cephalic papillae (arrowhead) and two amphidial pores (arrow) surrounding the oral opening (O). Scale bar = 2µm; **(C)** Lateral view showing the vulva (V), anus (A) and a projection at the end of the tail (T). Scale bar = 20µm; **(D)** Ventral view of the posterior portion showing the vulva (V) and the anus (A). Scale bar = 50µm; **(E)** Vulva opening with eggs (E). Scale bar = 10µm; **(F)** Lateral view of the female worm showing the anus (A) and details of the projection at the end of the tail (TP). Scale bar = 10µm.

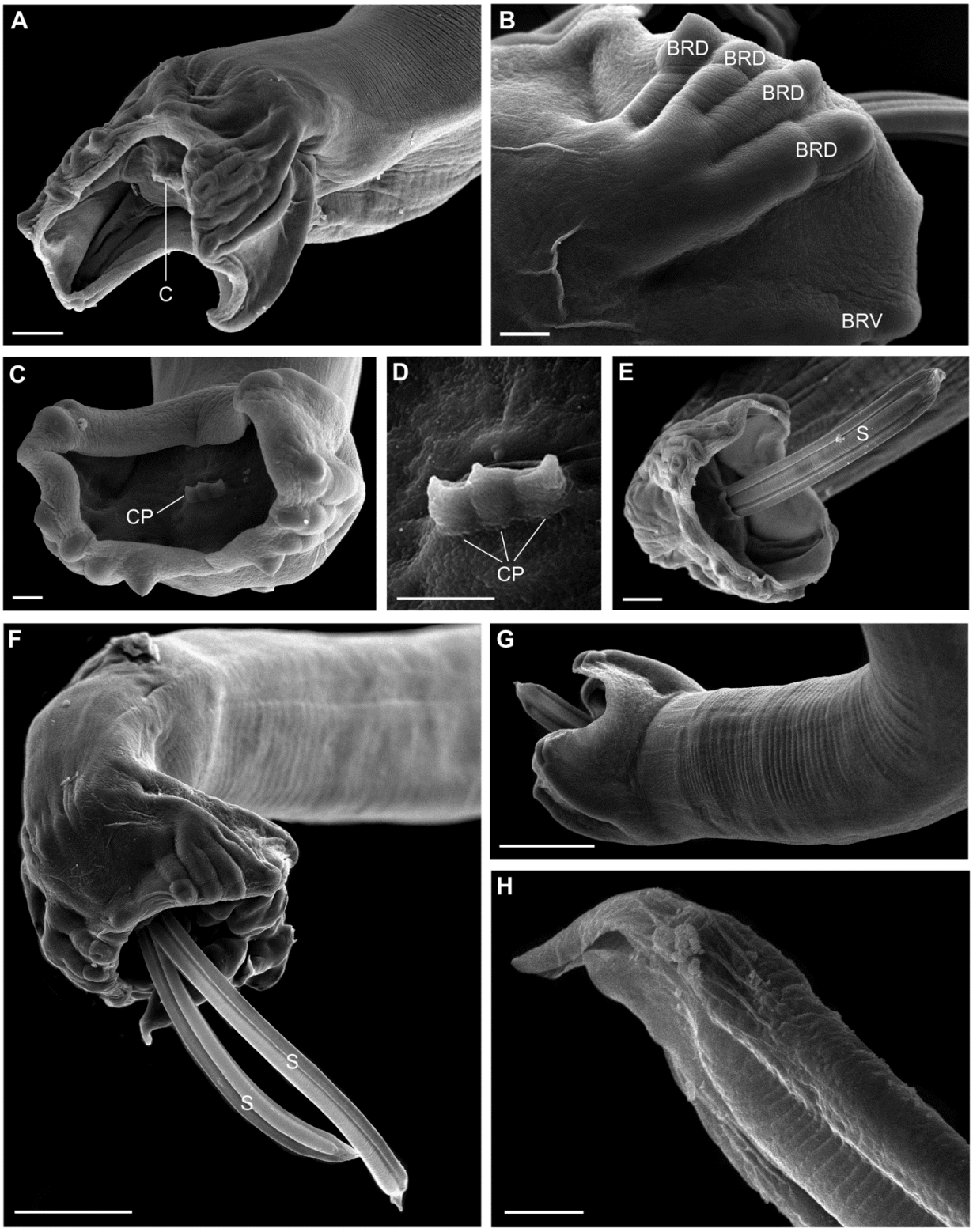

Fig. 5: Micrographs of the adult male *A. costaricensis*. **(A)** Posterior portion with the copulatory bursa surrounding the cloaca (C). Scale bar = 20µm; **(B)** Details of the copulatory bursa of the dorsal (BDR) and ventral (BVR) bursal rays. Scale bar = 10µm; **(C)** Copulatory bursa showing the three cloacal pappilae (CP). Scale bar = 10µm; **(D)** Details of the cloacal opening with three papillae (CP). Scale bar = 5µm; **(E)** Copulatory bursa showing projection of one of the spicules (S). Scale bar = 20µm; **(F)** Copulatory bursa with the projection of two spicules (S). Scale bar = 50µm; **(G)** Details of the spicule with a striated flange and a pointed end. Scale bar = 5µm; **(H)** Anterior extremity showing six cephalic papillae (arrowhead) and two amphidial pores (arrow) surrounding the oral opening (O). Scale bar = 5µm.

Resultados complementares 1

Análise das estruturas internas do parasito em suas diferentes fases evolutivas (vermes adultos, L1 e L3) utilizando microscopia confocal de varredura a laser (MCVL) e microscopia de luz de cortes histológicos.

A. Metodologia

Obtenção das diferentes fases de desenvolvimento do parasita

As larvas (L1) foram obtidas a partir de fezes de *Sigmodon hispidus* com mais de 30 dias de infecção. As larvas (L3) foram coletadas de caramujos da espécie *Biomphalaria glabrata* com 30 dias de infecção. Os vermes adultos (machos e fêmeas) foram coletados de roedores da espécie *S. hispidus* com 40 dias de infecção. Para maiores detalhes, consultar a metodologia descrita no Artigo 3.

Análise histológica

Amostras de L1, L3 e vermes adultos foram fixadas em formalina Millonig de Carson e incluídas em parafina. Os espécimes foram cortados na espessura de 5 µm, montados em lâminas de vidro, desparafinados e corados pelas técnicas de hematoxilina-eosina (H-E), Giemsa de Lennert, Reticulina de Gomori e *Sirius Red* (SR). As lâminas foram analisadas em microscópio de luz (Zeiss Axio Observer Z1).

Microscopia de luz

Amostras de vermes adultos (machos e fêmeas) frescas também foram analisadas em microscopio de luz (Zeiss Axio Observer Z1). Alguns espécimes de machos e fêmeas foram levados para a lupa de dissecção para retirada de espermatozoides e ovos, respectivamente.

Microscopia Confocal

As amostras das diferentes fases evolutivas foram fixadas em formalina Millonig de Carson e coradas com Carmim clorídrico *overnight.* As lâminas

foram montadas com goma de Damar e observadas em micorscopio confocal (Carl Zeiss LSM 510 META) equipado com laser HeNe 543nm e filtro 560.

B. Resultados

Análise histológica

Nas lâminas de vermes adultos, observarmos o sistema digestivo e a presença de sangue no interior do intestino (Figura 2). Visualizamos ainda, cortes transversais de fêmeas mostrando ovário com ovos maduros em seu interior (Figura 3a). Observamos também que o ovário apresenta um aspecto cordonal (Figura 3b), o intestino com epitélio ciliado (Figura 4a), útero repleto de ovos maduros (Figuras 4a, 4b) e ovos encapsulados no interior do útero (Figura 4c). Nos cortes histológicos de machos adultos, observamos o interior dos testículos, que também apresentam aspecto cordonal (Figura 8a). Na porção anterior do testículo observamos a presença de espermátides (Figura 8b). Além disso, visualizamos o interior da bolsa copuladora repleta de espermatozoides (Figura 9a), a abertura cloacal e as dois espículos com seus respectivos gubernáculos (Figura 9b). Nos cortes histológicos das formas larvares (L1 e L3) não foi possível definir nenhuma estrutura (Figuras 10c, 10d).

Microscopia de luz

Por esta técnica, observamos a morfologia dos ovos não-fecundados (Figuras 6a, 6b), que são arredondados e não apresentam casca, e fecundados (Figura 6c), que após a fecundação passam a apresentar uma fina casca. Os espermatozoides são arredondados e aflagelados (Figura 7). Analisamos os vermes adultos inteiros, onde observamos, na porção posterior da fêmea, o ânus e a vulva (Figura 5a) e no macho, a bolsa copuladora composta por seus raios bursais e, em seu interior, os espículos (Figura 5b).

Microscopia Confocal

Por esta técnica, pudemos observamos em L1, com clareza, apenas o início do trato digestivo da larva (Figura 10a), formado pelo esôfago e o ânus; em L3, observamos todo o trato digestivo e o aparelho reprodutor (Figura 10b).

Nos vermes adultos, visualizamos o intestino, o esôfago e a junção esôfago-intestinal (Figura 11c). Nas fêmeas, registramos a entrada de espermatozoides na vulva (Figuras 11a, 11b). Observamos ainda a porção posterior do macho, mostrando a bolsa copuladora (Figura 12a) e o interior do testículo repleto de espermatozoides (Figura 12b).

Figuras – Resultados Complementares 1

1

Figura 2 Corte histológico longitudinal da região anterior de verme adulto de *A. costaricensis* mostrando o esôfago e o intestino, este último contendo sangue (Giemsa, barra 500 µm).

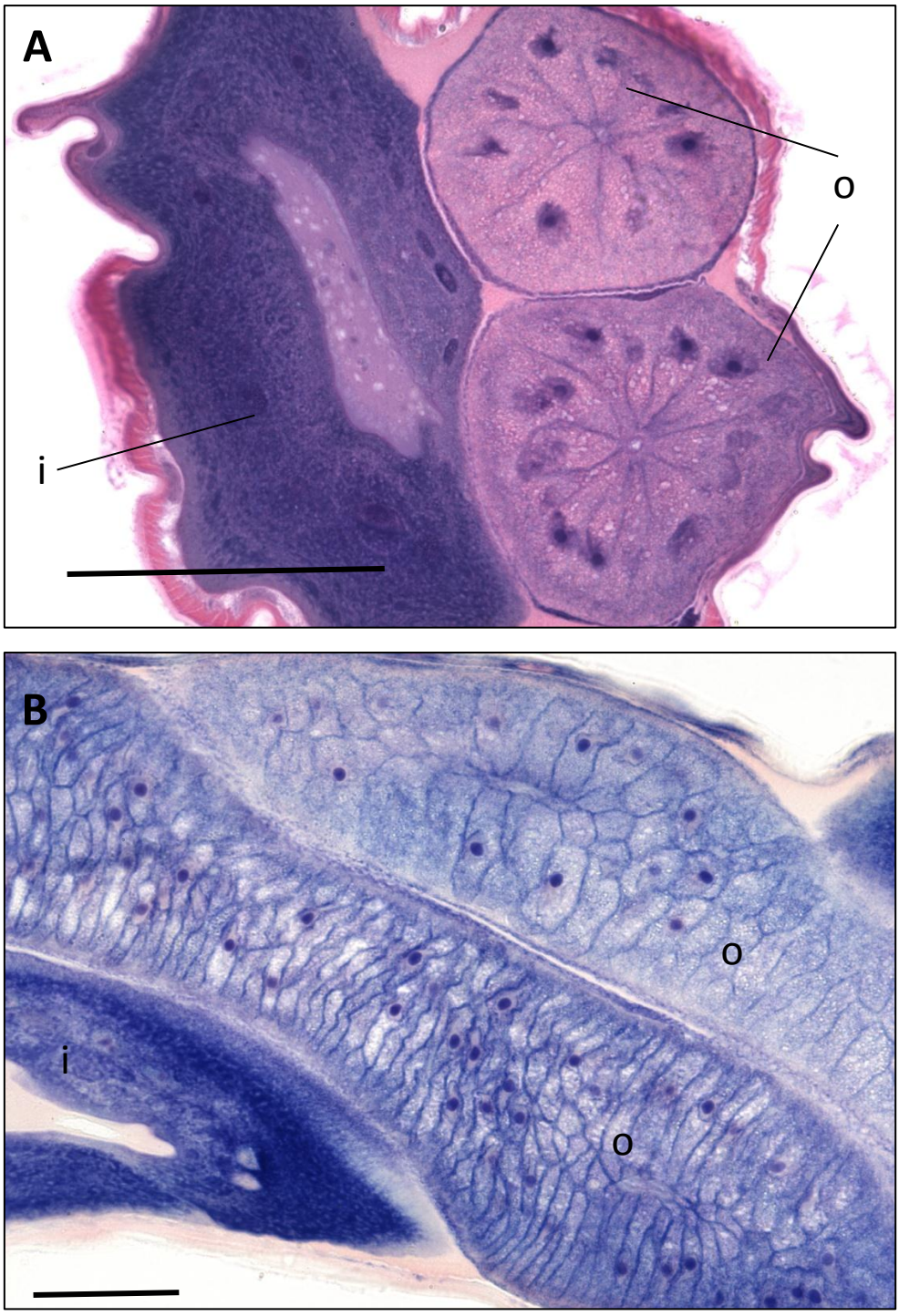

Figura 3: Corte histológico de fêmea adulta. **(A)** Corte transversal de *A. costaricensis* mostrando dois ovários (o) contendo ovos maduros e o intestino (i) (HE, barra 500 µm); **(B)** Corte longitudinal mostrando dois ovários (o) e o intestino (i) (Giemsa, barra 500 µm).

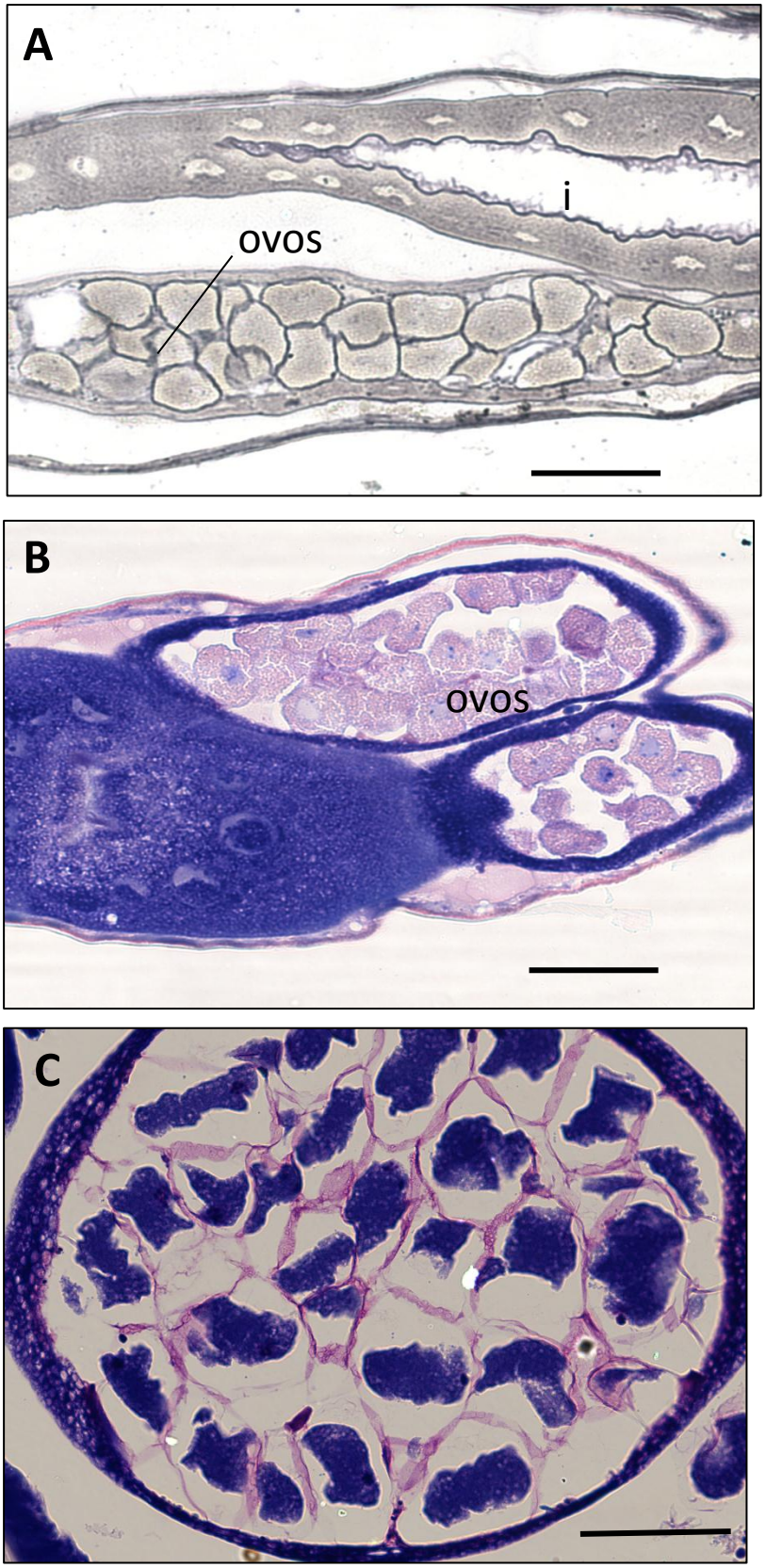

Figura 4: Fêmea adulta de *A. costaricensis*. **(A)** Útero repleto de ovos maduros e o intestino (i) com epitélio ciliado (Reticulina, barra 500 µm); **(B)** corte lateral evidenciando o intestino (i) e o útero contendo ovos (Giemsa, barra 500 µm); **(C)** Corte lateral mostrando ovos fertilizados contendo casca no interior do útero (Giemsa, barra 500 µm).

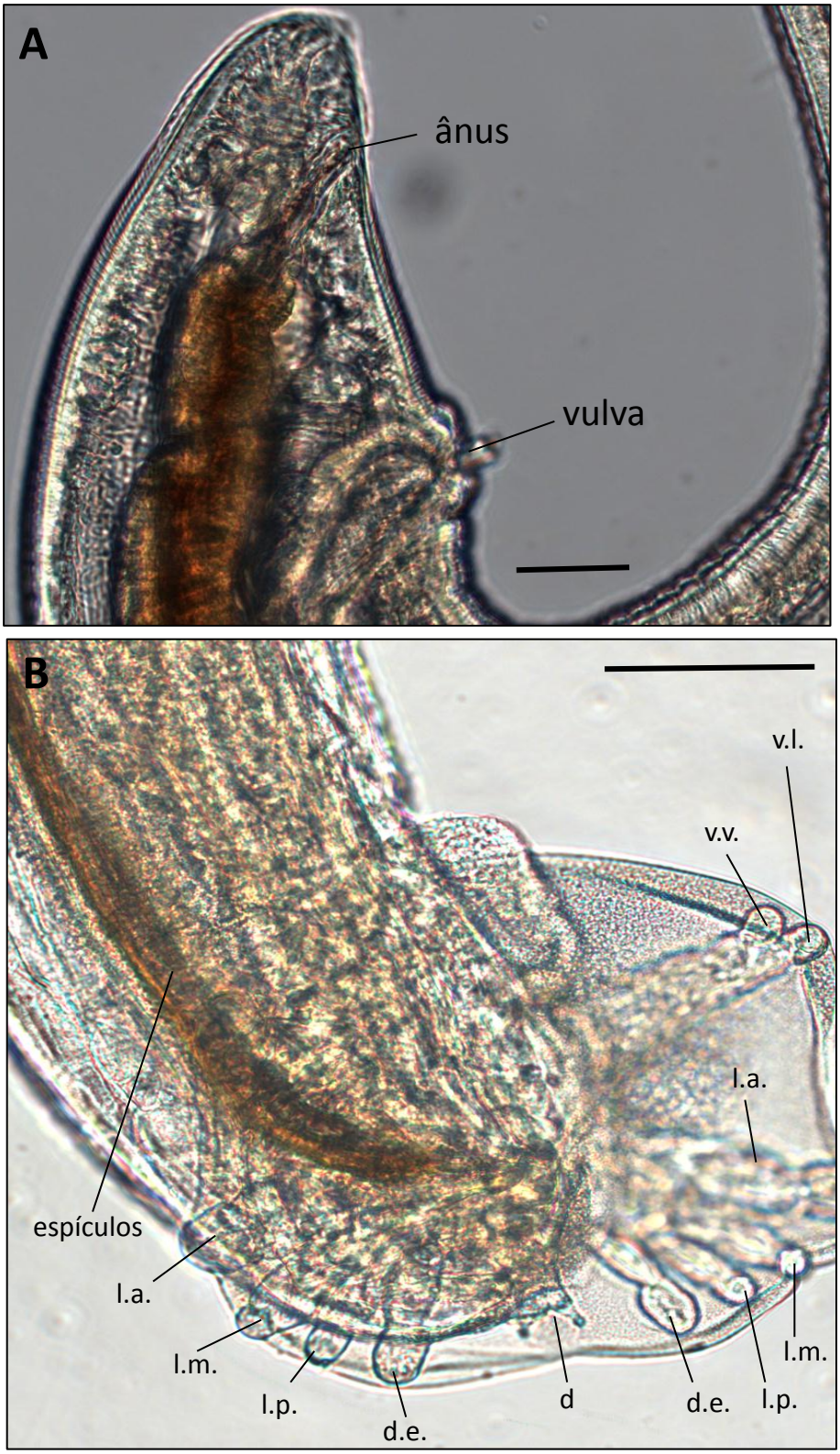

Figura 5: Vermes adultos de *A. costaricensis.* Fêmea (A) e Macho (B) (barra 500 µm). **(A)** Foto de uma fêmea mostrando vulva e ânus; **(B)** Foto de um macho evidenciando a bolsa copuladora formada por raios bursais (v.v.- ventro ventral, v.l.- ventro lateral, l.a.- lateral anterior, l.p.- lateral posterior, d.e.- dorsal externo, d – dorsal) e dois espículos em seu interior.

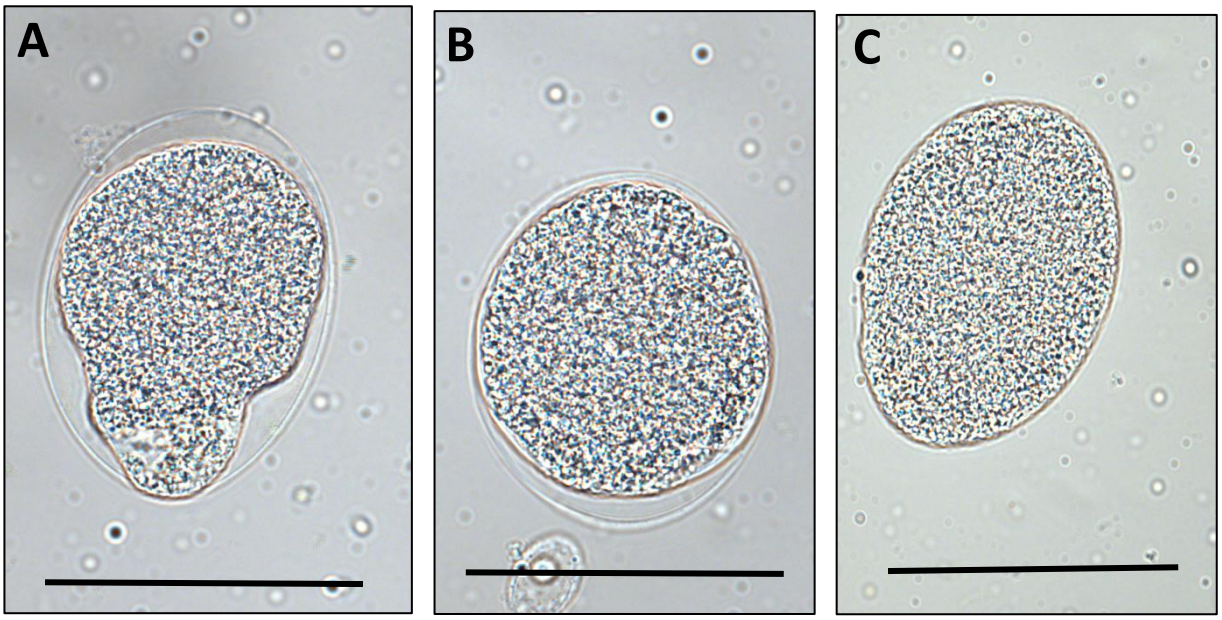

Figura 6: Fotos de campo claro de ovos (barra 500 µm). **(A)** e **(B)** ovos fertilizados contendo casca; **(C)** ovo não fertilizado

Figura 7: Foto de campo claro de espermatozoides (barra 500 µm)

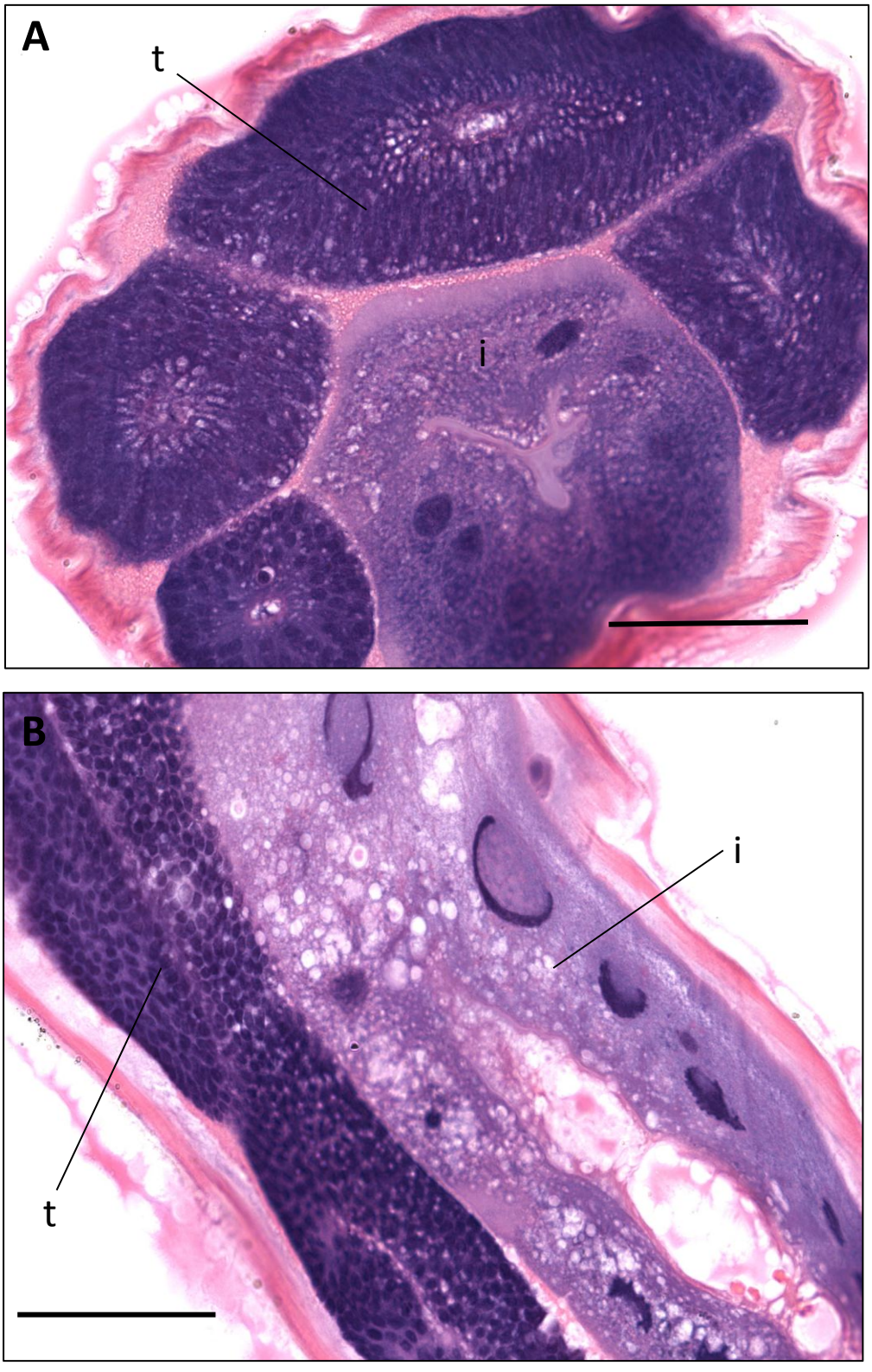

Figura 8: Cortes histológicos de macho adulto **(A)** Corte transversal mostrando o testículo (t) e o intestino (i) (HE, barra 500 µm); **(B)** Corte longitudinal mostrando a porção anterior do testículo (t) contendo espermátides e o intestino (i) (HE, barra 500 µm)

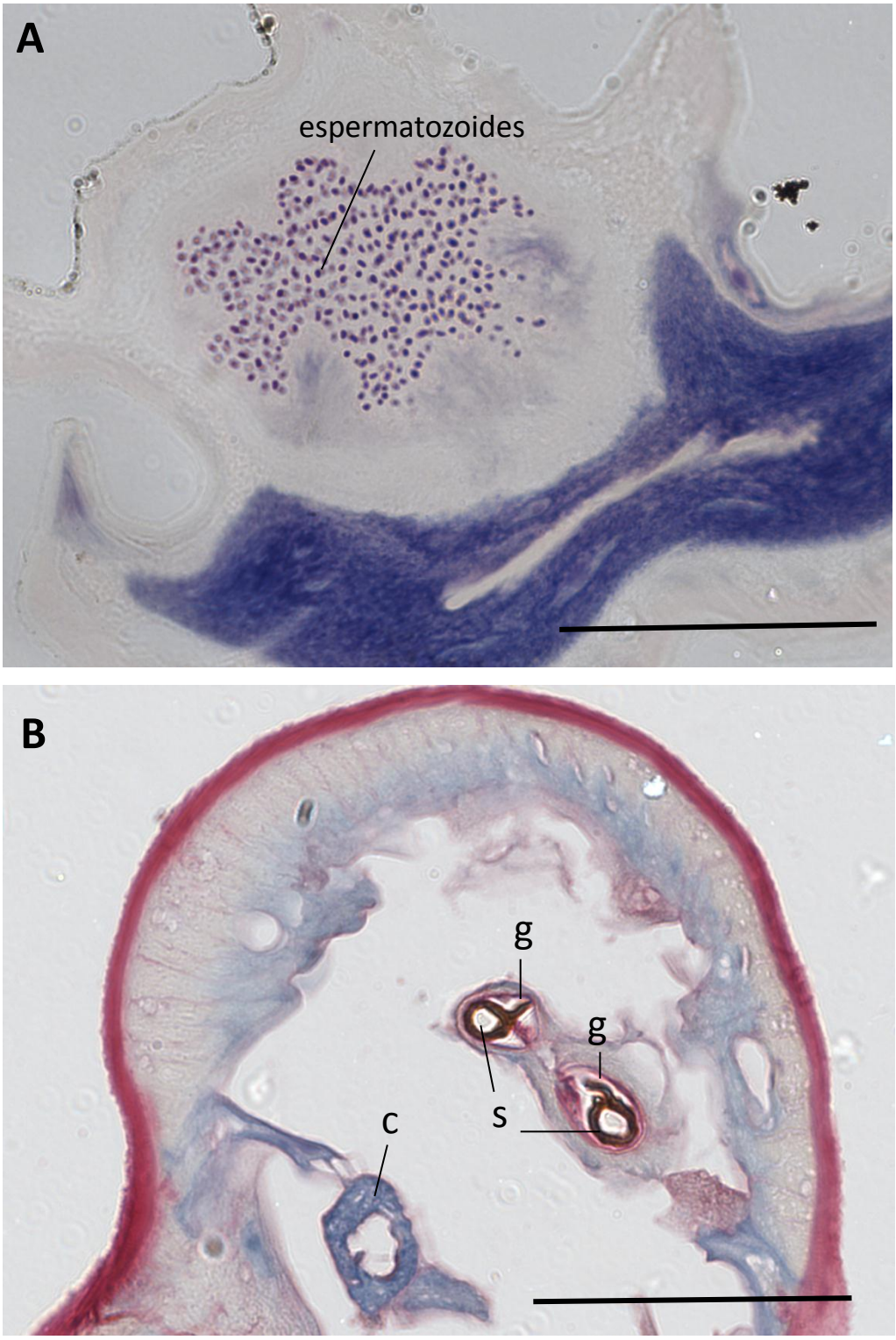

Figura 9: Cortes histológicos da porção posterior de machos adultos. **(A)** bolsa copuladora repleta de espermatozoides (Giemsa, barra 500 µm); **(B)** evidenciação das espículos, gubernáculo (g) e da cloaca (c) (SR, barra 500 µm).

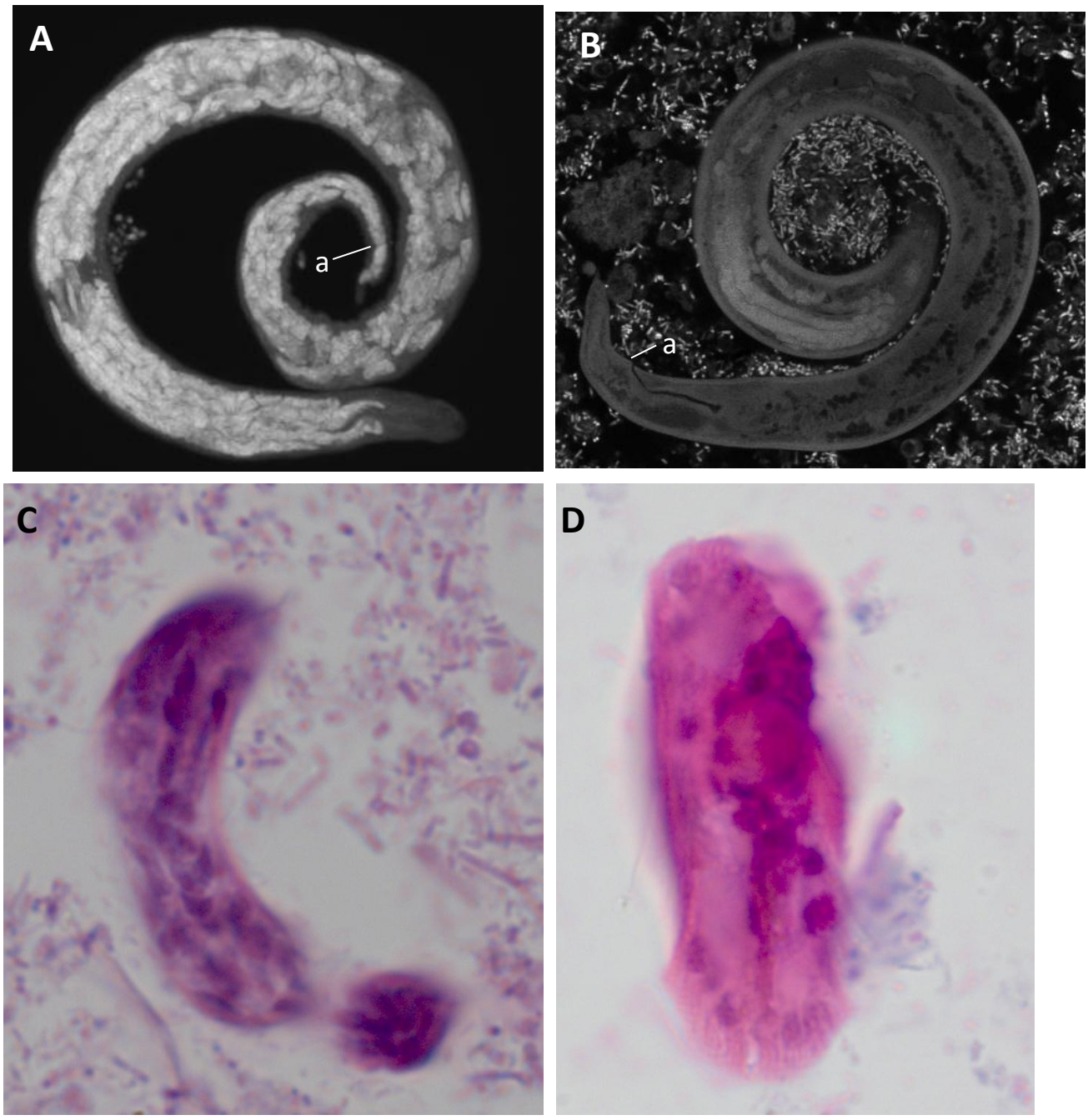

Figura 10: **(A)** / **(C)** Larvas de primeiro estágio (L1); **(B)** / **(D)** Larvas de terceiro estágio (L3). **(A)** Reconstrução tridimensional de L1 evidenciando o interior da larva repleto de grânulos onde só é possível indicar a localização do ânus; **(B)** Corte tomográfico de L3 evidenciando um interior mais diferenciado, onde podemos observar claramente o intestino e os ovários tubulares, além da abertura anal; **(C)** corte histológico de L1; **(D)** corte histológico de L3.

Figura 11: Porção posterior da fêmea adulta recém fecundada. **(A)** corte tomográfico mostrando a vulva (v) e o canal uterino repleto de espermatoizes (e) e o útero com ovos (o) fecundados; **(B)** ampliação da entrada da vulva mostrando os espermatozoides (e) em seu interior; **(C)** junção esôfago-intestinal (j) do verme adulto.

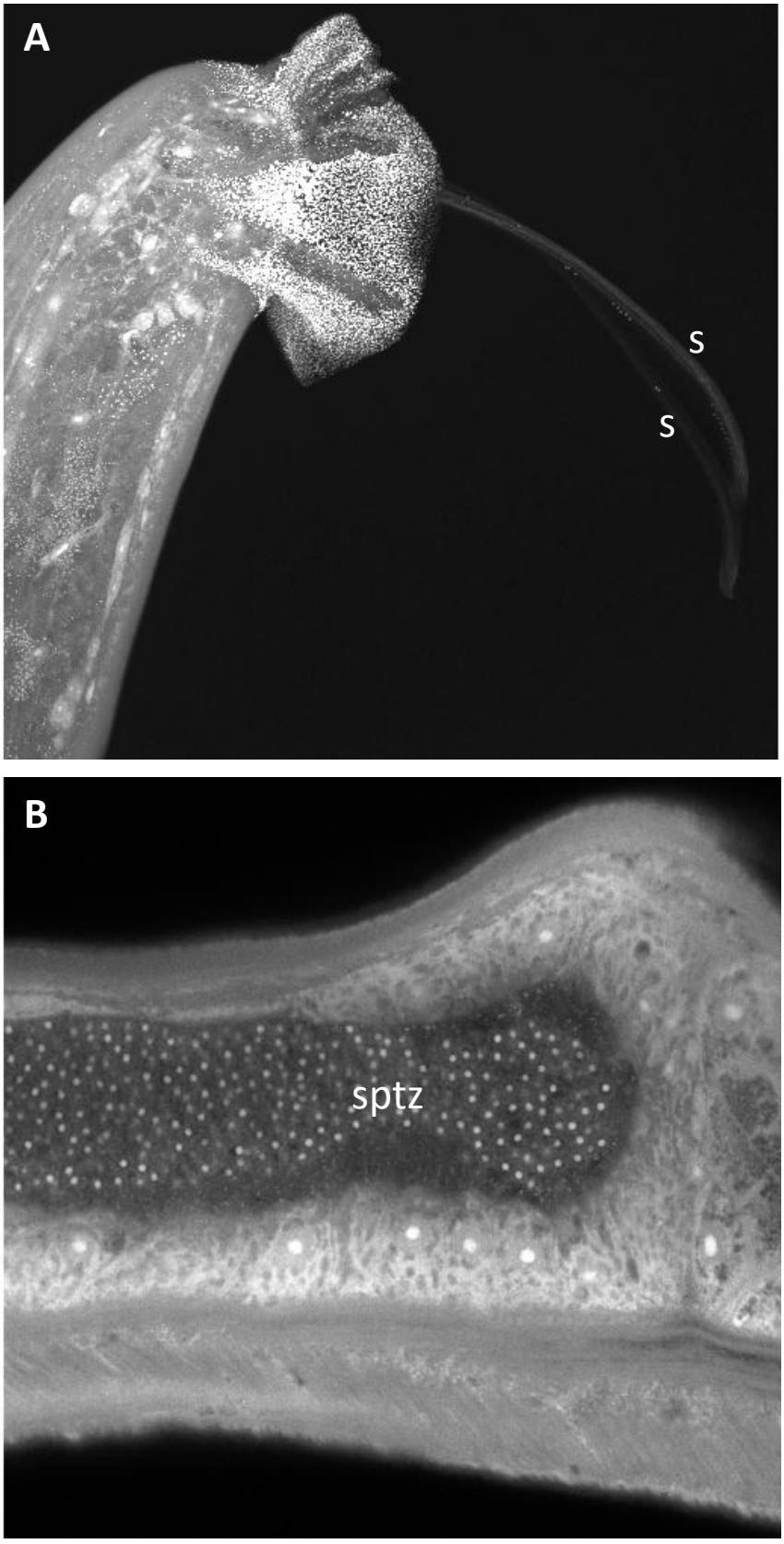

Figura 12: Machos adultos. **(A)** Reconstrução tridimensional da porção posterior mostrando a bolsa copuladora e as espículos projetadas (s); **(B)** Reconstrução tridimensional; em detalhe, o testículo repleto de espermatozoides (sptz).

Artigo 2

Comprehensive proteomic profiling of adult Angiostrongylus costaricensis, a human parasitic nematode (publicado no *Journal of Proteomics* 74:1545-59 (2011)

JOURNAL OF PROTEOMICS 74 (2011) 1545–1559

available at www.sciencedirect.com

ScienceDirect

www.elsevier.com/locate/jprot

Comprehensive proteomic profiling of adult *Angiostrongylus costaricensis*, a human parasitic nematode

Karina M. Rebello[a,b,d], *Juliana S.L. Barros*[a,b], *Ester M. Mota*[b], *Paulo C. Carvalho*[a,c,d], *Jonas Perales*[a,d], *Henrique L. Lenzi*[b], *Ana G.C. Neves-Ferreira*[a,d,*]

[a]*Toxinology Laboratory, Oswaldo Cruz Institute (IOC), Fiocruz, Rio de Janeiro, Brazil*
[b]*Pathology Laboratory, Oswaldo Cruz Institute (IOC), Fiocruz, Rio de Janeiro, Brazil*
[c]*Center for Technological Development in Health (CDTS), Fiocruz, Rio de Janeiro, Brazil*
[d]*Rio de Janeiro Proteomic Network, Brazil*

ARTICLE INFO

Available online 10 May 2011

Keywords:
Angiostrongylus costaricensis
Nematode
Proteome
Immunogenic proteins

ABSTRACT

Angiostrongylus costaricensis is a nematode helminth that causes an intestinal acute inflammatory process known as abdominal angiostrongyliasis, which is a poorly understood human disease occurring in Latin America. Our aim was to study the proteomic profiles of adult parasites focusing on immunogenic proteins. Total cellular extracts from both genders showed similar 2-DE profiles, with 60% of all protein spots focused between pH 5–7 and presenting molecular masses from 20.1 to 66 kDa. A total of 53 different dominant proteins were identified in our dataset and were mainly associated with the following over-represented Gene Ontology Biological Process terms: "macromolecule metabolic process", "developmental process", "response to stress", and "biological regulation". Female and male immunoblots showed similar patterns of reactive proteins. Immunoreactive spots identified by MALDI-PSD were found to represent heat shock proteins, a putative abnormal DAuer Formation family member, and galectins. To date, very few biochemical analyses have focused on the nematode *Angiostrongylus costaricensis*. As such, our results contribute to a better understanding of its biology and the mechanisms underlying the host–parasite relationship associated with this species. Moreover, our findings represent a first step in the search for candidate proteins for diagnostic assays and the treatment of this parasitic infection.

1. Introduction

There are 15 *Angiostrongylus* species, of which only two represent a public health concern related to causing abdominal angiostrongyliasis and eosinophilic meningoencephalitis in humans: *A. costaricensis* and *A. cantonensis*, respectively [1,2]. *A. cantonensis*, a rat lungworm, frequently occurs in outbreaks with case numbers ranging from tens to hundreds [3]. Cases have been detected throughout Southeast Asia, the South Pacific, Madagascar, Africa, the Caribbean, and the continents of Australia and North America [4,5]. Over 2827 cases of *A. cantonensis* meningitis have been reported in approximately 30 countries [3,4]. This species was recently also detected in Brazil [6,7]. Additionally, *A. costaricensis* produces abdominal angiostrongyliasis; its biological cycle was described by Morera (1973) [8] (Fig. 1). This disease was first described in Costa Rica [9]; other cases have been reported from the United States to northern Argentina [10]. Although this infection is enzootic in Texas [11], the only case of autochthonous human infection reported in the United States [12] was later identified

* *Corresponding author at:* Laboratório de Toxinologia, Pavilhão Ozório de Almeida, Instituto Oswaldo Cruz, Fiocruz. Av. Brasil, 4365 – Manguinhos, 21040–900 Rio de Janeiro, Brazil. Tel.: +55 21 2562 1381; fax: +55 21 2562 1410.
E-mail address: anag@ioc.fiocruz.br (A.G.C. Neves-Ferreira).

1874-3919/$ – see front matter © 2011 Elsevier B.V. All rights reserved.
doi:10.1016/j.jprot.2011.04.031

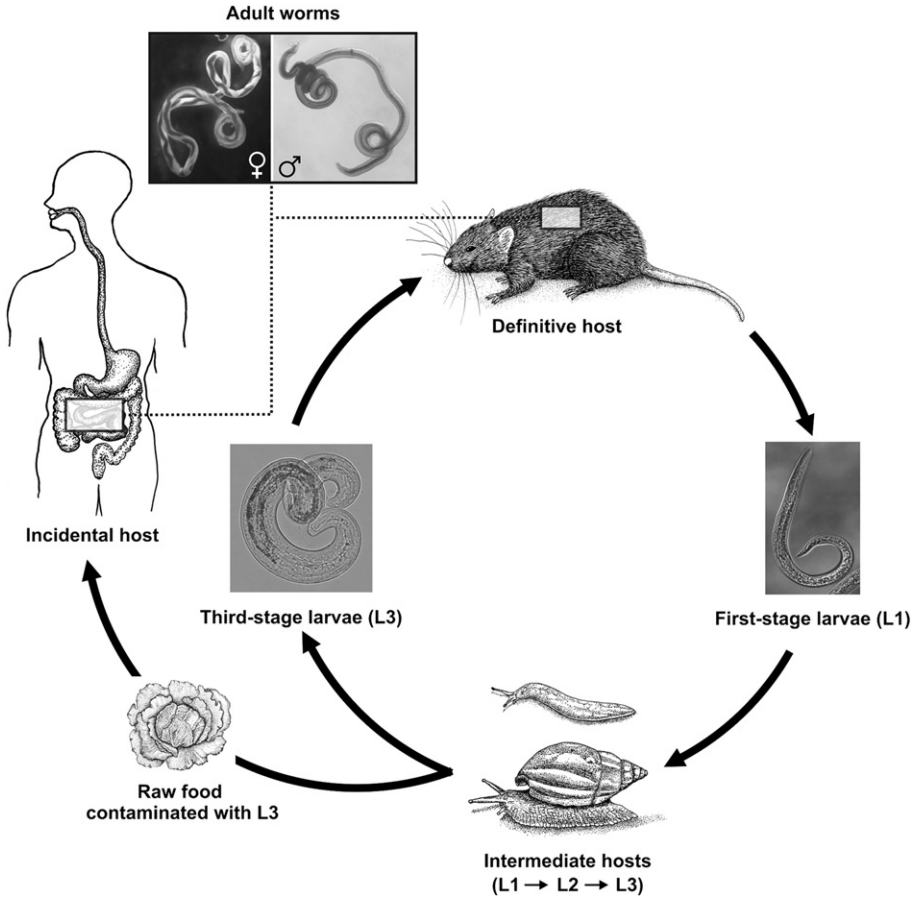

Fig. 1 – The biological life cycle of *Angiostrongylus costaricensis*. *A. costaricensis* is normally found in *Sigmodon hispidus*, *Rattus rattus* and other definitive hosts. The first stage larvae (L1) in the definitive hosts migrate into the intestinal lumen and are eliminated with the feces. Mollusks eat the contaminated feces or are externally infected via their epidermis, and second (L2) and third stage larvae (L3) develop in these hosts. The L3 are infectious to both definitive hosts and humans, who are incidental hosts. Infection with these parasites occurs through the ingestion of infected mollusks or unwashed vegetables contaminated with mucous of mollusks containing L3 *A. costaricensis* (see the Introduction for more details).

as a case of anisakiasis; however the authors replied maintaining the original diagnosis [13]. Even though abdominal angiostrongyliasis has been considered a public health problem in Costa Rica, its first reported outbreak occurred in Guatemala, where raw mint (eaten separately or as an ingredient in ceviche) was the likely vehicle of infection [14].

Several rodents are known to be definitive hosts of *A. costaricensis*, whereas its intermediate hosts are represented by mollusks of the *Veronicellidae* family [15]. More recently, it was shown that dogs can act as a reservoir host for *A. costaricensis* [16]. The parasite spreads to humans by means of the consumption of raw vegetables containing third-stage larvae (L3) developed in mollusks [17]. Currently, the explosive expansion of the giant snail *Achatina fulica* in many areas of Brazil has the potential to increase the transmission of *A. costaricensis* and *A. cantonensis* throughout the entire country [18–20]. A low number of infective L3 are apparently required to establish infection in vertebrate hosts, including humans [21]. According to serological studies, the number of clinical cases may be higher than the number of cases presenting symptomatic disease [22]. As shown by a preliminary evaluation, the antibody response to these infections gradually decreases over time, indicating that the worms do not survive for a long period in humans [23,24]. These observations suggest that abdominal angiostrongyliasis can spontaneously recede and should be better substantiated with a more sensitive and specific serum diagnostic test due to the existence of broad cross-reactivity among helminths of different species. Unfortunately, attempts to increase the specificity of immunodiagnostic tests usually lead to lower sensitivity, and vice-versa [23]. More extensive observations with clinical, parasitological and serological follow-ups are required for better evaluation of the prognostic value of serological and other molecular methods associated with abdominal angiostrongyliasis [24]. It is of note that some patients develop a severe abdominal disease that is only cured by surgery that removes the affected intestinal segment. The adult worms tend to aggregate in the more affected areas, and patients can be cured with this surgery. Longitudinal studies have not yet been performed due to the limitations of diagnostic tests and the inefficacy of antiparasitic drugs. In conclusion, abdominal angiostrongyliasis is clearly an underdiagnosed disease [25]. Better knowledge about the distribution of this human infection will depend on awareness of the

disease among medical personnel, on epidemiologic surveys of the infection in regional mollusk populations and on reliable serological tests based on well-defined antigens that are still not available [22–28]. Pathologists should be on constant alert during histopathological analysis of cecal appendix and intestinal segments with intense eosinophilia; a detailed analysis can sometimes reveal eggs, vasculitis and even adult worms in unexpected material [29].

The nematode species comprising the genus *Angiostrongylus* were initially grouped into two subgenera, *Angiostrongylus* and *Parastrongylus*; these two subgenera have been elevated to full genera status [30,31], but this taxonomic treatment has not been generally accepted [2]. Certain *Angiostrongylus* species, such as *A. cantonensis*, *A. costaricensis*, *A. dujardini* and *A. malaysiensis*, have been recategorized [31] as belonging to the genus *Parastrongylus* [32] based on differences in the morphology of the parasite male bursa and the final mammalian host [33]. All phylogenetic analyses that have been carried out to date do not support the assignment of the component species to two genera or subgenera, i.e., *Angiostrongylus* and *Parastrongylus* [2]. More recently, a molecular analysis using restriction fragment length polymorphisms (RFLPs) allowed the differentiation of *A. cantonensis*, *A. costaricensis* and *A. vasorum* [34]. The molecular differentiation and phylogenetic trees of *Angiostrongylus* species have been defined based on sequences from small-subunit ribosomal DNA [33], internal transcribed spacer 2 (ITS-2)[35], mitochondrial cytochrome-c oxidase subunit (COI) [2] and a 66-kDa protein gene of *A. cantonensis* [36]. Based on COI sequences and the 66-kDa protein gene of *A. cantonensis*, two major clades were defined: (1) *A. cantonensis* and *A. malaysiensis*, and (2) *A. costaricensis* and *A. vasorum* [2,36]. In the study based on COI analysis, a Costa Rican isolate of *A. costaricensis* was found to be quite different from a Brazilian isolate, with an uncorrected p-distance of 11.39%. The COI and ITS-2 results indicate the possibility that the Costa Rica and Brazil isolates could be cryptic species [2,35]. In both maximum-parsimony and maximum-likelihood analyses, *A. costaricensis* was found to be the most distant taxon and possibly to represent the earliest divergence group in evolutionary history [36].

Our group [37,38] showed the life cycle of *A. costaricensis* in its natural vertebrate host (*Sigmodon hispidus*) and in a mouse model to be much more complex than originally described by Morera [8]. These studies have revealed that the L3 stage alternatively goes through two migratory courses during its development into an adult worm: a lymphatic/venous–arterial pathway and a venous portal pathway. The former is considered to represent the primary pathway because it is used by most of the larvae. Like other metastrongylides, *A. costaricensis* passes over the pulmonary circulation to migrate from the lymphatic system to the arterial circulation, where they circulate for some days before reaching their definitive habitat in the mesenteric arteries of the terminal ileum and cecum. Oviposition by mature females begins 15 days after this and defines two important periods from the pathological point of view: pre- and post-oviposition. The former depends on worms in different stages of development, and the latter essentially depends on egg deposition in tissues.

Due to the disease characteristics associated with these nematodes, the incubation period in humans is highly variable; it can range from 14 days [39] to approximately 49–79 days [40] and even to more than one year [41].The main clinical signs and symptoms of the disease are also variable and include palpable abdominal masses (tumor-like masses), abdominal pain and rigidity, fever, anorexia, vomiting, diarrhea, intestinal obstipation, hepatomegaly, jaundice, abdominal distension, emaciation, unproductive cough, nausea, intestinal obstruction, perforation or bleeding and painful rectal examination. The radiologic findings related to the disease are intestinal dilatation or obstruction, hydro-air levels, tumor-like masses, intestinal wall thickening and rigidity and spasticity of the intestinal wall. Leukograms usually present leukocytosis with eosinophilia (>10–70%). The main areas of localization of the lesions are in the cecum, ascending colon, appendix, and small intestine [14,42–44]. Some cases can essentially evolve with hepatic lesions, such as nodules or focal necrosis [45–48], which are partially explained by the secondary portal pathway [37,38]. Using two different animal models (Swiss Webster mice and *Sigmodon hispidus* rats), we showed that during its life cycle, *A. costaricensis* presents an alternative migration to hepatic veins as a normal event in the venous portal pathway, in which the nematode matures and lays fertile eggs inside the liver. *A. costaricensis* adult worms can then reach the liver through branches of the hepatic artery and portal vein.

The proportion of cases that are oligosymptomatic or asymptomatic is unknown, and abdominal angiostrongyliasis appears not to always represent a persistent infection [22,44]. The mortality rate among symptomatic cases ranges from 1.8 to 7.4% [14,44]. It is important to note that even in the pre-oviposition phase, vascular lesions were observed to occur in *S. hispidus* expressed as an inflammatory reaction in the abdominal lymphatic circulation (lymphangitis and perilymphangitis constituted by macrophages, eosinophils, and neutrophils) and periarteritis with or without fibrosis, fibrinoid necrosis of the muscular layer, and micro-hemorrhages in the arterial wall [38]. These events could explain some rare human cases with a short incubation period. The diagnosis of abdominal angiostrongyliasis is confirmed by the identification of eggs, larva, or adult worms of *A. costaricensis* in surgical specimens [48]. Larvogenesis is not a frequent event in human cases and the eggs are sometimes limited to the morula stage.

A comparative histopathological study of confirmed and suspected cases of *A. costaricensis* infection revealed two types of macroscopic features: a predominant thickening of the intestinal wall (pseudoneoplastic pattern) and congestive necrotic lesions (ischemic-congestive pattern). Microscopically, three fundamental histopathological findings were detected, defining a triplet that establishes the diagnosis of probable abdominal angiostrongyliasis: (1) a massive infiltration of eosinophils in all layers of the intestinal wall; (2) a granulomatous reaction; and (3) eosinophilia vasculitis affecting arteries, veins, lymphatic structures and capillaries. The eosinophilic arteritis is usually centripetal, originating in the adventitia [44]. A definitive diagnosis relies on the identification of adult worms in arterial vessels (more rarely in veins) following surgical intervention (Fig. 2A–F). No treatment has thus far proven to be effective against the disease; moreover, treatment with some antiparasitic drugs can even worsen the course of the disease through unknown mechanisms [10]. Recently, it was shown that intranasal vaccination against

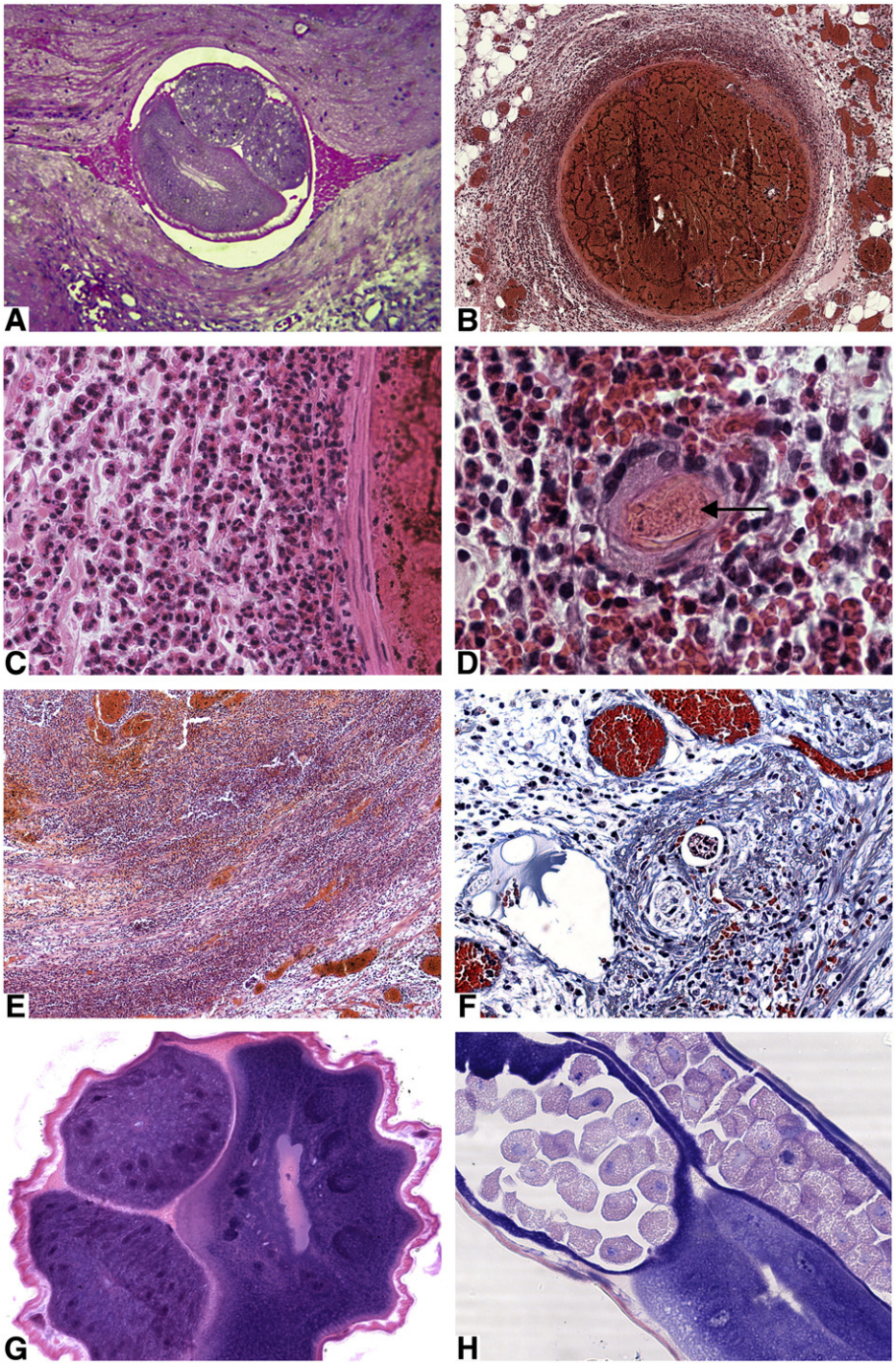

Fig. 2 – Histological lesions of abdominal angiostrongyliasis caused by *Angiostrongylus costaricensis*. (A) Female adult worm in a mesenteric artery of an infected *Sigmodon hispidus* individual showing the intestine (on the left) and the two ovaries (on the right).The parasite is located in the interface between the arterial endothelial layer and a thrombus [Hematoxylin–eosin (HE) 80×]. (B) Eosinophilic periarteritis with thrombus on human cecal appendix (HE 10×). (C) Detail of eosinophilic periarteritis full of eosinophils (HE 63×). (D) Immature egg (arrow head) in a human cecal wall, surrounded by a giant cell in the middle of the inflammatory infiltrate (HE 100×). (E) Injury of a human cecal muscle layer by intense inflammatory infiltrate (HE 10×). (F) Eggs in morula stage surrounded by inflammatory cells in a human cecal subserosa layer; the blood vessels are dilated and congested (Masson's trichrome stain 10×). (G) Transversal section of an isolated female adult worm surrounded by a clear muscle layer under the cuticle; the structure on the right is the intestine with its central lumen, and on the left, two anterior ovaries (immature segment) can be observed (Lennert's Giemsa 63×). (H) Longitudinal section of an isolated female adult worm presenting the two uteri full of eggs; the darker structure corresponds to the intestine (Lennert's Giemsa 40×).

A. costaricensis with synthetic antigens and recombinant peptides belonging to the catalytic region of the serine/threonine phosphatase 2A (PP2a) protein of the parasite results in a protective immune response in C57Bl/6 mice [49].

Even though nematodes are one of the most numerous and diverse phyla of animals on earth, including several human parasitic helminths, few studies have employed proteomic approaches to study their biology. One of the main limitations to performing such studies is the scarcity of genomic information available, which may hamper faster progress in this area [50]. In addition to the model organisms *Caenorhabditis elegans* [51] and *C. briggsae* [52], only five nuclear genomes from nematodes have been published: *Brugia malayi* [53], a major human filarial parasite; *Meloidogyne incognita* [54] and *M. hapla* [55], plant pathogens; *Pristionchus pacificus* [56], a beetle-associated species used as a model system in evolutionary biology; and *Trichinella spiralis* [57], a food-borne zoonotic parasite.

Most of the proteomic studies on nematodes have been performed on the free-living soil worm *C. elegans*, which is a convenient model system for *in vivo* studies of various physiological problems relevant to human diseases. Proteomics has contributed to the characterization of *C. elegans* nematodes by improving genome annotation and allowing analyses of phenotypic changes following RNAi treatment (targeted gene suppression), the performance of quantitative studies under various biological conditions and the profiling of protein expression during development and aging (for review, see Ref. [58]). In addition to revealing new diagnostic and therapeutic targets, high-throughput technologies could provide key insights related to comprehending mechanisms such as how the parasites invade host tissues and modulate their protective immune response [59,60].

In studies on parasitic nematodes, a widely adopted approach is to focus on the investigation of their secretomes. Apart from mediating interactions with the host (including modification of defense signaling pathways), excretory/secretory proteins may be an important source of potential immunogens to be used for diagnostics and vaccine development [61]. Several studies have thus far employed electrophoresis and/or liquid chromatography followed by MS/MS to identify secreted proteins from the helminths *Haemonchus contortus* [62], *Trichinella spiralis* and *T. pseudospiralis* [63,64], *Teladorsagia circumcincta* [65] and *Brugia malayi* [66–68]. Other proteomic studies on nematodes have focused on analyzing gender- and/or species-specific antigens [69–71], as well as the plasticity of protein expression patterns under different environmental conditions [72,73].

The aim of the present study was to comparatively identify the most abundant proteins in crude extracts from female and male *Angiostrongylus costaricensis*, particularly their immunogenic proteins.

2. Materials and methods

2.1. Parasites

The life cycle of the parasites was maintained at the laboratory using *Sigmodon hispidus* rodents and the snail *Biomphalaria glabrata* as definitive and intermediate hosts, respectively. Three-month-old rats were orally infected with 30 L3 larvae/animal. Adult worms were recovered by dissection of the mesenteric arteries of cotton rats after 40 days of infection [38]. They were extensively rinsed in PBS, segregated according to gender, weighted, and then stored at −80 °C until further use. Discrimination between genders was based on classical morphological criteria: females are usually longer and thinner than males and present an intestine full of blood, and males exhibit typical copulatory bursa with several rays and two copulatory spicules [8,74,75]. All procedures with animals were approved by the Animal Ethics Committee at Fiocruz (CEUA license # P0246/05) and were carried out in accordance with the *International Guiding Principles for Biomedical Research Involving Animals*, as issued by the *Council for the International Organizations of Medical Sciences*.

2.2. Optimization of protein extraction procedures

Protein extraction was performed after maceration of the worms (10 mg) in microcentrifuge tubes containing an abrasive resin (Sample Grinding Kit, GE Healthcare) and 150 μL of one of the following extraction solutions: (A) 1% SDS, 60 mM DTT and 40 mM Tris base; (B) 8 M urea, 4% CHAPS, 60 mM DTT, 40 mM Tris base and 1% v/v IPG buffer (same pH range of the IPG strip); (C) 7 M urea, 2 M thiourea, 4% CHAPS, 40 mM Tris base, 60 mM DTT and 1% v/v IPG buffer (same pH range of the IPG strip). Extraction with solution C was also performed in the presence of the Complete™ Protease Inhibitor Cocktail (Roche, Basel, Switzerland), following the manufacturer's instructions. After incubation for 1 h at room temperature with gentle shaking, cellular debris and resin were spun out (16,000 ×*g*, 15 min), and proteins were precipitated from the supernatant overnight with cold ethanol/acetone [1(protein extract):4 (ethanol):4 (acetone) v/v] at −20 °C. The precipitated proteins were sedimented at 16,000 ×*g* for 30 min, washed 3 times with ethanol/acetone/water (4:4:2 v/v) and solubilized overnight at 4 °C in extraction solution C without Tris base. Aliquots collected at each extraction step were assayed for total protein content using the 2-D Quant Kit (GE Healthcare).

2.3. SDS-PAGE

Protein extracts were initially analyzed by homogeneous SDS-PAGE (12%) in the Mini-Protean II system (Bio-Rad Laboratories) under reducing conditions using 4% stacking gels [76]. Additionally, low molecular weight markers from GE Healthcare were used and gels were stained with 0.2% CBB R-250.

2.4. 2-DE

Total cellular extracts of female and male adult worms were fractionated first on Immobiline DryStrips (IPG 11 cm pH 3–11 NL or 11/18 cm pH 4–7)(GE Healthcare) and then by homogeneous 15% SDS-PAGE as previously described [77]. Following in-gel sample rehydration at 30 V for 12 h, the following IEF electric conditions for 18 cm IPG strips were used: 200 V/1 h, 500 V/1 h, 1000 V/1 h, 1000–8000 V/30 min, and 8000 V/7 h (60,000 VhT). For 11 cm IPG strips, the maximum voltage was limited to 6000 V/6 h (44,000 VhT). Gels were stained with colloidal CBB G-250 or Sypro Ruby (Invitrogen) for total protein

visualization or incubated with the glycan-specific stain ProQ-Emerald (Invitrogen) for the detection of glycoproteins, as specified by the manufacturer's instructions. CBB-stained gels were scanned using an Image Scanner (GE Healthcare), and image analysis was performed using Image Master 2D Platinum 7.0 software (GE Healthcare). Spot detection was automatically performed with minimal manual editing. For each gender, three independent sample preparations were analyzed by 2-DE. Protein spot abundances were expressed as a mean ± standard deviation. Comparisons of spot abundances between female and male groups were performed using Student's t-test ($p \leq 0.01$). Fluorescent images were acquired on a Typhoon Trio scanner (GE Healthcare) with a resolution of 100 μm and photomultiplier (PTM) values adjusted to optimize sensitivity and avoid oversaturation. The excitation/emission wavelengths for Sypro Ruby and ProQ-Emerald were 488/610 and 532/520, respectively.

2.5. Characterization of immunogenic proteins

Immediately after electrophoresis, the proteins on 2-DE gels were transferred to PVDF membranes (Immun-Blot™ 0.2 μm, BioRad) at 270 mA for 3 h using the TE77 PWR semi-dry blotter (Amersham Biosciences). Two 2-DE gels were transferred at the same time by stacking them vertically in a multi-layered stack. After blocking unoccupied membrane sites overnight with TBS containing 0.05% Tween 20 and 5% skim milk, the PVDF membrane was incubated for 2 h with pooled serum taken from Swiss Webster mice 28 days after experimental infection with *A. costaricensis* (1/1000 v/v dilution in freshly prepared blocking solution). After washing 3× for 10 min with TBS containing 0.05% Tween 20, the membranes were further incubated for 2 h with the secondary antibody HRP-conjugated sheep anti-mouse IgG (whole antibody, GE Healthcare)(1/25,000 dilution in TBS+0.05% Tween 20). The membranes were washed again with TBS+ Tween 20 and then incubated between two cellophane sheets with the SuperSignal West Dura Chemiluminescent Substrate (Thermo Scientific) prepared according to the manufacturer's instructions. Each membrane/cellophane "sandwich" was exposed to Hyperfilm ECL Film (GE Healthcare) for 3 min. The spots on 2-DE blots were matched to their homologues in 2-DE gels using Image Master 2D Platinum 7.0 software (GE Healthcare).

2.6. Protein analysis by mass spectrometry

In-gel protein digestion, N-terminal chemical derivatization of tryptic peptides with 4-sulphophenyl isothiocyanate (SPITC), and sample desalting with C18 ZipTip micropipette tips (Millipore) were performed as previously described [78]. All MS spectra were acquired in positive ion reflector mode on an AB Sciex MALDI-TOF/TOF 5800 Mass Spectrometer using Explorer software, version 4.0.0. An aliquot (0.3 μL) of the desalted tryptic digest was deposited onto the target plate immediately before the addition of an equal volume of a saturated matrix solution [10 mg/mL α-cyano-4-hydroxycinnamic acid (Aldrich, Milwaukee, WI) in 50% acetonitrile/0.1% trifluoroacetic acid]. After sample drying at room temperature, both MS and MALDI-PSD data were acquired with a 1 kHz laser. Typically, 2040 and 2000 shots were accumulated for spectra in MS mode and PSD mode, respectively. Up to 20 of the most intense ion signals with a signal-to-noise ratio above 30 were selected as precursors for MALDI-PSD acquisition, excluding common trypsin autolysis peaks and matrix ion signals. External calibration in MS mode was performed using a mixture of five peptides: des-Arg1-Bradykinin (*m/z*) 904.4680; angiotensin I (*m/z*) 1296.6850; Glu1-fibrinopeptide B (*m/z*) 1570.6770; ACTH (1–17) (*m/z*) 2093.0870 and ACTH (18–39) (*m/z*) 2465.1990. MALDI-PSD spectra were externally calibrated using known fragment ion masses observed in the spectrum of angiotensin I.

2.7. Database searching and gene ontology analysis

Following data acquisition, peak lists from uninterpreted spectra were created using the Peaks-to-Mascot script of 5800 Explorer software (Applied Biosystems) and uploaded to the online Mascot search engine (Matrix Science). The search considered carbamidomethylation as a static modification and methionine oxidation, propionamide cysteine and N-terminal derivatization with SPITC as variable modifications. Up to two missed cleavages were accepted. The spectra were searched against NCBInr. Peaks Studio 5.2 [79] was used as an extra measure to confirm the interpretation of tandem spectra identified as described above; the same modification settings and protein database were used. We used PatternLab's Gene Ontology Explorer (GOEx) module [80,81] to further interpret our list of identified proteins. First, we used Goanna [82] to

Table 1 – Quantitative analysis of extraction yields and protein recovery after different sample preparation methods. Protein concentration was measured using the 2D-Quant-kit assay.

	Extraction solutions	Extraction yield (μg ptn/mg worm)			% Recovery after EtOH precipitation		
		Mean	SD	n	Mean	SD	n
Female	A	105.74	2.77	4	ND		
	B	86.11	9.06	4	60.78	6.86	4
	C	84.10	11.71	11	91.52	8.83	10
	C + inhibitor cocktail	81.34	8.58	2	ND		
Male	C	87.12	11.24	7	95.67	4.02	6

ND, not determined; n, number of independent replicates.

assign GO terms to each identified protein by Blasting [83] them against the online SwissProt, TrEMBLE, and UniProt databases. This generated a text file containing each protein's accessions number and the corresponding GO terms. This file, together with the Gene Ontology database [84] (OBO v 1.2 downloaded from geneontology.org in March 1st 2011), served as an input to GOEx so that statistically over-represented GO terms ($p \leq 0.01$) could be determined according to the hypergeometric distribution.

3. Results and discussion

3.1. *Optimization of protein extraction*

Female specimens of *A. costaricensis* are longer than male worms [8,74] and were recovered in higher numbers in infected *Sigmodon hispidus*. Therefore, the optimization of protein extraction conditions was performed only in females. Table 1 shows the quantitative results from grinding these parasites under different extraction conditions. Assuming SDS-based solution A as the gold standard (100% extraction efficiency), we showed that both solutions B (containing urea as caothropic agent) and C (containing urea/thiourea) were efficient in extracting approximately 80% of whole worm proteins. Qualitatively, SDS-PAGE profiles from all extraction conditions showed comparable patterns of protein bands with different staining intensities over the entire range of molecular masses from 14.4 kDa to more than 97 kDa (Fig. 3). After the addition of a protease inhibitor cocktail to solution C, no changes were observed in the extraction yield or the SDS-PAGE profile, indicating that proteolysis is not a major concern under the denaturing conditions used here. Because protease inhibitors can additionally modify proteins and cause charge artifacts, they were not used in this study. Proteins were precipitated with a mixture of cold ethanol/acetone so that contaminants that might impair subsequent 2-DE analysis, such as salts and nucleic acids, could be removed [85]. No qualitative differences were observed in the unidimensional protein profiles of samples extracted with solution C before and after precipitation (Fig. 3). Regarding the recovery of proteins from ethanol/acetone

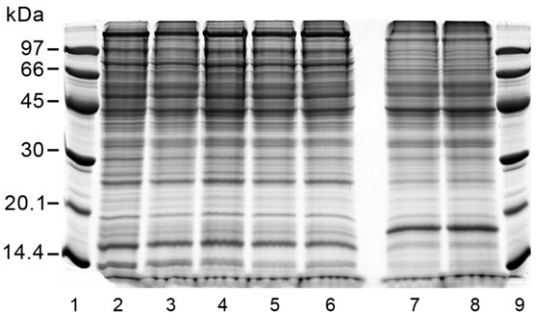

Fig. 3 – SDS-PAGE of protein extracts from adult *Angiostrongylus costaricensis* nematodes. Whole worms were ground in different solutions to optimize extraction conditions. The composition of solutions A–C is described in the Materials and methods section. Lanes 1 and 9, molecular mass markers; lane 2, female proteins extracted with solution A; lane 3, female proteins extracted with solution B; lane 4, female proteins extracted with solution C; lane 5, female proteins extracted with solution C +Complete™ protease inhibitor cocktail; lane 6, female proteins extracted with solution C and precipitated with ethanol/acetone; lane 7, male proteins extracted with solution C; lane 8, male proteins extracted with solution C and precipitated with ethanol/acetone. Gels (12%) were run under reducing conditions and stained with CBB R-250. The same amounts of protein (20 μg/10 μL) were applied in lanes 2–8.

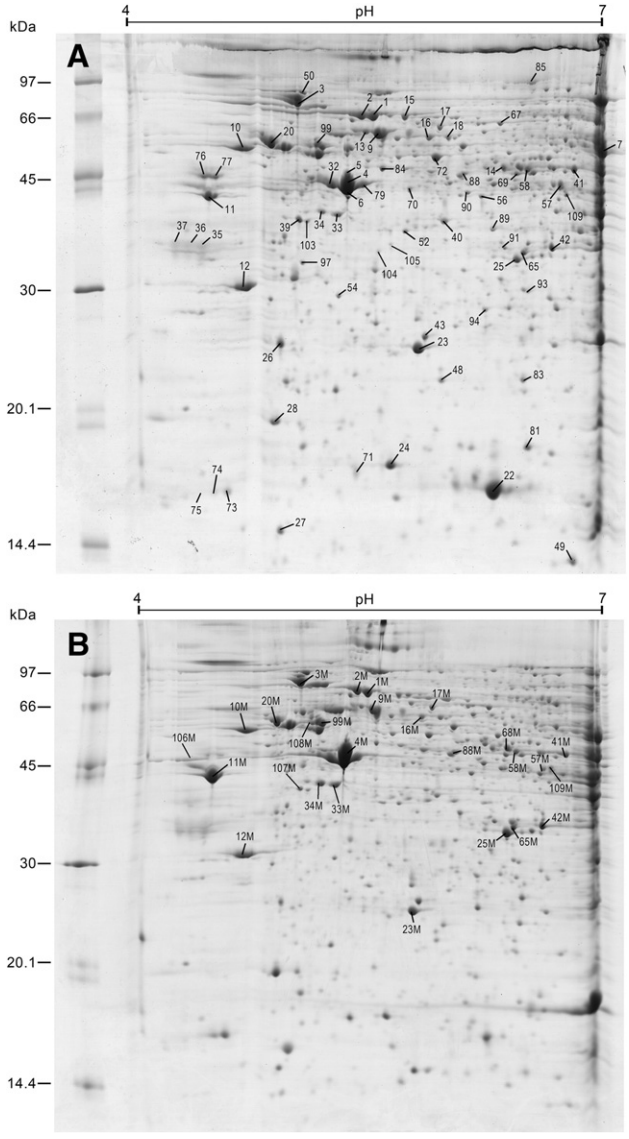

Fig. 4 – 2-DE gels of total protein extracts from adult *Angiostrongylus costaricensis* nematodes. Proteins (0.5 mg) from female (A) and male (B) worms extracted with solution C were separated by 2-DE on 18 cm IPG strips pH 4–7, followed by 15% SDS-PAGE. Gels were run under reducing conditions and stained with colloidal CBB G-250. The migration of molecular mass markers is shown on the acidic side of the gel. Numbers refer to the spot identity used in the tables. The letter M placed after the spot number indicates male proteins. Numbers without a letter refer to female proteins. Representative images of three independent replicates are shown.

pellets, the use of thiourea in combination with high concentrations of urea [86] dramatically increased the solubilization power of solution C as compared to solution B (Table 1). Under optimized conditions, male samples ground in solution C showed approximately the same extraction yield and percentage of protein recovery as females (Table 1). SDS-PAGE profiles were similar for both genders, although differences in the intensity distribution of the protein bands were evident (Fig. 3).

3.2. Two-dimensional analysis of protein extracts

To improve electrophoretic separation, extracts of female or male adult worms were independently fractionated by 2-DE. Using 11 cm IPG strips, pH 3–11 NL, approximately 800 protein spots were visualized by colloidal CBB staining (Fig. 1, Supplementary data). Although the body morphology and size are significantly different in female and male worms [87], their 2-DE profiles were similar, with less than 30% of unmatched spots being observed (which were concentrated in the more basic regions of the gels). Most protein spots (≈ 60%) from both genders were focused between pH 5 and 7, with molecular masses ranging from 20.1 to 66 kDa. In such broad-range IPG strips, more than one protein may be focused within the same gel spot [88]. Therefore, we decided to further improve the proteome analysis by using 18 cm medium-range IPG strips, pH 4–7 (Fig. 4). Approximately 1000 protein spots were detected between pH 4–7 on each individual gel. No significant gender-specific differences in expression levels were observed for 75% of these spots. Of the remaining 25% of protein spots, 7.5% and 10.4% were uniquely detected in female or male worms, respectively. These could represent true gender-specific proteins or quantitative differences between males and females (with the least abundant spots falling under the sensitivity threshold of the detection method used). Whether such differences represent biologically important variations remains to be determined.

3.3. Protein identification by MALDI-PSD MS

In an attempt to better characterize the protein profiles of *A. costaricensis* parasites, the most abundant spots shown in Fig. 4 were excised and analyzed by MALDI-PSD (Table 2 and Supplementary Table 1). It is important to note that only 12 gene sequences can be retrieved from the NCBInr database for *A. costaricensis* nematodes, all of which code for mitochondrial proteins. Hence, most of the uninterpreted experimental tandem spectra were matched to predicted fragment patterns from homologous species. To simplify the interpretation of the MALDI-PSD spectra, tryptic peptides were chemically derivatized with SPITC before MS analysis. This simple N-terminal sulfonation reaction leads to the formation of a much cleaner spectrum (almost exclusively) comprised of y-series ions, as b-series products are neutralized by a strongly negative modifying group [78,89]. Because the derivatization reaction is not 100% efficient, both derivatized and non-derivatized peptides were observed in most cases. Of the 106 dominant protein spots excised from 2-DE gels from females, 72 (68%) were identified by mass spectrometry. For male samples, 27 out of the 46 processed spots (59%) were positively identified. Although 16 spots gave rise to good quality MALDI-PSD spectra, they could not be identified; these peptide ions probably correspond to genes that have yet to be described.

3.4. Interpretation of the identification results

The GOEx tool [81] was used to search for associations between our MS data and Gene Ontology (GO) terms [84]. Several GO terms were statistically over-represented in our dataset, from which we highlight the following biological process terms: a) related to "macromolecule metabolic process" (GO:0009059-macromolecule biosynthetic process, GO:0019538-protein metabolic process, GO:0006508-proteolysis); b) related to "developmental process" (GO:0002164-larval development, GO:0048513-organ development, GO:0055115-entry into diapose); c) related to "response to stress" (GO:0006979-response to oxidative stress, GO:0006986-response to unfolded protein) and d) related to "biological regulation" (GO:0040008-regulation of growth, GO:0048518-positive regulation of biological process). The corresponding proteins for each enriched GO term are listed in Supplementary Table 2.

Not surprisingly, several of the most abundant proteins identified in *A. costaricensis* extracts were cytoskeleton-associated proteins, such as actin, myosin light chain, alpha tubulin, tropomyosin and collagen. These proteins play important roles in maintaining the body shape and muscle integrity of the nematodes [71,90,91]. The somatic musculature in nematodes is technically a part of the body wall, and it functions together with the pseudocoel and the cuticle as a hydrostatic skeleton [92] (Fig. 2G). Identified proteins involved in energy metabolism included, but were not limited to, cytochrome c oxydase, ATP synthase, enolase, glutamine synthetase, glutamate ammonia ligase, methionine adenosyltransferase and ABC transporter. Enolase is a multifaceted glycolytic protein that was traditionally thought to be restricted to the cytosol. Interestingly, some years ago, it was described on the surface of some helminths, where it binds to plasminogen and may be involved in the degradation of the host's extracellular matrix [93–96]. Proteins that directly interfere with host effector mechanism were also detected in the present proteomic study. Some of these are anti-oxidant proteins, such as peroxiredoxin, thioredoxin, translationally controlled tumor protein and aldehyde dehydrogenase. They effectively detoxify host-generated reactive oxygen species that could otherwise damage parasite cellular components, such as proteins, lipids and nucleic acids. Therefore, antioxidant proteins constitute a key factor favoring parasite survival inside the intravascular (mainly arterial) system, and thus contribute to the host–parasite relationship. These proteins are being investigated as putative protective antiparasite vaccines [97]. Other noteworthy identified proteins include As37 and cyclophilins, which are members of the immunoglobulin family. The latter is a folding helper enzyme belonging to the peptidyl-prolyl cis–trans isomerase class [98]. Both proteins have previously been described in other parasitic nematodes, such as *Haemonchus contornus* [62] and *Brugia malayi* [67], although their role in the parasites' immune evasion remains unknown. Finally, we identified a 14-3-3 protein, a 30 kDa polypeptide belonging to a highly conserved family of molecules that regulate intracellular signal transduction and the cell cycle [99]. This protein has also been

observed in other helminths, such as *Echinococcus multilocularis*, *E. granulosus*[100] and *Schistosoma mansoni*. In the last species, the 14-3-3 protein is believed to be involved in parasite growth and survival [101] and is being evaluated as a vaccine candidate against schistosomiasis [102].

The systematic profiling of *A. costaricensis* proteins described above contributes to our understanding of the parasite's physiology. For example, this comprehensive molecular characterization may eventually help to explain why traditional anthelmintic drugs seem to induce erratic migration of these parasites, instead of killing them, which may exacerbate the consequences of the infection [10]. Proteomics could additionally unveil important molecules involved in host–parasite crosstalk, leading to the development of more effective therapeutic interventions for controlling the disease. For example, immunoreactive proteins from *A. costaricensis* nematodes are largely unknown, contributing to the difficulty involved in specifically diagnosing abdominal angiostrongyliasis in humans. A number of severe cases are confirmed through histopathological examination of specimens obtained after surgical treatment. Such drastic intervention may be necessary for the correction of intestinal perforations or obstructions that are eventually observed in angiostrongyliasis infections [25,29]. The first immunochemical investigations have used antigen preparations made from crude adult worm [22–24,103,104] or egg [28,105] extracts from *A. costaricensis*. However, it is well known that crude antigenic preparations are not suitable for immunodiagnosis due to their broad cross-reactivity with other helminth species. Ideally, purified antigens specific to the parasite should be used in immunodiagnostic tests [23].

3.5. *Analysis of immunogenic proteins*

In the present study, we exploited proteomic tools to specifically identify immunogenic proteins in *A. costaricensis*. These proteins were recognized after blotting 2-DE gels loaded with male or female total protein extracts onto PVDF membranes probed with antisera from Swiss Webster mice experimentally infected with *A. costaricensis* (Fig. 5). Overall, the immunoblots for both sexes showed similar profiles of reactive proteins, although some inter-gender variations were detected. One of the most striking differences observed was a stronger response for a group of 30–40 kDa female antigens focused between pH 4.5–5.5. Accordingly, when comparing adult worm antigens obtained under mild (non-denaturing) conditions in ELISA tests, Graeff-Teixeira et al. [103] reported that whole female extracts were twice as sensitive as male extracts in recognizing a proven acute human *A. costaricensis* infection. It was suggested that the strong antigenicity of eggs produced by female worms may contribute to explaining such differences [28]. In fact, each female presents a large number of eggs inside two uteri, which were obligatorily included in the proteomic analysis of the female pool (Fig. 2H).

Identifying immunoreactive spots on Western blots corresponding to CBB-stained proteins was not simple, mainly due to the poor correlation between immunogenicity and protein abundance, as described previously for other helminth parasites [62,67]. For example, actin spots were not recognized by antisera from infected mice although they represent the most abundant protein in the worm extracts. This was not unexpected because actin is a major constituent of eukaryotic cells and is widely observed throughout the animal kingdom, usually together with myosin [106,107]. It is unknown whether actin plays a critical role in *A. costaricensis* intestinal epithelial endocytosis [108]. On the other hand, strongly immunogenic proteins focused in the central region of the male blot corresponded to regions of the gel where several faintly CBB-stained spots (or no spots at all) could be detected (Fig. 2, Supplementary data). To further improve these results, we are presently carrying out assays for the direct detection of antigens in the polyacrylamide gels and/or immunoprecipitation (pull-down) followed by nLC–MS/MS analysis.

The only immunoreactive protein spots detected by mice antisera that could be unequivocally identified by MALDI-PSD were heat shock proteins (HSPs)[spots # 1(M), 2(M) and 3], a putative abnormal DAuer Formation family member [spot # 3 M] and galectins [spots # 25(M), 42(M) and 65(M)] (Fig. 5). HSPs and galectins, as well as several other non-immunogenic proteins of *A. costaricensis*, were found in multiple protein spots, indicating the presence of protein isoforms. Indeed, when staining the gels with ProQ-Emerald, a glycan-specific reagent, several protein spots were shown to be glycosylated (Fig. 3, Supplementary data), a common feature among helminth parasite antigens [109]. HSPs act as molecular chaperones, regulating protein folding in the cell. These proteins are related to the adaptive response of the parasite to the host immune system. Furthermore, in various infectious disease models, vaccination strategies using HSPs have induced significant protection [110]. Although HSPs also present a particularly high degree of structural conservation during evolution that must reflect the perpetuation of functions necessary for cell survival [111], their immunogenicity is highly dependent on the presence of functional phagocytic cells in the host [112]. Calreticulin and disulfide isomerase are other proteins related to protein folding that were identified in *A. costaricensis* extracts. In contrast to the HSPs, they were not immunogenic. Calreticulin is a well conserved 46 kDa protein that plays important roles in the regulation of key cellular functions [113]. This protein has been identified as a potent virulence factor in *Trypanosoma cruzi* [114], as necessary for stress responses and fertility in *C. elegans* [115] and as involved in immune responses in *Hekigmosomoides polygyrus* [116] and in *Necator americanus* [117]. Protein disulfide isomerase is a multi-functional enzyme that, in addition to its enzymatic activity involved in protein folding, seems to be essential for viability and extracellular matrix formation in *C. elegans* nematodes [118].

In male blots, immunogenic spot #3M was identified as a DAuer formation protein. In female blots, the corresponding less reactive spot matched an HSP. A BLASTp search in the NCBInr database indicated high sequence similarity (91%) between a Dauer formation protein and Heat Shock Protein 90. Dauer formation (*daf*) genes have been described as controlling both larval development and adult longevity in *C. elegans* [119,120]. These genes can prolong larval development under adverse environmental conditions, such as a lack of food and/or high temperature [121]. They also extend the adult lifespan during restricted nutrition periods and changes in temperature [122].

Table 2 – Summary list of the most abundant protein spots of *A. costaricensis* adult extracts identified by MALDI-PSD MS. The letter M placed after the spot number indicates male proteins. Numbers without a letter refer to female proteins. Protein analysis was performed by running the Mascot search engine against the NCBInr database. For a more detailed description of all identified proteins, see Supplementary Table 1.

Spot no.	Protein name
1, 1M, 2, 2M, 3	Heat shock protein
3M	Putative abnormal DAuer formation family member
4, 4M, 5, 6	Actin
7	Elongation factor 1 alpha
9, 9M	Heat shock protein
10, 10M	Calreticulin
11, 11M	Tropomyosin
12, 12M	Fourteen-three-three family member
13	Heat shock protein
14	Methionine adenosyltransferase
15	COLlagen family member
16, 16M	CCT-2
17, 17M, 18	Chaperonin containing TCP-1 family member
20, 20M	Protein disulfide isomerase
22, 23, 23M	Peroxiredoxin
24	Hypothetical protein Rsph17025_3168
25, 25M	Galectin
26	Translationally controlled tumor protein
27	D-aminoacylase domain protein
28	*C. briggsae* CBR-MLC-2.2 protein
32	Actin
33, 33M, 34, 34M	As37
35, 36, 37	Putative Lin-5 (five) interacting protein
39	Ribosomal protein, small subunit family member
40	Stress-induced-phosphoprotein 1
41, 41M	Enolase
42, 42M	Galectin
43	PREDICTED: similar to mitochondrial truncated thioredoxin-dependent peroxide reductase precursor
48	Predicted protein
49	ABC transporter related
50	Hypothetical protein T05E11.3
52	NAD-dependent epimerase/dehydratase
54	20S proteasome alpha5 subunit
56	Hypothetical protein F17C11.9
57, 57M	Glutamate–ammonia ligase
58, 58M	Enolase
65, 65M	Galectin
67	Chaperonin containing TCP-1 family member
68M	Ubiquinol-Cytochrome c oxidoReductase complex family member
69	CRE-AHCY-1 protein
70	Uracil-DNA glycosylase
71	Cytochrome C oxidase family member
72	Hypothetical protein BURPS1710b_A0185
73, 74	Alkali myosin light chain
75	SUMO (ubiquitin-related) homolog family member (smo-1)
76, 77	Putative nucleosome binding protein
79	Putative beta-actin
81	Hypothetical protein ckrop_1216
83	CalPoNin family member
84	PREDICTED: similar to aldehyde dehydrogenase 1A2 isoform 2
85	Primosomal protein N '
88M	Hypothetical protein
89	Hypothetical protein Y24D9A.8
90	Activator of 90 kDa heat shock protein ATPase homolog 1
91	Galectin-1
93	*C. briggsae* CBR-PAS-6 protein
94	Heat shock protein
97	Predicted protein
99, 99M	Alpha tubulin
103	Protein farnesyltransferase/geranylgeranyltransferase putative
104	Hypothetical protein
105	Hypothetical protein Y46G5A.19

Table 2 (*continued*)

Spot no.	Protein name
106M	Putative nucleosome binding protein
107M	Putative histone-binding protein Caf1
108M	Alpha tubulin
109, 109M	Glutamate–ammonia ligase

Galectins were also recognized by mice antisera as immunogenic proteins in *A. costaricensis*. They were identified in several spots and are members of the galactoside-binding lectin family, being characterized by a typical motif of conserved amino acids in their carbohydrate recognition domain(s) [123]. The biological function of nematode galectins is not well understood, although they may be important for survival and interaction with the host [124]. Additionally, they seem to be involved in mediating immune recognition and modulation of the host response via an unknown mechanism, which may involve downregulation of the host's innate immunity [125]. Based on their primary structure and subunit architecture, galectins have been classified as proto (subunit molecular mass 14.5–16 kDa), chimera (29–35 kDa) and tandem repeat (32–36 kDa) types [126] or galectins 1–12 [127]. These proteins have been described in several organisms and in *C. elegans* galectin-1 appears to be associated with the cuticle and pharynx of the adult worm [128].

4. Conclusions

To our knowledge, this work represents the first systematic effort to characterize the proteome of male and female *A. costaricensis* worms. Several important features of these proteomes were uncovered, such as the identity of the dominant proteins in adult nematode extracts and the overall characteristics of antigens detected by antisera from infected rats. These results will certainly contribute to improving our understanding of the host–parasite relationship, as well as assisting searches for candidate proteins for diagnostic assays and the treatment of abdominal angiostrongyliasis.

Supplementary materials related to this article can be found online at doi:10.1016/j.jprot.2011.04.031.

Acknowledgements

This research was supported by Brazilian grants from Fiocruz (PAPES V and PDTIS), Conselho Nacional de Desenvolvimento Científico e Tecnológico (CNPq), Fundação de Amparo à Pesquisa do Estado do Rio de Janeiro (FAPERJ) and Coordenação de Aperfeiçoamento de Pessoal de Nível Superior (CAPES). We thank the staff of the Toxinology and Pathology Laboratories-IOC/Fiocruz for excellent technical assistance. We gratefully acknowledge Dr. André Teixeira S. Ferreira and Dr. Richard H. Valente (Toxinology Laboratory-IOC/Fiocruz) for their assistance with the mass spectrometric analysis. We also thank Monique R. O. Trugilho (Toxinology Laboratory-IOC/Fiocruz) for helping with 2-DE gel image analysis. We are grateful to Heloisa M. N. Diniz and Cristina S. Ferreira (Image Production and Treatment Service - IOC/Fiocruz) for processing the figures and creating the life cycle cartoon. KMR thanks CAPES for her PhD fellowship. PCC thanks CAPES/Fiocruz 30–2006 for his fellowship.

REFERENCES

[1] Morera P, Céspedes R. *Angiostrongylus costaricensis* n. sp. (Nematoda: Metastrongyloidea), a new lungworm occurring in man in Costa Rica. Rev Biol Trop 1971;18:173–85.
[2] Eamsobhana P, Lim PE, Solano G, Zhang H, Gan X, Yong HS. Molecular differentiation of *Angiostrongylus* taxa (Nematoda: Angiostrongylidae) by cytochrome c oxidase subunit I (COI) gene sequences. Acta Trop 2010;116:152–6.
[3] Wang QP, Lai DH, Zhu XQ, Chen XG, Lun ZR. Human angiostrongyliasis. Lancet Infect Dis 2008;8:621–30.
[4] Kliks MM, Palumbo NE. Eosinophilic meningitis beyond the Pacific Basin: the global dispersal of a peridomestic zoonosis caused by *Angiostrongylus cantonensis*, the nematode lungworm of rats. Soc Sci Med 1992;34:199–212.
[5] Pien FD, Pien BC. *Angiostrongylus cantonensis* eosinophilic meningitis. Int J Infect Dis 1999;3:161–3.
[6] Caldeira RL, Mendonça CL, Goveia CO, Lenzi HL, Graeff-Teixeira C, Lima WS, et al. First record of molluscs naturally infected with *Angiostrongylus cantonensis* (Chen, 1935) (Nematoda: Metastrongylidae) in Brazil. Mem Inst Oswaldo Cruz 2007;102:887–9.
[7] Maldonado Jr A, Simões RO, Oliveira AP, Motta EM, Fernandez MA, Pereira ZM, et al. First report of *Angiostrongylus cantonensis* (Nematoda: Metastrongylidae) in *Achatina fulica* (Mollusca: Gastropoda) from Southeast and South Brazil. Mem Inst Oswaldo Cruz 2010;105:938–41.
[8] Morera P. Life history and redescription of *Angiostrongylus costaricensis* Morera and Céspedes, 1971. Am J Trop Med Hyg 1973;22:613–21.
[9] Céspedes R, S. J., Mekbel S, Troper L, Müllner F, Morera P. Granulomas entéricos y linfáticos con intensa eosinofilia tissular producidos por un estrongilideo (Strongylata). Acta Med Costarric 1967;10:325–55.
[10] Morera P, Bontempo I. Acción de algunos antihelminticos sobre *Angiostrongylus costaricensis*. Rev Méd Hosp Nac Niños Costa Rica 1985;20:165–74.
[11] Ubelaker JE, Hall NM. First report of *Angiostrongylus costaricensis* Morera and Céspedes 1971 in the United States. J Parasitol 1979;65:307.
[12] Hulbert TV, Larsen RA, Chandrasoma PT. Abdominal angiostrongyliasis mimicking acute appendicitis and Meckel's diverticulum: report of a case in the United States and review. Clin Infect Dis 1992;14:836–40.
[13] Ash LR. Human anisakiasis misdiagnosed as abdominal angiostrongyliasis. Clin Infect Dis 1993;16:332–4.

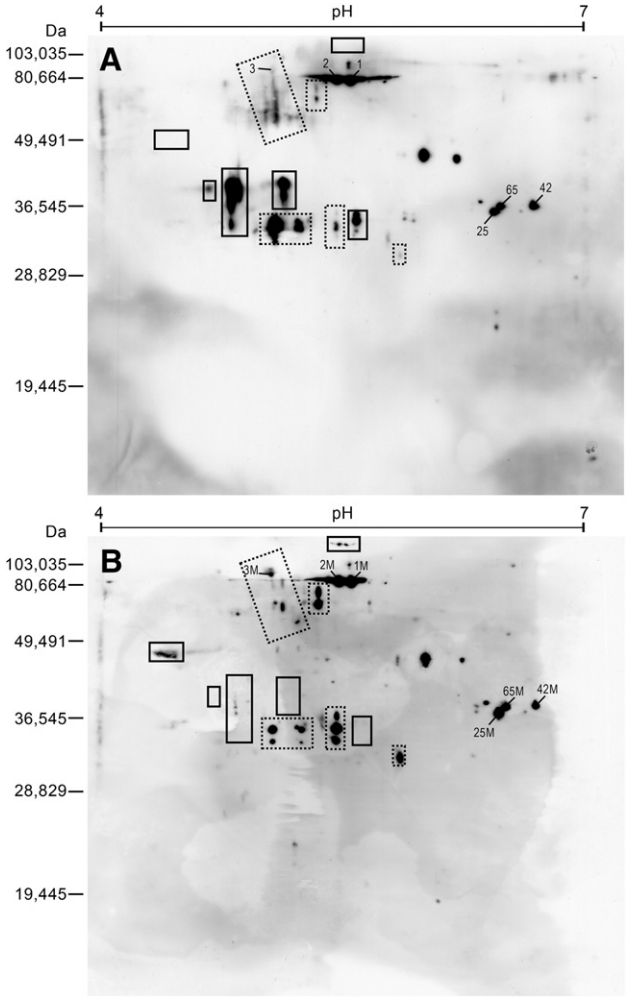

Fig. 5 – 2-DE/immunoblot of protein extracts from adult *Angiostrongylus costaricensis* nematodes. Proteins (0.1 mg) from female (A) and male (B) worms extracted with solution C were fractionated on 18 cm IPG strips pH 4–7, followed by 15% SDS-PAGE (reducing conditions), and further electroblotted onto a PVDF membrane that was probed with antisera from mice infected with *A. costaricensis*. After incubation with an anti-mouse secondary antibody conjugated to HRP, the membrane was developed by the addition of an ECL substrate. The migration of pre-stained molecular mass markers is indicated on the acidic side of the gel. Dotted-line boxes enclose protein spots with different signal intensities on female and male blots. Regions containing reactive spots exclusively found in one gender are indicated by solid-line boxes. Numbers refer to the spot identity used in the tables. The letter M placed after the spot number indicates male proteins. Numbers without a letter refer to female proteins.

[14] Kramer MH, Greer GJ, Quiñonez JF, Padilla NR, Hernández B, Arana BA, et al. First reported outbreak of abdominal angiostrongyliasis. Clin Infect Dis 1998;26:365–72.
[15] Morera P, Ash LR. Studies on the intermediate host of *Angiostrongylus costaricensis* (Morera and Céspedes, 1971). Bol Chil Parasitol 1970;25:135.
[16] Rodriguez R, Agostini AA, Porto SM, Olivaes AJ, Branco SL, Genro JP, et al. Dogs may be a reservoir host for *Angiostrongylus costaricensis*. Rev Inst Med Trop Sao Paulo 2002;44:55–6.
[17] Mendonça CL, Carvalho OS, Mota EM, Lenzi HL. Development of *Angiostrongylus costaricensis* Morera and Cespedes 1971 (Nematoda: Angiostrongylidae) larvae in the intermediate host *Sarasinula marginata* (Semper 1885) (Mollusca: Soleolifera). Parasitol Res 2008;102:861–5.
[18] Carvalho Odos S, Teles HM, Mota EM, Lafeta C, de Mendonça GF, Lenzi HL. Potentiality of *Achatina fulica* Bowdich, 1822 (Mollusca: Gastropoda) as intermediate host of the *Angiostrongylus costaricensis* Morera & Céspedes 1971. Rev Soc Bras Med Trop 2003;36:743–5.
[19] Graeff-Teixeira C. Expansion of *Achatina fulica* in Brazil and potential increased risk for angiostrongyliasis. Trans R Soc Trop Med Hyg 2007;101:743–4.
[20] Thiengo SC, Maldonado A, Mota EM, Torres EJ, Caldeira R, Carvalho OS, et al. The giant African snail *Achatina fulica* as natural intermediate host of *Angiostrongylus cantonensis* in Pernambuco, northeast Brazil. Acta Trop 2010;115:194–9.
[21] Rambo PR, Agostini AA, Graeff-Teixeira C. Abdominal angiostrongyliasis in southern Brazil—prevalence and parasitic burden in mollusc intermediate hosts from eighteen endemic foci. Mem Inst Oswaldo Cruz 1997;92:9–14.
[22] Graeff-Teixeira C, Goulart AH, de Brum CO, Laitano AC, Sievers-Tostes C, Zanini GM, et al. Longitudinal clinical and serological survey of abdominal angiostrongyliasis in Guapore, southern Brazil, from 1995 to 1999. Rev Soc Bras Med Trop 2005;38:310–5.
[23] Geiger SM, Laitano AC, Sievers-Tostes C, Agostini AA, Schulz-Key H, Graeff-Teixeira C. Detection of the acute phase of abdominal angiostrongyliasis with a parasite-specific IgG enzyme linked immunosorbent assay. Mem Inst Oswaldo Cruz 2001;96:515–8.
[24] Palominos PE, Gasnier R, Rodriguez R, Agostini AA, Graeff-Teixeira C. Individual serological follow-up of patients with suspected or confirmed abdominal angiostrongyliasis. Mem Inst Oswaldo Cruz 2008;103:93–7.
[25] Graeff-Teixeira C, Camillo-Coura L, Lenzi HL. Abdominal angiostrongyliasis—an under-diagnosed disease. Mem Inst Oswaldo Cruz 1987;82(Suppl 4):353–4.
[26] Morera P. Angiostrongiliasis abdominal, Un problema de salud pública ? Rev Asoc Guatem Parasitol Med Trop 1987;2: 9–11.
[27] Morera P, Amador JA. Prevalencia de la angiostrongilosis abdominal y la distribución estacional de la precipitación. Rev Costarric Salud Pública 1998;7:1–14.
[28] Mesen-Ramirez P, Abrahams-Sandi E, Fernandez-Quesada K, Morera P. *Angiostrongylus costaricensis* egg antigen for the immunodiagnosis of abdominal angiostrongyliasis. J Helminthol 2008;82:251–4.
[29] Graeff-Teixeira C, Camillo-Coura L, Lenzi HL. Histopathological criteria for the diagnosis of abdominal angiostrongyliasis. Parasitol Res 1991;77:606–11.
[30] Chabaud AG. Description of *Stefanskostrongylus dubosti* n. sp., parasite of Potamogale and attempt at classification of Angiostrongylidae nematodes. Ann Parasitol Hum Comp 1972;47:735–44.
[31] Ubelaker JE. Systematics of species referred to the genus *Angiostrongylus*. J Parasitol 1986;72:237–44.
[32] Baylis HS. On a collection of nematodes from Nigerian mammals (chiefly rodents). Parasitology 1928;20:280–304.
[33] Fontanilla IK, Wade CM. The small subunit (SSU) ribosomal (r) RNA gene as a genetic marker for identifying infective 3rd juvenile stage *Angiostrongylus cantonensis*. Acta Trop 2008;105:181–6.
[34] Caldeira RL, Carvalho OS, Mendonça CL, Graeff-Teixeira C, Silva MC, Ben R, et al. Molecular differentiation of *Angiostrongylus costaricensis*, *A. cantonensis*, and *A. vasorum*

by polymerase chain reaction-restriction fragment length polymorphism. Mem Inst Oswaldo Cruz 2003;98: 1039–43.
[35] Jefferies R, Shaw SE, Viney ME, Morgan ER. *Angiostrongylus vasorum* from South America and Europe represent distinct lineages. Parasitology 2009;136:107–15.
[36] Eamsobhana P, Lim PE, Zhang H, Gan X, Yong HS. Molecular differentiation and phylogenetic relationships of three Angiostrongylus species and *Angiostrongylus cantonensis* geographical isolates based on a 66-kDa protein gene of *A. cantonensis* (Nematoda: Angiostrongylidae). Exp Parasitol 2010;126:564–9.
[37] Mota EM, Lenzi HL. *Angiostrongylus costaricensis* life cycle: a new proposal. Mem Inst Oswaldo Cruz 1995;90:707–9.
[38] Mota EM, Lenzi HL. *Angiostrongylus costaricensis*: complete redescription of the migratory pathways based on experimental *Sigmodon hispidus* infection. Mem Inst Oswaldo Cruz 2005;100:407–20.
[39] Vázquez JJ, Boils PL, Sola JJ, Carbonell F, de Juan Burgueño M, Giner V, et al. Angiostrongyliasis in a European patient: a rare cause of gangrenous ischemic enterocolitis. Gastroenterology 1993;105:1544–9.
[40] Neafie RC, Marty AM. Unusual infections in humans. Clin Microbiol Rev 1993;6:34–56.
[41] Silvera CT, Ghali VS, Roven S, Heimann J, Gelb A. Angiostrongyliasis: a rare cause of gastrointestinal hemorrhage. Am J Gastroenterol 1989;84:329–32.
[42] Loria-Cortes R, Lobo-Sanahuja JF. Clinical abdominal angiostrongylosis. A study of 116 children with intestinal eosinophilic granuloma caused by *Angiostrongylus costaricensis*. Am J Trop Med Hyg 1980;29:538–44.
[43] Lobo Sanahuja F, Loria Cortes R, Gonzalez G. Abdominal angiostrongylosis. Clinical aspects, treatment and review of the literature. Bol Med Hosp Infant Mex 1987;44:4–9.
[44] Graeff-Teixeira C, Camillo-Coura L, Lenzi HL. Clinical and epidemiological aspects of abdominal angiostrongyliasis in southern Brazil. Rev Inst Med Trop Sao Paulo 1991;33:373–8.
[45] Morera P, Perez F, Mora F, Castro L. Visceral larva migrans-like syndrome caused by *Angiostrongylus costaricensis*. Am J Trop Med Hyg 1982;31:67–70.
[46] Duarte Z, Morera P, Vuong PN. Abdominal angiostrongyliasis in Nicaragua: a clinico-pathological study on a series of 12 cases reports. Ann Parasitol Hum Comp 1991;66:259–62.
[47] Vázquez JJ, Sola JJ, Boils PL. Hepatic lesions induced by *Angiostrongylus costaricensis*. Histopathology 1994;25:489–91.
[48] Rodriguez R, Dequi RM, Peruzzo L, Mesquita PM, Garcia E, Fornari F. Abdominal angiostrongyliasis: report of two cases with different clinical presentations. Rev Inst Med Trop Sao Paulo 2008;50:339–41.
[49] Solano-Parada J, Gonzalez-Gonzalez G, Torro LM, dos Santos MF, Espino AM, Burgos M, et al. Effectiveness of intranasal vaccination against *Angiostrongylus costaricensis* using a serine/threonine phosphatase 2 A synthetic peptide and recombinant antigens. Vaccine 2010;28:5185–96.
[50] Harris TW, Antoshechkin I, Bieri T, Blasiar D, Chan J, Chen WJ, et al. WormBase: a comprehensive resource for nematode research. Nucleic Acids Res 2010;38:D463–7.
[51] The_C.elegans_Sequencing_Consortium. Genome sequence of the nematode *C. elegans*: a platform for investigating biology. Science 1998;282:2012–8.
[52] Stein LD, Bao Z, Blasiar D, Blumenthal T, Brent MR, Chen N, et al. The genome sequence of *Caenorhabditis briggsae*: a platform for comparative genomics. PLoS Biol 2003;1:E45.
[53] Ghedin E, Wang S, Spiro D, Caler E, Zhao Q, Crabtree J, et al. Draft genome of the filarial nematode parasite *Brugia malayi*. Science 2007;317:1756–60.
[54] Abad P, Gouzy J, Aury JM, Castagnone-Sereno P, Danchin EG, Deleury E, et al. Genome sequence of the metazoan plant-parasitic nematode *Meloidogyne incognita*. Nat Biotechnol 2008;26:909–15.
[55] Opperman CH, Bird DM, Williamson VM, Rokhsar DS, Burke M, Cohn J, et al. Sequence and genetic map of *Meloidogyne hapla*: A compact nematode genome for plant parasitism. Proc Natl Acad Sci U S A 2008;105:14802–7.
[56] Dieterich C, Clifton SW, Schuster LN, Chinwalla A, Delehaunty K, Dinkelacker I, et al. The *Pristionchus pacificus* genome provides a unique perspective on nematode lifestyle and parasitism. Nat Genet 2008;40:1193–8.
[57] Mitreva M, Jasmer DP, Zarlenga DS, Wang Z, Abubucker S, Martin J, et al. The draft genome of the parasitic nematode *Trichinella spiralis*. Nat Genet 2011;43:228–35.
[58] Shim YH, Paik YK. *Caenorhabditis elegans* proteomics comes of age. Proteomics 2010;10:846–57.
[59] Mitreva M, Zarlenga DS, McCarter JP, Jasmer DP. Parasitic nematodes — from genomes to control. Vet Parasitol 2007;148:31–42.
[60] Barrett J. Forty years of helminth biochemistry. Parasitology 2009:1–10.
[61] Ranganathan S, Garg G. Secretome: clues into pathogen infection and clinical applications. Genome Med 2009;1: 113.
[62] Yatsuda AP, Krijgsveld J, Cornelissen AW, Heck AJ, de Vries E. Comprehensive analysis of the secreted proteins of the parasite *Haemonchus contortus* reveals extensive sequence variation and differential immune recognition. J Biol Chem 2003;278:16941–51.
[63] Robinson M, Gare D, Connolly B. Profiling excretory/secretory proteins of muscle larvae by two-dimensional gel electrophoresis and mass spectrometry. Vet Parasitol 2005;132:37–41.
[64] Robinson MW, Greig R, Beattie KA, Lamont DJ, Connolly B. Comparative analysis of the excretory–secretory proteome of the muscle larva of *Trichinella pseudospiralis* and *Trichinella spiralis*. Int J Parasitol 2007;37:139–48.
[65] Craig H, Wastling JM, Knox DP. A preliminary proteomic survey of the in vitro excretory/secretory products of fourth-stage larval and adult *Teladorsagia circumcincta*. Parasitology 2006;132:535–43.
[66] Moreno Y, Geary TG. Stage- and gender-specific proteomic analysis of *Brugia malayi* excretory–secretory products. PLoS Negl Trop Dis 2008;2:e326.
[67] Hewitson JP, Harcus YM, Curwen RS, Dowle AA, Atmadja AK, Ashton PD, et al. The secretome of the filarial parasite, *Brugia malayi*: proteomic profile of adult excretory–secretory products. Mol Biochem Parasitol 2008;160:8–21.
[68] Bennuru S, Semnani R, Meng Z, Ribeiro JM, Veenstra TD, Nutman TB. *Brugia malayi* excreted/secreted proteins at the host/parasite interface: stage- and gender-specific proteomic profiling. PLoS Negl Trop Dis 2009;3:e410.
[69] Dea-Ayuela MA, Bolas-Fernandez F. Two-dimensional electrophoresis and mass spectrometry for the identification of species-specific *Trichinella* antigens. Vet Parasitol 2005;132:43–9.
[70] Calvo E, Flores-Romero P, Lopez JA, Navas A. Identification of proteins expressing differences among isolates of *Meloidogyne* spp. (Nematoda: Meloidogynidae) by nano-liquid chromatography coupled to ion-trap mass spectrometry. J Proteome Res 2005;4:1017–21.
[71] Yan F, Xu L, Liu L, Yan R, Song X, Li X. Immunoproteomic analysis of whole proteins from male and female adult *Haemonchus contortus*. Vet J 2010;185:174–9.
[72] Islam MK, Miyoshi T, Yokomizo Y, Tsuji N. The proteome expression patterns in adult *Ascaris suum* under exposure to aerobic/anaerobic environments analyzed by two-dimensional electrophoresis. Parasitol Res 2004;93:96–101.
[73] Morgan C, LaCourse EJ, Rushbrook BJ, Greetham D, Hamilton JV, Barrett J, et al. Plasticity demonstrated in the proteome of a parasitic nematode within the intestine of different host strains. Proteomics 2006;6:4633–45.

[74] Thiengo SC, Vicente JJ, Pinto RM. Redescription of *Angiostrongylus (Paranstrongylus) costaricensis* Morera & Céspedes (nematoda: metastrongyloidea) from brazilian strain. Rev Bras Zool 1997;14:839–44.
[75] Ubelaker JE. Systematics of species referred to the genus *Angiostrongylus*. J Parasitol 1986;72:237–44.
[76] Laemmli UK. Cleavage of structural proteins during the assembly of the head of bacteriophage T4. Nature 1970;227: 680–5.
[77] Rocha SL, Neves-Ferreira AG, Trugilho MR, Chapeaurouge A, Leon IR, Valente RH, et al. Crotalid snake venom subproteomes unraveled by the antiophidic protein DM43. J Proteome Res 2009;8:2351–60.
[78] León IR, Neves-Ferreira AGC, Valente RH, Mota EM, Lenzi HL, Perales J. Improved protein identification efficiency by mass spectrometry using N-terminal chemical derivatization of peptides from *Angiostrongylus costaricensis*, a nematode with unknown genome. J Mass Spectrom 2007;42:781–92.
[79] Ma B, Zhang K, Hendrie C, Liang C, Li M, Doherty-Kirby A, et al. PEAKS: powerful software for peptide de novo sequencing by tandem mass spectrometry. Rapid Commun Mass Spectrom 2003;17:2337–42.
[80] Carvalho PC, Fischer JSG, Chen EI, Yates JR, Barbosa VC. PatternLab for proteomics: a tool for differential shotgun proteomics. BMC Bioinformatics 2008;9:316.
[81] Carvalho PC, Fischer JSG, Chen EI, Domont GB, Carvalho MGC, Degrave WM, et al. GO Explorer: A gene-ontology tool to aid in the interpretation of shotgun proteomics data. Proteome Sci 2009;7:6.
[82] McCarthy FM, Wang N, Magee GB, Nanduri B, Lawrence ML, Camon EB, et al. AgBase: a functional genomics resource for agriculture. BMC Genomics 2006;7:229.
[83] Altschul SF, Gish W, Miller W, Myers EW, Lipman DJ. Basic local alignment search tool. J Mol Biol 1990;215:403–10.
[84] Ashburner M, Ball CA, Blake JA, Botstein D, Butler H, Cherry JM, et al. Gene ontology: tool for the unification of biology. The Gene Ontology Consortium. Nat Genet 2000;25:25–9.
[85] Görg A, Weiss W, Dunn MJ. Current two-dimensional electrophoresis technology for proteomics. Proteomics 2004;4:3665–85.
[86] Rabilloud T. Use of thiourea to increase the solubility of membrane proteins in two-dimensional electrophoresis. Electrophoresis 1998;19:758–60.
[87] Ishih A, Rodriguez BO, Sano M. Scanning electron microscopic observations of first and third-stage larvae and adults of *Angiostrongylus costaricensis*. Southeast Asian J Trop Med Public Health 1990;21:568–73.
[88] Carrette O, Burkhard PR, Sanchez JC, Hochstrasser DF. State-of-the-art two-dimensional gel electrophoresis: a key tool of proteomics research. Nat Protoc 2006;1:812–23.
[89] Garcia-Murria MJ, Valero ML, Sanchez del Pino MM. Simple chemical tools to expand the range of proteomics applications. J Proteomics 2011;74:137–50.
[90] Kiel M, Josh P, Jones A, Windon R, Hunt P, Kongsuwan K. Identification of immuno-reactive proteins from a sheep gastrointestinal nematode, *Trichostrongylus colubriformis*, using two-dimensional electrophoresis and mass spectrometry. Int J Parasitol 2007;37:1419–29.
[91] Weinkopff T, Atwood III JA, Punkosdy GA, Moss D, Weatherly DB, Orlando R, et al. Identification of antigenic *Brugia* adult worm proteins by peptide mass fingerprinting. J Parasitol 2009;95:1429–35.
[92] Roberts L, Janovy JJ. Foundations in Parasitology. 5th edition. Chicago, USA: Wm.C.Brown Publishers; 1996. p. 659.
[93] Jolodar A, Fischer P, Bergmann S, Buttner DW, Hammerschmidt S, Brattig NW. Molecular cloning of an alpha-enolase from the human filarial parasite *Onchocerca volvulus* that binds human plasminogen. Biochim Biophys Acta 2003;1627:111–20.
[94] Bernal D, de la Rubia JE, Carrasco-Abad AM, Toledo R, Mas-Coma S, Marcilla A. Identification of enolase as a plasminogen-binding protein in excretory-secretory products of *Fasciola hepatica*. FEBS Lett 2004;563:203–6.
[95] Ramajo-Hernandez A, Perez-Sanchez R, Ramajo-Martin V, Oleaga A. *Schistosoma bovis*: plasminogen binding in adults and the identification of plasminogen-binding proteins from the worm tegument. Exp Parasitol 2007;115:83–91.
[96] Perez-Sanchez R, Valero ML, Ramajo-Hernandez A, Siles-Lucas M, Ramajo-Martin V, Oleaga A. A proteomic approach to the identification of tegumental proteins of male and female *Schistosoma bovis* worms. Mol Biochem Parasitol 2008;161:112–23.
[97] Chiumiento L, Bruschi F. Enzymatic antioxidant systems in helminth parasites. Parasitol Res 2009;105:593–603.
[98] Bell A, Monaghan P, Page AP. Peptidyl-prolyl cis–trans isomerases (immunophilins) and their roles in parasite biochemistry, host–parasite interaction and antiparasitic drug action. Int J Parasitol 2006;36:261–76.
[99] Bridges D, Moorhead GB. 14-3-3 proteins: a number of functions for a numbered protein. Sci STKE 2005;2005:re10.
[100] Siles-Lucas M, Nunes CP, Zaha A, Breijo M. The 14-3-3 protein is secreted by the adult worm of *Echinococcus granulosus*. Parasite Immunol 2000;22:521–8.
[101] McGonigle S, Loschiavo M, Pearce EJ. 14-3-3 proteins in *Schistosoma mansoni*; identification of a second epsilon isoform. Int J Parasitol 2002;32:685–93.
[102] Schechtman D, Tarrab-Hazdai R, Arnon R. The 14-3-3 protein as a vaccine candidate against schistosomiasis. Parasite Immunol 2001;23:213–7.
[103] Graeff-Teixeira C, Agostini AA, Camillo-Coura L, Ferreira-da-Cruz MF. Seroepidemiology of abdominal angiostrongyliasis: the standardization of an immunoenzymatic assay and prevalence of antibodies in two localities in southern Brazil. Trop Med Int Health 1997;2:254–60.
[104] Geiger SM, Graeff-Teixeira C, Soboslay PT, Schulz-Key H. Experimental *Angiostrongylus costaricensis* infection in mice: immunoglobulin isotype responses and parasite-specific antigen recognition after primary low-dose infection. Parasitol Res 1999;85:200–5.
[105] Bender AL, Maurer RL, da Silva MC, Ben R, Terraciano PB, da Silva AC, et al. Eggs and reproductive organs of female *Angiostrongylus costaricensis* are more intensely recognized by human sera from acute phase in abdominal angiostrongyliasis. Rev Soc Bras Med Trop 2003;36:449–54.
[106] Lehman W, Szent-Gyorgyi AG. Regulation of muscular contraction. Distribution of actin control and myosin control in the animal kingdom. J Gen Physiol 1975;66:1–30.
[107] Otey CA, Kalnoski MH, Lessard JL, Bulinski JC. Immunolocalization of the gamma isoform of nonmuscle actin in cultured cells. J Cell Biol 1986;102:1726–37.
[108] Galletta BJ, Cooper JA. Actin and endocytosis: mechanisms and phylogeny. Curr Opin Cell Biol 2009;21:20–7.
[109] Dell A, Haslam SM, Morris HR, Khoo KH. Immunogenic glycoconjugates implicated in parasitic nematode diseases. Biochim Biophys Acta 1999;1455:353–62.
[110] Zugel U, Kaufmann SH. Role of heat shock proteins in protection from and pathogenesis of infectious diseases. Clin Microbiol Rev 1999;12:19–39.
[111] Lindquist S, Craig EA. The heat-shock proteins. Annu Rev Genet 1988;22:631–77.
[112] Suto R, Srivastava PK. A mechanism for the specific immunogenicity of heat shock protein-chaperoned peptides. Science 1995;269:1585–8.

[113] Michalak M, Corbett EF, Mesaeli N, Nakamura K, Opas M. Calreticulin: one protein, one gene, many functions. Biochem J 1999;344(Pt 2):281–92.
[114] Ramírez G, Valck C, Ferreira VP, López N, Ferreira A. Extracellular *Trypanosoma cruzi* calreticulin in the host–parasite interplay. Trends Parasitol 2011;27:115–22.
[115] Park BJ, Lee DG, Yu JR, Jung SK, Choi K, Lee J, et al. Calreticulin, a calcium-binding molecular chaperone, is required for stress response and fertility in *Caenorhabditis elegans*. Mol Biol Cell 2001;12:2835–45.
[116] Rzepecka J, Rausch S, Klotz C, Schnoller C, Kornprobst T, Hagen J, et al. Calreticulin from the intestinal nematode *Heligmosomoides polygyrus* is a Th2-skewing protein and interacts with murine scavenger receptor-A. Mol Immunol 2009;46:1109–19.
[117] Kasper G, Brown A, Eberl M, Vallar L, Kieffer N, Berry C, et al. A calreticulin-like molecule from the human hookworm *Necator americanus* interacts with C1q and the cytoplasmic signalling domains of some integrins. Parasite Immunol 2001;23:141–52.
[118] Winter AD, McCormack G, Page AP. Protein disulfide isomerase activity is essential for viability and extracellular matrix formation in the nematode *Caenorhabditis elegans*. Dev Biol 2007;308:449–61.
[119] Larsen PL, Albert PS, Riddle DL. Genes that regulate both development and longevity in *Caenorhabditis elegans*. Genetics 1995;139:1567–83.
[120] Curran SP, Ruvkun G. Lifespan regulation by evolutionarily conserved genes essential for viability. PLoS Genet 2007;3: e56.
[121] Cassada RC, Russell RL. The dauerlarva, a post-embryonic developmental variant of the nematode *Caenorhabditis elegans*. Dev Biol 1975;46:326–42.
[122] Klass MR. Aging in the nematode *Caenorhabditis elegans*: major biological and environmental factors influencing life span. Mech Ageing Dev 1977;6:413–29.
[123] Leffler H, Carlsson S, Hedlund M, Qian Y, Poirier F. Introduction to galectins. Glycoconj J 2004;19:433–40.
[124] Young AR, Meeusen EN. Galectins in parasite infection and allergic inflammation. Glycoconj J 2004;19:601–6.
[125] Dzik JM. Molecules released by helminth parasites involved in host colonization. Acta Biochim Pol 2006;53:33–64.
[126] Hirabayashi J, Kasai K. The family of metazoan metal-independent beta-galactoside-binding lectins: structure, function and molecular evolution. Glycobiology 1993;3:297–304.
[127] Leffler H. Introduction to galectins. Trends Glycosci Glycotechnol 1997;45:9–19.
[128] Arata Y, Akimoto Y, Hirabayashi J, Kasai K, Hirano H. An immunohistochemical study of the 32-kDa galectin (beta-galactoside-binding lectin) in the nematode *Caenorhabditis elegans*. Histochem J 1996;28:201–7.

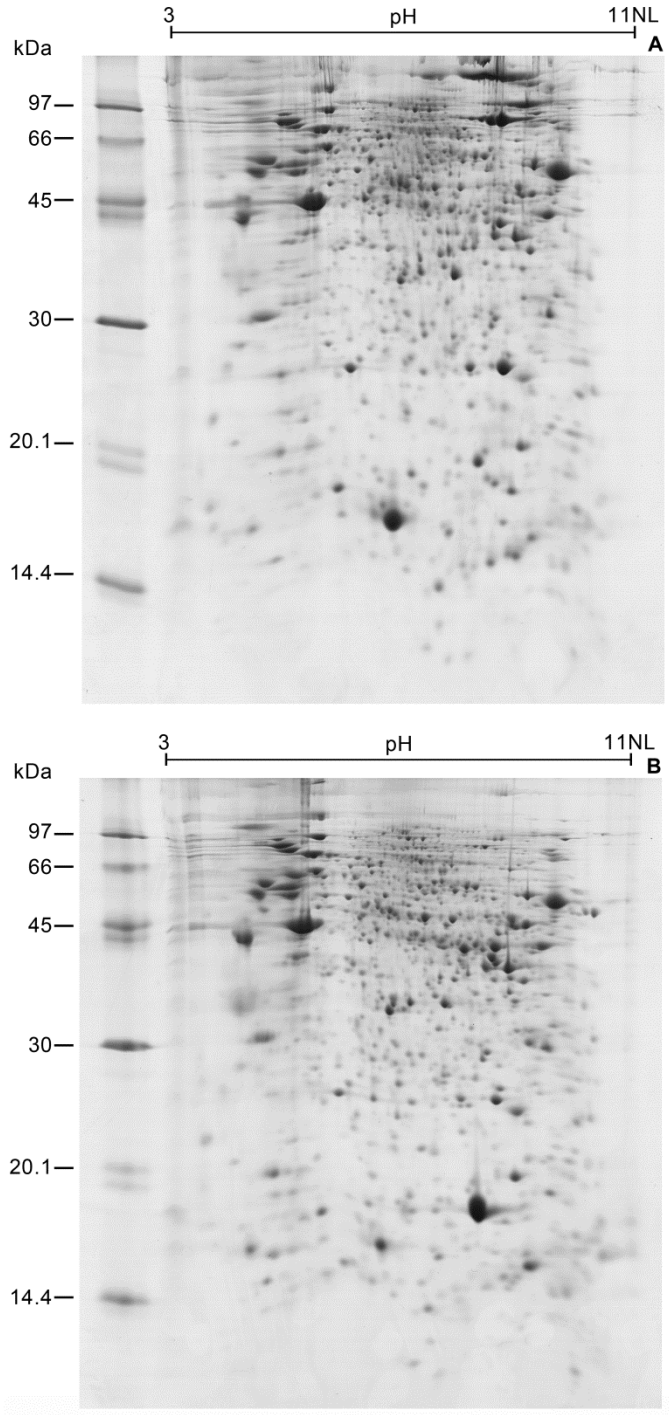

Supplementary Fig. 1. 2-DE gels of total protein extracts from adult *Angiostrongylus costaricensis* nematodes. Proteins (0.2 mg) from female (A) and male (B) worms extracted with solution C were fractionated on 11 cm IPG strips pH 3–11 NL, followed by 15% SDS-PAGE. Gels were run under reducing conditions and stained with colloidal CBB G-250. The migration of molecular mass markers is shown on the acid side of the gel. Gels were run under reducing conditions and stained with colloidal CBB G-250.

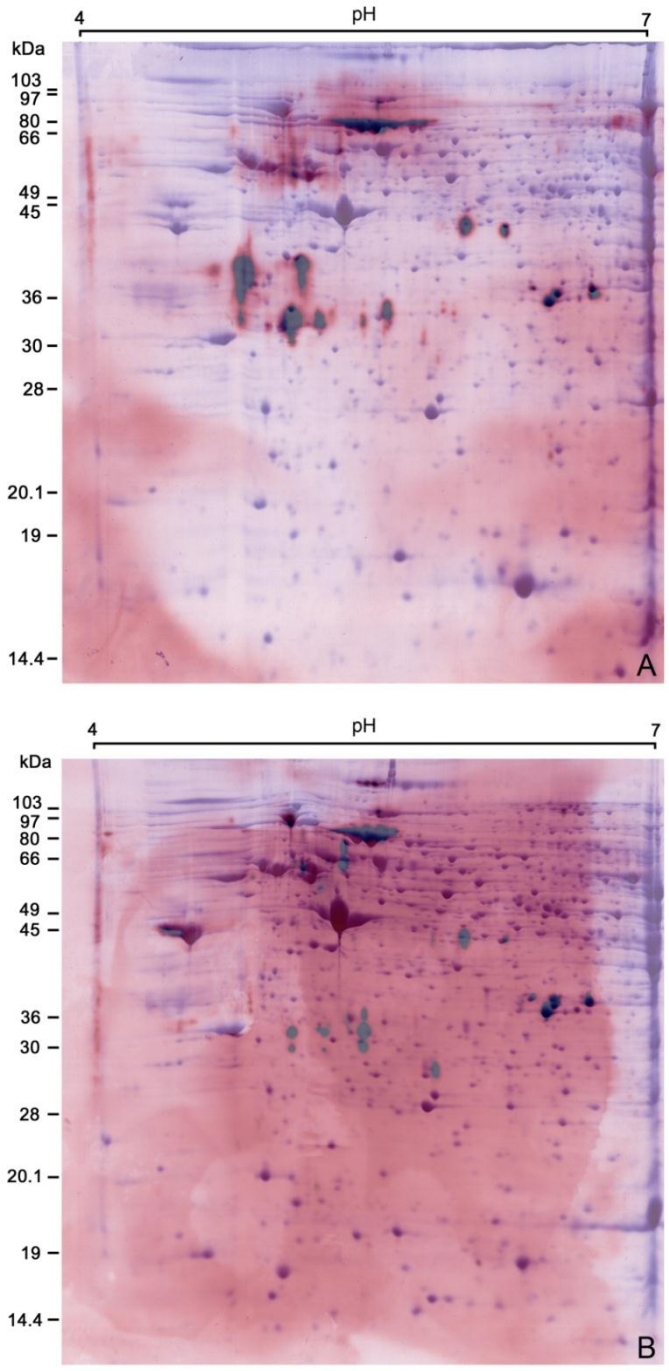

Supplementary Fig. 2. Overlay of 2-DE-immunoblots (red) and Coomassie-stained 2-DE gels (blue) run on 18 cm IPG strips, pH 4–7. (A) Female samples; (B) male samples.

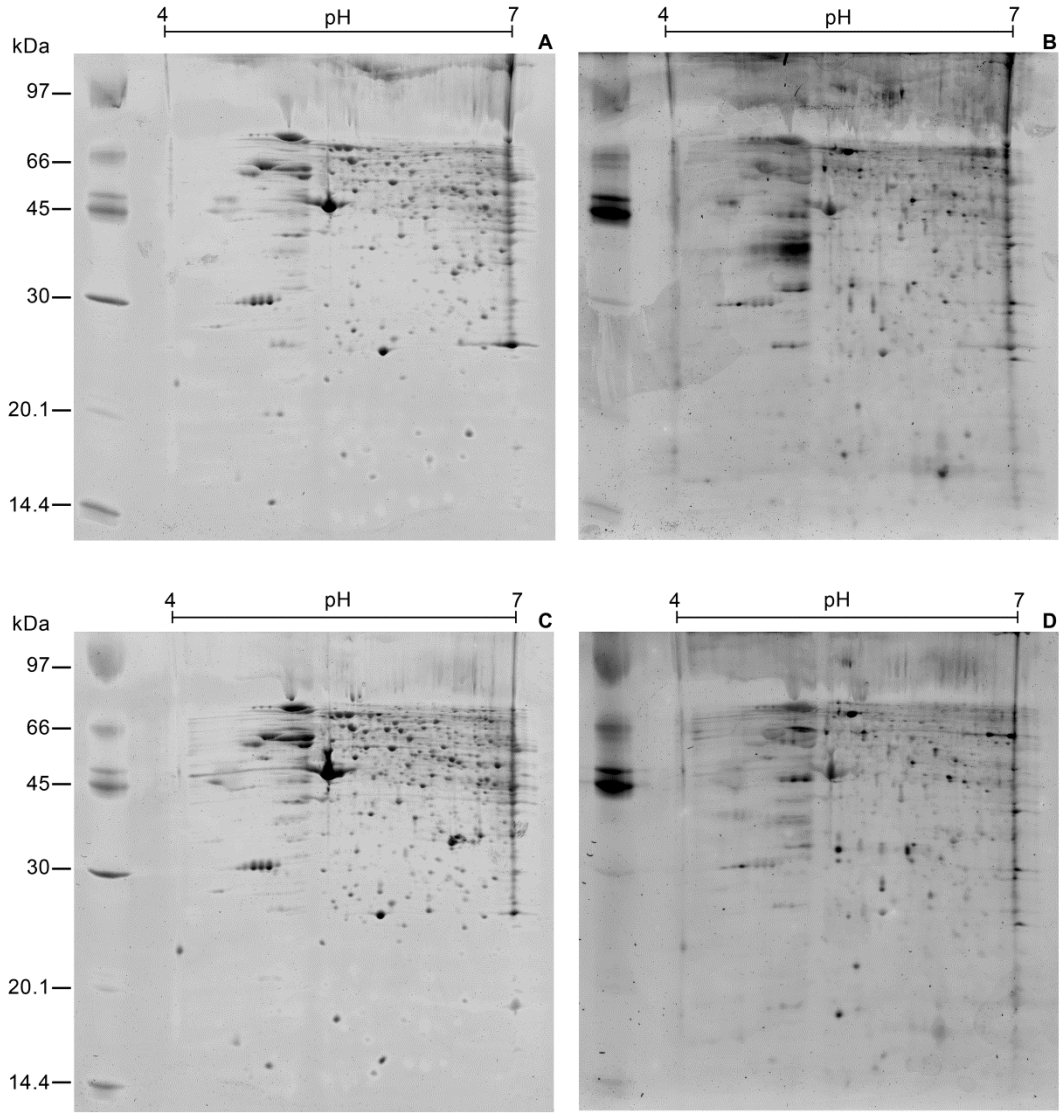

Supplementary Fig. 3. Multiplex analysis of total protein extracts (0.2 mg) from adult *Angiostrongylus costaricensis*nematodes. 2-DE gels were run on 11 cm IPG strips pH 4–7 followed by 15% SDS-PAGE. Proteins from female and male worms were extracted with solution C, precipitated with ethanol/acetone and resolubilized in the same solution without Tris base. The same gel was sequentially stained with Pro-Q (A, C) Emerald and SYPRO Ruby (B, D) fluorescent dyes. Gels were run under reducing conditions.

Supplementary Table 1 - Detailed list of the most abundant protein spots of *A. costaricensis* adult extracts identified by MALDI-PSD MS. The letter M placed after the spot number indicates male proteins. Numbers without a letter refer to female proteins. Protein analysis was performed by running the Mascot search engine against the NCBInr database. Peptides equally identified by the Peaks search engine are indicated.

Spot no.	Protein name	Protein ID (NCBI)	Mascot protein score	Mascot ion score	Peaks	MS/MS sequences	Precursor mass (Da)	Mass error (ppm)	No. peptides	Protein family
1	Heat shock protein [*Bursaphelenchus xylophilus*]	gi|110433182	408	69	X	K.VEIIANDQGNR.T	1227.6207	20,30	4	Heat shock protein (HsP)
				40	X	K.SQVNDIVLVGGSTR.I	1443.7682	11,90		
				63	X	R.TTPSYVAFTDTER.L	1486.6940	11,20		
				120	X	K.SQVNDIVLVGGSTR.I + SPITC (N-term)	1658.7393	-15.15		
				92	X	K.STAGDTHLGGEDFDNR.M	1690.7183	6,68		
				107	X	R.TTPSYVAFTDTER.L + SPITC (N-term)	1701.6651	-11.79		
				111	X	K.STAGDTHLGGEDFDNR.M + SPITC (N-term)	1905.6894	-9.70		
1M	Hsp70 protein [*Mitsukurina owstoni*]	gi|21427320	106	20	X	K.AVITVPAYFNDSQR.Q	1579.7995	3,21	3	Heat shock protein (HsP)
				28	X	K.STAGDTHLGGEDFDNR.M	1690.7183	-1.95		
				86	X	K.STAGDTHLGGEDFDNR.M + SPITC (N-term)	1905.6894	-19.67		
2	Heat shock protein 70A [*Caenorhabditis elegans*]	gi|156352	325	28	X	K.VEIIANDQGNR.T	1227.6207	30,00	4	Heat shock protein (HsP)
				77	X	K.DAGAIAGLNVLR.I + SPITC (N-term)	1383.6275	16,30		
				117	X	K.VEIIANDQGNR.T + SPITC (N-term)	1442.5918	1,94		
				37	X	R.TTPSYVAFTDTER.L	1486.6940	25,40		
				32	X	K.STAGDTHLGGEDFDNR.M	1690.7183	22,00		
				94	X	K.STAGDTHLGGEDFDNR.M + SPITC (N-term)	1905.6894	0,74		
2M	Heat shock protein [*Bursaphelenchus xylophilus*]	gi|110433182	408	39	X	R.FEELCADLFR.N + Carbamidomethyl (C)	1298.5965	8.25	4	Heat shock protein (HsP)
				86	X	K.DAGAIAGLNVLR.I + SPITC (N-term)	1383.6275	-11,75		
				67	X	R.FEELCADLFR.N + Carbamidomethyl (C); SPITC (N-term)	1513.5676	0.61		
				136	X	K.SQVNDIVLVGGSTR.I + SPITC (N-term)	1658.7393	-18.71		
				32	X	K.STAGDTHLGGEDFDNR.M	1690.7183	2.13		
				93	X	K.STAGDTHLGGEDFDNR.M + SPITC (N-term)	1905.6894	-11.12		
3	Heat shock protein 90 [*Haemonchus contortus*]	gi|255091016	355	35	X	K.TKPIWTR.N	900.5181	25,10	6	Heat shock protein (HsP)
				34	X	R.ALLFVPQR.A	942.5651	16,70		
				55	X	K.LGIHEDSTNR.K	1140.5523	10,90		
				68	X	R.ALLFVPQR.A + SPITC (N-term)	1157.5362	-12.82		
				38	X	K.DAVANSAFVER.V	1177.5727	3,81		
				67	X	K.EDQTEVLEER.R	1246.5677	2,98		
				82	X	K.LGIHEDSTNR.K + SPITC (N-term)	1355.5234	-13.43		
				65	X	K.GVVDSEDLPLNISR.E	1512.7784	3,00		
3M	Putative abnormal DAuer formation family member [*Angiostrongylus cantonensis*]	gi|256251566	419	28		R.ALLFVPQR.A	942.5651	31,20	6	
				45		K.MAEFLR.Y + SPITC (N-term)	980.3554	9.39		
				72	X	R.ALLFVPQR.A + SPITC (N-term)	1157.5362	-5.56		
				42		K.HFSVEGQLEFR.A	1347.6572	21,40		
				76		K.LGIHEDSTNR.K + SPITC (N-term)	1355.5234	-11.29		
				95	X	K.DAVANSAFVER.V + SPITC (N-term)	1392.5438	-10.12		
				23		K.GVVDSEDLPLNISR.E	1512.7784	8.36		
				90	X	K.GVVDSEDLPLNISR.E + SPITC (N-term)	1727.7495	-32.49		
4	Actin [*Caenorhabditis elegans*]	gi|6626	538	60	X	K.AGFAGDDAPR.A	975.4410	30,10	6	Actin
				63	X	R.GYSFTTTAER.E	1131.5197	24,30		
				90	X	R.GYSFTTTAER.E + SPITC (N-term)	1346.4907	5,93		
				33	X	R.AVFPSIVGRPR.H + SPITC (N-term)	1412.6693	23,70		
				65	X	K.QEYDESGPSIVHR.K	1515.6954	36,80		
				65	X	K.IWHHTFYNELR.V + SPITC (N-term)	1729.7130	13,00		
				115	X	K.SYELPDGQVITVGNER.F	1775.8690	24,60		

4M	Actin [*Caenorhabditis elegans*]	gi|6626	402	30	X	K.IIAPPER.K + SPITC (N-term)	1009.4361	21,10	5	Actin
				82	X	K.AGFAGDDAPR.A + SPITC (N-term)	1190.4121	7.84		
				95	X	R.GYSFTTTAER.E + SPITC (N-term)	1346.4907	12,00		
				30	X	K.QEYDESGPSIVHR.K	1515.6954	32,60		
				80	X	K.QEYDESGPSIVHR.K + SPITC (N-term)	1730.6665	6.68		
				115	X	K.SYELPDGQVITVGNER.F + SPITC (N-term)	1990.8401	-0.88		
5	Actin [*Caenorhabditis elegans*]	gi|6626	412	61	X	K.AGFAGDDAPR.A	975.4410	25,20	6	Actin
				55	X	R.GYSFTTTAER.E	1131.5197	19,60		
				86	X	R.GYSFTTTAER.E + SPITC (N-term)	1346.4907	-0.60		
				33	X	R.AVFPSIVGRPR.H + SPITC (N-term)	1412.6693	17,80		
				64	X	K.QEYDESGPSIVHR.K	1515.6954	33,30		
				55	X	K.IWHHTFYNELR.V + SPITC (N-term)	1729.7130	9.64		
				113	X	K.SYELPDGQVITVGNER.F	1775.8690	21,10		
6	Actin [*Caenorhabditis elegans*]	gi|6626	412	71	X	K.AGFAGDDAPR.A	975.4410	34,20	6	Actin
				68	X	R.GYSFTTTAER.E	1131.5197	29,00		
				90	X	R.GYSFTTTAER.E + SPITC (N-term)	1346.4907	13,10		
				29	X	R.AVFPSIVGRPR.H + SPITC (N-term)	1412.6693	27,70		
				61	X	K.QEYDESGPSIVHR.K	1515.6954	42,90		
				89	X	K.QEYDESGPSIVHR.K + SPITC (N-term)	1730.6665	30,20		
				99	X	K.SYELPDGQVITVGNER.F	1775.8690	31,60		
7	Elongation factor 1 alpha [*Hylesinus varius*]	gi|12007194	141	49	X	K.GWTVER.K + SPITC (N-term)	961.3422	22,20	2	Ras_like_GTPase
				47	X	K.IGGIGTVPVGR.V	1024.6030	38,90		
9	Heat Shock Protein family member (Hsp-60) [*Caenorhabditis elegans*]	gi|17555558	191	34	X	K.APGFGDNRK.N + SPITC (N-term)	1175.4488	3.93	4	Heat Shock Protein (HsP)
				73	X	R.VTDALCATR.A + Carbamidomethyl (C); SPITC (N-term)	1220.4624	12,60		
				61	X	R.AAVEEGIVPGGGVALLR.S	1606.9043	28,50		
				22		K.ANEEAGDGTTCATVLAR.A + Propionamide ©	1748.7999	26,00		
9M	Putative heat shock protein [*Angiostrongylus cantonensis*]	gi|256251570	149	48	X	K.EDTLLLR.G + SPITC (N-term)	1073.4521	29,00	3	Chaperonin_like
				72	X	R.VTDALCATR.A + Carbamidomethyl (C); SPITC (N-term)	1220.4624	24,00		
				29	X	R.AAVEEGIVPGGGVALLR.S	1606.9043	34,40		
10	Calreticulin [*Necator americanus*]	gi|3687326	96	48	X	K.AHAAETFEK.L	1002.4770	30,40	2	Calreticulim
				49	X	K.KPEDWDER.E	1073.4778	39,80		
10M	Calreticulin [*Wucheria bancrofti*]	gi|164604795	60	41	X	GEWKPK + SPITC (N-term)	958.3677	18,15	2	Calreticulim
				60	X	KPEDWDER	1073.4778	16,94		
11	RecName: Full=Tropomyosin, muscle [*Trichostrongylus colubriformis*]	gi|136098	246	51	X	K.IVELEEELR.V	1128.6026	33,50	4	Tropomyosin
				39	X	R.MTLLEEELER.A	1261.6224	20,60		
				82	X	K.IVELEEELR.V + SPITC (N-term)	1343.5737	5,75		
				85	X	K.VQEAEAEVAALNR.R	1398.7103	28,60		
				40	X	K.EVDRLEDELVHEK.E + SPITC (N-term)	1824.7658	9,59		
11M	Tropomyosin [*Ascaris lumbricoides*]	gi|154466686	373	49	X	R.AEFAER.S + SPITC (N-term)	936.3106	-13.52	7	Tropomyosin
				39	X	K.IVELEEELR.V	1128.6026	-11.07		
				31	X	R.MTLLEEELER.A	1261.6224	-22.94		
				46	X	K.IEKDNALDR.A + SPITC (N-term)	1287.5223	-25.64		
				88	X	K.IVELEEELR.V + SPITC (N-term)	1343.5737	-35.93		
				57		K.VQEAEAEVAALNR.R	1398.7103	-14.11		
				75	X	R.MTLLEEELER.A + SPITC (N-term)	1476.5934	-43.02		
				32	X	K.KVQEAEAEVAALNR.R	1526.8052	-10.02		
				26	X	K.EVDRLEDELVHEK.E + SPITC (N-term)	1824.7658	-30.20		
12	Fourteen-three-three family member (ftt-2) [*Caenorhabditis elegans*]	gi|17568359	192	72	X	K.MQPTHPIR.L + SPITC (N-term)	1193.4780	44,30	2	14_3_3
				49	X	K.MQPTHPIR.L + Oxidation (M); SPITC (N-term)	1209.4729	39,10		
				120	X	K.VTELGAELSNEER.N + SPITC (N-term)	1660.6709	30,30		

12M	14-3-3b protein [*Meloidogyne incognita*]	gi|40388674	427	29	X	K.MQPTHPIR.L	978.5069	26.9	6	14_3_3
				60	X	K.LAEQAER.Y + SPITC (N-term)	1030.3848	-0.06		
				30	X	K.MKGDYYR.Y + SPITC (N-term)	1146.3933	-7.18		
				63	X	K.MQPTHPIR.L + SPITC (N-term)	1193.4780	-2.99		
				37	X	K.MQPTHPIR.L + Oxidation (M); SPITC (N-term)	1209.4729	-8.67		
				57	X	K.DSTLIMQLLR.D + SPITC (N-term)	1443.6247	-6,12		
				28	X	K.VTELGAELSNEER.N	1445.6998	10,70		
				114	X	K.VTELGAELSNEER.N + SPITC (N-term)	1660.6709	-14.77		
				77	X	K.SQQSYQEAFDIAK.D + SPITC (N-term)	1728.6759	-22.11		
13	Putative heat shock protein [*Angiostrongylus cantonensis*]	gi|256251570	143	56	X	K.EDTLLLR.G + SPITC (N-term)	1073.4521	16,70	3	
				67	X	R.VTDALCATR.A + Carbamidomethyl (C); SPITC (N-term)	1220.4624	14,10		
				20	X	R.AAVEEGIVPGGGVALLR.S	1606.9043	22,70		
14	Methionine adenosyltransferase [*Obelia sp* . KJP-2004]	gi|46909373	142	53	X	R.SAAYAAR.W + SPITC (N-term)	923.3265	16,80	2	S_AdoMet_syntM
				89	X	R.MDGGACIPLR.V + Carbamidomethyl (C); Oxidation (M); SPITC (N-term)	1319.4767	35,20		
15	COLlagen family member (col-71) *[Caenorhabditis elegans]*	gi|17537301	56	56	X	K.DGGIFFEDGTR.R	1212.5411	47,60	1	Col_cuticule_N
16	CCT-2 [*Caenorhabditis elegans*]	gi|1046266	94	37	X	R.IHPQTIISGYR.R	1283.6986	31.30	1	Chaperonin_like
				94	X	R.IHPQTIISGYR.R + SPITC (N-term)	1498.6697	-12.99		
16M	CCT-2 [*Caenorhabditis elegans*]	gi|1046266	81	81	X	R.IHPQTIISGYR.R + SPITC (N-term)	1498.6697	-29.41	1	Chaperonin_like
17	Chaperonin Containing TCP-1 family member (cct-5) [*Caenorhabditis elegans*]	gi|25144674	213	63	X	K.SHILAAR.A + SPITC (N-term)	981.4160	10,40	3	Chaperonin_like
				57	X	K.AVTIFVR.G + SPITC (N-term)	1019.4569	9,08		
				94	X	R.EQISLATQVVR.M + SPITC (N-term)	1457.6643	2,23		
17M	Chaperonin Containing TCP-1 family member (cct-5) [*Caenorhabditis elegans*]	gi|25144674	214	49	X	K.SHILAAR.A + SPITC (N-term)	981.4160	-22.85	3	Chaperonin_like
				57	X	K.AVTIFVR.G + SPITC (N-term)	1019.4569	-17.99		
				108	X	R.EQISLATQVVR.M + SPITC (N-term)	1457.6643	-34.95		
18	Chaperonin Containing TCP-1 family member (cct-7) [*Caenorhabditis elegans*]	gi|17564182	100	29		R.GGAEQFIAETER.S	1306.6153	28,90	1	Chaperonin_like
				100	X	R.GGAEQFIAETER.S + SPITC (N-term)	1521.5864	-1.31		
20	Protein disulfide isomerase [*Ancylostoma caninum*]	gi|46249431	235	54	X	K.SHNLLFVSK.E	1043.5764	36,70	5	ER_PDI
				60	X	K.NFDQVAR.D + SPITC (N-term)	1063.3851	41,30		
				61	X	K.VIDYTGDR.T + SPITC (N-term)	1152.4216	29,30		
				59	X	K.YADHENIIIAK.M	1285.6666	28,20		
				60	X	K.YADHENIIIAK.M + SPITC (N-term)	1500.6377	18,80		
20M	Protein disulfide isomerase [*Ancylostoma caninum*]	gi|46249431	142	51	X	K.NFDQVAR.D + SPITC (N-term)	1063.3851	-23.81	3	Thiredoxin_like
				64	X	K.VIDYTGDR.T + SPITC (N-term)	1152.4216	-29.05		
				28	X	K.YADHENIIIAK.M + SPITC (N-term)	1500.6377	-48.36		
22	Peroxiredoxin [*Haemonchus contortus*]	gi|47499100	300	50	X	K.DDEGIAYR.G	937.4141	33,90	4	Thioredoxin_like
				60	X	R.SVDETLR.L + SPITC (N-term)	1033.3845	9.53		
				67	X	K.HGEVCPAGWTPGK.E + Carbamidomethyl (C)	1394.6401	9.53		
				123	X	K.DYGVLKDDEGIAYR.G + SPITC (N-term)	1827.7444	10.60		
23	Peroxiredoxin [*Haemonchus contortus*]	gi|47499100	302	54	X	K.DDEGIAYR.G	937.4141	33,90	4	Thioredoxin_like
				60	X	R.SVDETLR.L + SPITC (N-term)	1033.3845	9,53		
				65	X	K.HGEVCPAGWTPGK.E + Carbamidomethyl (C)	1394.6401	15,90		
				123	X	K.DYGVLKDDEGIAYR.G + SPITC (N-term)	1827.7444	10,60		
23M	Peroxiredoxin [*Haemonchus contortus*]	gi|47499100	202	41	X	K.DDEGIAYR.G	937.4141	38,20	3	Thiredoxin_like
				32	X	R.GLFIIDPK.G + SPITC (N-term)	1116.4984	1.47		
				22	X	K.DYGVLKDDEGIAYR.G	1612.7733	29,30		
				129	X	K.DYGVLKDDEGIAYR.G + SPITC (N-term)	1827.7444	3.64		

24	Hypothetical protein Rsph17025_3168 [*Rhodobacter sphaeroides* ATCC 17025]	gi|146279199	61	61		R.QSDFDRFER.A	1198.5367	-32.93	1	WHTH_gntR
25	Galectin [*Teladorsagia circumcincta*]	gi|1935060	250	117	X	R.NSLISNEWGNEER.E + SPITC (N-term)	1761.6722	-32.54	4	GLECT
				50	X	K.ELKEYEHR.L + SPITC (N-term)	1317.5118	-20.60		
				72	X	K.GEWGKEER.K + SPITC (N-term)	1204.4277	-27.15		
				36	X	K.EYEHR.L + SPITC (N-term)	947.2902	-5.62		
25M	Galectin [*Teladorsagia circumcincta*]	gi|1935060	81	32	X	K.EYEHR.L + SPITC (N-term)	947.2902	-44.08	2	GLECT
				49	X	R.NSLISNEWGNEER.E	1546.7012	-46.83		
26	Translationally controlled tumor protein [*Ostertagia ostertagi*]	gi|215262522	142	49	X	R.GIDIVLNHK.L	1007.5764	-5.13	4	TCTP
				63	X	R.GIDIVLNHK.L + SPITC (N-term)	1222.5475	-16.14		
				79	X	R.MAEGAGDGQVAIIEYR.D	1678.7984	12,70		
				53	X	R.MAEGAGDGQVAIIEYR.D + Oxidation (M)	1694.7934	-1.56		
27	D-aminoacylase domain protein [*Gemmata obscuriglobus* UQM 2246]	gi|168703938	61	27		K.IAAVGMVGKVEGAR.E + Oxidation (M)	1372.7497	-25.31	1	Metalllo-dependent hydrolases
				61		K.IAAVGMVGKVEGAR.E + Oxidation (M); SPITC (N-term)	1587.7207	-46.88		
28	C. briggsae CBR-MLC-2.2 protein [*Caenorhabditis briggsae*]	gi|268577393	93	52		K.EAFGIMDQNK.D + Oxidation (M)	1167.5230	-5.13	4	EFH
				41		K.RGEPLDEDEIK.A	1299.6306	6,54		
				41		K.EAFGIMDQNK.D + Oxidation (M); SPITC (N-term)	1382.4941	-18.57		
				20		K.RGEPLDEDEIK.A + SPITC (N-term)	1514.6017	-18.88		
32	Actin [*Caenorhabditis elegans*]	gi|6626	447	48	X	K.AGFAGDDAPR.A	975.4410	20,60	7	Actin
				47	X	K.IIAPPER.K + SPITC (N-term)	1009.4361	3,40		
				55	X	R.GYSFTTTAER.E	1131.5197	17,30		
				43	X	K.IIAPPERK.Y + SPITC (N-term)	1137.5311	-3.98		
				82	X	K.AGFAGDDAPR.A + SPITC (N-term)	1190.4121	-10.31		
				90	X	R.GYSFTTTAER.E + SPITC (N-term)	1346.4907	-5.58		
				47	X	R.AVFPSIVGRPR.H + SPITC (N-term)	1412.6693	8,86		
				108	X	K.QEYDESGPSIVHR.K	1515.6954	15,90		
				111	X	K.QEYDESGPSIVHR.K + SPITC (N-term)	1730.6665	0,67		
				78	X	K.SYELPDGQVITVGNER.F	1775.8690	16,70		
33	As37 [*Ascaris suum*]	gi|22036079	289	68	X	K.APHFPQQPVAR.Q	1246.6571	33.20	4	Ig
				60	X	K.APHFPQQPVAR.Q	1325.5744	27,20		
				52	X	K.FEVPQGAPTFTR.K	1348.6776	31.00		
				61	X	K.APHFPQQPVAR.Q + SPITC (N-term)	1461.6282	12,20		
				101	X	R.DDGQVMVMEFR.A + SPITC (N-term)	1540.5455	13,70		
				120	X	K.FEVPQGAPTFTR.K + SPITC (N-term)	1563.6487	8.94		
				59	X	R.DDGQVMVMEFR.A + 2 Oxidation (M); SPITC (N-term)	1572.5353	6.54		
33M	As37 [*Ascaris suum*]	gi|22036079	264	42	X	K.APHFPQQPVAR.Q	1246.6571	-16.12	4	Ig
				49	X	K.DAGQFVCTAK.N + Carbamidomethyl (C); SPITC (N-term)	1310.4730	33,10		
				34	X	R.DDGQVMVMEFR.A	1325.5744	13,40		
				16	X	K.FEVPQGAPTFTR.K	1348.6776	24,70		
				59	X	K.APHFPQQPVAR.Q + SPITC (N-term)	1461.6282	-4.21		
				76	X	R.DDGQVMVMEFR.A + SPITC (N-term)	1540.5455	-4.21		
				87	X	K.FEVPQGAPTFTR.K + SPITC (N-term)	1563.6487	-12.74		
				67	X	R.DDGQVMVMEFR.A + 2 Oxidation (M); SPITC (N-term)	1572.5353	-14.83		

34	As37 [*Ascaris suum*]	gi|22036079	289	68	X	K.APHFPQQPVAR.Q	1246.6571	33,20	4	Ig
				60	X	R.DDGQVMVMEFR.A	1325.5744	27,20		
				52	X	K.FEVPQGAPTFTR.K	1348.6776	31,00		
				61	X	K.APHFPQQPVAR.Q + SPITC (N-term)	1461.6282	12,20		
				101	X	R.DDGQVMVMEFR.A + SPITC (N-term)	1540.5455	13,70		
				120	X	K.FEVPQGAPTFTR.K + SPITC (N-term)	1563.6487	8,94		
				59	X	R.DDGQVMVMEFR.A + 2 Oxidation (M); SPITC (N-term)	1572.5353	6,54		
34M	As37 [*Ascaris suum*]	gi|22036079	291	61	X	K.APHFPQQPVAR.Q	1246.6571	6,20	4	Ig
				38	X	K.DAGQFVCTAK.N + Carbamidomethyl (C); SPITC (N-term)	1310.4730	-13.94		
				40	X	R.DDGQVMVMEFR.A	1325.5744	-5.88		
				38	X	K.FEVPQGAPTFTR.K	1348.6776	3,75		
				74	X	K.APHFPQQPVAR.Q + SPITC (N-term)	1461.6282	-19.74		
				89	X	R.DDGQVMVMEFR.A + SPITC (N-term)	1540.5455	-21.47		
				91	X	K.FEVPQGAPTFTR.K + SPITC (N-term)	1563.6487	-23.62		
				84	X	R.DDGQVMVMEFR.A + 2 Oxidation (M); SPITC (N-term)	1572.5353	-27.16		
35	Putative Lin-5 (Five) Interacting protein [*Angiostrongylus cantonensis*]	gi|256016521	64	44	X	K.GSCDHCPIPR.T + 2 Carbamidomethyl ©	1197.5019	15,90	1	Collagen
				64	X	K.GSCDHCPIPR.T + 2 Carbamidomethyl (C); SPITC (N-term)	1412.4730	-5.58		
36	Putative Lin-5 (Five) Interacting protein [*Angiostrongylus cantonensis*]	gi|256016521	72	24	X	K.GSCDHCPIPR.T + 2 Carbamidomethyl ©	1197.5019	19,10	1	Collagen
				72	X	K.GSCDHCPIPR.T + 2 Carbamidomethyl (C); SPITC (N-term)	1412.4730	-16.14		
37	Putative Lin-5 (Five) Interacting protein [*Angiostrongylus cantonensis*]	gi|256016521	56	32	X	K.GSCDHCPIPR.T + 2 Carbamidomethyl (C); SPITC (N-term)	1197.5019	30,30	1	Colagen
				56	X	K.GSCDHCPIPR.T + 2 Carbamidomethyl (C); SPITC (N-term)	1412.4730	3,06		
39	Ribosomal protein, small subunit family member (rps-0) [*Caenorhabditis elegans*]	gi|17554768	245	49	X	R.EILILR.G + SPITC (N-term)	970.4616	4,29	4	RPS2
				68	X	R.LLVISDPR.I + SPITC (N-term)	1126.5151	-11.16		
				64	X	K.FAAHTGATAIFGR.F	1318.6782	11,30		
				127	X	K.FAAHTGATAIFGR.F + SPITC (N-term)	1533.6493	-7.16		
40	Stress-induced-phosphoprotein 1 *[Ascaris suum]*	gi|324512662	100	48	X	K.LMEFQR.A + SPITC (N-term)	1037.3769	30.6	2	TPR
				38		K.LMEFQR.A + Oxidation (M); SPITC (N-term)	1053.3718	23,90		
				52	X	R.EAGIIQMR.- + SPITC (N-term)	1131.4511	19,60		
41	Enolase [Haemonchus contortus]	gi|301015486	66	18	X	K.NFCVTQQR.D + Carbamidomethyl (C)	1051.4869	29,90	1	TIM_phosphatase binding
				66	X	K.NFCVTQQR.D + Carbamidomethyl (C); SPITC (N-term)	1266.4580	2,14		
41M	Enolase [*Haemonchus contortus*]	gi|301015486	207	65	X	K.NFCVTQQR.D + Carbamidomethyl (C); SPITC (N-term)	1266.4580	0.33	2	TIM_phosphatase binding
				142	X	R.AAVPSGASTGVHEALELR.D + SPITC (N-term)	1978.8877	1.89		
42	RecName: Full=32 kDa beta-galactoside-binding lectin; AltName: Full=Galectin-1	gi|6225602	362	47	X	K.GDSFDIR.I + SPITC (N-term)	1023.3426	-14.36	5	GLECT
				53	X	R.FTSFAHR.Q + SPITC (N-term)	1079.3953	-11.30		
				29	X	K.EFKDYEHR.L	1122.5094	5,99		
				68	X	K.EFKDYEHR.L + SPITC (N-term)	1337.4805	-16.87		
				64	X	R.NGDIALHFNPR.F + SPITC (N-term)	1467.6023	-12.00		
				40	X	K.SADFSGNDVPLHISVR.F	1712.8482	-0.51		
				134	X	K.SADFSGNDVPLHISVR.F + SPITC (N-term)	1927.8193	-18.55		
42M	RecName: Full=32 kDa beta-galactoside-binding lectin; AltName: Full=Galectin-1	gi|6225602	220	24	X	K.DYEHR.L + SPITC (N-term)	933.2745	28,10	4	GLECT
				53	X	K.GDSFDIR.I + SPITC (N-term)	1023.3426	7.43		
				50	X	R.FTSFAHR.Q + SPITC (N-term)	1079.3953	17,40		
				94	X	K.SADFSGNDVPLHISVR.F + SPITC (N-term)	1927.8193	-2.63		

43	PREDICTED: similar to mitochondrial truncated thioredoxin-dependent peroxide reductase precursor [*Strongylocentrotus purpuratus*]	gi|115712104	115	35	X	R.GLFLIDPEGVVR.H	1313.7343	13,20	3	Thioredoxin_like
				115	X	R.GLFLIDPEGVVR.H + SPITC (N-term)	1528.7054	-5.58		
				69		R.SVDEALR.L + SPITC (N-term)	1003.3739	2,61		
48	Predicted protein [*Laccaria bicolor* S238N-H82]	gi|170093093	164	26	X	K.HVVFGK.V + SPITC (N-term)	900.3622	4,86	3	Cyclophilin
				49	X	K.SIYGDR.F + SPITC (N-term)	924.3106	13,10		
				24	X	K.NFMIQGGDFTR.G	1284.5921	22,90		
				90	X	K.NFMIQGGDFTR.G + SPITC (N-term)	1499.5632	6,15		
				89	X	K.NFMIQGGDFTR.G + Oxidation (M); SPITC (N-term)	1515.5581	-0.86		
49	ABC transporter related [*Pyrobaculum islandicum* DSM 4184]	gi|119871557	69	49	X	R.VELATVLAQRPR.V	1351.7936	22,00	1	P_loop NTPase
				69	X	R.VELATVLAQRPR.V + SPITC (N-term)	1566.7646	-1,36		
50	Hypothetical protein T05E11.3 [*Caenorhabditis elegans*]	gi|17542208	171	61		K.TFEINPR.H + SPITC (N-term)	1090.4212	12,40	3	HATPase_c
				38		K.AEKHEFQAEVNR.M	1456.7059	-4.35		
				49		R.GIVDSDDLPLNVSR.E	1498.7627	14,70		
				61		K.AEKHEFQAEVNR.M + SPITC (N-term)	1671.6769	-20.83		
52	NAD-dependent epimerase/dehydratase *[Micromonospora aurantiaca ATCC 27029]*	gi|302866601	59	59	X	R.ATVEWFR.S + SPITC (N-term)	1122.4263	-28.03	1	NADB_Rossman
54	20S proteasome alpha5 subunit *[Brugia malayi]*	gi|170588333	154	59	X	K.LGSTSLGIR.T + SPITC (N-term)	1117.4896	9,41	2	Ntn_hydrolase
				95		R.GVNTFSPEGR.I + SPITC (N-term)	1277.4805	3,45		
56	hypothetical protein F17C11.9 *[Caenorhabditis elegans]*	gi|17559824	58	58	X	R.TYLVGER.I + SPITC (N-term)	10.514.103	33,00	1	GST_C
57	Glutamate--ammonia ligase [*Homo sapiens*]	gi|31831	96	29	X	R.FILHR.V + SPITC (N-term)	899.3782	21,00	2	GLn_synt_C
				25	X	R.DIVEAHYR.A	1001.4930	29,20		
				67	X	R.DIVEAHYR.A + SPITC (N-term)	1216.4641	-0.73		
57M	Glutamate--ammonia ligase [*Homo sapiens*]	gi|31831	97	30	X	R.FILHR.V + SPITC (N-term)	899.3782	21,00	2	GLn_synt_C
				67	X	R.DIVEAHYR.A	1216.4641	-0.73		
58	Enolase [*Haemonchus contortus*]	gi|301015486	242	45	X	R.QIYDSR.G + SPITC (N-term)	995.3477	29,70	3	TIM_phosphatase binding
				40	X	K.NFCVTQQR.D + Carbamidomethyl (C); SPITC (N-term)	1266.4580	32,60		
				137	X	R.AAVPSGASTGVHEALELR.D + SPITC (N-term)	1978.8877	12,80		
58M	Enolase [*Haemonchus contortus*]	gi|301015486	198	32	X	R.QIYDSR.G + SPITC (N-term)	995.3477	21,70	2	TIM_phosphatase binding
				41	X	K.NFCVTQQR.D + Carbamidomethyl (C); SPITC (N-term)	1266.4580	33,60		
				125	X	R.AAVPSGASTGVHEALELR.D + SPITC (N-term)	1978.8877	2,68		
65	Galectin [*Haemonchus contortus*]	gi|7542332	292	53	X	K.GDSFDIR.I + SPITC (N-term)	1023.3426	2,54	5	GLECT
				50	X	R.FTSFAHR.Q + SPITC (N-term)	1079.3953	0,65		
				67	X	K.SYPVPYR.S + SPITC (N-term)	1095.4154	-8.54		
				29	X	K.EFKDYEHR.L	1122.5094	9,29		
				51	X	R.NGDIALHFNPR.F	1252.6313	8,28		
				74	X	K.EFKDYEHR.L + SPITC (N-term)	1337.4805	-14.10		

65M	Galectin [*Haemonchus contortus*]	gi|7542332	343	24	X	K.DYEHR.L + SPITC (N-term)	933.2745	-1.83	6	GLECT
				53	X	K.GDSFDIR.I + SPITC (N-term)	1023.3426	-14.46		
				47	X	R.FTSFAHR.Q + SPITC (N-term)	1079.3953	-12.14		
				33	X	K.SYPVPYR.S + SPITC (N-term)	1095.4154	-20.31		
				39	X	K.EFKDYEHR.L + SPITC (N-term)	1337.4805	-23.97		
				60	X	K.SADFSGNDVPLHISVR.F	1712.8482	-3.08		
				134	X	K.SADFSGNDVPLHISVR.F + SPITC (N-term)	1927.8193	-14.97		
67	Chaperonin containing TCP-1 family member (cct-6) [*Caenorhabditis elegans*]	gi|25144678	102	63		R.GLVLDHGAR.H + SPITC (N-term)	1151.4852	21,70	2	Chaperonin_like
				39		K.DAIHDGLR.A + SPITC (N-term)	1110.4223	25,60		
68M	Ubiquinol-Cytochrome c oxidoReductase complex family member (ucr-1) *[Caenorhabditis elegans]*	gi|17553678	60	60	X	R.FTGSEYR.Y + SPITC (N-term)	1073.3583	-11.21	1	Peptidase_M16
69	CRE-AHCY-1 protein [*Caenorhabditis remanei*]	gi|308505972	143	28	X	K.FDNLYGIR.E	996.5029	47,40	2	NADB_Rossmann
				67	X	K.FDNLYGIR.E + SPITC (N-term)	1211.4740	31.4		
				75	X	R.HIILLAEGR.L + SPITC (N-term)	1235.5791	-18.41		
70	Uracil-DNA glycosylase [*Bacteroides sp* . 3_1_23]	gi|299147640	63	63		K.IFTDAVIR.K + SPITC (N-term)	1148.4995	-20.22	1	UDG
71	Cytochrome C oxidase family member (cco-2) [*Caenorhabditis elegans*]	gi|17555666	90	31	X	R.FLEAIK.I + SPITC (N-term)	934.3928	-0.10	2	Cty_c_oxidase_Va
				59	X	K.VVEAALR.A + SPITC (N-term)	971.4205	1,51		
72	Hypothetical protein BURPS1710b_A0185 [*Burkholderia pseudomallei* 1710b]	gi|76818840	66	66		R.AAAAGKLDPVR.A + SPITC (N-term)	1282.5798	46,50	1	
73	Alkali myosin light chain [*Setaria digitata*]	gi|251762815	96	96	X	K.IDGTQIGDVVR.A + SPITC (N-term)	1386.5908	0.51	1	EFh
74	alkali myosin light chain *[Setaria digitata]*	gi|251762815	96	96	X	K.IDGTQIGDVVR.A + SPITC (N-term)	1386.5908	-0.92	1	EFh
75	SUMO (ubiquitin-related) homolog family member (smo-1) [*Caenorhabditis elegans*]	gi|17508217	128	49	X	R.FLFDGR.R + SPITC (N-term)	968.3521	12,00	2	UBQ
				79	X	K.VVGQDSNEVHFR.V + SPITC (N-term)	1600.6399	-8.34		
76	Putative nucleosome binding protein [*Angiostrongylus cantonensis*]	gi|256016665	86	21	X	R.ADFEVGQVLR.D	1132.5877	28,90	1	PTZ00007
				86	X		1347.5588	5,09		
77	Putative nucleosome binding protein [*Angiostrongylus cantonensis*]	gi|256016665	77	20	X	R.ADFEVGQVLR.D	11.325.877	31,20	1	PTZ00007
				77	X	R.ADFEVGQVLR.D + SPITC (N-term)	1347.5588	0,79		
79	Putative beta-actin (aa 27-375) [*Mus musculus*]	gi|49868	343	19	X	R.AVFPSIVGR.S	944.5444	35,20	5	Actin
				53	X	K.IIAPPER.K + SPITC (N-term)	1009.4361	-1,36		
				87	X	R.AVFPSIVGR.S + SPITC (N-term)	1159.5154	-3,55		
				103	X	R.GYSFTTTAER.E + SPITC (N-term)	1346.4907	-6.03		
				101	X	K.QEYDESGPSIVHR.K	1515.6954	26,00		
				84	X	K.QEYDESGPSIVHR.K + SPITC (N-term)	1730.6665	-3.20		
				62		K.SYELPDGQVITVGNER.F	1775.8690	21,70		
81	Hypothetical protein ckrop_1216 [*Corynebacterium kroppenstedtii* DSM 44385]	gi|237785799	86	44	X	R.EWGLDEFISIR.D	1363.6772	0.24	1	Sigma_70
				86	X	R.EWGLDEFISIR.D + SPITC (N-term)	1578.6483	-19.49		

83	CalPoNin family member (cpn-1) [*Caenorhabditis elegans*]	gi|17506301	118	118	X	K.GATASGLNMGNTR.H + Oxidation (M); SPITC (N-term)	1479.5541	-0.46	1	CH
84	PREDICTED: similar to aldehyde dehydrogenase 1A2 isoform 2 [*Strongylocentrotus purpuratus*]	gi|115899350	140	49	X	R.LGSPWR.T + SPITC (N-term)	929.3524	2,91	2	ALDH-SF
				91	X	K.VAFTGSTEIGR.I + SPITC (N-term)	1351.5537	-29.05		
85	Primosomal protein N ' [*Roseiflexus sp* . RS-1]	gi|148655390	61	61	X	K.SFGVGTQR.V + SPITC (N-term)	1065.4008	-28.62	1	DEXDc
88M	Hypothetical protein [*Angiostrongylus cantonensis*]	gi|256016687	490	42		R.QTSGWR.E + SPITC (N-term)	948.3218	-18.21	7	Calponin
				23		K.TGFGMPR.Q + SPITC (N-term)	979.3350	-27.27		
				87		K.GQTGFGSPR.D + SPITC (N-term)	1120.4066	-36.78		
				72		K.GMTGFGVPR.D + SPITC (N-term)	1135.4249	-40.25		
				88		R.GEMPHDEGTTSR.Q + SPITC (N-term)	1530.5174	-43.08		
				119		R.NTTVALLQAQEQR.S + SPITC (N-term)	1685.7501	-37.25		
				58		R.RPEVPFWSGQDEAR.H + SPITC (N-term)	1887.7668	-23.85		
89	Hypothetical protein Y24D9A.8 [*Caenorhabditis elegans*]	gi|25153750	71	70		K.TQVMAASFR.N + SPITC (N-term)	1224.4726	-19.97	1	
				71			1240.4675	-42.22		
90	Activator of 90 kDa heat shock protein ATPase homolog 1 [*Homo sapiens*]	gi|6912280	84	36	X	K.WGEGDPR.W + SPITC (N-term)	1030.3273	-38.41	2	SRBPCC
				48	X	R.WIVEER.A + SPITC (N-term)	1045.3997	-36.06		
91	RecName: Full=32 kDa beta-galactoside-binding lectin; AltName: Full=Galectin-1	gi|6225602	89	28		K.DYEHR.L + SPITC (N-term)	933.2745	7,19	2	GLECT
				61		R.FTSFAHR.Q + SPITC (N-term)	1079.3953	-0.46		
93	C. briggsae CBR-PAS-6 protein [*Caenorhabditis briggsae*]	gi|268557826	191	103	X	K.LQANTQYYGR.R + SPITC (N-term)	1427.5598	8,56	2	Ntn_hydrolase
				88	X	R.FLQTECSSWR.W + Carbamidomethyl (C); SPITC (N-term)	1527.5581	10,30		
94	Heat Shock Protein family member (hsp-25) [*Caenorhabditis elegans*]	gi|71982751	112	32		R.RIDVNR.S + SPITC (N-term)	986.4062	34,10	2	Alpha_crystallin _Hsps_p23_like
				80		R.EYNQEFLLPR.G + SPITC (N-term)	1522.6221	15,60		
97	Predicted protein *[Laccaria bicolor S238N-H82]*	gi|170111260	61	61	X	R.DIVNEAAR.R + SPITC (N-term)	1101.4219	-33.03	1	Cyclophilin
99	Alpha tubulin [*Onchocerca volvulus*]	gi|63029700	312	59	X	K.EDAANNYAR.G	1022.4417	26,80	5	Tubulin_FtsZ
				61	X	K.EDAANNYAR.G + SPITC (N-term)	1237.4128	-6.51		
				89	X	K.YMAVCLLYR.G + Carbamidomethyl (C); SPITC (N-term)	1402.5542	-2.97		
				68	X	K.YMAVCLLYR.G + Carbamidomethyl (C); Oxidation (M); SPITC (N-term)	1418.5491	-13.24		
				43	X	R.LISQVVSSITASLR.F	1472.8562	13,10		
				42	X	R.AIMVDLEPTVVDEIR.T	1698.8862	10,30		
				26		R.AIMVDLEPTVVDEIR.T + Oxidation (M)	1714.8811	-0.94		
				78	X	R.NLDVERPSYTNLNR.I + SPITC (N-term)	1904.8145	5.58		
99M	Alpha tubulin [*Onchocerca volvulus*]	gi|63029700	320	84	X	K.EDAANNYAR.G + SPITC (N-term)	1237.4128	10,50	5	Tubulin_FtsZ
				89	X	K.YMAVCLLYR.G + Carbamidomethyl (C); SPITC (N-term)	1402.5542	9.01		
				81	X	K.YMAVCLLYR.G + Carbamidomethyl (C); Oxidation (M); SPITC (N-term)	1418.5491	-0.62		
				42	X	R.AIMVDLEPTVVDEIR.T	1698.8862	22.30		
				27	X	R.AIMVDLEPTVVDEIR.T + Oxidation (M)	1714.8811	-3.62		
				81	X	R.NLDVERPSYTNLNR.L + SPITC (N-term)	1904.8145	16.40		
				24	X	R.AFVHWYVGEGMEEGEFSEAR.E	2329.0110	32,50		

103	Protein farnesyltransferase/geranylgeranyltransferase putative [*Albugo laibachii* Nc14]	gi|325181745	104	67		R.NNSAWNHR.W + SPITC (N-term)	1212.4189	3.83	2	PPTA
				37		K.NYQVWHHR.R + SPITC (N-term)	1353.5131	0.06		
104	Hypothetical protein [*Angiostrongylus cantonensis*]	gi|256016587	114	44	X	K.EGGDAFVR.A + SPITC (N-term)	1064.3692	0.80	3	
				68		K.TCEIYTDMGR.F + Carbamidomethyl (C); Oxidation (M); SPITC (N-term)	1475.4826	-9.72		
				30		K.RYEDVSPSFADSR.E + SPITC (N-term)	1742.6665	4.74		
105	Hypothetical protein Y46G5A.19 [*Caenorhabditis elegans*]	gi|25154106	139	139	X	R.VLIIGGGDGGILR.E + SPITC (N-term)	1453.7058	-11,79	1	AdoMet_MTases
106M	Putative nucleosome binding protein [*Angiostrongylus cantonensis*]	gi|256016665	251	48	X	R.DNIINR.A + SPITC (N-term)	958.3637	7.29	3	PTZ00007
				68		R.ADFEVGQVLR.D	1132.5877	15,20		
				77	X	R.ADFEVGQVLR.D + SPITC (N-term)	1347.5588	-9.16		
				125		R.NEDDEEDDSHEIMR.A	1732.6482	11,90		
				42		R.NEDDEEDDSHEIMR.A + Oxidation (M)	1748.6431	2.46		
				93	X	R.NEDDEEDDSHEIMR.A + SPITC (N-term)	1947.6193	5.61		
				74		R.NEDDEEDDSHEIMR.A + Oxidation (M); SPITC (N-term)	1963.6142	5.10		
107M	Putative histone-binding protein Caf1 [*Trichinella spiralis*]	gi|316979260	68	68		K.TVAIWDLR.N + SPITC (N-term)	1187.5103	-14.67	1	WD40
108M	Alpha tubulin [*Onchocerca volvulus*]	gi|63029700	284	46	X	K.EDAANNYAR.G	1022.4417	13,30	4	Tubulin_FtsZ
				76	X	K.EDAANNYAR.G + SPITC (N-term)	1237.4128	-7.72		
				75	X	K.YMAVCLLYR.G + Carbamidomethyl (C); SPITC (N-term)	1402.5542	-6.67		
				68	X	K.YMAVCLLYR.G + Carbamidomethyl (C); Oxidation (M); SPITC (N-term)	1418.5491	-20.29		
				48	X	R.AIMVDLEPTVVDEIR.T	1698.8862	15,20		
				85	X	R.NLDVERPSYTNLNR.L + SPITC (N-term)	1904.8145	5.89		
109	Glutamate--ammonia ligase [*Homo sapiens*]	gi|31831	97	30		R.FILHR.V + SPITC (N-term)	899.3782	29,90	2	GLn_synt_C
				67	X	R.DIVEAHYR.A + SPITC (N-term)	1216.4641	8.15		
109M	Glutamate--ammonia ligase [*Homo sapiens*]	gi|31831	97	30		R.FILHR.V + SPITC (N-term)	899.3782	32,80	2	GLn_synt_C
				67	X	R.DIVEAHYR.A + SPITC (N-term)	1216.4641	13,20		

Supplementary Table 2 - List of protein entries assigned to over-represented GO terms (Biological Process category)		
GO term	**Term description**	**Protein entries from our dataset**
Macromolecule metabolic process		
GO:0009059	Macromolecule biosynthetic process	17554768 (ribosomal protein), 237785799 (hypothetical protein ckrop_1216), 148655390 (primosomal protein N´), 12007194 (elongation factor 1 alpha)
GO:0019538	Protein metabolic process	17554768 (ribosomal protein), 17542208 (hypothetical protein T05E11.3), 170093093 (predicted protein), 146086176 (20S proteasome subunit alpha 5), 268557826 (CBR-PAS-6 protein), 25144678 (chaperonin containing TCP-1), 6912280 (ATPase homolog 1), 255091016 (HSP 90), 17555558 (HSP-60), 256251570 (HSP), 25144674 (chaperonin containing TCP-1); 17564182 (chaperonin containing TCP-1), 3687326 (calreticulin1), 1046266 (CCT-2), 256251566 (DAUER)
GO:0006508	Proteolysis	146086176 (20S proteasome subunit alpha 5), 268557826 (CBR-PAS-6 protein)
Developmental process		
GO:0002164	Larval development	6626 (actin), 17554768 (ribosomal protein), 17542208 (hypothetical protein T05E11.3), 301015486 (enolase)
GO:0048513	Organ development	6626 (actin), 17554768 (ribosomal protein), 301015486 (enolase), 25144756 (ATP synthase), 17508217 (SUMO homolog), 25144678 (chaperonin containing TCP-1), 25144674 (chaperonin containing TCP-1), 17564182 (chaperonin containing TCP-1), 268577393 (cbr-mlc-2.2 protein), 1046266 (CCT-2)
GO:0055115	Entry into diapause	17568359 (14-3-3 protein), 40388674 (14-3-3b protein)
Response to stress		
GO:0006979	Response to oxidative stress	47499100 (peroxiredoxin), 17555558 (HSP), 256251570 (HSP)
GO:0006986	Response to unfolded protein	17555558 (HSP), 256251570 (HSP)
Biological regulation		
GO:0040008	Regulation of growth	17554768 (ribosomal protein), 17542208 (hypothetical protein T05E11.3), 301015486 (enolase), 25144756 (ATP synthase), 17508217 (SUMO homolog), 308505972 (CRE-AHCY-1), 47499100 (peroxiredoxin), 25144674 (chaperonin containing TCP-1), 17568359 (14-3-3 protein), 215262522 (translationally controled tumor protein), 268577393 (CBR-MLC-2.2 protein), 40388674 (14-3-3b protein)
GO:0048518	Positive regulation of biological process	17554768 (ribosomal protein), 17542208 (hypothetical protein T05E11.3), 301015486 (enolase), 25144756 (ATP synthase), 17508217 (SUMO homolog), 47499100 (peroxiredoxin), 25144674 (chaperonin containing TCP-1), 17568359 (14-3-3 protein), 215262522 (translationally controled tumor protein), 268577393 (CBR-MLC-2.2 protein), 40388674 (14-3-3b protein)

Artigo 3

Proteolytic activity in the adult and larval stages of the human roundworm parasite Angiostrongylus costaricensis (A ser publicado no *Memórias do Instituto Oswaldo Cruz vol. 107(6)*(2012) manuscrito MIOC-3560).

Proteolytic activity in the adult and larval stages of the human roundworm parasite *Angiostrongylus costaricensis*

Karina Mastropasqua Rebello[1,2,3], Caroline Reis de Siqueira[1,3], Erika Louise Ribeiro[1,3], Richard Hemmi Valente[1,3], Ester Maria Mota[2], Jonas Perales[1,3], Ana Gisele da Costa Neves-Ferreira[1,3]/+, Henrique Leonel Lenzi[2†]

[1]Laboratório de Toxinologia, [2]Laboratório de Patologia, Instituto Oswaldo Cruz-Fiocruz, Rio de Janeiro, RJ, Brasil [3]Rede Proteônica do Rio de Janeiro, Fundação de Amparo à Pesquisa do Estado do Rio de Janeiro, Rio de Janeiro, RJ, Brasil

Angiostrongylus costaricensis *is a nematode that causes abdominal angiostrongyliasis, a widespread human parasitism in Latin America. This study aimed to characterize the protease profiles of different developmental stages of this helminth. First-stage larvae (L1) were obtained from the faeces of infected* Sigmodon hispidus *rodents and third-stage larvae (L3) larvae were collected from mollusks* Biomphalaria glabrata *previously infected with L1. Adult worms were recovered from rodent mesenteric arteries. Protein extraction was performed after repeated freeze-thaw cycles followed by maceration of the nematodes in 40 mM Tris base. Proteolysis of gelatin was observed by zymography and found only in the larval stages. In L3, the gelatinolytic activity was effectively inhibited by orthophenanthroline, indicating the involvement of metalloproteases. The mechanistic class of the gelatinases from L1 could not be precisely determined using traditional class-specific inhibitors. Adult worm extracts were able to hydrolyze haemoglobin in solution, although no activity was observed by zymography. This haemoglobinolytic activity was ascribed to aspartic proteases following its effective inhibition by pepstatin, which also inhibited the haemoglobinolytic activity of L1 and L3 extracts. The characterization of protease expression throughout the* A. costaricensis *life cycle may reveal key factors influencing the process of parasitic infection and thus foster our understanding of the disease pathogenesis.*

Key words: *Angiostrongylus costaricensis* - metalloproteases - aspartic proteases – haemoglobin - zymography

Angiostrongylus costaricensis (Morera & Cespedes 1970) is a nematode that causes abdominal angiostrongyliasis (AA), a human helminthiasis characterized by abdominal eosinophilic ileocolitis. Adult worms live inside the mesenteric arteries of rodents (definitive hosts). Eggs laid by females hatch to release first-stage larvae (L1), which migrate into the intestinal lumen and are eliminated with the faeces. The L1 larvae infect mollusks (intermediate hosts) and further develop into infective third-stage larvae (L3), which subsequently develop into adult worms in the mammalian hosts. Humans are incidental hosts and may become infected through the ingestion of infected mollusks or unwashed vegetables (Morera 1973). This parasitic disease has been reported throughout Central and South America (Morera & Cespedes 1971, Incani et al. 2007, Palominos et al. 2008). In endemic areas, such as the southern region of Brazil, epidemiological and clinical features are used as diagnostic indications of AA (Agostini et al. 1983, 1984, Ayala 1987, Graeff-Teixeira et al. 1991, 2005, Bender et al. 2003, Mesen-Ramirez et al. 2008, Ben et al. 2010, Abrahams-Sandi et al. 2011). However, AA is a disease with unspecified clinical manifestations. To date, the only way to achieve an accurate diagnosis is through surgical intervention to find intra-arterial worms or eggs trapped in small capillaries in histological sections. Moreover, an effective pharmacological treatment for AA does not currently exist (Morera & Bontempo 1985, Terada et al. 1993, Tungtrongchitr et al. 1993). Previous studies using noninvasive tools to diagnose AA have shown that available serological tests are not effective due to both nonspecific cross-reactivity issues and the diversity of humoral responses (Graeff-Teixeira et al. 1997, Geiger et al. 2001). A published method based on a polymerase chain reaction may eventually improve our ability to diagnose the disease, although the results are still preliminary (da Silva et al. 2003). Moreover, many studies have assessed different types of therapies with limited success, such as treatment with anthelmintic drugs (Morera & Bontempo 1985, Mentz & Graeff-Teixeira 2003, Bohrer Mentz et al. 2007), anti-inflammatory drugs (Fante et al. 2008) and antithrombotic agents (Rodriguez et al. 2011). The present consensus is that anthelmintic drug administration is not recommended given that it usually induces the erratic migration of worms instead of killing them (Morera & Bontempo 1985). Therefore, new targets for the diagnosis and treatment of this helminthic disease are urgently needed.

Proteases are interesting biomarkers for the detection of diseases and account for roughly 10% of all current pharmacological targets (Lim & Craik 2009). They catalyze the cleavage of peptide bonds in proteins and, based on their mechanism of catalysis, are classified into

Financial support: FIOCRUZ (PAPES V, PDTIS), CNPq, FAPERJ, CAPES
KMR has CAPES fellowship.
† *In memoriam*
+ Corresponding author: anag@ioc.fiocruz.br
Received 10 November 2011
Accepted 9 May 2012

six distinct classes: serine, cysteine, metallo, aspartic, glutamic and threonine proteases (Lopez-Otin & Bond 2008, Rawlings et al. 2012). Proteolytic enzymes have been implicated in several aspects of helminth development (Tort et al. 1999), including moulting (Hong et al. 1993, Rhoads et al. 1998), hatching (Xu & Dresden 1986) and excystment (Chung et al. 1995). Moreover, parasite-derived proteases are key elements in the process of host colonization by the infective larval stages of several helminths. In addition to assisting in connective tissue invasion and feeding, these enzymes help parasitic organisms to evade the host immune response and prevent blood coagulation (McKerrow 1989, Dzik 2006). They are major virulence factors because they play a variety of roles establishing, maintaining and exacerbating the infection (McKerrow et al. 2006). Proteases of different mechanistic classes may be expressed in the parasite intestines or may constitute their excretory-secretory products. They are presently considered to be potential targets for the next generation of antiparasite interventions (Dalton 2003). The aim of this study was to evaluate the presence of proteases in crude extracts of *A. costaricensis* nematodes at different developmental stages. We hypothesize that, as is true for other helminth nematodes, proteolysis is most likely involved in the nutrition, development and pathogenicity of *A. costaricensis.*

MATERIALS AND METHODS

Chemicals - Protease inhibitors [pepstatin A, L-trans-epoxysuccinyl-L-leucylamido-(4-guanidino)-butane (E-64), orthophenanthroline, 4-(amidinophenyl) methanesulphonyl fluoride (APMSF), ethylenediaminetetraacetic acid (EDTA) and ethyleneglycol bis(2-aminoethyl ether)-N,N,N',N' tetraacetic acid (EGTA)], dithiotreitol (DTT), human haemoglobin and Coomassie R-250 were purchased from Sigma-Aldrich (St Louis, USA). The Sample Grinding kit, 2-D Quant kit and protein low molecular weight standards for sodium dodecyl sulfate polyacrylamide gel electrophoresis (SDS-PAGE) were from GE Healthcare (Chalfont St Giles, UK). All other chemicals were of analytical reagent grade.

Ethics - All procedures with animals were approved by the Animal Ethical Committee at Oswaldo Cruz Foundation (license # P0246/05) and conducted in accordance with the International Guiding Principles for Biomedical Research Involving Animals, as issued by the Council for the International Organizations of Medical Sciences.

Parasite life cycle - Adult and larval stages of *A. costaricensis* nematodes were obtained from the normal life cycle of the parasites, which were kept in the laboratory through their successive passages in mollusks *Biomphalaria glabrata* (intermediate hosts) and rodents *Sigmodon hispidus* (definitive hosts), as previously described (Mota & Lenzi 2005).

L1 - Three-month-old rodents were used after 30 days of being orally infected with L3 of *A. costaricensis* per animal. Faeces collected from these animals were added to 50 mL of water. L1 was decanted from the faeces suspension using a modified Baermann apparatus. The modification consisted of a funnel directly connected to a haemolysis tube through a latex hose (Barcante et al. 2003). After 12 h, 50 mL of the sediment containing L1 were recovered and centrifuged at 2,000 g for 10 min at room temperature (RT). The supernatant was discarded and the remaining pellet was resuspended in 10 mL of water. After gentle agitation, suspension aliquots (100 µL) were transferred to Petri dishes for counting and evaluation of the morphology of the larvae using an inverted light microscope. A discontinuous Percoll gradient was then used to separate L1 from small debris and bacteria as previously described (Graeff-Teixeira et al. 1999). This method takes advantage of the change in density that occurs when *A. costaricensis* larvae are killed, allowing for the separation of dead L1 from live ones. Following the purification step, the Percoll was removed by five cycles of phosphate buffered saline (PBS) washing and centrifugation at 2,500 *g* for 10 min at 20ºC.

L3 - The infective L3 were obtained from mollusks previously infected with L1. Briefly, mollusks were crushed and the tissues were homogenized and digested in an acid-pepsin solution (0.5% pepsin and 0.2% HCl) for 2 h at 37ºC (Wallace 1969, Mota & Lenzi 2005). Host cellular debris was removed from the digests by centrifugation at 2,000 *g* for 10 min. The infective larvae were then isolated according to Baermann's modified technique and counted as previously described for L1.

Adult worms (male and female) - Adult worms were recovered by dissection of the mesenteric arteries of *S. hispidus* rats 40 days after the infection (Wallace 1969, Mota & Lenzi 2005). They were extensively rinsed in PBS, segregated according to gender (Rebello et al. 2011), weighted and then stored at -80ºC until further use.

Protein extraction – Samples containing 80,000 L1 or 30,000 L3 were resuspended in 300 µL of 40 mM Tris base in 1.5 mL microcentrifuge tubes containing abrasive resin (Sample Grinding Kit). Protein extraction was performed by a combination of 10 freeze-thaw cycles in liquid nitrogen followed by grinding for 2 min. Adult worms (13 males or 7 females) were separately ground for 5 min in 1.5 mL microcentrifuge tubes containing abrasive resin and 150 µL of 40 mM Tris base. The optimization of the protein extraction procedures was performed on female samples only and included sample grinding in two additional extraction solutions: 40 mM Tris base with 1% Triton X-100 or 40 mM Tris base with 1% SDS. Cell debris was removed by centrifugation at 16,000 *g* for 10 min and the protein content of the supernatants was measured using the 2-D Quant kit and bovine serum albumin as the standard.

Zymography - The proteolytic activity of crude extracts of larvae and adult worms was analyzed by zymography using 12% T SDS-PAGE (T = total concentration of acrylamide and bis-acrylamide) (Laemmli 1970), containing 0.1% copolymerized gelatin (Heussen & Dowdle 1980). Protein extracts (2 µg) were diluted (v/v) in sample buffer without ß-mercaptoethanol and loaded onto gels. The gels were run at 12 mA and 4ºC. After electrophoresis, the gels were incubated for 1 h at RT in 2.5% (v/v) Triton X-100 for SDS removal and enzyme renaturation.

The effect of pH on the proteolytic activity was determined by incubating Triton X-100-treated gels for 12 h at 37ºC in the following buffers: 0.1 M sodium citrate containing 1 mM $CaCl_2$ (pH 3.0 or 5.5), 0.1 M sodium phosphate containing 1 mM $CaCl_2$ (pH 7.0), 0.1 M Tris containing 1 mM $CaCl_2$ (pH 7.4), 0.1 M glycine-NaOH containing 1 mM $CaCl_2$ (pH 10) and 0.2 M KCl-NaOH containing 1 mM $CaCl_2$ (pH 12). Zymograms were stained with 0.2% Coomassie Brilliant Blue (R-250) in methanol:acetic acid solution (40:10 v/v) and destained in the same solution without the dye. They were scanned with the ImageScanner III (GE HealthCare) and analyzed by the Image Master 2D Elite software (GE HealthCare).

Haemoglobin proteolysis in solution - Haemoglobin hydrolysis was assayed after the incubation of human haemoglobin (0.5 mL; 2 mg/mL) with crude extracts of larvae or adult nematodes (50 µg) at 37ºC for 1 h, 5 h or 18 h in the presence of 1 mM DTT. Digestions were conducted in the following buffers: 0.1 M sodium acetate, pH 3.0 or 5.0, and 0.1 M sodium phosphate, pH 7.4. The reaction was stopped by the addition of sample buffer (Laemmli 1970) and boiling for 5 min; the hydrolysates were further analyzed by 15% T SDS-PAGE under reducing conditions. Protein extracts (50 µg) from the gut tissue of female worms were also tested upon the haemoglobin substrate as described above (18 h hydrolysis).

Inhibition of proteolytic activity - The following protease inhibitors were used to identify the mechanistic class of the proteases in protein extracts (molar concentrations used are indicated): 10 µM E-64, 10 mM and 100 mM orthophenanthroline, 10 mM EDTA; 10 mM EGTA, 1 µM pepstatin A and 100 µM APMSF. They were included in the buffer in which the zymograms were incubated overnight following enzyme renaturation. To assay for the inhibition of haemoglobinolytic activity in solution, the inhibitors were added to the appropriate digestion buffer.

RESULTS

The optimization of protein extraction conditions was performed only in female adult worms, which are longer and more abundant than male worms (Rebello et al. 2011). Equivalent sample amounts (~3.5 mg of worm/replicate for each condition) were ground in three different solutions followed by the estimation of protein recoveries by the 2-D Quant kit (Table). Quantitatively, when compared to the assumed 100% extraction efficiency (obtained with 40 mM Tris base containing 1% SDS), 40 mM Tris base containing 1% Triton X-100 or 40 mM Tris base solutions allowed for the recovery of 81% and 45% of total worm proteins, respectively. Although detergents did not impair the proteolytic activity, the inhibitory efficiency of chelating agents was reduced in the presence of SDS. Therefore, to avoid interference in the inhibition assays, all protein extracts further used in this study were prepared in 40 mM Tris base without any detergents, albeit with lower efficiency of protein recovery.

The zymographic analysis involves protein separation by SDS-PAGE copolymerized with a substrate within the polyacrylamide gel matrix. Following renaturation by the exchange of the SDS with a nonionic detergent, proteolytic activity was visualized *in situ* as clear bands against a dark blue background where the protease had digested the substrate (Wilkesman & Kurz 2009). Calcium chloride was included in the hydrolysis buffer to improve the detection of calcium-dependent proteases (ex.: metalloproteases, serine proteases) which could eventually be present in the nematode extracts. This technique has proven extremely useful for the detection of a wide range of proteases from parasites, animals and plants (d'Avila-Levy et al. 2001, Santos et al. 2009). A drawback of the technique is that some enzymes do not renature correctly and hence cannot be detected (Wilkesman & Kurz 2009).

A pronounced gelatinolytic activity was observed for the protein extracts of L1 and L3 larvae, the migratory stages of the parasite. For both larval stages, gelatinolytic activity was detected at a neutral and an alkaline pH, with optimal activity observed at pH 7.4 (Fig. 1A). The SDS-PAGE analysis of the larval extracts (Fig. 2B) showed a complex pattern of protein bands, with molecular masses ranging from 97 to less than 14.4 kDa. On the other hand, most proteolytic bands showed apparent molecular masses greater than 40 kDa (Fig. 2A). To determine the mechanistic class of the gelatinases of *A. costaricensis*, their susceptibility to the following protease inhibitors was analyzed: APMSF (irreversible inhibitor of serine proteases), E-64 (irreversible inhibitor of cysteine proteases), pepstatin (reversible inhibitor of aspartic proteases), orthophenanthroline, EDTA or EGTA (reversible inhibitors of metal-dependent proteases) (Fig. 3). The gelatinolytic activity of L3 extracts was insensitive to APMSF, E-64 and pepstatin, but was readily inhibited by orthophenanthroline, EDTA or EGTA, suggesting the major involvement of zinc metalloproteases. The proteolytic activity of L1 extracts upon gelatin was only partially inhibited by orthophenanthroline or EDTA. On the other hand, EGTA strongly inhibited the gelatinolytic activity of L1 extracts; this metal chelator has a very high affinity for calcium ions, suggesting the presence of calcium-dependent proteases in this sample. Given that APMSF, E-64 and pepstatin did not affect this enzymatic activity either, the mechanistic class of

TABLE

Quantitative analysis of different sample preparation methods for female adult worms

	Extraction yield (µg ptn/mg worm)[a]		
Extraction solutions	Mean	SD	n
40 mM Tris	23.82	1.98	3
40 mM Tris + 1% Triton X-100	43.25	5.12	3
40 mM Tris + 1% SDS	53.10	1.47	3

a: protein concentration was measured using the 2-D Quant kit assay; n: number of independent replicates; SD: standard deviation; SDS: sodium dodecyl sulphate.

the gelatinases of L1 larvae could not be precisely determined. Worm extracts of male and female adults were unable to hydrolyze copolymerized gelatin over the wide range of pH values tested (not shown).

DISCUSSION

Host haemoglobin is a major substrate for the proteolytic enzymes produced by nematodes that feed on blood (Williamson et al. 2003). The present study showed that protein extracts from larvae (Fig. 4) or adult worms (Fig. 5) of *A. costaricensis* hydrolyze human haemoglobin in vitro after 18 h and 5 h of incubation, respectively. No hydrolysis of haemoglobin was observed after 1 h of incubation (not shown). Interestingly, haemoglobin-degrading activity was also observed in protein extracts from isolated gut tissue of adult worms, with optimum activity observed at pH 3.0 (Fig. 1B). The same pH behaviour was observed in crude extracts from adult worms and larvae (not shown). It is possible to observe blood inside the intestines of *A. costaricensis* adult worms, thus suggesting that the parasite haemoglobinolytic protease may be involved in the degradation of blood components of the host. These proteases may be responsible for the degradation of haemoglobin and other host proteins during intracellular residence, as already observed for schistosomes (McKerrow et al. 2006). The haemoglobinolytic activity of *A. costaricensis* extracts was effectively inhibited by pepstatin, while APMSF, E-64 and orthophenanthroline had no inhibitory effect (Figs 4, 5). These results indicate the presence of aspartic proteases in larvae and adult worms.

Metalloprotease activity has been already reported in several helminths (Lun et al. 2003, Quiñones et al. 2006, Williamson et al. 2006), including *Angiostrongylus cantonensis* (Lee et al. 2004, Lai et al. 2005). These enzymes belong to a diverse group of enzymes that utilize coordination to a metal ion (usually zinc) to exert catalysis and have a powerful degrading effect on extracellular matrix components (Rawlings & Barrett 1995). Because L1 and L3 larvae from *A. costaricensis* do not possess a bucal stylet (Ishih et al. 1990), one can speculate that the important gelatinolytic activity observed by zymography may assist in parasite penetration into both the mollusk tegument and the intestinal wall. For example, the infective larvae of *Strongyloides stercoralis* secretes a metalloprotease that is thought to be involved in the invasive process, facilitating the tissue penetration of the host skin (McKerrow et al. 1990, Gomez Gallego et al. 2005). Similarly, the secreted metalloproteases of *Ancylostoma caninum* appear to trigger the activation of the third-stage infective larvae, including ecdysis and penetration of host tissues (Hotez et al. 1990, Hawdon et al. 1995, Williamson et al. 2006). Metalloproteases have also been identified in extracts and excretory-secretory samples of *A. cantonensis* and may be associated with parasite dissemination and/or pathogenesis (Lai et al. 2005).

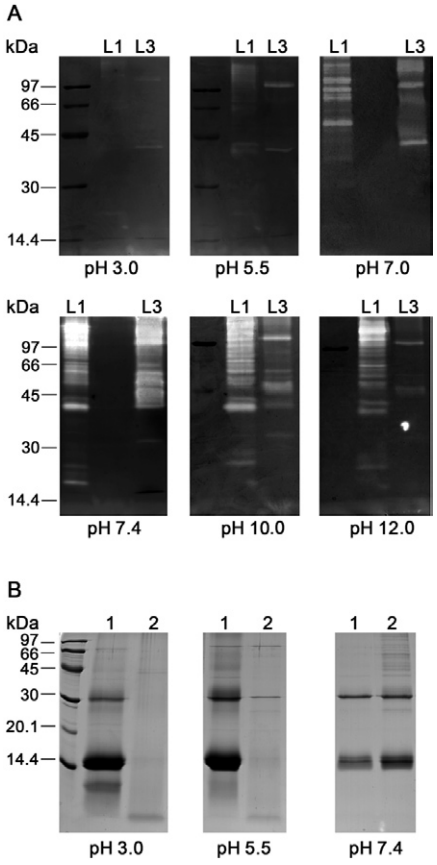

Fig. 1: A: gelatin zymograms showing the proteolytic activity of the protein extracts of first (L1) and third (L3) stage larvae of *Angiostrongylus costaricensis* nematodes. Samples (2 µg) were loaded onto 12% sodium dodecyl sulfate polyacrylamide gel electrophoresis (SDS-PAGE) copolymerized with 0.1% gelatin. After the electrophoretic separation, the zymograms were incubated for 18 h at 37ºC at different pHs (see Materials and Methods for the description of buffers composition). The zymograms were stained with Coomassie Brilliant Blue R250; B: SDS-PAGE (12%) analysis of haemoglobin degradation by protein extracts (50 µg) from the gut tissue of female worms (18 h hydrolysis) tested at different pHs; 1: haemoglobin (negative control); 2: haemoglobin + protein extract (positive control). Gels were stained with Coomassie Blue. Molecular mass standards are shown on the left side of the gel.

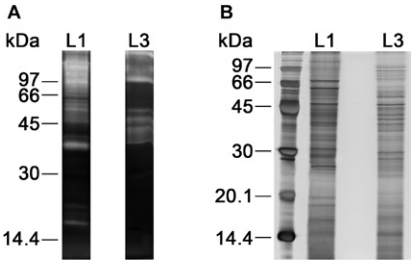

Fig. 2A: comparison of zymographic and electrophoretic profiles of protein extracts of first (L1) and third (L3) stage larvae of *Angiostrongylus costaricensis* nematodes. Samples (2 µg) were loaded onto 12% sodium dodecyl sulfate polyacrylamide gel electrophoresis (SDS-PAGE) copolymerized with 0.1% gelatin. After the electrophoretic separation, the zymograms were incubated for 18 h at 37ºC in 0.1 M Tris containing 1 mM $CaCl_2$, pH 7.4. They were stained with Coomassie Brilliant Blue R250. B: SDS-PAGE (12%) analysis of crude extracts (2 µg) stained with silver nitrate. Molecular mass standards are shown on the left side of the gel.

Several aspartic proteases have also been described in different parasitic nematodes, including hookworms (Williamson et al. 2004), *S. stercoralis* (Gallego et al. 1998), *Haemonchus contortus* (Longbottom et al. 1997) and *Onchocerca volvulus* (Jolodar et al. 2004) and in the free-living nematode *Caenorhabditis elegans* (Geier et al. 1999). In the hookworms, these proteases play an important role in haemoglobin digestion in the intestine and in tissue degradation during the larvae migration in the mammalian host (Williamson et al. 2003). A recent study showed that the expression level of the aspartic protease gene in *A. cantonensis* varies during the life cycle of the nematode and differs between male and female adult worms (Hwang et al. 2010). Some nematodes express aspartic proteases in eggs and in early stages of development, but a clear function has not yet been ascribed to these enzymes (Yang et al. 2009).

Aspartic proteases are proteolytic enzymes characterized by the presence of two catalytic aspartic acid residues at their active site. These enzymes play a key role in the digestion of haemoglobin by schistosomes (Brinkworth et al. 2001, Koehler et al. 2007), *Plasmodium falciparum* (Francis et al. 1997, Banerjee et al. 2002), *Necator americanus* (Brown et al. 1995, 1999) and *A. caninum* (Williamson et al. 2003). Interestingly, cysteine protease activity was not detected under the experimental conditions tested. This type of protease is the most widely reported class of protease in parasitic nematodes and has been shown to hydrolyze gelatin in addition to other substrates (Yatsuda et al. 2006, Kasny et al. 2007, Liu et al. 2010). Cysteine proteases are associated with several biological processes, such as tissue penetration, feeding and evasion of host immune response (Sajid & McKerrow 2002).

From a biological point of view, it is interesting to note that L1 extracts showed stronger gelatinolytic activity than L3 extracts. L1 larvae penetrate mollusks through oral (Morera 1973) and/or percutaneous infections (Thiengo 1996, Mendonca et al. 1999) and moult twice inside the intermediate host. We hypothesize that the ability of gelatinases to hydrolyze extracellular matrix components is important for tissue invasion. The stronger gelatinolytic activity of L1 larvae may ensure its successful penetration through the mollusk's surface and muscular layers. However, L3 larvae may also make use of gelatinolytic enzymes to penetrate the vertebrate intestinal wall and reach the circulatory system, as already described for the infective stage of several parasite nematodes (Hotez et al. 1990, Zhan et al. 2002, Lai et al. 2005, Lee & Yen 2005). L3 become adult worms inside the blood vessels, where these last will live their entire lives. L1 may be eventually found in the systemic circulation, although this results from an alternative migratory route in rodents (Mota & Lenzi 2005, Fontoura et al. 2007). Therefore, it was not surprising to find that the proteolytic activity against haemoglobin was more pronounced in L3 larvae and adult worms. These developmental stages of the parasite remain in direct contact with blood most of their lifetime.

In summary, in this study we investigated the presence of proteolytic activity in crude protein extracts from different life cycle stages of *A. costaricensis*. Several metalloproteases with gelatinolytic activity were observed in the protein extracts from L1 and L3 larvae, but not in adult

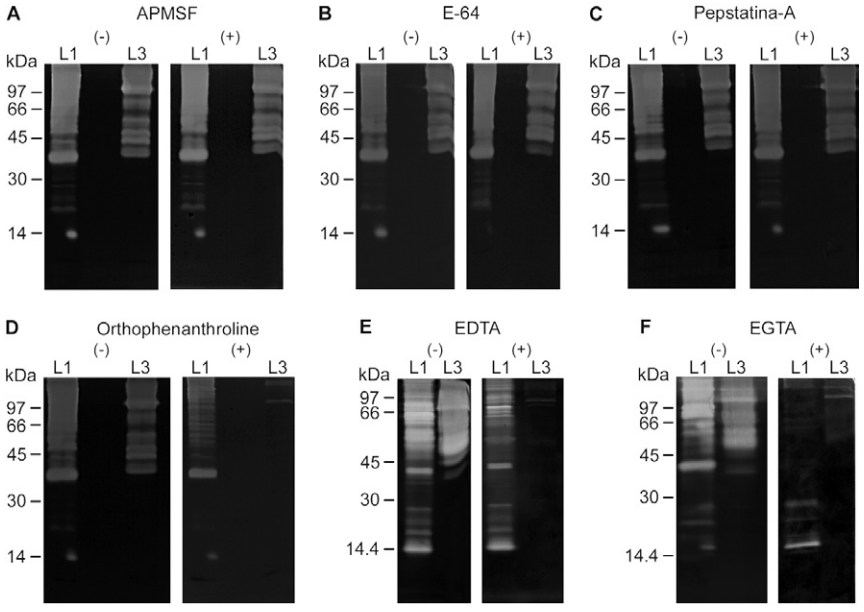

Fig. 3: effect of protease inhibitors on the zymographic profiles of the protein extracts of first (L1) and third (L3) larvae of *Angiostrongylus costaricensis* nematodes. L1 or L3 samples were loaded onto 12% sodium dodecyl sulfate polyacrylamide gel electrophoresis copolymerized with 0.1% gelatin. After the electrophoretic separation, the zymograms were incubated for 18 h at 37ºC in 0.1 M Tris containing 1 mM $CaCl_2$, pH 7.4. The proteolytic activity was assayed in the absence (-) or presence (+) of each one of the protease inhibitors [A: 100 µM 4-(amidinophenyl) methanesulphonyl fluoride (APMSF); B: 10 µM L-trans-epoxysuccinyl-L-leucylamido-(4-guanidino)-butane (E-64); C: 1 µM pepstatin-A; D: 10 mM orthophenanthroline; E: 10 mM ethylenediaminetetraacetic acid (EDTA); F: 10 mM ethyleneglycol bis(2-aminoethyl ether)-N,N,N',N' tetraacetic acid (EGTA)]. Zymograms were stained with Coomassie Brilliant Blue R250. Molecular mass standards are shown on the left side of the gel.

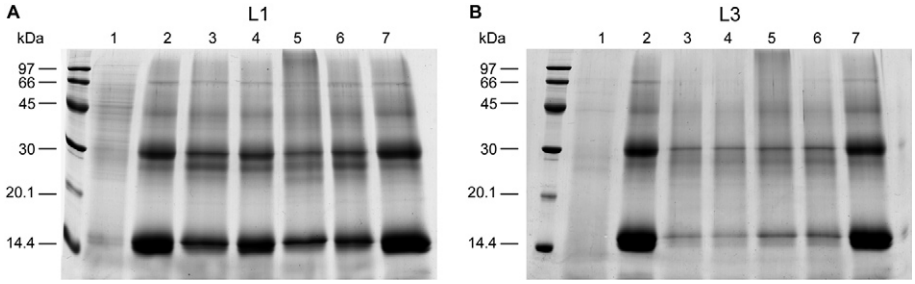

Fig. 4: human haemoglobin hydrolyzed by protein extracts of first-stage larvae (L1) (A) or third-stage larvae (L3) (B) of *Angiostrongylus costaricensis* nematodes. Haemoglobin solubilised in 0.1 M sodium citrate buffer pH 3.0 was incubated with 50 µg of larval extracts for 18 h at 37ºC. To assay for inhibition, the haemoglobin substrate was incubated with the larval extract in the presence of different protease inhibitors. Lane 1: crude larval extract; 2: haemoglobin (negative control); 3: haemoglobin + larval extract (positive control); 4: haemoglobin + larval extract + 10 µM L-trans-epoxysuccinyl-L-leucylamido-(4-guanidino)-butane; 5: haemoglobin + larval extract + 10 mM orthophenanthroline; 6: haemoglobin + larval extract + 100 µM 4-(amidinophenyl) methanesulphonyl fluoride; 7: haemoglobin + larval extract + 1 µM pepstatin. Sodium dodecyl sulfate polyacrylamide gel electrophoresis (15%) were stained with Coomassie Brilliant Blue R250. Molecular mass standards are shown on the left side of the gel.

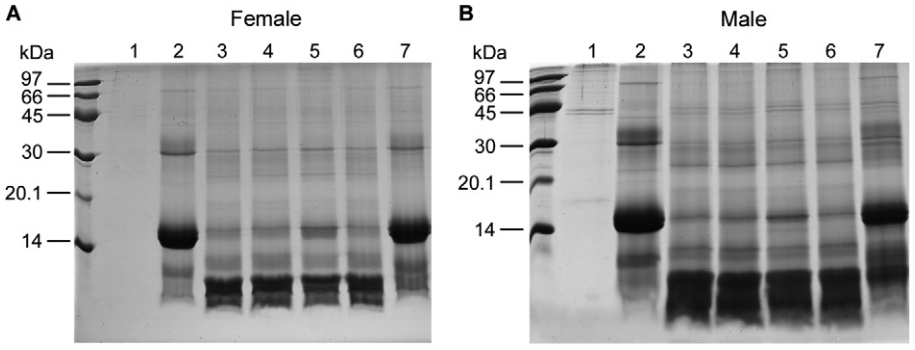

Fig. 5: human haemoglobin hydrolyzed by protein extracts of adult female (A) or male (B) *Angiostrongylus costaricensis* nematodes. Haemoglobin solubilised in 0.1 M sodium citrate buffer pH 3.0 was incubated with 50 µg of worm extracts for 5 h at 37ºC. To assay for inhibition, the haemoglobin substrate was incubated with the worm extract in the presence of different protease inhibitors. Lane 1: crude worm extract; 2: haemoglobin (negative control); 3: haemoglobin + worm extract (positive control); 4: haemoglobin + worm extract + 10 µM L-trans-epoxysuccinyl-L-leucylamido-(4-guanidino)-butane; 5: haemoglobin + worm extract + 10 mM orthophenanthroline; 6: haemoglobin + worm extract + 100 µM 4-(amidinophenyl) methanesulphonyl fluoride; 7: haemoglobin + worm extract + 1 µM pepstatin. Sodium dodecyl sulfate polyacrylamide gel electrophoresis (15%) were stained with Coomassie Brilliant Blue R250. Molecular mass standards are shown on the left side of the gel.

worm extracts. They showed optimal activity at neutral to alkaline pH. At low pH, haemoglobinolytic enzymes characterized as aspartic proteases were detected both in larvae and adult worms. The results suggest that these haemoglobin-degrading proteases should ideally exert their activity under an acid environment, such as the intestine. Although the biological function of the proteases from *A. costaricensis* remains unknown, they represent an attractive target for the development of diagnostic tests and vaccines for the control of abdominal angiostrongyliasis.

ACKNOWLEDGEMENTS

To Heloisa MN Diniz, for processing the figures.

REFERENCES

Abrahams-Sandi E, Mesén-Ramirez P, Suarez-Chacon D, Fernández-Quesada K 2011. An indirect immunofluorescence antibody test employing whole eggs as the antigen for the diagnosis of abdominal angiostrongyliasis. *Mem Inst Oswaldo Cruz 106*: 390-393.

Agostini AA, Marcolan AM, Lisot JM, Lisot JU 1984. Angiostrongilíase abdominal. Estudo anátomo-patológico de quatro casos observados no Rio Grande do Sul, Brasil. *Mem Inst Oswaldo Cruz 79*: 443-445.

Agostini AA, Peixoto A, Caleffi AL, Dexhaimer A, Camargo RR 1983. Angiostrongilíase abdominal: três casos observados no Rio Grande do Sul. *Rev Assoc Med Rio Grande do Sul* 27: 200-203.

Ayala MA 1987. Angiostrongiloidíase abdominal. Seis casos observados no Paraná e em Santa Catarina, Brasil. *Mem Inst Oswaldo Cruz 82*: 29-36.

Banerjee R, Liu J, Beatty W, Pelosof L, Klemba M, Goldberg DE 2002. Four plasmepsins are active in the *Plasmodium falciparum* food vacuole, including a protease with an active-site histidine. *Proc Natl Acad Sci USA 99*: 990-995.

Barcante JM, Barcante TA, Dias SR, Vieira LQ, Lima WS, Negrao-Correa D 2003. A method to obtain axenic *Angiostrongylus vasorum* first-stage larvae from dog feces. *Parasitol Res 89*: 89-93.

Ben R, Rodrigues R, Agostini AA, Graeff-Teixeira C 2010. Use of heterologous antigens for the immunodiagnosis of abdominal angiostrongyliasis by an enzyme-linked immunosorbent assay. *Mem Inst Oswaldo Cruz 105*: 914-917.

Bender AL, Maurer RL, da Silva MC, Ben R, Terraciano PB, da Silva AC, Graeff-Teixeira C 2003. Eggs and reproductive or-

gans of female *Angiostrongylus costaricensis* are more intensely recognized by human sera from acute phase in abdominal angiostrongyliasis. *Rev Soc Bras Med Trop 36*: 449-454.

Bohrer Mentz M, Dallegrave E, Agostini A, Graeff-Teixeira C 2007. Phenantroline, lovastatin and mebendazole do not inhibit oviposition in the murine experimental infection with *Angiostrongylus costaricensis*. *Parasitol Res 100*: 379-382.

Brinkworth RI, Prociv P, Loukas A, Brindley PJ 2001. Hemoglobin-degrading, aspartic proteases of blood-feeding parasites: substrate specificity revealed by homology models. *J Biol Chem 276*: 38844-38851.

Brown A, Burleigh JM, Billett EE, Pritchard DI 1995. An initial characterization of the proteolytic enzymes secreted by the adult stage of the human hookworm *Necator americanus*. *Parasitology 110*: 555-563.

Brown A, Girod N, Billett EE, Pritchard DI 1999. *Necator americanus* (human hookworm) aspartyl proteinases and digestion of skin macromolecules during skin penetration. *Am J Trop Med Hyg 60*: 840-847.

Chung YB, Kong Y, Joo IJ, Cho SY, Kang SY 1995. Excystment of *Paragonimus westermani* metacercariae by endogenous cysteine protease. *J Parasitol 81*: 137-142.

Dalton J 2003. Helminth vaccines: from mining genomic information for vaccine targets to systems used for protein expression. *Int J Parasitol 33*: 621-640.

da Silva AC, Graeff-Teixeira C, Zaha A 2003. Diagnosis of abdominal angiostrongyliasis by PCR from sera of patients. *Rev Inst Med Trop Sao Paulo 45*: 295-297.

d'Avila-Levy CM, Melo AC, Vermelho AB, Branquinha MH 2001. Differential expression of proteolytic enzymes in endosymbiont-harboring *Crithidia* species. *FEMS Microbiol Lett 202*: 73-77.

Dzik JM 2006. Molecules released by helminth parasites involved in host colonization. *Acta Biochim Pol 53*: 33-64.

Fante CA, Dieterish S, Rodriguez R 2008. Betamethasone and aqueous extract of *Arctium lappa* for treating angiostrongyliasis. *Rev Soc Bras Med Trop 41*: 654-657.

Fontoura GD, Maurer RL, Oliveira CM, Graeff-Teixeira C 2007. Abdominal angiostrongyliasis in rodent experimental infection: evidence for systemic circulation of first stage larvae. *Parasitol Int 56*: 227-229.

Francis SE, Sullivan DJ Jr, Goldberg DE 1997. Hemoglobin metabolism in the malaria parasite *Plasmodium falciparum*. *Annu Rev Microbiol 51*: 97-123.

Gallego SG, Slade RW, Brindley PJ 1998. A cDNA encoding a pepsinogen-like, aspartic protease from the human roundworm parasite *Strongyloides stercoralis*. *Acta Trop 71*: 17-26.

Geier G, Banaj HJ, Heid H, Bini L, Pallini V, Zwilling R 1999. Aspartyl proteases in *Caenorhabditis elegans*. Isolation, identification and characterization by a combined use of affinity chromatography, two-dimensional gel electrophoresis, microsequencing and databank analysis. *Eur J Biochem 264*: 872-879.

Geiger SM, Abrahams-Sandi E, Soboslay PT, Hoffmann WH, Pfaff AW, Graeff-Teixeira C, Schulz-Key H 2001. Cellular immune responses and cytokine production in BALB/c and C57BL/6 mice during the acute phase of *Angiostrongylus costaricensis* infection. *Acta Trop 80*: 59-68.

Gomez Gallego S, Loukas A, Slade RW, Neva FA, Varatharajalu R, Nutman TB, Brindley PJ 2005. Identification of an astacin-like metallo-proteinase transcript from the infective larvae of *Strongyloides stercoralis*. *Parasitol Int 54*: 123-133.

Graeff-Teixeira C, Agostini AA, Camillo-Coura L, Ferreira-da-Cruz MF 1997. Seroepidemiology of abdominal angiostrongyliasis: the standardization of an immunoenzymatic assay and prevalence of antibodies in two localities in southern Brazil. *Trop Med Int Health 2*: 254-260.

Graeff-Teixeira C, Camillo-Coura L, Lenzi HL 1991. Clinical and epidemiological aspects of abdominal angiostrongyliasis in southern Brazil. *Rev Inst Med Trop Sao Paulo 33*: 373-378.

Graeff-Teixeira C, Geiger S, Walderich B, Hoffmann W, Abrahams E, Schulz-Key H 1999. Isolation of *Angiostrongylus costaricensis* first-stage larvae from rodent feces on a Percoll gradient. *J Parasitol 85*: 1170-1171.

Graeff-Teixeira C, Goulart AH, Brum C de O, Laitano AC, Sievers-Tostes C, Zanini GM, Bered PL, Morassutti A, Geiger S, Abrahms-Sandi E, Oliveira FT, Maurer RL, Aguiar LF, Garrido CT, da Silva AC, Rodriguez R, Schulz-Key H, Agostini AA 2005. Longitudinal clinical and serological survey of abdominal angiostrongyliasis in Guaporé, southern Brazil, from 1995 to 1999. *Rev Soc Bras Med Trop 38*: 310-315.

Hawdon JM, Jones BF, Perregaux MA, Hotez PJ 1995. *Ancylostoma caninum*: metalloprotease release coincides with activation of infective larvae *in vitro*. *Exp Parasitol 80*: 205-211.

Heussen C, Dowdle EB 1980. Electrophoretic analysis of plasminogen activators in polyacrylamide gels containing sodium dodecyl sulfate and copolymerized substrates. *Anal Biochem 102*: 196-202.

Hong X, Bouvier J, Wong MM, Yamagata GY, McKerrow JH 1993. *Brugia pahangi*: identification and characterization of an aminopeptidase associated with larval molting. *Exp Parasitol 76*: 127-133.

Hotez P, Haggerty J, Hawdon J, Milstone L, Gamble HR, Schad G, Richards F 1990. Metalloproteases of infective *Ancylostoma* hookworm larvae and their possible functions in tissue invasion and ecdysis. *Infect Immun 58*: 3883-3892.

Hwang KP, Chang SH, Wang LC 2010. Alterations in the expression level of a putative aspartic protease in the development of *Angiostrongylus cantonensis*. *Acta Trop 113*: 289-294.

Incani RN, Caleiras E, Martin M, Gonzalez C 2007. Human infection by *Angiostrongylus costaricensis* in Venezuela: first report of a confirmed case. *Rev Inst Med Trop Sao Paulo 49*: 197-200.

Ishih A, Rodriguez BO, Sano M 1990. Scanning electron microscopic observations of first and third-stage larvae and adults of *Angiostrongylus costaricensis*. *Southeast Asian J Trop Med Public Health 21*: 568-573.

Jolodar A, Fischer P, Buttner DW, Miller DJ, Schmetz C, Brattig NW 2004. *Onchocerca volvulus:* expression and immunolocalization of a nematode cathepsin D-like lysosomal aspartic protease. *Exp Parasitol 107*: 145-156.

Kasny M, Mikes L, Dalton JP, Mountford AP, Horak P 2007. Comparison of cysteine peptidase activities in *Trichobilharzia regenti* and *Schistosoma mansoni* cercariae. *Parasitology 134*: 1599-1609.

Koehler JW, Morales ME, Shelby BD, Brindley PJ 2007. Aspartic protease activities of schistosomes cleave mammalian hemoglobins in a host-specific manner. *Mem Inst Oswaldo Cruz 102*: 83-85.

Laemmli UK 1970. Cleavage of structural proteins during the assembly of the head of bacteriophage T4. *Nature 227*: 680-685.

Lai SC, Jiang ST, Chen KM, Lee HH 2005. Matrix metalloproteinases activity demonstrated in the infective stage of the nematodes, *Angiostrongylus cantonensis*. *Parasitol Res 97*: 466-471.

Lee HH, Chou HL, Chen KM, Lai SC 2004. Association of matrix metalloproteinase-9 in eosinophilic meningitis of BALB/c mice caused by *Angiostrongylus cantonensis*. *Parasitol Res 94*: 321-328.

Lee JD, Yen CM 2005. Protease secreted by the infective larvae of *Angiostrongylus cantonensis* and its role in the penetration of mouse intestine. *Am J Trop Med Hyg 72*: 831-836.

Lim MD, Craik CS 2009. Using specificity to strategically target proteases. *Bioorg Med Chem 17*: 1094-1100.

Liu YH, Han YP, Li ZY, Wei J, He HJ, Xu CZ, Zheng HQ, Zhan XM, Wu ZD, Lv ZY 2010. Molecular cloning and characterization of cystatin, a cysteine protease inhibitor, from *Angiostrongylus cantonensis*. *Parasitol Res 107*: 915-922.

Longbottom D, Redmond DL, Russell M, Liddell S, Smith WD, Knox DP 1997. Molecular cloning and characterisation of a putative aspartate proteinase associated with a gut membrane protein complex from adult *Haemonchus contortus*. *Mol Biochem Parasitol 88*: 63-72.

Lopez-Otin C, Bond JS 2008. Proteases: multifunctional enzymes in life and disease. *J Biol Chem 283*: 30433-30437.

Lun HM, Mak CH, Ko RC 2003. Characterization and cloning of metallo-proteinase in the excretory/secretory products of the infective-stage larva of *Trichinella spiralis*. *Parasitol Res 90*: 27-37.

McKerrow JH 1989. Parasite proteases. *Exp Parasitol 68*: 111-115.

McKerrow JH, Brindley P, Brown M, Gam AA, Staunton C, Neva FA 1990. *Strongyloides stercoralis*: identification of a protease that facilitates penetration of skin by the infective larvae. *Exp Parasitol 70*: 134-143.

McKerrow JH, Caffrey C, Kelly B, Loke P, Sajid M 2006. Proteases in parasitic diseases. *Annu Rev Pathol 1*: 497-536.

Mendonca CLGF, Carvalho OS, Mota EM, Pelajo-Machado M, Caputo LFG, Lenzi HL 1999. Penetration sites and migratory routes of *Angiostrongylus costaricensis* in the experimental intermediate host (*Sarasinula marginata*). *Mem Inst Oswaldo Cruz 94*: 549-556.

Mentz MB, Graeff-Teixeira C 2003. Drug trials for treatment of human angiostrongyliasis. *Rev Inst Med Trop Sao Paulo 45*: 179-184.

Mesen-Ramirez P, Abrahams-Sandi E, Fernandez-Quesada K, Morera P 2008. *Angiostrongylus costaricensis* egg antigen for the immunodiagnosis of abdominal angiostrongyliasis. *J Helminthol 82*: 251-254.

Morera P 1973. Life history and redescription of *Angiostrongylus costaricensis* Morera and Céspedes, 1971. *Am J Trop Med Hyg 22*: 613-621.

Morera P, Bontempo I 1985. Acción de algunos antihelminticos sobre *Angiostrongylus costaricensis*. *Rev Med Hosp Nac Niños (Costa Rica) 20*: 165-174.

Morera P, Cespedes R 1970. *Angiostrongylus costaricensis* n. sp. (Nematoda: Metastrongyloidea), a new lungworm occurring in man in Costa Rica. *Rev Biol Trop 18*: 173-185.

Morera P, Cespedes R 1971. Angiostrongilosis abdominal. Uma nueva parasitosis humana. *Acta Med Costarric 14*: 173-189.

Mota EM, Lenzi HL 2005. *Angiostrongylus costaricensis*: complete redescription of the migratory pathways based on experimental *Sigmodon hispidus* infection. *Mem Inst Oswaldo Cruz 100*: 407-420.

Palominos PE, Gasnier R, Rodriguez R, Agostini AA, Graeff-Teixeira C 2008. Individual serological follow-up of patients with suspected or confirmed abdominal angiostrongyliasis. *Mem Inst Oswaldo Cruz 103*: 93-97.

Quiñones AM, Torres RJ, Rubin MR 2006. Biochemical detection, pharmacological inhibition and phylogenetic analysis of *Caenorhabditis elegans* metalloproteases. *BIOS 77*: 113-126.

Rawlings ND, Barrett AJ 1995. Evolutionary families of metallopeptidases. *Methods Enzymol 248*: 183-228.

Rawlings ND, Barrett AJ, Bateman A 2012. MEROPS: the database of proteolytic enzymes, their substrates and inhibitors. *Nucleic Acids Res 40*: D343-350.

Rebello KM, Barros JS, Mota EM, Carvalho PC, Perales J, Lenzi HL, Neves-Ferreira AG 2011. Comprehensive proteomic profiling of adult *Angiostrongylus costaricensis*, a human parasitic nematode. *J Proteomics 74*: 1545-1559.

Rhoads ML, Fetterer RH, Urban JF Jr 1998. Effect of protease class-specific inhibitors on *in vitro* development of the third to fourth-stage larvae of *Ascaris suum*. *J Parasitol 84*: 686-690.

Rodriguez R, Porto SM, Dos Santos Ferrari R, Marcolan AM, da Silva AC, Graeff-Teixeira C, Fornari F 2011. Outcomes in mice with abdominal angiostrongyliasis treated with enoxaparin. *Parasitol Res 109*: 787-792.

Sajid M, McKerrow JH 2002. Cysteine proteases of parasitic organisms. *Mol Biochem Parasitol 120*: 1-21.

Santos LO, Marinho FA, Altoe EF, Vitorio BS, Alves CR, Britto C, Motta MC, Branquinha MH, Santos AL, d'Avila-Levy CM 2009. HIV aspartyl peptidase inhibitors interfere with cellular proliferation, ultrastructure and macrophage infection of *Leishmania amazonensis*. *PLoS ONE 4*: e4918.

Terada M, Kino H, Akyol CV, Sano M 1993. Effects of mebendazole on *Angiostrongylus costaricensis* in mice, with special reference to the timing of treatment. *Parasitol Res 79*: 441-443.

Thiengo SC 1996. Mode of infection of *Sarasinula marginata* (Mollusca) with larvae of *Angiostrongylus costaricensis* (Nematoda). *Mem Inst Oswaldo Cruz 91*: 277-278.

Tort J, Brindley PJ, Knox D, Wolfe KH, Dalton JP 1999. Proteinases and associated genes of parasitic helminths. *Adv Parasitol 43*: 161-266.

Tungtrongchitr A, Ishih A, Terada M, Radomyos P 1993. Effects of sensitization on efficacy of mebendazole in mice infected with adult *Angiostrongylus costaricensis*. *Trop Med Parasitol 44*: 322-326.

Wallace GRL 1969. Techniques for recovering and identifying larvae of *Angiostrongylus cantonensis* from mollusks. *Malacologia 7*: 427-438.

Wilkesman J, Kurz L 2009. Protease analysis by zymography: a review on techniques and patents. *Rec Pat Biotechnol 3*: 175-184.

Williamson AL, Brindley PJ, Knox DP, Hotez PJ, Loukas A 2003. Digestive proteases of blood-feeding nematodes. *Trends Parasitol 19*: 417-423.

Williamson AL, Lecchi P, Turk BE, Choe Y, Hotez PJ, McKerrow JH, Cantley LC, Sajid M, Craik CS, Loukas A 2004. A multi-enzyme cascade of hemoglobin proteolysis in the intestine of blood-feeding hookworms. *J Biol Chem 279*: 35950-35957.

Williamson AL, Lustigman S, Oksov Y, Deumic V, Plieskatt J, Mendez S, Zhan B, Bottazzi ME, Hotez PJ, Loukas A 2006. *Ancylostoma caninum* MTP-1, an astacin-like metalloprotease secreted by infective hookworm larvae, is involved in tissue migration. *Infect Immun 74*: 961-967.

Xu YZ, Dresden MH 1986. Leucine aminopeptidase and hatching of *Schistosoma mansoni* eggs. *J Parasitol 72*: 507-511.

Yang Y, Wei H, Qin W, Zheng J 2009. Expression and characterization of aspartic protease gene in eggs and larvae stage of *Ancylostoma caninum*. *Parasitol Res 104*: 1327-1333.

Yatsuda AP, Bakker N, Krijgsveld J, Knox DP, Heck AJ, de Vries E 2006. Identification of secreted cysteine proteases from the parasitic nematode *Haemonchus contortus* detected by biotinylated inhibitors. *Infect Immun 74*: 1989-1993.

Zhan B, Hotez PJ, Wang Y, Hawdon JM 2002. A developmentally regulated metalloprotease secreted by host-stimulated *Ancylostoma caninum* third-stage infective larvae is a member of the astacin family of proteases. *Mol Biochem Parasitol 120*: 291-296.

Resultados complementares 2

Caracterização do conteúdo de proteases dos extratos das diferentes fases evolutivas (vermes adultos, L1 e L3) utilizando substratos sintéticos fluorogênicos. Estes resultados foram obtidos durante o período de doutorado sanduíche na *University of California, San Francisco*, USA (novembro 2011-fevereiro 2012), sob orientação do Dr. James McKerrow.

A. Metodologia

Ensaios de hidrólise de substrato fluorogênico em solução

Os parasitos (L1, L3, machos e fêmeas) foram macerados com resina abrasiva (*Sample Grinding Kit*, GE Healthcare) em tubos contendo 40 mM de Tris, por 5 min. Em seguida, apenas as larvas passaram por ciclos de congelamento e descongelamento em nitrogênio líquido para lise completa. Após centrifugação (16.000 x g / 15 min), foram feitas dosagens de proteína dos sobrenadantes dos extratos de parasitas utilizando o *2D Quant kit* (GE - Heathcare). Após ensaios iniciais de padronização utilizando diluições seriadas dos extratos, as seguintes quantidades de proteína foram empregadas nos testes de atividade enzimática (volume final 1 µL): 8,3 µg, 8,5 µg, 8,9 µg e 8,7 µg de proteínas de L1, L3, fêmea e macho, respectivamente.

Os substratos cumarínicos foram preparados na concentração de 10 mM em dimetilsulfóxido (DMSO) e estocados a 4°C, só sendo diluídos em tampão para sua concentração final de uso (10 µM) no momento do ensaio. Os substratos testados foram: Boc-Leu-Gly-Arg-7-amino-4-methyl-coumarin (AMC)(Sigma), Z-Arg-Arg-AMC, Z-Arg-Arg-Leu-Arg-AMC, Z-Phe-Arg-AMC, Tyr-AMC, Z-Val-Val-Arg-AMC (Bachem)(substratos para serino-proteases) e MeoSuc-Ala-Ala-Pro-Met-AMC, Suc-Ala-Ala-Pro-Ala-AMC)(Enzyme Systems Products), Z-Phe-Val-Arg-AMC, Suc-Leu-Leu-Val-Tyr-AMC (Bachem) (substratos para cisteíno-proteases).

A determinação do pH ótimo de atividade enzimática dos extratos de L1, L3, machos e fêmeas sobre os substratos foi realizada no intervalo de pH 5,5 a 9,0 utilizando-se os tampões citrato-fosfato 0,2 M (pHs 5,5 ; 6,0 ; 6,5), fosfato de sódio 0,2 M (pHs 7,0 e 7,5) ou glicina-NaOH 0,2 M (pHs 8,0 e 9,0). Os

ensaios foram realizados em placas de 96 poços preta, em um volume final de 200 µL. As diferentes amostras foram incubadas na presença do substrato e a detecção dos produtos de hidrólise foi feita em fluorímetro, por 30 minutos, utilizando 355 nm de comprimento de onda de excitação e 460 nm para emissão da fluorescência.

O efeito dos inibidores classe-específicos sobre a atividade enzimática dos extratos de L1, L3, vermes machos e fêmeas foi determinado no pH ótimo das enzimas. Nestes ensaios, as amostras foram pré-incubadas com o substrato à temperatura ambiente, por 30 minutos, na presença de um dos seguintes inibidores de proteases: 10 µM de E-64 (inibidor de cisteíno-protease), 1 mM de PMSF, 1 mM de benzamidina (inibidores de serino-protease), 10 mM de ortofenantrolina, 10 mM de EDTA (inibidores de metalo-proteases) ou 1 µM de pepstatina-A (inibidor de aspártico-proteases).

Purificação de serino-proteases de L1 de *A. costaricensis*

Extratos de L1 foram aplicados em uma coluna de afinidade benzamidina-Sepharose fast flow (GE Healthcare), utilizando o cromatógrafo líquido de alta eficiência Ettan (GE Healthcare). A coluna foi equilibrada em tampão Tris-HCl 0,05 M, contendo NaCl 0,5 M, pH 7,4 e eluída com tampão glicina 0,05 M, pH 3,0, a uma velocidade de fluxo de 0.5 mL/min. Frações de 1,0 mL foram coletadas em tubos contendo 100 µL de Tris-HCl 1 M, pH 9 para evitar a desnaturação das amostras em pH ácido. Outro cuidado adotado foi a coleta das frações em gelo, para minimizar eventual proteólise.

A atividade enzimática das frações coletadas da coluna foi avaliada sobre substrato cromogênico N_{α}-Benzoyl-L-arginina 4-nitroanilida (BAPNA) (Sigma Aldrich), específico para serino-proteases. Os ensaios foram realizados segundo o protocolo descrito por (Preiser *et al.*, 1975), utilizando-se uma alíquota de100 µL de cada uma das amostras e 700 µL de substrato BAPNA (1mg/mL), diluído em tampão Tris-HCl 0,1 M, pH 8,0, contendo cloreto de cálcio (relação 1:1 v/v). As reações de hidrólise foram monitoradas por 30 min, a 37°C, sendo interrompidas pela adição de 300 µL de ácido acético 30% (v/v). A detecção dos produtos de hidrólise do substrato cromogênico foi feita por espectrofotometria, utilizando-se um comprimento de onda de 410 nm.

As frações eluídas da coluna de benzamidina que mostraram atividade enzimática sobre o substrato BAPNA foram precipitadas no *freezer*, por 12 horas, com 4 volumes etanol + 4 volumes acetona + 2 volumes de água. Após centrifugação e lavagem com uma mistura de etanol 40%, acetona 40%, os precipitados foram solubilizados com uréia 8 M, seguido de redução das proteínas com DTT e alquilação com iodoacetamida. Após diluição da uréia para 1 M, as proteínas foram tripsinizadas por 16 horas, a 37°C. Os peptídeos trípticos foram dessalinizados em microcolunas POROS R2 e submetidos à cromatografia de fase reversa em coluna capilar Magic C18 AQ 200 Å (30 cm x 75 µm; Michrom Bioresources Inc) utilizando o nanocromatógrafo Proxeon Easy II (Thermo) acoplado ao espectrômetro de massas LTQ-Orbitrap XL (Thermo).

A aquisição de dados no Orbitrap foi feita no modo *data-dependent*, alternando automaticamente entre o MS no Orbitrap a 60.000 de resolução (FWHM @ m/z 400) e o MS2 no *linear trap*. Para cada MS, até dez íons mais intensos foram selecionados para fragmentação por CID (*Collision Induced Dissociation)* (Swanson & Washburn, 2005). Os arquivos brutos do LTQ-Orbitrap (extensão RAW) foram convertidos em listas de massas (formato MS2) pelo software RAWXtract. Através do algoritmo de busca ProLuCID (Xu *et al.*, 2006), estes valores de massa obtidos experimentalmente foram confrontados com listas de massas teóricas geradas pela digestão tríptica *in silico* das sequências de *C. elegans* depositadas no banco de dados UniProtKB (http://www.uniprot.org). Para filtrar identificações de baixa qualidade e validar os resultados obtidos, empregamos o algoritmo SEPro (*Search Engine Processor*) (http://pcarvalho.com/patternlab/sepro.shtml).

B. Resultados

Ensaios de hidrólise de substrato fluorogênicos em solução

Inicialmente, avaliamos a capacidade de hidrólise dos extratos de L1, L3, macho e fêmea sobre os diferentes substratos fluorogênicos indicados na Tabela 2. Os substratos Boc-Leu-Gly-Arg-AMC e Tyr-AMC, preferenciais para os extratos de formas larvares e vermes adultos, respectivamente, foram utilizados nos ensaios de determinação do pH ótimo de atividade enzimática

das proteases, sob as condições analisadas. Constatamos que L1 e L3 apresentam um pH ótimo de atividade de 8,0, enquanto que extratos de vermes adultos tiveram pH ótimo de 7.5 (Figura 15).

A hidrólise do substrato Boc-Leu-Gly-Arg-AMC, específico para serino-proteases, por extratos de L1 foi inibida apenas na presença de PMSF e benzamidina, ambos inibidores de serino-proteases (Figura 18). A hidrólise deste mesmo substrato pelo extrato de L3 foi inibida pela presença dos inibidores de metaloproteases ortofenantrolina e EDTA (Figura 20). Vale ressaltar que, dependendo das concentrações de enzima utilizadas, podemos observar a clivagem de qualquer substrato peptídico pelos extratos testados. Efetivamente, a especificidade do mecanismo de ação deve ser definida utilizando-se inibidores classe-específicos e não apenas substratos (que não são tão específicos). Neste caso, como a atividade de L3 foi inibida eficientemente pela presença de quelantes de metal, os dados sugerem a presença de metaloproteases. No caso dos extratos de L1, a presença de serino-proteases parece indiscutível.

Os extratos de vermes adultos (macho e fêmea) hidrolisaram preferencialmente o substrato Tyr-AMC. No entanto, a classe de proteases envolvida nesta atividade enzimática não foi determinada nas fêmeas adultas, pois nenhum dos inibidores testados mostrou-se eficaz. Este mesmo teste de inibição não foi feito nos machos em função da escassez de amostra.

Purificação de serino-proteases de L1 de *A. costaricensis*

O perfil cromatográfico do extrato de L1 após a coluna de afinidade com benzamidina mostrou uma fração majoritária que não interagiu com a coluna e um segundo pico eluído apenas com tampão glicina, em pH ácido (Figura 13). A fração ligada à coluna apresentou atividade enzimática sobre BAPNA comparável com a fração não-ligada, apesar de conter cerca de 5 vezes menos proteína (estimado pela área relativa do pico cromatográfico), indicando um aumento da atividade específica. Por SDS-PAGE (Laemmli, 1970), observamos o enriquecimento de pelo menos duas bandas principais na fração ligada à coluna de afinidade, com massas moleculares estimadas entre 30 e 45 kDa (Figura 14, círculo vermelho). Em função da pouca quantidade de proteína, houve necessidade de revelar o gel com nitrato de prata por bastante tempo. A

alta sensibilidade do processo de revelação permitiu a visualização de bandas artefatuais de queratina (50-68 kDa) que normalmente contaminam tampões e amostras (Yokota *et al.*, 2000).

Para confirmar a purificação de serino-proteases, a etapa seguinte consistiu na análise da fração ligada à coluna por espectrometria de massas utilizando nLC-nESI-MS/MS. Os espectros de MS2 gerados foram confrontados com um banco de dados contendo as sequências de *C. elegans* do UniProtKB, complementado com 246 sequências dos contaminantes mais comuns (ex.: queratinas, tripsina, albumina). Para permitir a validação dos resultados através do cálculo do *false discovery rate* (FDR), todas as sequências foram invertidas, gerando um conjunto adicional de sequências fictícias (sequências iscas ou *decoy*). As proteínas de L1 identificadas na fração ligada à coluna de benzamidina estão listadas na Tabela 3. Nossos dados permitiram a identificação de 425 peptídeos (0% FDR, erro $\leq$ 8 ppm) que mapearam para 68 proteínas classificadas em 27 grupos que compartilhavam ao menos um peptídeo. Cerca de 50% destes peptídeos corresponderam a sequências de contaminantes (principamente queratinas). Dentre os peptídeos restantes, aproximadamente 30% identificaram proteínas estruturais de nematoide, indicadas em azul na Tabela 3 (ex.: componentes de citoesqueleto, matriz extracelular, cutícula e/ou músculo). Identificamos também algumas proteínas envolvidas com resposta a estresse e processos metabólicos, além de histonas e a proteína 14-3-3-*like*. Devido à natureza iônica da benzamidina, acreditamos que a presença destas proteínas na fração que se ligou à coluna seja consequência de interações inespecíficas. Não conseguimos identificar serino-proteases nesta fração, mesmo quando fizemos buscas contra um banco de dados de sequências de nematoides utilizando o algoritmo Peaks (dados não mostrados). A pesquisa no UniProtKB com as palavras “serine protease” e “Angiostrongylus” revela a inexistência de sequências desta classe de proteases depositadas. Além da limitação de informação de sequência nos bancos de dados, a pouca quantidade de amostra também é um fator limitante importante. Atualmente, além de juntar maior quantidade de massa parasitária para repetir o experimento sob condições experimentais otimizadas, estamos selecionando os espectros de boa qualidade sem identificação para serem submetidos à análise por sequenciamento *de novo* em associação com BLAST.

Figuras – Resultados Complementares 2

Tabela 2: Atividade enzimática de extratos proteicos de *A. costaricensis* testada contra um painel de substratos sintéticos fluorogênicos preferenciais para cisteíno (C)- e/ou serino-proteases (S). A atividade enzimática foi classificada como intensa (+++), moderada (++), fraca (+) ou ausente (-).

Classe	Substrato Fluorogênico	L1
S	Boc-Leu-Gly-Arg-AMC	+++
S/C	Tyr-AMC	++
S	Suc-Ala-Ala-Pro-Ala-AMC	--
S	N-Benzoyl-Phe-Val-Arg-AMC	+
S	Meo-Suc-Ala-Ala-Pro-Met-AMC	--
C	Z-Arg-Arg-Leu-Arg-AMC	--
C	Z-Val-Val-Arg-AMC	+++
S/C	Suc-Leu-Leu-Val-Tyr-AMC	+
C	Z-Arg-Arg-AMC	++
C/S	Z-Phe-Arg-AMC	+

Substrato Fluorogênico	Macho
Boc-Leu-Gly-Arg-AMC	--
Tyr-AMC	+++
Suc-Ala-Ala-Pro-Ala-AMC	--
N-Benzoyl-Phe-Val-Arg-AMC	--
Meo-Suc-Ala-Ala-Pro-Met-AMC	--
Z-Arg-Arg-Leu-Arg-AMC	--
Z-Val-Val-Arg-AMC	--
Suc-Leu-Leu-Val-Tyr-AMC	--
Z-Arg-Arg-AMC	--
Z-Phe-Arg-AMC	--

Substrato Fluorogênico	L3
Boc-Leu-Gly-Arg-AMC	+++
Tyr-AMC	--
Suc-Ala-Ala-Pro-Ala-AMC	--
N-Benzoyl-Phe-Val-Arg-AMC	--
Meo-Suc-Ala-Ala-Pro-Met-AMC	--
Z-Arg-Arg-Leu-Arg-AMC	--
Z-Val-Val-Arg-AMC	++
Suc-Leu-Leu-Val-Tyr-AMC	--
Z-Arg-Arg-AMC	--
Z-Phe-Arg-AMC	--

Substrato Fluorogênico	Fêmea
Boc-Leu-Gly-Arg-AMC	++
Tyr-AMC	+++
Suc-Ala-Ala-Pro-Ala-AMC	+
N-Benzoyl-Phe-Val-Arg-AMC	--
Meo-Suc-Ala-Ala-Pro-Met-AMC	++
Z-Arg-Arg-Leu-Arg-AMC	--
Z-Val-Val-Arg-AMC	--
Suc-Leu-Leu-Val-Tyr-AMC	--
Z-Arg-Arg-AMC	--
Z-Phe-Arg-AMC	--

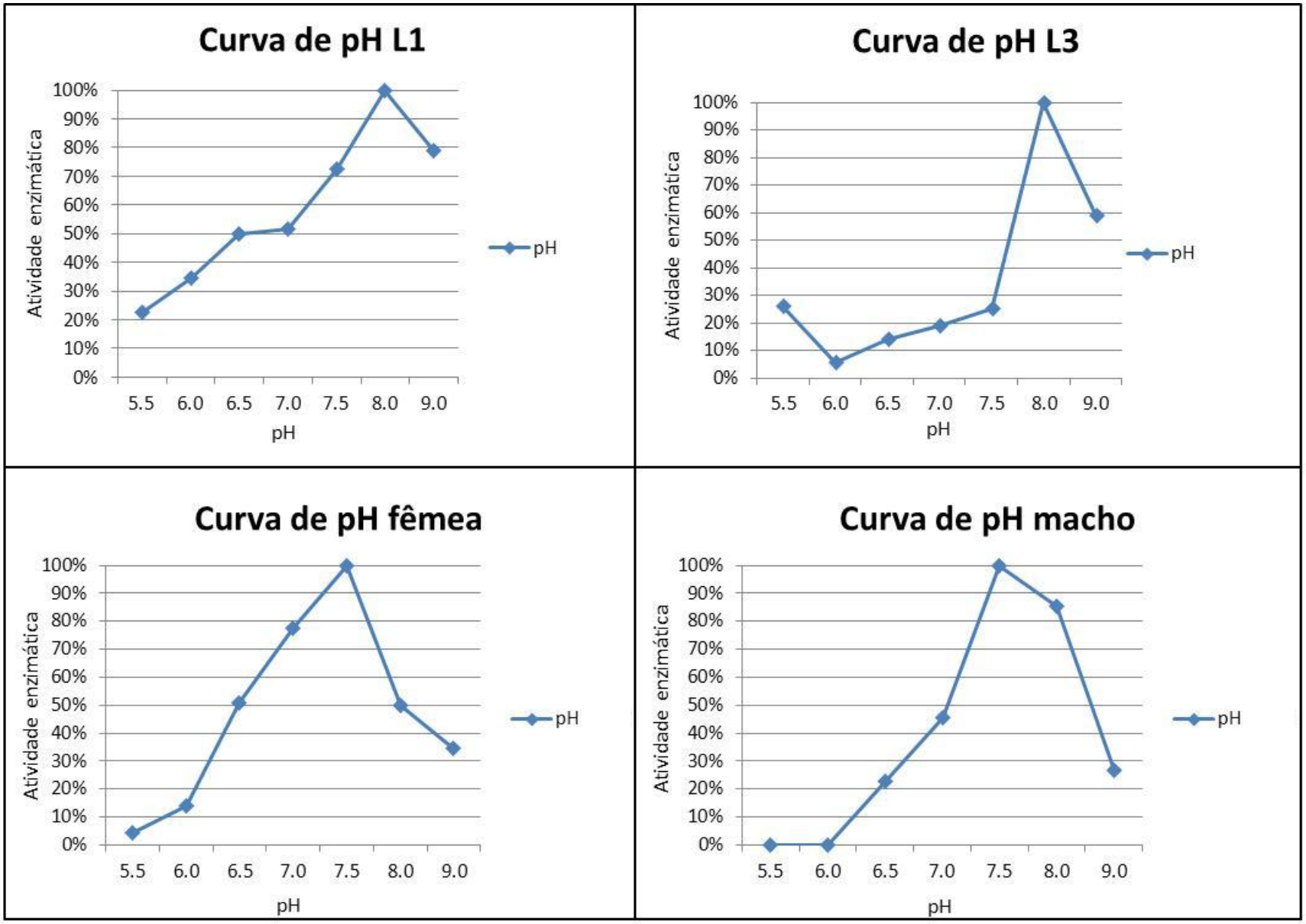

Figura 13: Curva pH ótimo para extratos de proteínas de *A. costaricensis* utilizando os substratos fluorogênicos N-t-Boc-Leu-Gli-Arg-AMC (L1 e L3) ou Tyr-AMC (macho e fêmea).

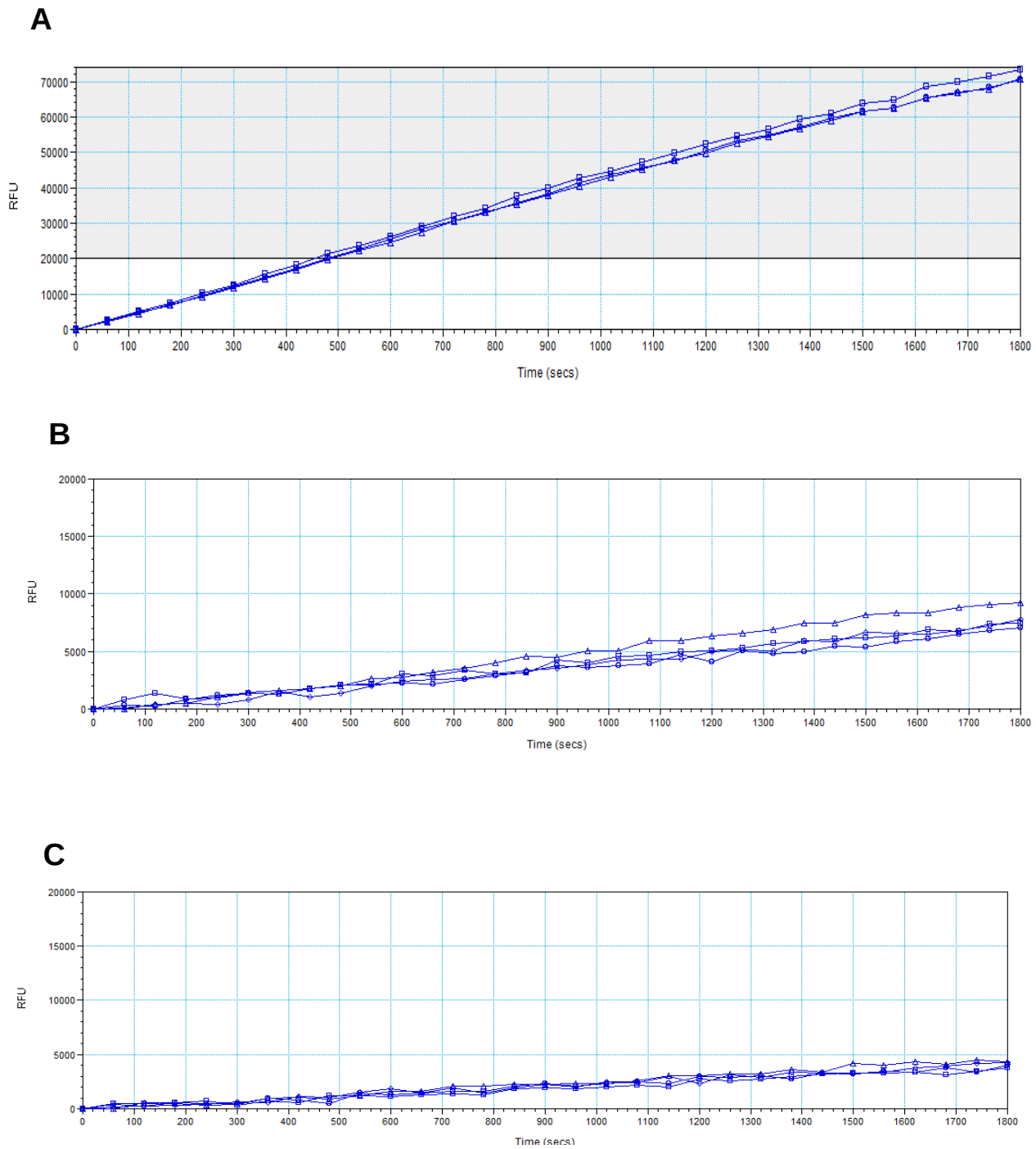

Figura 14: Hidrólise enzimática dos diferentes substratos fluorogênicos (10 µM, pH 8,0) pelo extrato de L1. (A) N-t-Boc-Leu-Gly-Arg-AMC, substrato para serino-proteases do tipo C3/C5 convertases; (B) N-Benzoyl-Phe-Val-Arg-AMC, substrato para serino-proteases do tipo trombina; (C) Suc-Leu-Leu-Val-Tyr-AMC, substrato para quimiotripsina-like e calpaínas-like

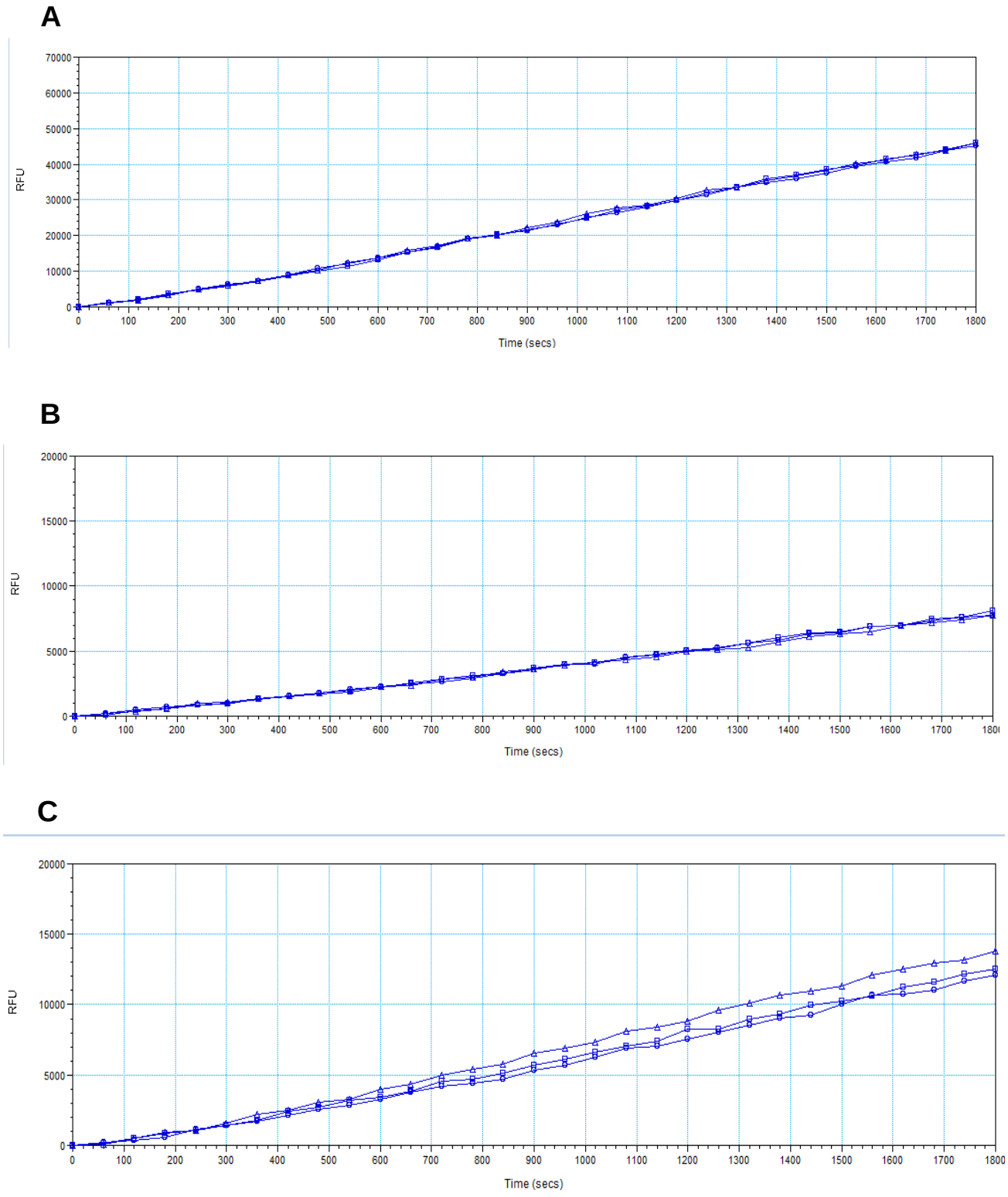

Figura 15: Hidrólise enzimática dos diferentes substratos fluorogênicos (10 µM, pH 8,0) pelo extrato de L1. (A) Z-Val-Val-Arg-AMC, substrato para catepsina S; (B) Z-Arg-Arg-AMC, substrato para catepsina-B; (C) TFA-Tyr-AMC, substrato para catepsina- B e quimiotripsina.

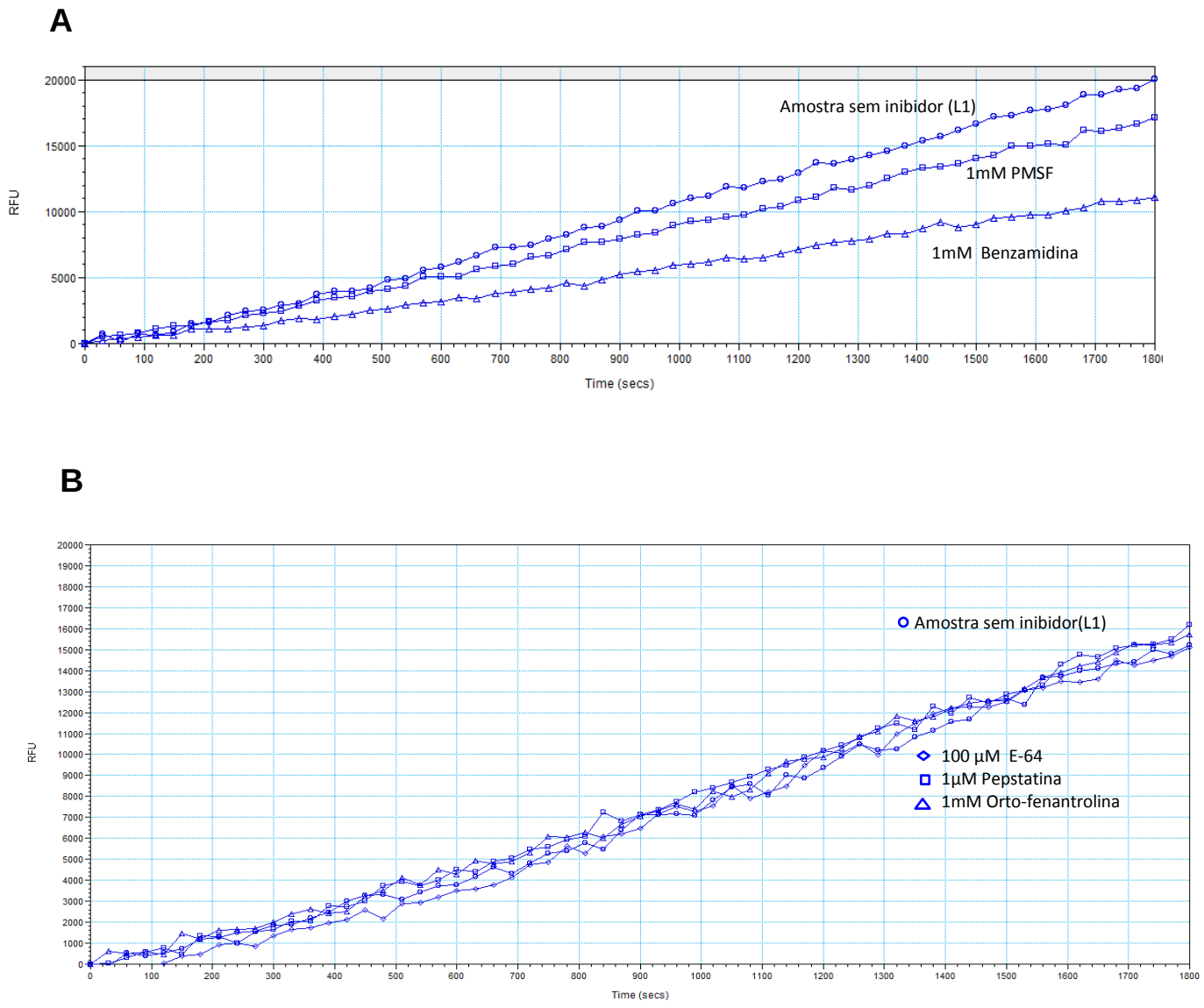

Figura 16: Hidrólise enzimática do substrato N-t-Boc-Leu-Gly-Arg-AMC (10 µM, pH 8,0) pelo extrato de L1 na presença de inibidores de proteases. (A) 1 mM de PMSF e 1 mM de benzamidina; (B) 100 µM de E-64, 1 µM de pepstatina e 1 mM de ortofenantrolina.

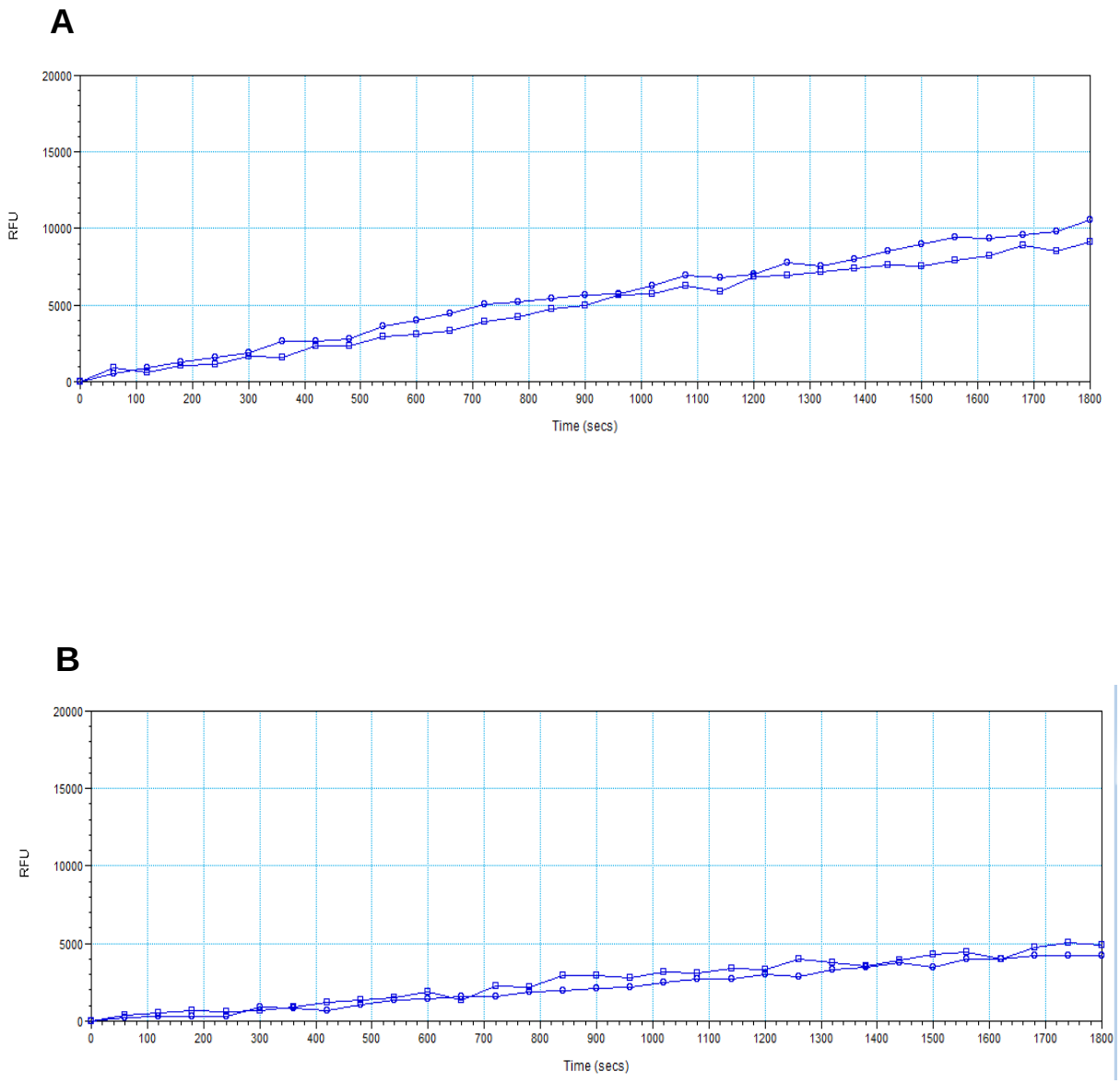

Figura 17: Hidrólise enzimática dos diferentes substratos fluorogênicos (10 µM, pH 8.0) pelo extrato de L3. (A) N-t-Boc-Leu-Gly-Arg-AMC, substrato para serino-proteases do tipo C3/C5 convertases; (B) Z-Val-Val-Arg-AMC, substrato para catepsina S.

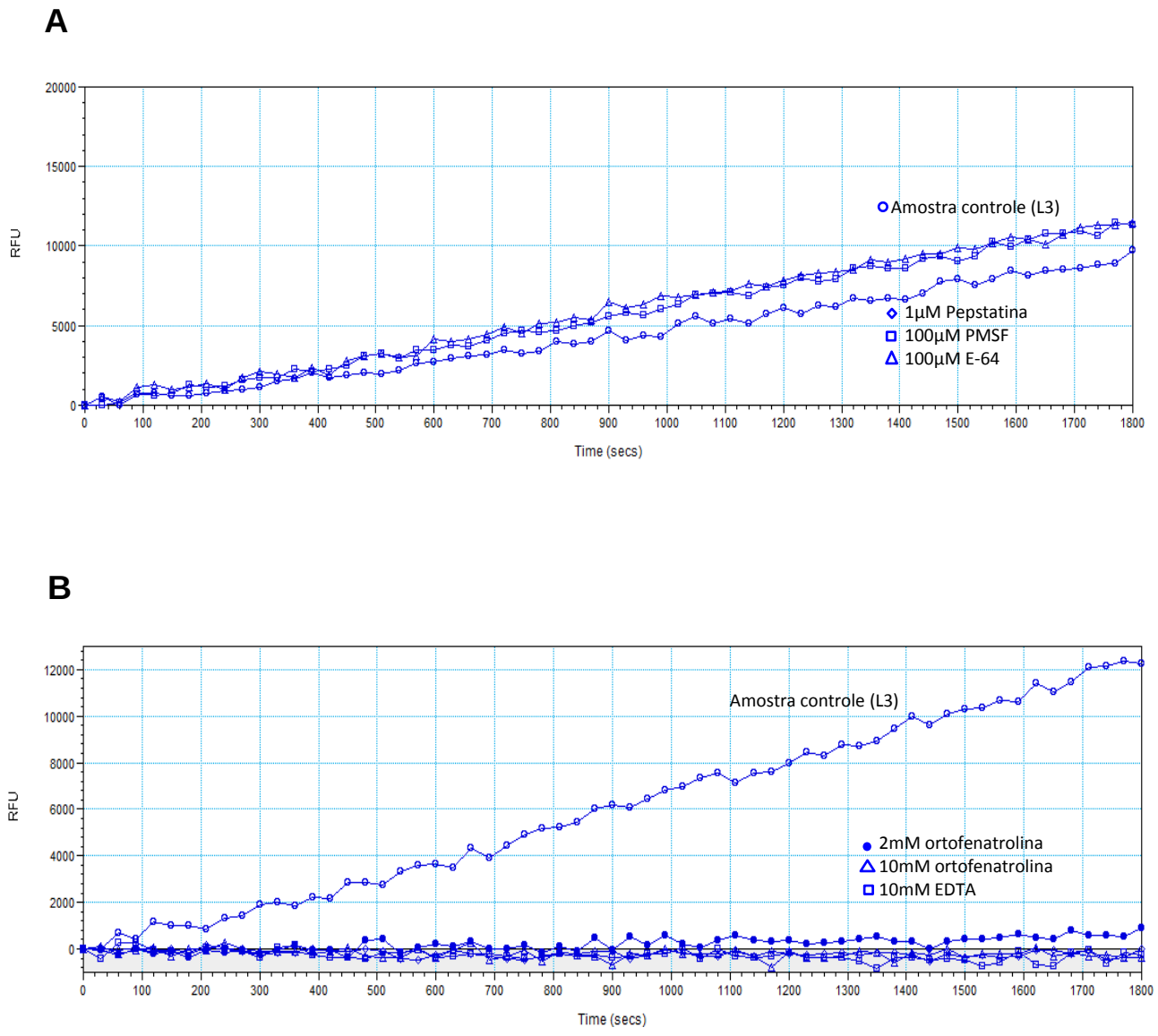

Figura 18: Hidrólise enzimática do substrato N-t-Boc-Leu-Gly-Arg-AMC (10 µM, pH 8,0) pelo extrato de L3 na presença de inibidores de proteases. (A) 1 µM de pepstatina, 100 µM de PMSF e 100 µM de E-64; (B) 2 mM e 10 mM de ortofenantrolina e 10 mM EDTA.

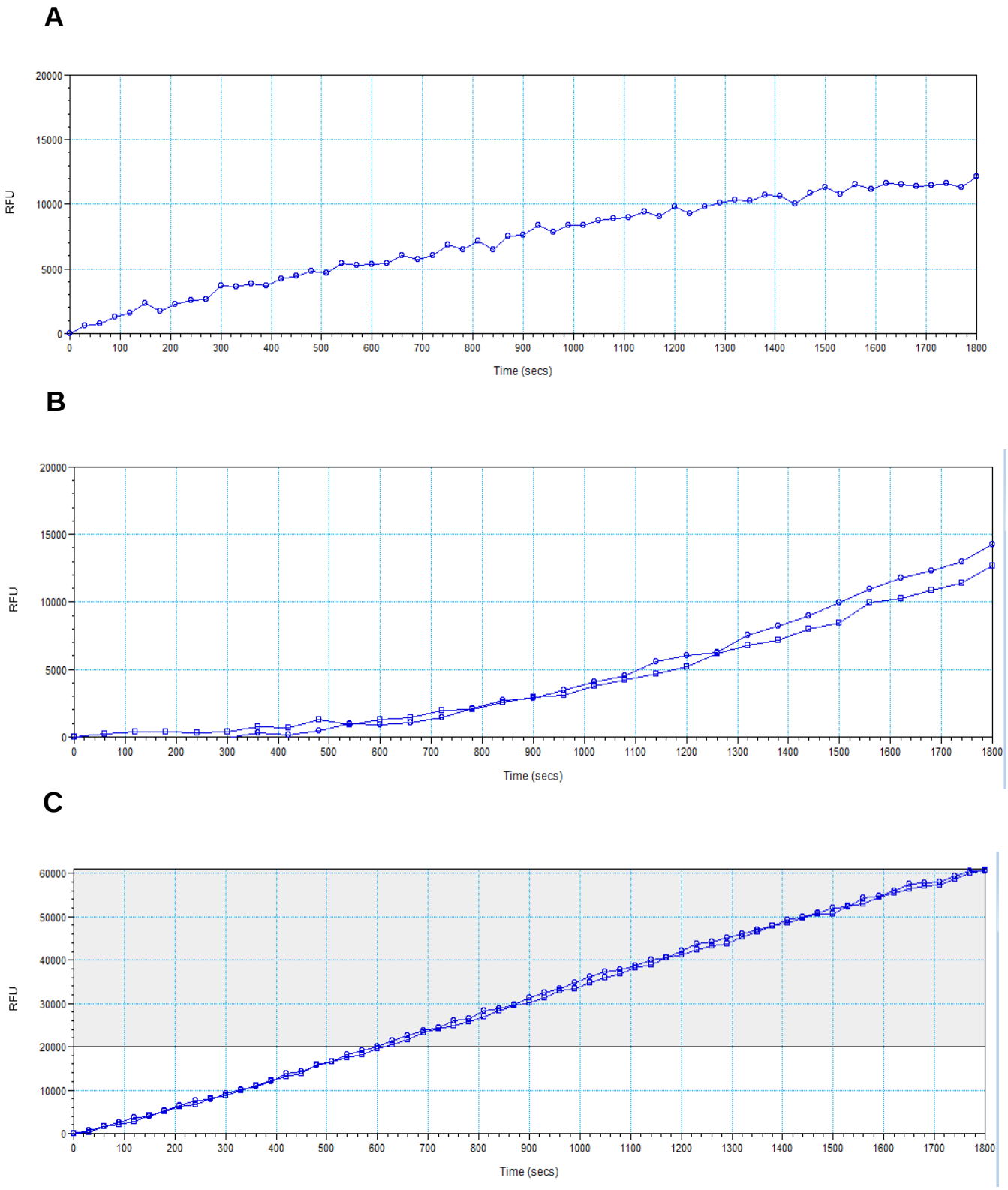

Figura 19: Hidrólise enzimática dos diferentes substratos fluorogênicos (10 µM, pH 8.0) pelo extrato de fêmea. (A) N-t-Boc-Leu-Gly-Arg-AMC, substrato para serino-proteases do tipo C3/C5 convertases; (B) Meo-Suc-Ala-Ala-Pro-Met-AMC, substrato para quimitripsina-like e serino proteases do tipo elastase; (C) TFA-Tyr-AMC, substrato para catepsina- B e

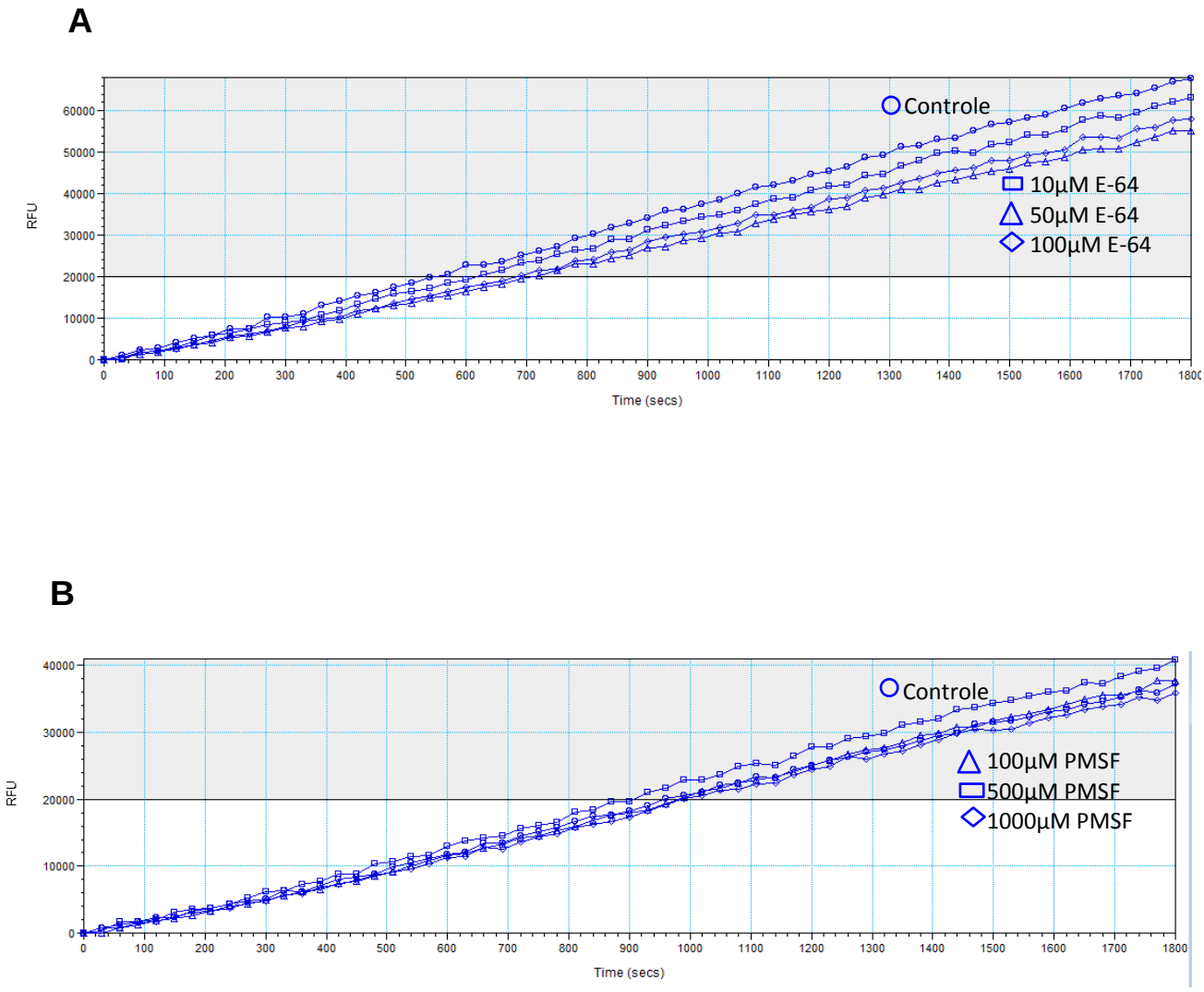

Figura 20: Hidrólise enzimática do substrato TFA-Tyr-AMC (10 µM, pH 8,0) pelo extrato de fêmea na presença de inibidores de proteases. (A) 10 µM, 50 µM, 100 µM de E-64 (B) 100 µM, 500 µM, 1000 µM de PMSF.

A

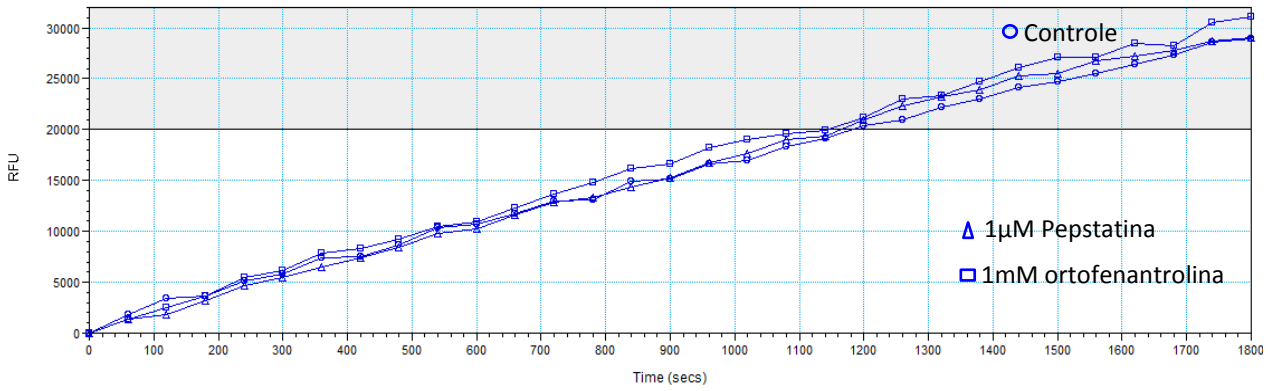

B

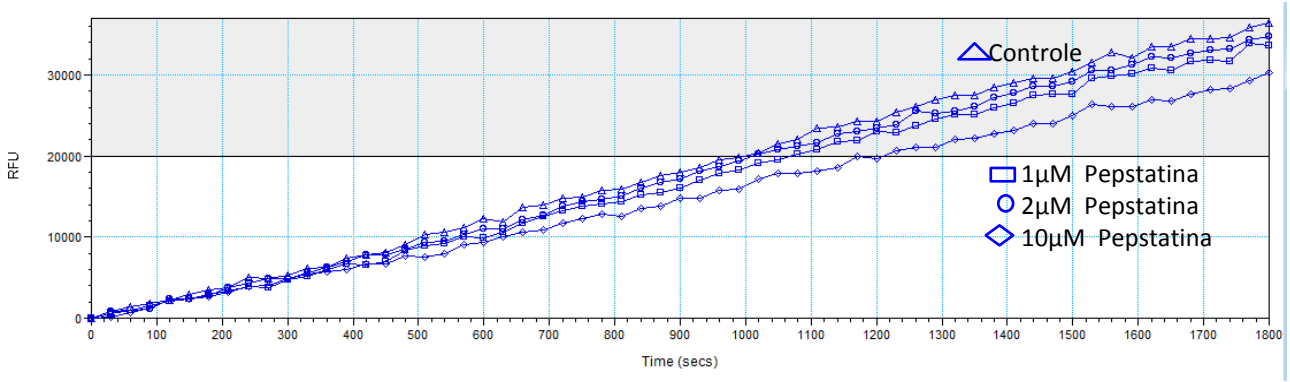

Figura 21: Hidrólise enzimática do substrato TFA-Tyr-AMC (10 µM, pH 8,0) pelo extrato de fêmea na presença de inibidores de proteases. (A) 1 µM Pepstatina e1 mM de ortofenatrolina; (B) 1 µM, 2 µM e 10 µM de pepstatina.

A

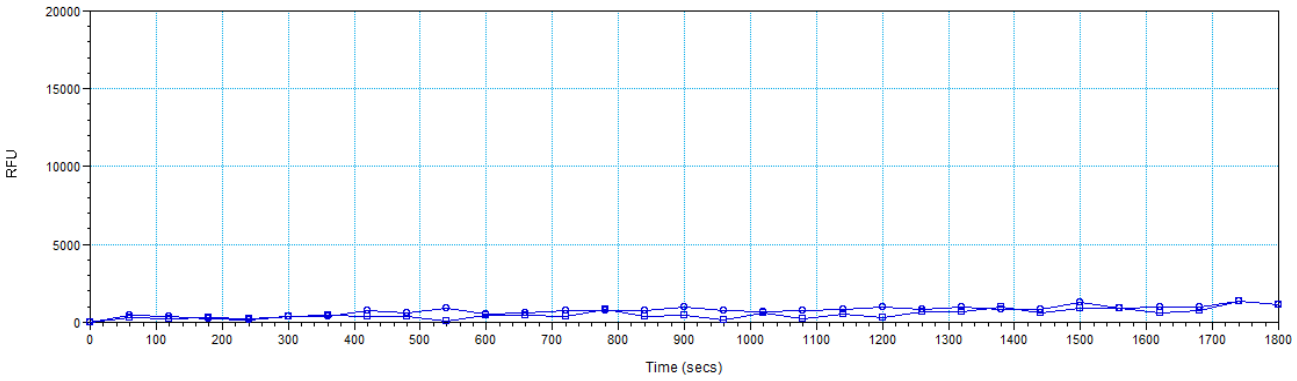

B

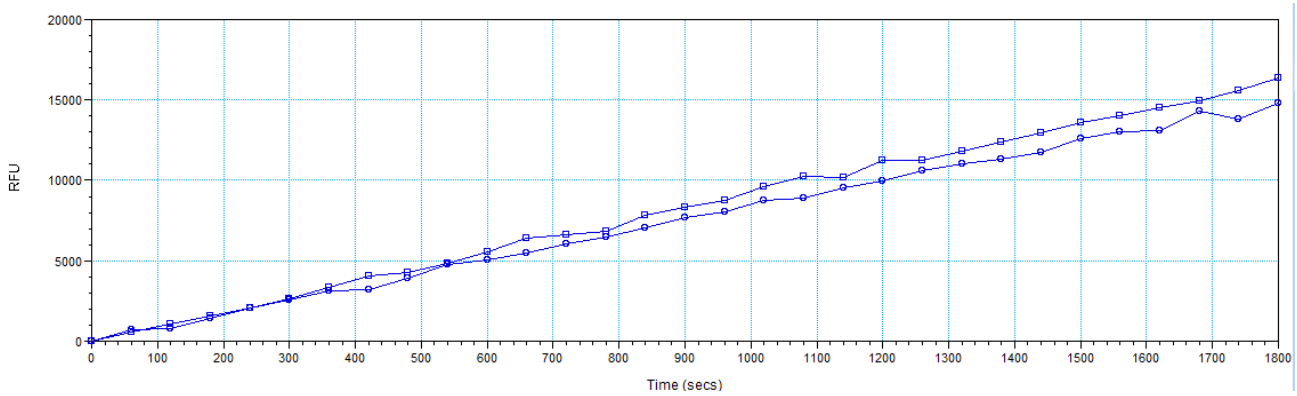

Figura 22: Hidrólise enzimática dos diferentes substratos fluorogênicos (10 µM, pH 8,0) pelo extrato de macho (A) Z-Val-Val-Arg-AMC, substrato para catepsina S; TFA-Tyr-AMC, substrato para catepsina- B e quimiotripsina.

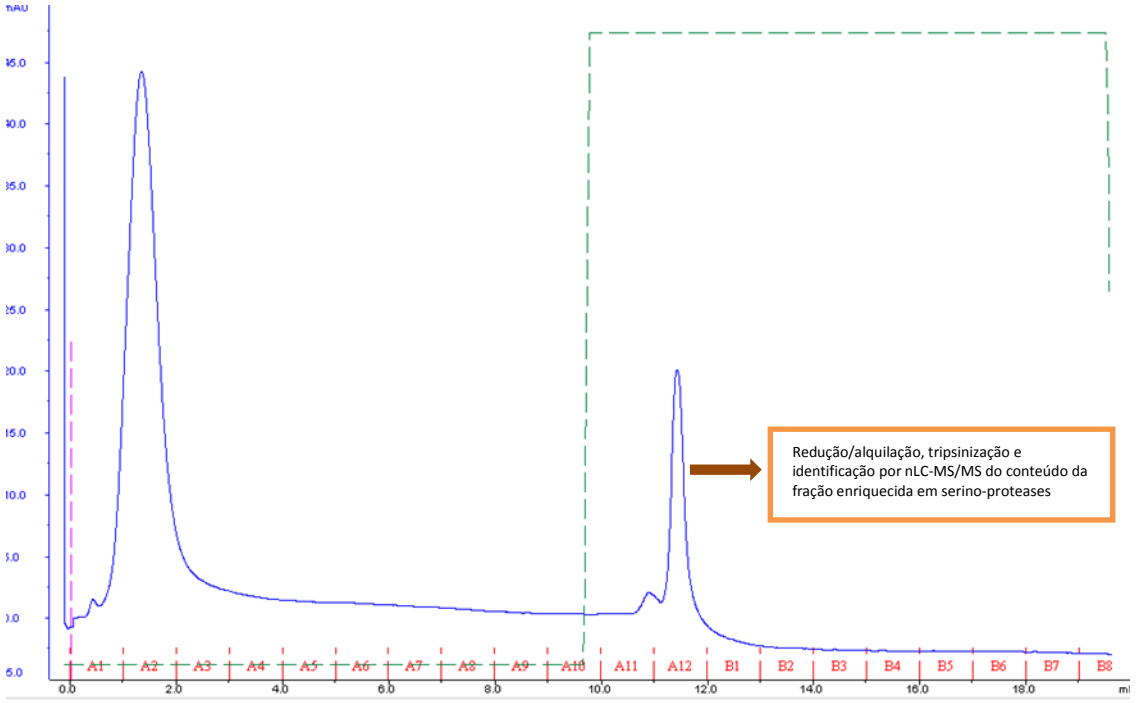

Figura 23: Cromatografia de afinidade de extrato de L1 de *A. costaricensis* em coluna HiTrap Benzamidina FF (1 mL). Tampão A: 50 mM Tris-HCl 0,5 M NaCl pH 7,4. Tampão B: 50 mM glicina-HCl pH 3,0. Picos de absorvância a 280 nm. A linha tracejada indica o gradiente de tampão B utilizado (0-100%). Fluxo 1 mL/min. Foram coletadas frações de 1 mL/tubo, neutralizadas imediatamente com solução de Tris base 1 M.

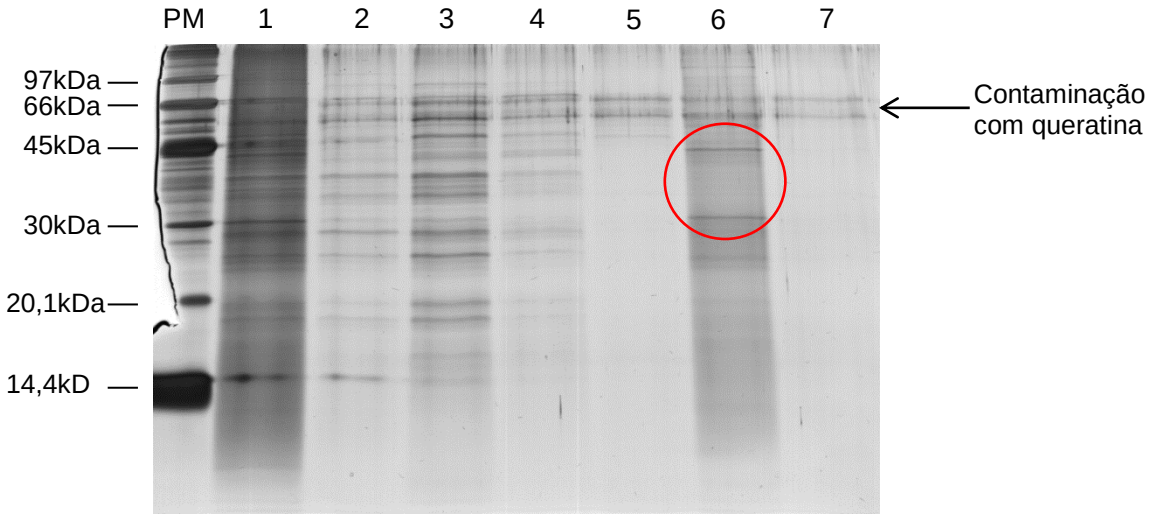

Figura 24: SDS-PAGE 15% em condições redutoras. (1) 1,1 µg do extrato bruto de L1; (2-4) 100µL de frações não- ligadas à coluna de benzamidina correspondentes aos tubos A1, A2, A3; (5-7) frações ligadas à coluna de benzamidina correspondentes aos tubos A11, A12, B1. PM: padrão de massa molecular (*Low range*- GE Healthcare).

Tabela 3: Proteínas do extrato de L1 de *A. costaricensis* que interagiram com a coluna HiTrap Benzamidina identificadas por nLC-nESI-LTQ-Orbitrap XL.

Número de acesso	Grupo	M+H$^+$	# Peptídeos	Cobertura	Descrição
P91910	1	50062	2	0.07	Tubulin alpha-3 chain
P62784	2	11344	5	0.5	Histone H4
P46561	3	57472	3	0.09	ATP synthase subunit beta, mitochondrial
Q19289	4	67090	2	0.04	Intermediate filament protein ifb-1
O76840	5	237427	3	0.02	Papilin
contaminant_TRYPSIN	6	23959	8	0.51	Trypsin
Q18688	7	80214	4	0.08	Heat shock protein 90
Q9U296	8	69474	2	0.04	Malic enzyme
P02566	9	224970	3	0.02	Myosin-4
Q18066	10	71786	3	0.06	Disorganized muscle protein 1
Q03755	11	45121	1	0.02	Cuticlin-1
P12844	12	225353	5	0.04	Myosin-3
Q27888	13	36024	2	0.07	L-lactate dehydrogenase
Q18817	14	49396	2	0.07	Protein BEN-1
P52275	14	50294	2	0.06	Tubulin beta-2 chain
O17921	14	50188	2	0.06	Protein TBB-1
contaminant_KERATIN07	15	50864	8	0.16	Keratin
contaminant_KERATIN10	15	44061	4	0.08	Keratin
contaminant_KERATIN02	15	61931	26	0.62	Keratin
contaminant_KERATIN03	15	59464	20	0.38	Keratin
contaminant_KERATIN05	15	51481	14	0.3	Keratin
contaminant_KERATIN04	15	49595	4	0.07	Keratin
contaminant_KERATIN11	15	48438	2	0.03	Keratin
contaminant_KERATIN12	15	47927	10	0.21	Keratin
contaminant_KERATIN08	15	50449	11	0.23	Keratin
contaminant_KERATIN06	15	49119	6	0.1	Keratin
contaminant_KERATIN15	16	64453	4	0.05	Keratin
contaminant_KERATIN14	16	65812	4	0.05	Keratin
contaminant_KERATIN13	16	65436	23	0.41	Keratin
contaminant_KERATIN20	16	53697	3	0.03	Keratin
contaminant_KERATIN17	16	62405	16	0.28	Keratin
contaminant_KERATIN18	16	59767	12	0.24	Keratin
contaminant_KERATIN22	16	65807	24	0.43	Keratin
contaminant_KERATIN21	16	39176	11	0.31	Keratin
contaminant_KERATIN16	16	57211	3	0.05	Keratin
Q6A8K1	17	40382	8	0.28	Protein ACT-4, isoform c
P10983	17	41750	8	0.27	Actin-1/3
O45815	17	41827	5	0.14	Protein ACT-5
P10984	17	41732	8	0.27	Actin-2
Q95ZL1	17	37236	7	0.28	Protein ACT-4, isoform b
P10986	17	41732	8	0.27	Actin-4
P41932	18	28155	4	0.17	14-3-3-like protein 1
Q20655	18	28032	9	0.33	14-3-3-like protein 2
Q95ZT1	18	22545	8	0.32	Protein FTT-2, isoform b
Q27249	19	29596	10	0.35	Tropomyosin isoforms c/e
Q22866	19	32965	15	0.34	Tropomyosin isoforms a/b/d/f
Q27484	20	13519	2	0.21	Probable histone H2B 3
Q22979	20	12138	2	0.24	Protein HIS-39
Q27894	20	13545	2	0.21	Histone H2B 2
P04255	20	13474	2	0.21	Histone H2B 1
Q27876	20	13559	2	0.21	Probable histone H2B 4
B6EU49	21	17115	2	0.14	Alkali myosin light chain long isoform
P53014	21	17115	2	0.14	Myosin, essential light chain
Q8ITY2	22	60595	6	0.13	Protein PCK-1, isoform b
Q8ITY1	22	41052	4	0.13	Protein PCK-1, isoform c
Q8ITY0	22	66613	8	0.14	Protein PCK-1, isoform d
O44906	22	73134	8	0.13	Protein PCK-1, isoform a
B3WFV3	23	63645	7	0.14	Protein UNC-15, isoform b
P10567	23	101870	14	0.19	Paramyosin
Q9U3B0	24	24049	2	0.11	Heat shock protein 60 (Fragment)
P50140	24	60045	3	0.07	Chaperonin homolog Hsp-60, mitochondrial
Q95XF6	25	13227	1	0.14	Protein Y73B3A.12
O16305	25	16795	2	0.22	Calmodulin
P90901	26	66472	2	0.04	Intermediate filament protein ifa-1
G5ECT5	26	68487	2	0.04	Protein IFA-1, isoform d
O45246	27	70377	2	0.04	Protein HSP-70
P09446	27	69661	4	0.08	Heat shock 70 kDa protein A
G5ECU5	27	70579	2	0.04	Protein F44E5.4

IV. Discussão

A angiostrongilíase abdominal (AA) é uma doença pouca conhecida e sub-diagnosticada, sendo em muitos casos confundida com outras enfermediadades. A inexistência de uma ferramenta diagnóstica etiológica eficaz impossibilita o conhecimento da prevalência dessa enfermidade no Brasil e em nos outros países da America Latina, como na Costa Rica, onde a doença é considerada um grave problema de saúde pública (Ubelaker & Hall, 1979; Demo & Pessat, 1986; Morera, 1988). Apesar de a maioria dos doentes brasileiros ser proveniente da região sul (Agostini *et al.*, 1984; Ayala, 1987), casos da doença já foram descritos em outros estados brasileiros (Ziliotto *et al.*, 1975; Barbosa *et al.*, 1980; Rocha *et al.*, 1991; Pena *et al.*, 1995). Apesar do grande potencial de expansão da AA, a literatura disponível sobre o nematoide *A. costaricensis* e sobre a angiostrongilíase abdominal é bastante limitada. Pouco se sabe a respeito da morfologia, fisiologia e metabolismo do nematoide causador desta doença.

O levantamento da literatura revela a existência de apenas três trabalhos utilizando técnicas de microscopia no estudo do *A. costaricensis*: um trabalho pioneiro (Morera & Cespedes, 1971) ilustrando as diferentes fases do ciclo através de desenhos obtidos por microscopia de campo claro; um manuscrito (Thiengo *et al.*, 1997) descrevendo uma cepa brasileira de *A. costaricensis* utilizando a mesma técnica anterior, mas com ênfase na morfometria dos vermes; um terceiro e único trabalho utilizando a técnica de microscopia de varredura (Ishih *et al.*, 1990) mostrando a topografia das diferentes fases de desenvolvimento do helminto. Desta forma, a primeira etapa deste estudo consistiu no estudo detalhado das morfologias interna e externa de vermes adultos (machos e fêmeas) e larvas de primeiro (L1) e terceiro (L3) estágios de *A. costaricensis*. Utilizamos técnicas de microscopia eletrônica de varredura e microscopia de luz de espécimes inteiros (Artigo 1), além de microscopia confocal e microscopia de luz de cortes histológicos (Resultados complementares 1).

De um modo geral, nossos resultados corroboraram os dados da literatura, contribuindo para ampliar o detalhamento morfológico do parasito. Como única exceção, podemos citar o número de papilas cefálicas

encontradas nos vermes adultos: encontramos quatro papilas e dois anfídios no entorno do orifício oral do helminto (Figuras 3b, 4h – Artigo 1), enquanto (Ishih *et al.*, 1990) relataram a presença de duas fileiras de seis papilas ao redor da boca. Dos dois lados da boca, entre as duas fileiras de papilas, relataram também a presença de dois ofídios. Os grupos de Thiengo e Morera relataram a presença de apenas seis papilas cefálicas. Anderson (1978) descreveu como chave taxonômica para classificação no gênero *Angiostrongylus* a presença de seis papilas cefálicas sensoriais circundando a boca, o que estaria de acordo com nossos achados. Mostramos ainda, pela primeira vez, a fotografia das três papilas presentes na abertura cloacal (Figuras 4c, 4d – Artigo 1) descritas originalmente por Morera & Cespedes, 1971, revistas por Thiengo *et al.*, 1997 e mostradas apenas por desenhos em câmara clara. As papilas, tanto cefálicas quanto cloacais, são órgãos sensorais auxiliares nos nematoides (Strote & Bonow, 1993). Através da microscopia de luz, visualizamos também a presença de papilas esofágica-intestinais nos vermes adultos (Figura 5b – Artigo 1) que nunca tinham sido observadas anteriormente. Estas papilas têm a função de regulação da ingesta de alimentos no intestino, como ocorre em outros nematoides (Hoberg *et al.*, 2010).

O estudo histológico das diferentes fases de desenvolvimento possibilitou a observação das estruturas internas dos vermes adultos (Figuras 2, 3, 4), tais como o gubernáculo, a cloaca e os ovos no interior do útero (Figuras 9, 3a, 3b, 4a, 4b, 4c). O mesmo não pôde ser evidenciado nas formas larvares devido a dificuldades da técnica de processamento; por se tratar de um material bastante diminuto (Figuras 10c, 10d), existe uma grande perda de amostra ao longo da preparação do material.

Portanto, utilizamos a microscopia confocal a laser, que nos permite fazer cortes ópticos no material. Observamos que as L1 estavam repletas de grânulos (Figuras 10a, 10c – Resultados complementares 1). Este resultado foi surpreendente, uma vez que esse aspecto granular normalmente é visto apenas em L2. Desta forma, ainda que não tenha sido possível visualizar as estruturas internas de L1, notamos que as L3 apresentam uma morfologia interna mais desenvolvida e definida; por exemplo, pudemos observar facilmente o aparelho digestivo completo desta forma larvar (Figura 10).

Na segunda parte do trabalho, analisamos o perfil de expressão proteica do *A. costaricensis* usando técnicas bioquímicas/proteômicas. Atualmente, os dois únicos trabalhos da literatura nesta área foram publicados por nosso grupo (León *et al.*, 2007; Rebello *et al.*, 2011), sendo que os resultados do artigo mais recente fazem parte desta tese (Artigo 2). Iniciamos a caracterização do proteoma deste nematoide utilizando vermes adultos, machos e fêmeas. Escolhemos esta fase em função da maior facilidade de obtenção de massa parasitária e também por representar uma etapa do ciclo biológico do parasito que se desenvolve no hospedeiro humano. Apesar de diferenças importantes quanto à morfologia e ao tamanho de machos e fêmeas, seus extratos proteicos mostraram perfis muito semelhantes quando fracionados em géis de eletroforese bidimensional. A maioria dos *spots* de ambos os sexos se concentrou na faixa de pH entre 5 e 7, com massas moleculares variando de 20,1 kDa a 66 kDa. Curiosamente, para cerca de 75% deles, não detectamos expressão diferencial entre machos e fêmeas; menos de 10% dos *spots* foi detectado em um dos gêneros apenas. As proteínas mais abundantes identificadas nos mapas bidimensionais de *A. costaricensis* se mostraram associadas aos seguintes termos do *Gene Ontology – Biological Process*: "processo metabólico de macromoléculas", "processo de desenvolvimento", "resposta à estresse" e "regulação biológica".

Padrões bastante similares entre machos e fêmeas também foram observados em *Angiostrongylus cantonensis* (Song *et al.*, 2012); as poucas proteínas identificadas que mostraram diferença de expressão entre os dois gêneros foram actina, galectina, peroxiredoxina, subunidade alfa de proteossoma e mioglobina indoleamina dioxigenase-*like*. Em nosso trabalho de proteoma descritivo, as três primeiras também foram identificadas nos extratos de vermes adultos de *A. costaricensis*. A actina é uma proteína de citoesqueleto bastante conservada nos nematoides e representou o *spot* de maior abundância relativa nos mapas bidimensionais de *A. costaricensis*. A peroxiredoxina é uma proteína multifuncional que pertence à superfamília das tioredoxinas e sua principal função é ajustar o estado redox celular deflagrado pela resposta imune do hospedeiro (Morassutti & Graeff-Teixeira, 2012). A função das galectinas nos helmintos ainda não está clara, apesar de alguns

autores levantarem a hipótese de estarem atuando como potenciais moduladores imunes em *Brugia malayi* (Hewitson *et al.*, 2008).

Recentemente, a análise do secretoma de fêmeas adultas de *A. cantonensis* (Morassutti *et al.*, 2012) revelou a presença de diversas proteínas, algumas delas também observadas em *A. costaricensis* (Rebello *et al.*, 2011), tais como peroxiredoxina, proteína de choque térmico 70, As37, actina, galectina e proteína disulfato isomerase. Várias das proteínas secretadas por *A. cantonensis* se mostraram imunorreativas, incluindo proteína de choque térmico, actina, peroxiredoxina, disulfalto isomerase, galectina, ferritina, aldolase, inibidor de aspartil protease, cisteíno-protease e hemoglobinase do tipo cisteíno-protease. No caso de *A. costaricensis* (Rebello *et al.*, 2011), os *immunoblots* de macho e fêmea apresentaram perfis bastante semelhantes de proteínas reativas, com algumas variações entre os gêneros. Identificamos como *spots* imunogênicos apenas as proteínas de choque térmico (HSPs), a proteína do estágio DAUER e as galectinas. O baixo número de identificação ocorreu devido à fraca correlação entre a imunorreatividade e a abundância dos *spots,* mesma dificuldade encontrada por outros autores (Yatsuda *et al.*, 2003; Robinson *et al.*, 2005).

É importante ressaltar que o desconhecimento sobre o genoma do *Angiostrongylus costaricensis* limita bastante a eficiência da metodologia de identificação utilizada, baseada na comparação de espectros de massa (MS2) não interpretados com informações de sequências depositadas em bancos de dados (Cottrell, 2011). Apenas recentemente, os genomas mitocondriais de *Angiostrongylus costaricensis* e *Angiostrongylus cantonensis* foram publicados (Lv *et al.*, 2012). Apesar da diversidade de nematoides existentes, somente sete genomas completos desta classe de helmintos foram publicados e estão depositados no GeneBank, dificultando ainda mais a identificação proteica por espectrometria de massas. São eles: *C. elegans, C. briggsae, Brugia malayi, Meloidogyne incognita, Pristionchus pacificus, Meloidogyne hapla e Trichinella spiralis* (Consortium, 1998; Stein *et al.*, 2003; Ghedin *et al.*, 2007; Abad *et al.*, 2008; Dieterich *et al.*, 2008; Opperman *et al.*, 2008; Mitreva *et al.*, 2011).

Dando prosseguimento às análises bioquímicas do *A. costaricensis*, partimos para o detalhamento do subproteoma representado por suas enzimas proteolíticas (degradoma) (Artigo 3). Proteases são considerados importantes

fatores de virulência, exercendo diferentes funções no estabelecimento, manutenção e exacerbação de infecções parasitárias (McKerrow *et al.*, 2006). Proteases de diferentes classes mecanísticas podem ser expressas nos intestinos dos parasitas ou podem constituir seus produtos de excreção-secreção. Atualmente, elas são consideradas alvos potenciais para uma nova geração de quimioterápicos com atividade antiparasitária (Dalton, 2003).

Inicialmente, para avaliarmos as proteases presentes nos extratos das diferentes fases de desenvolvimento do *A. costaricensis,* utilizamos a técnica de zimografia, baseada na eletroforese em gel de poliacrilamida desnaturante, copolimerizado com gelatina como substrato proteico (Heussen & Dowdle, 1980). Trata-se de uma técnica comumente utilizada para identificar a presença de proteases nos mais diversos organismos (D'Avila-Levy *et al.*, 2003; D'Avila-Levy *et al.*, 2005; Cuervo *et al.*, 2006). Após a separação eletroforética, o gel é incubado com o detergente não-iônico Triton X-100, que desloca o SDS das proteínas, possibilitando seu reenovelamento. De volta à conformação nativa, as proteases degradam o substrato presente no seu entorno, o que pode ser facilmente visualizado na forma de bandas coradas negativamente após incubação do gel com azul de Coomassie. Eventualmente, algumas proteínas não renaturam corretamente e não podem ser detectadas por esta técnica (Wilkesman & Kurz, 2009).

Para complementar os resultados de zimografia, avaliamos a atividade proteolítica dos extratos sobre hemoglobina, substrato proteico normalmente hidrolisado por organismos hematófagos (Williamson *et al.*, 2003). O *Angiostrongylus costaricensis* é um helminto cujo *habitat* definitivo são os ramos das artérias mesentéricas intestinais do hospedeiro vertebrado. Os vermes adultos nitidamente se alimentam de sangue, principalmente as fêmeas, cujo intestino é geralmente visualizado repleto deste fluido biológico (Rebello *et al.*, 2011). Assim, utilizamos este ensaio para verificar se os vermes adultos sabidamente hematófagos degradam hemoglobina em solução e também se as formas larvares eram capazes de hidrolisar esse substrato proteico.

Através dos ensaios de zimografia em gelatina e hidrólise de hemoglobina em solução, detectamos a presença de metaloproteases na fase infectante do nematoide (L3) e de hemoglobinases do tipo aspártico-proteases

em L1, L3, fêmeas e machos adultos (Artigo 3). A presença de metaloproteases já foi descrita no secretoma de L3 de *A. cantonensis* (Lai *et al.*, 2005). Dados da literatura indicam que as proteases secretadas por larvas infectantes facilitam sua penetração na pele e na parede intestinal de humanos (Tort *et al.*, 1999). Em alguns helmintos, as metaloproteases também parecem estar envolvidas na degradação de componentes da matriz extracelular (Petralanda *et al.*, 1986). A presença de proteases ácidas em helmintos parasitas capazes de hidrolisar hemoglobina foi descrita pela primeira vez em 1959 (Timms & Bueding, 1959). A presença de hemoglobinases do tipo aspártico proteases foi descrita nos nematoides *A. cantonensis*, *Dirofalaria immmitis*, *Trichuris muris* e *Ascaris suum* (Maki *et al.*, 1982). A distribuição anatômica dessas enzimas proteolíticas pode variar nas diferentes espécies. A atividade enzimática mais pronunciada foi detectada no intestino de *A. cantonensis*, *D. immitis* e *A. suum*. De modo menos intenso, extratos de órgãos reprodutivos e da parede do corpo dos helmintos analisados também degradaram a hemoglobina. O pH ótimo de hidrólise da hemoglobina foi entre pH 3,1- 4,6 (Maki *et al.*, 1982). Outro relato importante na literatura descreve a expressão diferencial de aspártico proteases em diferentes fases de desenvolvimento do *A. cantonensis* (Hwang *et al.*, 2010). Neste trabalho, os autores mostraram que a expressão do gene que codifica aspártico proteases é bastante diminuta nas larvas infectantes (L3) quando comparado com fêmeas adultas. E ainda, que a expressão do gene é muito maior nas fêmeas adultas do que nos machos adultos (Hwang *et al.*, 2010).

É importante mencionar que os extratos de L1 de *A. costaricensis* mostraram uma atividade gelatinolítica mais intensa do que os extratos de L3. As larvas de primeiro estágio penetram nos moluscos por via oral (Morera, 1973) ou por infecções percutâneas (Thiengo, 1996; Mendonça *et al.*, 1999) e, no seu interior, sofrem duas mudas. Podemos especular que a atividade gelatinásica seja importante para permitir a hidrólise de componentes da matriz extracelular e consequente invasão dos tecidos. Assim, a forte atividade gelatinolítica de L1 deve garantir a sua penetração bem sucedida pela superfície do molusco e através das camadas musculares. No entanto, as L3 também devem utilizar as enzimas gelatinolíticas para penetrar a parede intestinal do vertebrado e alcançar o sistema circulatório, tal como já descrito

para a fase infecciosa de diversos nematoides parasitas (Hotez *et al.*, 1990; Zhan *et al.*, 2002; Lai *et al.*, 2005; Lee & Yen, 2005). As larvas de terceiro estágio tornam-se adultas no interior dos vasos sanguíneos, onde estes últimos viverão durante toda sua vida. As larvas podem eventualmente ser encontradas na circulação sistêmica do roedor, embora isso seja uma rota migratória alternativa (Mota & Lenzi, 2005; Fontoura *et al.*, 2007). Desta forma, não foi surpreendente observar que a hidrólise da hemoglobina foi maior nas L3 e nos vermes adultos do que nas L1.

Para avançar na caracterização do degradoma do *A. costaricensis*, partimos para o mapeamento da especificidade de clivagem dos sítios catalíticos de suas enzimas proteolíticas. Para isso, utilizamos uma biblioteca de substratos sintéticos fluorogênicos com diferentes aminoácidos na posição P1 (Schechter & Berger, 1967). Nestes substratos, o grupamento fluorogênico 7-amino 4-metilcumarina (AMC) está ligado à carboxila C-terminal do substrato peptídico. Quando o substrato é hidrolisado, há liberação do AMC que, uma vez excitado a 360 nm, emite fluorescência detectável a 460 nm (Sojka *et al.*, 2007). Utilizando um painel de substratos sintéticos e inibidores específicos para proteases de diferentes classes mecanísiticas, detectamos a presença de serino-proteases nos extratos de L1 (Figuras 16, 17, 18) e confirmamos a presença de metaloproteases nos extratos de L3 (Figuras 19, 20). Observamos ainda que as serino-proteases presentes em L1 clivam preferencialmente os substratos que possuem arginina na posição P1.

As principais representantes do grupo das serino-proteases são as tripsinas, as quimiotripsinas e as elastases. Apesar da similaridade de suas estruturas primária e terciária (Shotton & Watson, 1970; Birktoft & Blow, 1972; Huber *et al.*, 1974), estas enzimas apresentam especificidades distintas. Tripsinas clivam cadeias peptídicas na porção carboxílica com maior eficiência de hidrólise sobre resíduos de aminoácidos básicos como lisina ou arginina, exceto quando seguidos de prolina (Brown & Wold, 1973; Hedstrom, 2002). As quimiotripsinas hidrolisam preferencialmente cadeias polipeptídicas na porção carboxílica em resíduos de aminoácidos hidrofóbicos com cadeia lateral aromática, como fenilalanina e triptofano (Hedstrom, 2002). As elastases hidrolisam cadeias proteicas na porção carboxílica em resíduos de aminoácidos hidrofóbicos apolares de cadeia lateral menos volumosa, como

glicina e valina (Hedstrom, 2002). Portanto, nossos dados usando um painel de diferentes substratos sintéticos parecem apontar para a presença de serino-proteases do tipo tripsina-*like* nos extratos de L1.

Dando continuidade ao estudo das enzimas proteolíticas, enriquecemos o extrato de L1 em seu conteúdo de serino-proteases utilizando cromatografia de afinidade em coluna de benzamidina. Para confirmação da purificação de serino-proteases, a etapa seguinte consistiu na análise da fração ligada à coluna por espectrometria de massas. Entretanto, provavelmente em função da inexistência de sequências de serino-proteases de Angiostrongylus nos bancos de dados, agravada pela pouca quantidade de material, ainda não conseguimos identificações de serino-proteases nesta fração.

V. Conclusão Geral e Perspectivas

Este trabalho de tese gerou uma quantidade importante de dados originais sobre a morfologia e a bioquímica do *Angiostrongylus costaricensis* em suas diferentes fases de desenvolvimento. Eles englobaram o detalhamento de diversas estruturas anatômicas deste helminto e a caracterização de seus diferentes padrões de expressão proteica, incluindo a caracterização dos subproteomas definidos por suas proteases e proteínas imunorreativas. Os resultados deverão contribuir para melhorar nossa compreensão acerca da biologia do *A. costaricensis* e da fisiopatologia da angiostrongilíase, uma doença ainda pouca conhecida mas em ampla expansão no Brasil.

A caracterização do proteoma e do secretoma das diferentes formas de desenvolvimento do *A. costaricensis* através da técnica de *shotgun proteomics* (nanocromatografia líquida acoplada à espectrometria de massas de alta resolução) constituem as perspectivas imediatas do trabalho. Pretendemos também mapear proteínas de interesse, *in situ,* através de imunomarcações sobre cortes do parasito e análise por microscopia. Os resultados desta próxima etapa do projeto certamente contribuirão de modo significativo para a geração de conhecimentos relevantes para o desenvolvimento de potenciais alvos para o diagnóstico e/ou tratamento da angiostrongilíase abdominal.

VI. Referências Bibiográficas

Abad P, Gouzy J, Aury JM, Castagnone-Sereno P, Danchin EG, Deleury E, Perfus-Barbeoch L, Anthouard V, Artiguenave F, Blok VC, Caillaud MC, Coutinho PM, Dasilva C, De Luca F, Deau F, Esquibet M, Flutre T, Goldstone JV, Hamamouch N, Hewezi T, Jaillon O, Jubin C, Leonetti P, Magliano M, Maier TR, Markov GV, McVeigh P, Pesole G, Poulain J, Robinson-Rechavi M, Sallet E, Segurens B, Steinbach D, Tytgat T, Ugarte E, van Ghelder C, Veronico P, Baum TJ, Blaxter M, Bleve-Zacheo T, Davis EL, Ewbank JJ, Favery B, Grenier E, Henrissat B, Jones JT, Laudet V, Maule AG, Quesneville H, Rosso MN, Schiex T, Smant G, Weissenbach J, Wincker P 2008. Genome sequence of the metazoan plant-parasitic nematode *Meloidogyne incognita*. *Nat Biotechnol.* 26: 909-915.

Abrahams-Sandí E 2007. Angiostrongiliasis abdominal: notas sobre el diagnóstico. *Rev Biomed* 18: 37-45.

Aebersold R, Goodlett DR 2001. Mass spectrometry in proteomics. *Chem Rev* 101: 269-295.

Agostini AA, Marcolan AM, Lisot JM, Lisot JU 1984. Abdominal angiostrongyliasis. Anatomo-pathological study of 4 cases observed in Rio Grande do Sul, Brazil. *Mem Inst Oswaldo Cruz* 79: 443-445.

Agostini AA, Peixoto A, Caleffi AL, Dexhaimer A, Camargo RR 1983. Angiostrongilíase abdominal: três casos observados no Rio Grande do Sul. *Rev Assoc Med Rio Grande do Sul* 27: 200-203.

Aguiar PH, Morera P, Pascual J 1981. First record of angiostrongylus cantonensis in Cuba. *Am J Trop Med Hyg* 30: 963-965.

Anderson RC, 1978, *Keys to genera of the Superfamily Metastrongyloidea*, In: CIH Keys to the nematodes parasites of vertebrates.UK, pp. 1-40.

Anderson RC, 2000, *Nematode Parasites of Vertebrates: Their Development and Transmission*, 2nd ed. Edition. CABI Publishing/CAB International, Wallingford, United Kingdom.

Ashton PD, Curwen RS, Wilson RA 2001. Linking proteome and genome: how to identify parasite proteins. *Trends Parasitol* 17: 198-202.

Ayala MA 1987. Abdominal angiostrongyloidiasis. 6 cases observed in Parana and in Santa Catarina, Brazil. *Mem Inst Oswaldo Cruz* 82: 29-36.

Baird JK, Neafie RC, Lanoie L, Connor DH 1987. Abdominal angiostrongylosis in an African man: case study. *Am J Trop Med Hyg* 37: 353-356.

Bakker N, Vervelde L, Kanobana K, Knox DP, Cornelissen AWCA, De Vries E, Yatsuda AP 2004 Vaccination against the nematode *Haemonchus contortus* with a thiol-binding fraction from the excretory/secretory products (ES). *Vaccine* 22: 618-628.

Barbosa H, Raick AN, Magalhaes AV, Otero PM 1980. [Abdominal angiostrongylosis]. *AMB Rev Assoc Med Bras* 26: 178-180.

Bennuru S, Meng Z, Ribeiro JM, Semnani RT, Ghedin E, Chan K, Lucas DA, Veenstra TD, Nutman TB 2011. Stage-specific proteomic expression patterns of the human filarial parasite Brugia malayi and its endosymbiont Wolbachia. *Proc Natl Acad Sci U S A* 108: 9649-9654.

Bethony J, Brooker S, Albonico M, Geiger SM, Loukas A, Diemert D, Hotez PJ 2006. Soil-transmitted helminth infections: ascariasis, trichuriasis, and hookworm. *Lancet* 367: 1521-1532.

Birktoft JJ, Blow DM 1972. Structure of crystalline -chymotrypsin. V. The atomic structure of tosyl- -chymotrypsin at 2 A resolution. *J Mol Biol* 68: 187-240.

Bjellqvist B, Ek K, Righetti PG, Gianazza E, Gorg A, Westermeier R, Postel W 1982. Isoelectric focusing in immobilized pH gradients: principle, methodology and some applications. *J. Biochem. Biophys. Methods* 6: 317-339.

Blaxter M 1998. *Caenorhabditis elegans* is a nematode. *Science* 282: 2041-2046.

Boussinesq M 2006. Loiasis. *Ann Trop Med Parasitol* 100: 715-731.

Brack M, Schropel M 1995. Angiostrongylus costaricensis in a black-eared marmoset. *Trop Geogr Med* 47: 136-138.

Brooker S, Clements AC, Bundy DA 2006. Global epidemiology, ecology and control of soil-transmitted helminth infections. *Adv. Parasitol.* 62: 221-261.

Brown WE, Wold F 1973. Alkyl isocyanates as active-site-specific reagents for serine proteases. Reaction properties. *Biochemistry* 12: 828-834.

Caldeira RL, Mendonça CL, Goveia CO, Lenzi HL, Graeff-Teixeira C, Lima WS, Mota EM, Pecora IL, Medeiros AM, Carvalho Odos S 2007. First record of molluscs naturally infected with *Angiostrongylus cantonensis* (Chen, 1935) (Nematoda: Metastrongylidae) in Brazil. *Mem Inst Oswaldo Cruz* 102: 887-889.

Campbell BG, Little MD 1988. The finding of *Angiostrongylus cantonensis* in rats in New Orleans. *Am J Trop Med Hyg* 38: 568-573.

Canas B, Lopez-Ferrer D, Ramos-Fernandez A, Camafeita E, Calvo E 2006. Mass spectrometry technologies for proteomics. *Brief Funct Genomic Proteomic* 4: 295-320.

CDC 2011. Progress toward global eradication of dracunculiasis, January 2010-June 2011. In MMWR Morb Mortal Wkly Rep (Unithed States), pp. 1450-1453.

Céspedes RS, J; Mekbel, S; Troper, L; Müllner, F; Morera P 1967. Granulomas entéricos y linfáticos con intensa eosinofilia tissular producidos por un estrongilideo (Strongylata). *Acta Med Costarric.* 10: 325-355.

Chabaud AG 1972. [Description of *Stefanskostrongylus dubosti* n. sp., parasite of Potamogale and attempt at classification of Angiostrongylinae nematodes]. *Ann Parasitol Hum Comp* 47: 735-744.

Chen HT 1935. Um Nouveau Nematode Pulmonaire, Pulmonema cantonensis n.g.n.sp., des Rats de Canton. *Ann Parasitol.*: 312-317.

Chen X, MacDonald MH, Khan F, Garrett WM, Matthews BF, Natarajan SS 2011. Two-dimensional proteome reference maps for the soybean cyst nematode *Heterodera glycines*. *Proteomics* 11: 4742-4746.

Chitwood BG, Chitwood MB, 1974, *Introduction to Nematology*Baltimore, Maryland, 334 p.

Consortium *Ce*S 1998. Genome sequence of the nematode *C. elegans*: a platform for investigating biology. *Science* 282: 2012-2018.

Cottrell JS 2011. Protein identification using MS/MS data. *J Proteomics* 74: 1842-1851.

Cox J, Mann M 2011. Quantitative, high-resolution proteomics for data-driven systems biology. *Annu Rev Biochem* 80: 273-299.

Craig H, Wastling JM, Knox DP 2006. A preliminary proteomic survey of the in vitro excretory/secretory products of fourth-stage larval and adult *Teladorsagia circumcincta*. *Parasitology* 132: 535-543.

Crompton DW 1999. How much human helminthiasis is there in the world? *J Parasitol* 85: 397-403.

Cuervo P, Saboia-Vahia L, Costa Silva-Filho F, Fernandes O, Cupolillo E, JB DEJ 2006. A zymographic study of metalloprotease activities in extracts and extracellular secretions of *Leishmania (Viannia) braziliensis* strains. *Parasitology* 132: 177-185.

D'Avila-Levy CM, Araujo FM, Vermelho AB, Soares RM, Santos AL, Branquinha MH 2005. Proteolytic expression in Blastocrithidia culicis: influence of the endosymbiont and similarities with virulence factors of pathogenic trypanosomatids. *Parasitology* 130: 413-420.

D'Avila-Levy CM, Souza RF, Gomes RC, Vermelho AB, Branquinha MH 2003. A metalloproteinase extracellularly released by Crithidia deanei. *Can J Microbiol* 49: 625-632.

da Silva AC, Graeff-Teixeira C, Zaha A 2003. Diagnosis of abdominal angiostrongyliasis by PCR from sera of patients. *Rev Inst Med Trop São Paulo.* 45: 295-297.

Dalton J 2003. *Fasciola hepatica* cathepsin L-like proteases: biology, function, and potential in the development of first generation liver fluke vaccines. *Int J Parasitol* 33: 1173-1181.

de Magalhaes AV, de Andrade GE, Koh IH, Soares Mdo C, Alves E, Tubino P, dos Santos Fde A, Raick AN 1982. [A new case of abdominal angiostrongyliasis]. *Rev. Inst. Med. Trop. Sao Paulo* 24: 252-256.

Demo OJ, Pessat OAN 1986. Angiostrongilosis abdominal. Primer caso humano encontrado em Argentina. *Prensa Médica Argentina* 73: 732-738.

Dieterich C, Clifton SW, Schuster LN, Chinwalla A, Delehaunty K, Dinkelacker I, Fulton L, Fulton R, Godfrey J, Minx P, Mitreva M, Roeseler W, Tian H, Witte H, Yang SP, Wilson RK, Sommer RJ 2008. The *Pristionchus pacificus* genome provides a unique perspective on nematode lifestyle and parasitism. *Nat Genet.* 40: 1193-1198.

Duarte Z, Morera P, Vuong PN 1991. Abdominal angiostrongyliasis in Nicaragua: a clinico-pathological study on a series of 12 cases reports. *Ann Parasitol Hum Comp.* 66: 259-262.

Eamsobhana P, Lim PE, Solano G, Zhang H, Gan X, Yong HS 2010. Molecular differentiation of *Angiostrongylus* taxa (Nematoda: Angiostrongylidae) by cytochrome c oxidase subunit I (COI) gene sequences. *Acta Trop.* 116: 152-156.

Erickson SM, Xi Z, Mayhew GF, Ramirez JL, Aliota MT, Christensen BM, Dimopoulos G 2009. Mosquito infection responses to developing filarial worms. *PLoS Negl Trop Dis* 3: e529.

Faust EC, Russell PF, Jung RC, 1970, *Craig and Faust´s clinical parasitology*, 8th Edition. Philadelphia, Lea & Febiger.

Fields S 2001. Proteomics. Proteomics in genomeland. *Science* 291: 1221-1224.

Fischer P, Bamuhiiga J, Buttner DW 1997. Occurrence and diagnosis of *Mansonella streptocerca* in Uganda. *Acta Trop* 63: 43-55.

Fontoura GD, Maurer RL, Oliveira CM, Graeff-Teixeira C 2007. Abdominal angiostrongyliasis in rodent experimental infection: evidence for systemic circulation of first stage larvae. *Parasitol Int* 56: 227-229.

Forner F, Foster LJ, Toppo S 2007. Mass spectrometry data analysis in the proteomics era. *Curr Bioinf* 2: 63-93.

Fröhlich T, Arnold GJ 2006. Proteome research based on modern liquid chromatography-tandem mass spectrometry: separation, identification and quantification. *J Neural Transm* 113: 973-994.

Geiger SM, Laitano AC, Sievers-Tostes C, Agostini AA, Schulz-Key H, Graeff-Teixeira C 2001. Detection of the acute phase of abdominal angiostrongyliasis with a parasite-specific IgG enzyme linked immunosorbent assay. *Mem Inst Oswaldo Cruz.* 96: 515-518.

Ghedin E, Wang S, Spiro D, Caler E, Zhao Q, Crabtree J, Allen JE, Delcher AL, Guiliano DB, Miranda-Saavedra D, Angiuoli SV, Creasy T, Amedeo P, Haas B, El-Sayed NM, Wortman JR, Feldblyum T, Tallon L, Schatz M, Shumway M, Koo H, Salzberg SL, Schobel S, Pertea M, Pop M, White O, Barton GJ, Carlow CK, Crawford MJ, Daub J, Dimmic MW, Estes CF, Foster JM, Ganatra M, Gregory WF, Johnson NM, Jin J, Komuniecki R, Korf I, Kumar S, Laney S, Li BW, Li W, Lindblom TH, Lustigman S, Ma D, Maina CV, Martin DM, McCarter JP, McReynolds L, Mitreva M, Nutman TB, Parkinson J, Peregrin-Alvarez JM, Poole C, Ren Q, Saunders L, Sluder AE, Smith K, Stanke M, Unnasch TR, Ware J, Wei AD, Weil G, Williams DJ, Zhang Y, Williams SA, Fraser-Liggett C, Slatko B, Blaxter ML, Scott AL 2007. Draft genome of the filarial nematode parasite *Brugia malayi*. *Science* 317: 1756-1760.

Gorg A, Drews O, Luck C, Weiland F, Weiss W 2009. 2-DE with IPGs. *Electrophoresis* 30 Suppl 1: S122-132.

Görg A, Weiss W, Dunn MJ 2004. Current two-dimensional electrophoresis technology for proteomics. *Proteomics* 4: 3665-3685.

Graeff-Teixeira C, Agostini AA, Camillo-Coura L, Ferreira-da-Cruz MF 1997. Seroepidemiology of abdominal angiostrongyliasis: the standardization of an immunoenzymatic assay and prevalence of antibodies in two localities in southern Brazil. *Trop Med Int Health.* 2: 254-260.

Graeff-Teixeira C, Camillo-Coura L, Lenzi HL 1991a. Clinical and epidemiological aspects of abdominal angiostrongyliasis in southern Brazil. *Rev Inst Med Trop São Paulo.* 33: 373-378.

Graeff-Teixeira C, Camillo-Coura L, Lenzi HL 1991b. Histopathological criteria for the diagnosis of abdominal angiostrongyliasis. *Parasitol Res.* 77: 606-611.

Graves PR, Haystead TAJ 2002. Molecular Biologist's Guide to Proteomics. *Microbiology and Molecular Biology Reviews* 66: 39-63.

Gustavsen K, Hopkins A, Sauerbrey M 2011. Onchocerciasis in the Americas: from arrival to (near) elimination. *Parasit Vectors* 4: 205.

Halton DW 2004. Microscopy and the helminth parasite. *Micron* 35: 361-390.

Halton DW, Gustafsson MKS 1996. Functional morphology of the platyhelminth nervous system. *Parasitology*: S47-S72.

Havercroft JC, Smith AL, Williams RH 1991. *Schistosoma mansoni*: immuno-localization of the calcium binding protein Sm20. *Parasite Immunol* 13: 593-604.

Hedstrom L 2002. Serine protease mechanism and specificity. *Chem Rev* 102: 4501-4524.

Heussen C, Dowdle EB 1980. Electrophoretic analysis of plasminogen activators in polyacrylamide gels containing sodium dodecyl sulfate and copolymerized substrates. *Anal Biochem.* 102: 196-202.

Hewitson JP, Harcus Y, Murray J, van Agtmaal M, Filbey KJ, Grainger JR, Bridgett S, Blaxter ML, Ashton PD, Ashford DA, Curwen RS, Wilson RA, Dowle AA, Maizels RM 2011. Proteomic analysis of secretory products from the model gastrointestinal nematode *Heligmosomoides polygyrus* reveals dominance of venom allergen-like (VAL) proteins. *J Proteomics* 74: 1573-1594.

Hewitson JP, Harcus YM, Curwen RS, Dowle AA, Atmadja AK, Ashton PD, Wilson A, Maizels RM 2008. The secretome of the filarial parasite, *Brugia malayi*: proteomic profile of adult excretory-secretory products. *Mol Biochem Parasitol.* 160: 8-21.

Hoberg EP, Kumsa B, Pilitt PA, Abrams A 2010. Synlophe structure in *Pseudomarshallagia elongata* (Nematoda: Trichostrongyloidea), abomasal parasites among Ethiopian ungulates, with consideration of other morphological attributes and differentiation within the Ostertagiinae. *J. Parasitol.* 96: 401-411.

Horton J 2003. Human gastrointestinal helminth infections: are they now neglected diseases? *Trends Parasitol* 19: 527-531.

Hotez P, Haggerty J, Hawdon J, Milstone L, Gamble HR, Schad G, Richards F 1990. Metalloproteases of infective *Ancylostoma* hookworm larvae and their possible functions in tissue invasion and ecdysis. *Infect. Immun* 58: 3883-3892.

Hotez PJ, Brindley PJ, Bethony JM, King CH, Pearce EJ, Jacobson J 2008. Helminth infections: the great neglected tropical diseases. *J Clin Invest* 118: 1311-1321.

Huber R, Kukla D, Bode W, Schwager P, Bartels K, Deisenhofer J, Steigemann W 1974. Structure of the complex formed by bovine trypsin and bovine pancreatic trypsin inhibitor. II. Crystallographic refinement at 1.9 A resolution. *J Mol Biol* 89: 73-101.

Hulbert TV, Larsen RA, Chandrasoma PT 1992. Abdominal angiostrongyliasis mimicking acute appendicitis and Meckel's diverticulum: report of a case in the United States and review. *Clin Infect Dis* 14: 836-840.

Hwang KP, Chang SH, Wang LC 2010. Alterations in the expression level of a putative aspartic protease in the development of *Angiostrongylus cantonensis*. *Acta Trop.* 113: 289-294.

Iabuki K, Montenegro MR 1979. Appendicitis caused by Angiostrongylus costaricensis. Presentation of a case. *Rev. Inst. Med. Trop. Sao Paulo* 21: 33-36.

Iriemenam NC, Oyibo WA, Fagbenro-Beyioku AF 2008. Dracunculiasis--the saddle is virtually ended. *Parasitol Res* 102: 343-347.

Ishih A, Rodriguez BO, Sano M 1990. Scanning electron microscopic observations of first and third-stage larvae and adults of *Angiostrongylus costaricensis*. *Southeast Asian J. Trop. Med. Public Health* 21: 568-573.

Juminer B, Roudier M, Raccurt CP, Pujol HP, Gerry F, Bonnet R 1992. Presence of abdominal angiostrongylosis in Guadeloupe. Apropos of 2 recent cases. *Bull Soc Pathol Exot* 85: 39-43.

Kramer MH, Greer GJ, Quiñonez JF, Padilla NR, Hernández B, Arana BA, Lorenzana R, Morera P, Hightower AW, Eberhard ML, Herwaldt BL 1998. First reported outbreak of abdominal angiostrongyliasis. *Clin Infect Dis* 26: 365-372.

Krushna NS, Shiny C, Dharanya S, Sindhu A, Aishwarya S, Narayanan RB 2009. Immunolocalization and serum antibody responses to *Brugia malayi* pepsin inhibitor homolog (Bm-33). *Microbiol Immunol* 53: 173-183.

Laemmli UK 1970. Cleavage of structural proteins during the assembly of the head of bacteriophage T4. *Nature* 227: 680-685.

Lai SC, Jiang ST, Chen KM, Lee HH 2005. Matrix metalloproteinases activity demonstrated in the infective stage of the nematodes, *Angiostrongylus cantonensis*. *Parasitol Res.* 97: 466-471.

Lambshead PJ, Brown CJ, Ferrero TJ, Hawkins LE, Smith CR, Mitchell NJ 2003. Biodiversity of nematode assemblages from the region of the Clarion-Clipperton Fracture Zone, an area of commercial mining interest. *BMC Ecol* 3: 1.

Lane CS 2005. Mass spectrometry-based proteomics in the life sciences. *CMLS Cellular and Molecular Life Sciences* 62: 848-869.

Lanfredi RM, Fraiha Neto H, Gomes DC 1998. Scanning electron microscopy of *Lagochilascaris minor* Leiper, 1909 (Nematoda: Ascarididae). *Mem Inst Oswaldo Cruz* 93: 327-330.

Lee JD, Yen CM 2005. Protease secreted by the infective larvae of *Angiostrongylus cantonensis* and its role in the penetration of mouse intestine. *Am J Trop Med Hyg.* 72: 831-836.

León IR, Neves-Ferreira AGC, Valente RH, Mota EM, Lenzi HL, Perales J 2007. Improved protein identification efficiency by mass spectrometry using N-terminal chemical derivatization of peptides from *Angiostrongylus costaricensis*, a nematode with unknown genome. *J Mass Spectrom.* 42: 781-792.

Lindo JF, Waugh C, Hall J, Cunningham-Myrie C, Ashley D, Eberhard ML, Sullivan JJ, Bishop HS, Robinson DG, Holtz T, Robinson RD 2002. Enzootic *Angiostrongylus cantonensis* in rats and snails after an outbreak of human eosinophilic meningitis, Jamaica. *Emerg Infect Dis* 8: 324-326.

Link AJ, Eng J, Schieltz DM, Carmack E, Mize GJ, Morris DR, Garvik BM, Yates JR, 3rd 1999. Direct analysis of protein complexes using mass spectrometry. *Nat Biotechnol* 17: 676-682.

Lv S, Zhang Y, Zhang L, Liu Q, Liu HX, Hu L, Wei FR, Steinmann P, Graeff-Teixeira C, Zhou XN, Utzinger J 2012. The complete mitochondrial genome of the rodent intra-arterial nematodes *Angiostrongylus cantonensis* and *Angiostrongylus costaricensis*. *Parasitol Res*.

Maki J, Furuhashi A, Yanagisawa T 1982. The activity of acid proteases hydrolysing haemoglobin in parasitic helminths with special reference to interspecific and intraspecific distribution. *Parasitology* 84: 137-147.

Maldonado Jr A, Simões R, Thiengo S, 2012, *Angiostrongyliasis in the Americas*, In: Zoonosis. pp. 303-320.

Maliska AM 2004. Microscopia eletrônica de varredura e microanálise, UFSC, ed. (Santa Catarina).

Mallick P, Kuster B 2010. Proteomics: a pragmatic perspective. *Nat Biotechnol* 28: 695-709.

Marques S, Barros-Battesti DM, Onofrio VC, Famadas KM, Faccini JL, Keirans JE 2004. Redescription of larva, nymph and adults of Ixodes (I .) loricatus Neumann, 1899 (Acari: Ixodidae) based on light and scanning electron microscopy. *Syst Parasitol* 59: 135-146.

McKerrow JH, Caffrey C, Kelly B, Loke P, Sajid M 2006. Proteases in parasitic diseases. *Annu Rev Pathol.* 1: 497-536.

Medeiros JF, Py-Daniel V, Barbosa UC 2011. Prevalence of *Mansonella ozzardi* among riverine communities in the municipality of Labrea, State of Amazonas, Brazil. *Rev Soc Bras Med Trop* 44: 186-190.

Mendonça CL, Carvalho OS, Mota EM, Pelajo-Machado M, Caputo LF, Lenzi HL 1999. Penetration sites and migratory routes of *Angiostrongylus costaricensis* in the experimental intermediate host (Sarasinula marginata). *Mem Inst Oswaldo Cruz* 94: 549-556.

Merrihew GE, Davis C, Ewing B, Williams G, Kall L, Frewen BE, Noble WS, Green P, Thomas JH, MacCoss MJ 2008. Use of shotgun proteomics for the identification, confirmation, and correction of *C. elegans* gene annotations. *Genome Res* 18: 1660-1669.

Millares P, Lacourse EJ, Perally S, Ward DA, Prescott MC, Hodgkinson JE, Brophy PM, Rees HH 2012. Proteomic profiling and protein identification by MALDI-TOF mass spectrometry in unsequenced parasitic nematodes. *PLoS One* 7: e33590.

Miller CL, Kinsella JM, Garner MM, Evans S, Gullett PA, Schmidt RE 2006. Endemic infections of *Parastrongylus (=Angiostrongylus) costaricensis* in two species of nonhuman primates, raccoons, and an opossum from Miami, Florida. *J Parasitol* 92: 406-408.

Mitreva M, Jasmer DP, Zarlenga DS, Wang Z, Abubucker S, Martin J, Taylor CM, Yin Y, Fulton L, Minx P, Yang SP, Warren WC, Fulton RS, Bhonagiri V, Zhang X, Hallsworth-Pepin K, Clifton SW, McCarter JP, Appleton J, Mardis ER, Wilson RK 2011. The draft genome of the parasitic nematode *Trichinella spiralis*. *Nat Genet.* 43: 228-235.

Morassutti AL, Graeff-Teixeira C 2012. Interface Molecules of *Angiostrongylus cantonensis*: Their Role in Parasite Survival and Modulation of Host Defenses. *Int J Inflam* 2012: 512097.

Morassutti AL, Levert K, Pinto PM, da Silva AJ, Wilkins P, Graeff-Teixeira C 2012. Characterization of *Angiostrongylus cantonensis* excretory-secretory proteins as potential diagnostic targets. *Exp Parasitol* 130: 26-31.

Morera P 1973. Life history and redescription of *Angiostrongylus costaricensis* Morera and Céspedes, 1971. *Am J Trop Med Hyg.* 22: 613-621.

Morera P 1988. Angiostrongilíase abdominal. Um problema de Saúde Pública ? *Rev. Soc. Bras. Med. Trop* 21: 81-83.

Morera P, 2001, *Abdominal angiostrongyliasis*, 8 ed Edition. W.B, Saunders, Philadelphia, .

Morera P, Bontempo I 1985. Acción de algunos antihelminticos sobre *Angiostrongylus costaricensis*. *Rev Méd Hosp Nac Niños (Costa Rica).* 20: 165-174.

Morera P, Cespedes R 1971. Angiostrongilosis abdominal. Uma nueva parasitosis humana. *Acta Med Costarric.* 14: 173-189.

Morera P, Cespedes R 2002. Angiostrongylus costaricensis n. sp. (Nematoda: Metastrongyloidea), a new lungworm occuring in man in Costa Rica. 1971. *Rev Biol Trop* 50: 783-796.

Morera P, Céspedes R 1971. *Angiostrongylus costaricensis* n. sp. (Nematoda: Metastrongyloidea), a new lungworm occuring in man in Costa Rica. *Rev Biol Trop.* 18: 173-185.

Mota EM, Lenzi HL 2005. *Angiostrongylus costaricensis*: complete redescription of the migratory pathways based on experimental *Sigmodon hispidus* infection. *Mem Inst Oswaldo Cruz.* 100: 407-420.

Murray PR, Rosenthal KS, Pfaller MA, 2006, *Microbiologia Médica*, Vol 5ª edRio de Janeiro, 945 p.

Nesvizhskii AI, Aebersold R 2005. Interpretation of shotgun proteomic data: the protein inference problem. *Mol Cell Proteomics* 4: 1419-1440.

O'Farrell PH 1975. High resolution two-dimensional electrophoresis of proteins. *J. Biol. Chem.* 250: 4007-4021.

Ohbayashi M, Kamiya M, Bhaibulaya M 1979. Studies on the parasite fauna of Thailand. I Two new metastrongylid nematodes, *Angiostrongylus siamensis* sp. n. and *Thaistrongylus harinasutai* gen. et sp. n. (Metastrongyloidea; Angiostrongylidae) from wild rats. *Jpn J Vet Res* 27: 5-10.

Opperman CH, Bird DM, Williamson VM, Rokhsar DS, Burke M, Cohn J, Cromer J, Diener S, Gajan J, Graham S, Houfek TD, Liu Q, Mitros T, Schaff J, Schaffer R, Scholl E, Sosinski BR, Thomas VP, Windham E 2008. Sequence and genetic map of *Meloidogyne hapla*: A compact nematode genome for plant parasitism. *Proc Natl Acad Sci U S A* 105: 14802-14807.

Page AP, Winter AD 2003. Enzymes involved in the biogenesis of the nematode cuticle. *Adv Parasitol* 53: 85-148.

Patterson SD, Aebersold RH 2003. Proteomics: the first decade and beyond. *Nat Genet* 33: 311-323.

Pena GP, Andrade Filho J, de Assis SC 1995. *Angiostrongylus costaricensis*: first record of its occurrence in the State of Espírito Santo, Brazil, and a review of its geographic distribution. *Rev. Inst. Med. Trop. São Paulo* 37: 369-374.

Petralanda I, Yarzabal L, Piessens WF 1986. Studies on a filarial antigen with collagenase activity. *Mol Biochem Parasitol* 19: 51-59.

Pien FD, Pien BC 1999. *Angiostrongylus cantonensis* eosinophilic meningitis. *Int J Infect Dis* 3: 161-163.

Preiser H, Schmitz J, Maestracci D, Crane RK 1975. Modification of an assay for trypsin and its application for the estimation of enteropeptidase. *Clin Chim Acta* 59: 169-175.

Quiros JL, Jimenez E, Bonilla R, Arce I, Hernandez C, Jimenez Y 2011. Abdominal angiostrongyliasis with involvement of liver histopathologically confirmed: a case report. *Rev Inst Med Trop São Paulo* 53: 219-222.

Rabilloud T, Chevallet M, Luche S, Lelong C 2010. Two-dimensional gel electrophoresis in proteomics: Past, present and future. *J Proteomics* 73: 2064-2077.

Raccurt CP, Blaise J, Durette-Desset MC 2003. [Presence of Angiostrongylus cantonensis in Haiti]. *Trop Med Int Health* 8: 423-426.

Rebello KM, Barros JS, Mota EM, Carvalho PC, Perales J, Lenzi HL, Neves-Ferreira AG 2011. Comprehensive proteomic profiling of adult *Angiostrongylus costaricensis*, a human parasitic nematode. *J. Proteomics* 74: 1545-1559.

Rey L, 2001, *Parasitologia*, 3 ed Edition. Guanabara Koogan, Rio de Janeiro.

Rey L, 2008, *Nematóides parasitos do homem*, In: Koogan, G. (Ed.) Parasitologia.Rio de Janeiro, pp. 437--484.

Righetti PG 2009. Happy bicentennial, electrophoresis! *J Proteomics* 73: 181-187.

Robinson MW, Gare DC, Connolly B 2005. Profiling excretory/secretory proteins of *Trichinella spiralis* muscle larvae by two-dimensional gel electrophoresis and mass spectrometry. *Vet Parasitol.* 132: 37-41.

Rocha A, Sobrinho JM, Salomao EC 1991. [Abdominal angiostrongyliasis. The first indigenous case reported in Minas Gerais]. *Rev Soc Bras Med Trop* 24: 265-268.

Ruiz PJ, Morera P 1983. Spermatic artery obstruction caused by Angiostrongylus costaricensis Morera and Cespedes, 1971. *Am J Trop Med Hyg* 32: 1458-1459.

Ruppert EE, Fox RS, Barnes RD, 1996, *Zoologia dos Invertebrados*, Vol 6ª edSão Paulo

Sanchez GA 1992. Intestinal perforation by *Angiostrongylus costaricensis*. A report of 2 cases. *Rev Med Panama* 17: 74-81.

Sawanyawisuth K, Pugkhem A, Mitchai J, Intapan PM, Anunnatsiri S, Limpawattana P, Chotmongkol V 2010. Abdominal angiostrongyliasis caused by *Angiostrongylus cantonensis*: a possible cause of eosinophilic infiltration in human digestive tract. *Pathol Res Pract* 206: 102-104.

Schechter I, Berger A 1967. On the size of the active site in proteases. I. Papain. *Biochem Biophys Res Commun* 27: 157-162.

Shim YH, Paik YK 2010. *Caenorhabditis elegans* proteomics comes of age. *Proteomics* 10: 846-857.

Shotton DM, Watson HC 1970. Three-dimensional structure of tosyl-elastase. *Nature* 225: 811-816.

Simonsen PE, Onapa AW, Asio SM 2010. *Mansonella perstans* filariasis in Africa. *Acta Trop* 120 Suppl 1: S109-120.

Sly DL, Toft JD, 2nd, Gardiner CH, London WT 1982. Spontaneous occurrence of *Angiostrongylus costaricensis* in marmosets (*Saguinus mystax*). *Lab Anim Sci* 32: 286-288.

Sojka D, Hajdusek O, Dvorak J, Sajid M, Franta Z, Schneider EL, Craik CS, Vancova M, Buresova V, Bogyo M, Sexton KB, McKerrow JH, Caffrey CR, Kopacek P 2007. IrAE: an asparaginyl endopeptidase (legumain) in the gut of the hard tick Ixodes ricinus. *Int J Parasitol* 37: 713-724.

Song Z, Huang H, Tan F, Zhang E, Hu J, Pan C 2012. Differential proteomics analysis of female and male adults of Angiostrongylus cantonensis. *Exp Parasitol* 131: 169-174.

Steen H, Mann M 2004. The ABC's (and XYZ's) of peptide sequencing. *Nat Rev Mol Cell Biol* 5: 699-711.

Stein LD, Bao Z, Blasiar D, Blumenthal T, Brent MR, Chen N, Chinwalla A, Clarke L, Clee C, Coghlan A, Coulson A, D'Eustachio P, Fitch DH, Fulton LA, Fulton RE, Griffiths-Jones S, Harris TW, Hillier LW, Kamath R, Kuwabara PE, Mardis ER, Marra MA, Miner TL, Minx P, Mullikin JC,

Plumb RW, Rogers J, Schein JE, Sohrmann M, Spieth J, Stajich JE, Wei C, Willey D, Wilson RK, Durbin R, Waterston RH 2003. The genome sequence of *Caenorhabditis briggsae*: a platform for comparative genomics. *PLoS Biol.* 1: E45.

Strote G, Bonow I 1993. Ultrastructural observations on the nervous system and the sensory organs of the infective stage (L3) of *Onchocerca volvulus* (Nematoda: Filarioidea). *Parasitol Res* 79: 213-220.

Swanson S, Washburn M 2005. The continuing evolution of shotgun proteomics. *Drug Discovery Today* 10: 719-725.

Taylor MJ, Hoerauf A, Bockarie M 2010. Lymphatic filariasis and onchocerciasis. *Lancet* 376: 1175-1185.

Thiengo S 1996. Mode of infection of *Sarasinula marginata* (Mollusca) with larvae of *Angiostrongylus costaricensis* (Nematoda). *Mem Inst Oswaldo Cruz* 91: 277-278.

Thiengo SC, Vicente JJ, Pinto RM 1997. Redescription of *Angiostrongylus (Paranstrongylus) costaricensis* Morera & Céspedes (nematoda: metastrongyloidea) from brazilian strain. *Rev Bras Zool* 14: 839 - 844.

Timms AR, Bueding E 1959. Studies of a proteolytic enzyme from *Schistosoma mansoni*. *Br J Pharmacol Chemother* 14: 68-73.

Tort J, Brindley PJ, Knox D, Wolfe KH, Dalton JP 1999. Proteinases and associated genes of parasitic helminths. *Adv Parasitol.* 43: 161-266.

Ubelaker JE, Hall NM 1979. First report of *Angiostrongylus costaricensis* Morera and Céspedes 1971 in the United States. *J Parasitol.* 65: 307.

Utzinger J, Keiser J 2004. Schistosomiasis and soil-transmitted helminthiasis: common drugs for treatment and control. *Expert Opin Pharmacother* 5: 263-285.

van Balkom BW, van Gestel RA, Brouwers JF, Krijgsveld J, Tielens AG, Heck AJ, van Hellemond JJ 2005. Mass spectrometric analysis of the Schistosoma mansoni tegumental sub-proteome. *J Proteome Res* 4: 958-966.

Vermelho AB, Pereira AF, Coelho RRR, Souto-Padrón T, 2011, *Práticas de Microbiologia*. Guanabara Koogan, Rio de Janeiro.

Waisberg J, Corsi CE, Rebelo MV, Vieira VT, Bromberg SH, dos Santos PA, Monteiro R 1999. Jejunal perforation caused by abdominal angiostrongyliasis. *Rev Inst Med Trop Sao Paulo* 41: 325-328.

Walther M, Muller R 2003. Diagnosis of human filariases (except onchocerciasis). *Adv Parasitol* 53: 149-193.

Washburn MP, Wolters D, Yates JR, 3rd 2001. Large-scale analysis of the yeast proteome by multidimensional protein identification technology. *Nat Biotechnol* 19: 242-247.

Wilkesman J, Kurz L 2009. Protease analysis by zymography: a review on techniques and patents. *Rec. Pat. Biotechnol.* 3: 175-184.

Wilkins MR, Pasquali C, Appel RD, Ou K, Golaz O, Sanchez JC, Yan JX, Gooley AA, Hughes G, Humphery-Smith I, Williams KL, Hochstrasser DF 1996. From proteins to proteomes: large scale protein identification by two-dimensional electrophoresis and amino acid analysis. *Bio/Technology* 14: 61-65.

Williamson AL, Brindley PJ, Knox DP, Hotez PJ, Loukas A 2003. Digestive proteases of blood-feeding nematodes. *Trends Parasitol.* 19: 417-423.

Wongkamchai S, Chiangjong W, Sinchaikul S, Chen ST, Choochote W, Thongboonkerd V 2011. Identification of *Brugia malayi* immunogens by an immunoproteomics approach. *J Proteomics* 74: 1607-1613.

Xu T, Venable JD, Park SK, Cociorva D, al. e 2006. ProLuCID, a fast and sensitive tandem mass spectra-based protein identification program. *Mol. Cell. Proteomics* 5: S:174.

Yates JR, 3rd 2004. Mass spectral analysis in proteomics. *Annu Rev Biophys Biomol Struct* 33: 297-316.

Yates JR, Ruse CI, Nakorchevsky A 2009. Proteomics by Mass Spectrometry: Approaches, Advances, and Applications. *Annual Review of Biomedical Engineering* 11: 49-79.

Yatsuda AP, Krijgsveld J, Cornelissen AW, Heck AJ, de Vries E 2003. Comprehensive analysis of the secreted proteins of the parasite *Haemonchus contortus* reveals extensive sequence variation and differential immune recognition. *J Biol Chem* 278: 16941-16951.

Yokota H, Mori K, Kaniwa H, Shibanuma T 2000. Elimination of artifactual bands from polyacrylamide gels. *Anal Biochem* 280: 188-189.

Zanini GM, Graeff-Teixeira C 1995. [Abdominal angiostrongyliasis: its prevention by the destruction of infecting larvae in food treated with salt, vinegar or sodium hypochlorite]. *Rev Soc Bras Med Trop* 28: 389-392.

Zanini GM, Graeff-Teixeira C 2001. Inactivation of infective larvae of Angiostrongylus costaricensis with short time incubations in 1.5% bleach solution, vinegar or saturated cooking salt solution. *Acta Trop* 78: 17-21.

Zhan B, Hotez PJ, Wang Y, Hawdon JM 2002. A developmentally regulated metalloprotease secreted by host-stimulated Ancylostoma caninum third-stage infective larvae is a member of the astacin family of proteases. *Mol. Biochem. Parasitol.* 120: 291-296.

Zhang X, Fang A, Riley CP, Wang M, Regnier FE, Buck C 2010. Multi-dimensional liquid chromatography in proteomics--a review. *Anal Chim Acta* 664: 101-113.

Zhu H, Bilgin M, Snyder M 2003. Proteomics. *Annu Rev Biochem* 72: 783-812.

Ziegelbauer K, Speich B, Mausezahl D, Bos R, Keiser J, Utzinger J 2012. Effect of sanitation on soil-transmitted helminth infection: systematic review and meta-analysis. *PLoS Med* 9: e1001162.

Ziliotto A, Jr., Kunzle JE, Fernandes LA, Prates-Campos JC, Britto-Costa R 1975. Angiostrongyliasis: report of a probable case. *Rev. Inst. Med. Trop. Sao Paulo* 17: 312-318.